Misdirection and guidance of regenerating motor axons
after experimental nerve injury and repair

Misdirection and guidance of regenerating motor axons after experimental nerve injury and repair

PROEFSCHRIFT

ter verkrijging van de graad van Doctor
aan de Universiteit Leiden,
op gezag van Rector Magnificus Prof. Mr. C.J.J.M. Stolker,
volgens besluit van het College voor Promoties
te verdedigen op dinsdag 21 mei 2013
klokke 16:15 uur

door

Godard de Ruiter

geboren te Nieuwerkerk a/d IJssel
in 1978

Promotiecommissie:
Promotor:
Prof. dr. M.J.A. Malessy
Co-promotor:
Prof. R.J. Spinner, Mayo Clinic, Rochester MN, VS
Overige leden:
Prof. dr. J.G. van Dijk
Prof. dr. J.N. Noordermeer
Prof. dr. J. Verhaagen, Nederlands Instituut voor Neurowetenschappen

Financial support for the printing of this thesis was generously provided by the Department of Neurosurgery LUMC, Stichting Researchfonds Bronovo, Implantcast, QMediq, Promedics, Biomet, InSpine, Krijnen Medical, ChipSoft.

Godard's stay in the USA was supported by the Sundt fellowship (Mayo Clinic), Leids Universitair Fonds (LUF), Janneke Fruin-Helb beurs, Stichting Fundatie van de Vrijvrouwe van Renswoude te 's Gravenhage, Stichting Mitialto, Stichting Dr. Hendrik Muller's Vaderlandsch Fonds, Lustra and Jo Keur Fonds

ISBN: 978-94-6191-726-3

Press: Ipscamp
Lay-out: Textcetera
Cover design: Jurgen Kuivenhoven

Contents

CHAPTER 1

Introduction Aims and Outline

Peripheral nerve injuries and repair

Peripheral nerve injuries are a common type of injury that can be caused by various mechanisms including, for example, sharp transection (as in iatrogenic injury), disruption due to fracture of long bones, and stretch injuries (as in adult traumatic and neonatal brachial plexus palsy). The exact incidence of traumatic nerve injuries in The Netherlands is not known. In Canada, a prevalence rate of 2.8% has been reported in the trauma population [1]. In Sweden, the incidence rate is 13.9 per 100,000 person years [2].

The peripheral nervous system has the capacity to regenerate and, depending on the severity of the nerve lesion, spontaneous recovery can occur. When the continuity of the nerve is lost or when a neuroma-in-continuity has formed, surgical intervention may be indicated. In sharp transection injuries nerve ends can be coapted directly without tension. In blunt or stretch injuries, however, direct suture of the nerve ends is often not possible without tension at the coaptation site. In these cases, a graft is needed to bridge the gap between the proximal and distal stumps. The introduction in the second half of the previous century of the operating microscope and surgical loupes, as well as the development of microsurgical techniques and the use of the autologous nerve graft to reestablish continuity of the injured nerves have considerably improved the outcome following nerve surgery. Despite these developments, however, functional recovery is often incomplete.

Timing of surgery

Several factors can account for the incomplete recovery. First of all, the timing of surgery is an important factor. The best chance of recovery is when nerve repair is performed directly after trauma, because the capacity for regeneration has been shown to decrease with time and because changes occur in the distal nerve and targets due to the prolonged period of denervation [3, 4]. In closed nerve traction or compression lesions, it can be difficult to predict whether the continuity of the nerve has been lost. The decision whether to await spontaneous recovery or perform surgical exploration within days is determined by various factors, for example, the extent of the neurological deficit and type of trauma. Electrophysiological analysis can be helpful in determining the extent of the nerve injury and in detecting early signs of muscle reinnervation.

Unfortunately, even after immediate repair, functional recovery of proximal injuries is limited because of the length axons have to elongate, from the site of the injury to the distal targets. For example, after reconstruction of brachial plexus injuries, it may take years before axons reach the hand (with a regeneration speed of 1-3 mm a day) [5]. Therefore, recovery of hand function is often poor. Novel strategies (e.g. electrical stimulation [6] and gene therapy [7]) have been developed which focus on increasing the speed of axonal regeneration in order to reduce the time between the nerve injury and target reinnervation. Alternatively, *sensory protection* (which is pursued by temporary reinnervation of a denervated muscle by transfer of a sensory branch to the distal nerve stump [8] or via side-to-side nerve grafts [9]) is used to slow the process of degeneration in the distal targets.

Misdirection or misrouting

Another factor, which plays a role in the incomplete recovery after nerve injury and repair, is misdirection or misrouting of regenerating axons. There is always a certain degree of misdirection, even following microsurgical coaptation of the individual fascicles, because the continuity of the endoneurial or basal lamina tubes cannot be restored and axons cross the coaptation site in a random way (**Figure 2, Chapter 2**). This misdirection of axons across the repair site may lead to reinnervation of inappropriate targets. In the repair of mixed nerves, for example, motor axons may be directed towards the skin, and vice versa, sensory axons towards the muscle. Even in the repair of a pure motor nerve innervating different muscles, axons may end up in pathways towards a different muscle, which might function antagonistically. In sensory nerve repair, misdirection may lead to an increased perceptual territory [10].

The first indication that axons are misdirected at the coaptation site dates back to the beginning of the 20th century. In his book on *degeneration and regeneration of the nervous system*, In 1928, Ramon y Cajal demonstrated [11] that a single axon can have multiple projections to different distal targets (**Figure 2, Chapter 2**). Since then, numerous studies have investigated accuracy of regeneration and reinnervation (**for review see Chapter 2**). As yet, however, the extent and impact of misdirection on the level of function is not known.

AIMS AND OUTLINE

The first aim of this thesis was *to quantify the degree of misdirection* and *to determine the impact of misdirection on functional recovery* after different types of nerve injury and repair. A sequential retrograde tracing technique was used to quantify the degree of misdirection. First, a tracer was injected into an intact nerve before the injury to label the original motoneuron pool. Subsequently, a second tracer was used at a specific period of time after the injury and repair to label the motoneurons that had regenerated to the same nerve branch. As a model, the rat sciatic nerve was chosen, not only because it is the most frequently used model in experiments on nerve regeneration, but also, because the nerve divides distally into a tibial and peroneal nerve branch; these have antagonistic functions: ankle plantar and dorsiflexion, respectively (**Figure 1, Chapter 4**). The degree of misdirection to either the peroneal or tibial nerve branch can thus be investigated. For this purpose, a new functional evaluation method was developed in collaboration with the motion analysis laboratory at Mayo Clinic. Equipment for analyzing motion, normally used in patients with neurological disorders, was adapted to assess the recovery of ankle plantar and dorsiflexion in rats after sciatic nerve injury. This new technique of ankle motion analysis was validated and compared to the current gold standard of walking track analysis (**Chapter 3)**. Sequential retrograde tracing and ankle motion analysis were subsequently used to quantify the degree of misdirection after different types of nerve injury and repair, and the impact on the

recovery of function respectively (**Chapter 4**). Different types of nerve injury (crush vs transection injury) and repair (direct coaptation vs autograft repair) were investigated to determine the impact of intact versus interrupted basal lamina tubes on misdirection, and nerve repair with one versus two coaptation sites.

The second aim of this thesis was to improve *guidance of regenerating motor axons* in the rat sciatic nerve model. In **Chapter 2** we reviewed several factors that may be involved in the routing of regenerating axons after nerve injury and repair. In recent years, different strategies have been developed that may guide and direct regenerating axons toward their correct target organ. Most of these guiding strategies have been investigated *in vitro* using neurite outgrowth assays of e.g. explanted dorsal root ganglion (DRG) cells. For example, physical guidance of neurites has been investigated using grooved microsurfaces. This research has shown that neurites orient parallel to the walls of microchannels [12]. Other examples include research on *in vitro* outgrowth of neurites on polymer filaments, with different shapes and coatings [13], and polymer surfaces patterned with gradients of peptides or neurotrophic factors to guide neurites in a certain direction [14]. Only a limited number of studies have investigated the influence on *in vivo* nerve regeneration. In the second part of this thesis we tried to improve the *in vivo* guidance of regenerating axons using two different tools: (1) *mechanical guidance* with *multichannel nerve tubes*, and (2) *biological guidance* with *gene therapy*.

Multichannel nerve tube

Single lumen nerve tubes, guides or conduits have been developed as an alternative for repair with an autologous nerve graft, mainly because of the disadvantages of the autograft, such as donor-site morbidity, limited availability and size mismatch with the injured nerve, necessitating the use of multiple pieces of grafts (so called cable grafts, **figure 1 Chapter 5**). Different single lumen nerve tubes are now available for clinical use (a review of the experimental and clinical data is provided in **Chapter 5**). Unfortunately, single lumen tubes are only effective in the repair of small defects (<3 cm). Furthermore, in larger mixed or motor nerves, repair with a single lumen nerve tube may lead to inappropriate target reinnervation due to the *dispersion of regenerating axons* across the lumen [15]. We have found similar results as shown by a decrease in *type grouping* in reinnervated gastrocnemius and anterior tibialis muscles after repair of a 1-cm sciatic nerve defect with a single lumen nerve tube [16].

Multichannel nerve tubes that have been developed for both experimental peripheral nerve [17-19] and spinal cord repair [20-23] may limit this axonal dispersion by separately guiding groups of regenerating axons inside the channels. To investigate the influence of multichannel structure on regeneration, we developed a single lumen and 7-channel nerve conduit from the polymer, poly(lactic co-glycolic acid) (PLGA). in collaboration with the bio-engineering laboratory at Mayo Clinic. These conduits were first analyzed *in vitro* for different ratios of lactic to

glycolic acid to assess certain nerve tube properties: permeability, flexibility, swelling and degradation (**Chapter 6**). Subsequently, in a pilot study we compared the accuracy of regeneration across a 1-cm gap after autograft repair and repair with single lumen or multichannel nerve tubes using sequential and simultaneous retrograde tracing (**Chapter 7**). The technique of sequential tracing has already been described above. In simultaneous tracing, the same tracers, FB and DY, were used, but were now applied at the same time to the tibial and peroneal nerve, respectively, to label motor axons that had regenerated to either one or both branches. Our hypothesis was that more double labeling (motoneurons with projections to both branches) would be observed after single lumen nerve tube repair compared with autograft repair due to dispersion of axonal branches originating from the same motoneuron, and, that multichannel nerve tube repair would limit this dispersion. In a second study, we additionally analyzed the influence of 2-, 4-channel conduits on regeneration using multichannel nerve tubes made of collagen (**Chapter 8**). Again, simultaneous retrograde tracing was performed to investigate the dispersion of regenerating axons across these conduits. In addition, functional recovery was assessed using ankle motion analysis.

Gene therapy

In addition to mechanical guidance through multichannel conduits, we also investigated the possibility of biological guidance with gene therapy by selective injection of a lentiviral vector encoding for GDNF (glial cell line-derived neurotrophic factor). This neurotrophic factor has been shown to improve motoneuron survival and regeneration after prolonged axotomy [24]. This study was performed at the Netherlands Institute for Neuroscience (NIN). Previous experiments from this institution have shown that the lentiviral vector encoding for GDNF (LV-GDNF), after injection into a nerve can transfect Schwann cells that subsequently produce GDNF [25]. We injected the same viral vector LV-GDNF into the peroneal nerve, after transection and repair of the sciatic nerve just proximal to the tibial-peroneal bifurcation (**Chapter 9**). The directing effect of selective LV-GDNF injection into the peroneal nerve branch was investigated after 4 weeks with the same simultaneous tracing method mentioned above. Our hypothesis was that more motoneurons would be labeled by the tracer applied to the peroneal nerve branch (DY) and fewer by the tracer applied to the tibial nerve branch (FB) after LV-GDNF injection into the peroneal nerve branch, when compared with the control groups (repair without viral vector injection and injection of a control vector encoding for green fluorescent protein).

Future directions

Finally, the last Chapter of this thesis (**Chapter 10 General discussion and future directions**), summarizes the results and discusses future directions of both mechanical and biological guidance.

REFERENCES

1. Noble, J., et al., *Analysis of upper and lower extremity peripheral nerve injuries in a population of patients with multiple injuries.* The Journal of Trauma: Injury, Infection, and Critical Care, 1998. **45**(1): p. 116-122.
2. Asplund, M., et al., *Incidence of traumatic peripheral nerve injuries and amputations in Sweden between 1998 and 2006.* Neuroepidemiology, 2009. **32**: p. 217-228.
3. Fu, S.Y. and T. Gordon, *Contributing factors to poor functional recovery after delayed nerve repair: prolonged denervation.* J Neurosci, 1995. **15**(5 Pt 2): p. 3886-95.
4. Fu, S.Y. and T. Gordon, *Contributing factors to poor functional recovery after delayed nerve repair: prolonged axotomy.* J Neurosci, 1995. **15**(5 Pt 2): p. 3876-85.
5. Guttmann, E., et al., *The rate of regeneration of nerve.* J Exp Biol, 1942. **19**: p. 14-44.
6. Al-Majed, A.A., et al., *Brief electrical stimulation promotes the speed and accuracy of motor axonal regeneration.* Journal of Neuroscience, 2000. **20**(7): p. 2602-08.
7. Tannemaat, M.R., et al., *From microsurgery to nanosurgery: how viral vectors may help repair the peripheral nerve.* Prog Brain Res, 2009. **175**: p. 173-86.
8. Elsohemy, A., et al., *Sensory protection of rat muscle spindles following peripheral nerve injury and reinnervation.* Plastic and Reconstructive surgery, 2009. **124**(6): p. 18601868.
9. Ladak, A., et al., *Side-to-side nerve grafts sustain chronically denervated peripheral nerve pathways during axons regeneration and result in improved functional reinnervation.* Neurosurgery, 2011. **68**(6): p. 1654-1666.
10. Dyck, P.J., et al., *Assessment of nerve regeneration and adaptation after median nerve reconnection and digital neurovascular flap transfer.* Neurology, 1988. **38**(10): p. 1586-91.
11. Cajal, S., *Degeneration and regeneration of the nervous system.* London: Oxford University Press, 1928.
12. Mahoney, M.J., et al., *The influence of microchannels on neurite growth and architecture.* Biomaterials, 2005. **26**: p. 771-778.
13. Ribeiro-Resende, V.T., et al., *Strategies for inducing the formation of bands of Büngner in peripheral nerve regeneration.* Biomaterials, 2009. **2009**(30): p. 5251-5259.
14. Yu, L.M.Y., J.H. Wosnick, and M.S. Shoichet, *Miniaturized system of neurotrophin patterning for guided regeneration.* J Neurosci Methods, 2008. **171**(253-263).
15. Brushart, T.M., et al., *Joseph H. Boyes Award. Dispersion of regenerating axons across enclosed neural gaps.* J Hand Surg [Am], 1995. **20**(4): p. 557-64.
16. Vleggeert-Lankamp, C.L., et al., *Type grouping in skeletal muscles after experimental reinnervation: another explanation.* Eur J Neurosci, 2005. **21**(5): p. 1249-56.
17. Bender, M.D., et al., *Multi-channeled biodegradable polymer/CultiSpher composite nerve guides.* Biomaterials, 2004. **25**(7-8): p. 1269-78.
18. Sundback, C., et al., *Manufacture of porous polymer nerve conduits by a*

novel low-pressure injection molding process. Biomaterials, 2003. **24**(5): p. 819-30.
19. Yang, Y., et al., *Neurotrophin releasing single and multiple lumen nerve conduits.* J Control Release, 2005. **104**(3): p. 433-46.
20. Friedman, J.A., et al., *Biodegradable polymer grafts for surgical repair of the injured spinal cord.* Neurosurgery, 2002. **51**(3): p. 742-51; discussion 751-2.
21. Moore, M.J., et al., *Multiple-channel scaffolds to promote spinal cord axon regeneration.* Biomaterials, 2006. **27**(3): p. 419-29.
22. Stokols, S. and M.H. Tuszynski, *The fabrication and characterization of linearly oriented nerve guidance scaffolds for spinal cord injury.* Biomaterials, 2004. **25**(27): p. 5839-46.
23. Chen, B.K., et al., *Axon regeneration through scaffold into distal spinal cord after transection.* J Neurotrauma, 2009. **26**(10): p. 1759-71.
24. Boyd, J.G. and T. Gordon, *Glial cell line-derived neurotrophic factor and brain-derived neurotrophic factor sustain the axonal regeneration of chronically axotomized motoneurons in vivo.* Exp Neurol, 2003. **183**(2): p. 610-9.
25. Tannemaat, M.R., et al., *Differential effects of lentiviral vector-mediated overexpression of nerve growth factor and glial cell line-derived neurotrophic factor on regenerating sensory and motor axons in the transected peripheral nerve.* Eur J Neurosci, 2008. **28**(8): p. 1467-79.

PART
ONE

MISDIRECTION OF MOTOR AXON REGENERATION

CHAPTER 2

Review on misdirection of regenerating axons after experimental nerve injury and repair

Godard C.W. de Ruiter, M.D. [1], Robert J. Spinner, M.D. [2], Joost Verhaagen, PhD [3, 4], Martijn J.A. Malessy, M.D. PhD [1,3]

[1] Department of Neurosurgery, Leiden University Medical Center, Leiden, The Netherlands
[2] Department of Neurosurgery, Mayo Clinic, Rochester, Minnesota USA
[3] Department of Neuroregeneration, Netherlands Institute for Neuroscience, Amsterdam, NL
[4] Department of Molecular and Cellular Neurobiology, Center for Neurogenomics and Cognition Research, Vrije Universiteit Amsterdam, The Netherlands

Part of this review is accepted for publication in the Journal of Neurosurgery

ABSTRACT

Misdirection of regenerating axons is one of the factors that can explain the limited results often found after nerve injury and repair. In the repair of mixed nerves innervating different distal targets (skin and muscle), misdirection may for example, lead to motor axons projecting towards skin, and vice versa, sensory axons projecting towards muscle. In the repair of motor nerves innervating different distal targets, misdirection may result in reinnervation of the wrong target muscle, which might function antagonistically. In sensory nerve repair, misdirection might give an increased perceptual territory. After median nerve repair, for example, this might lead to a dysfunctional hand.

Different factors may be involved in the misdirection of regenerating axons and there may be various mechanisms which can later correct for misdirection. In this review, we discuss these different factors and mechanisms that act along the pathway of the regenerating axon. In addition, we review recently developed evaluation methods that can be used to investigate the accuracy of regeneration after nerve injury and repair (including the use of transgenic fluorescent mice, retrograde tracing techniques, and motion analysis).

INTRODUCTION

Functional recovery after nerve injury and repair is often disappointing, despite the capacity of the peripheral nervous system to regenerate. Several factors can explain this incomplete recovery. First of all, the timing of surgery is an important factor. The best chances for recovery are when nerve repair is performed directly after the injury, because (1) the capacity of regeneration has been shown to decrease with time (fewer neurons from which axons regenerate), and (2) changes occur in the distal nerve and targets due to the prolonged period of denervation (such as fragmentation of the basal lamina tubes and decrease in the number of Schwann cells [1-3]). The type of injury and possibilities for repair may also influence the functional outcome: the recovery following graft repair, for example, is reduced compared with direct coaptation repair. If the patient is older, the chance of functional recovery will be decreased [4].

Another factor that can explain poor recovery after nerve injury and repair is misdirection or misrouting of regenerating axons. Misdirection can explain the difference in recovery for different types of nerves (mixed, motor and sensory nerves). In the repair of mixed nerves that innervate different distal targets (skin and muscle), misdirection may lead to motor axons projecting towards skin, and sensory axons projecting towards muscle. In the repair of a motor nerve that innervates different target muscles, motor axons may be misdirected to antagonistic muscles. As for example following repair of the sciatic nerve, that distally divides into the tibial and peroneal nerve branches involved in ankle plantar and dorsiflexion, respec-

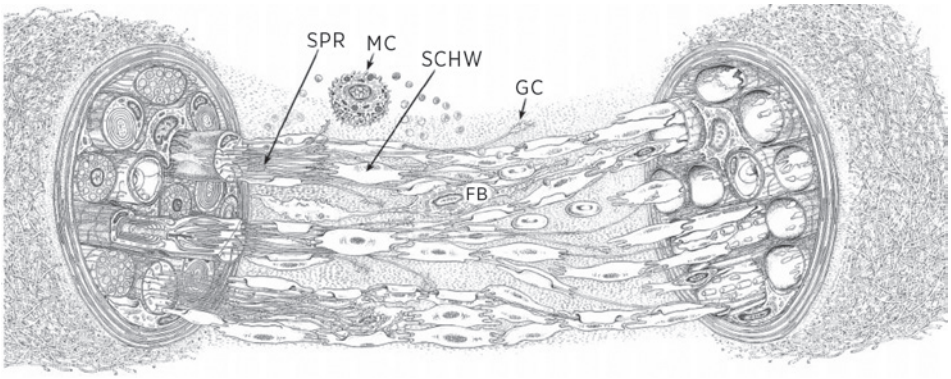

Figure 1

Local cellular response to nerve transection. Sprouting occurs at the cut axonal ends in the proximal nerve segment (left). Sprouts (SPR) arising from one myelinated axons form a regenerating unit surrounded by common basal lamina. At the tip of each sprout there is a growth cone (GC). Sprouts advance over the zone of injury in immediate association with Schwann cells (SCHW). In the injury zone there are macrophages, fibroblasts (FB), mast cells (MC), and blood corpuscle elements. In the distal segment sprouts attach to the band of Bügner and become enclosed in the Schwann cell cytoplasm. Axonal misdirection is frequent. (Figure obtained with permission from article by Lundborg [54]).

tively [5]. In sensory nerve repair misdirection may limit outcome: after repair of the median nerve at the wrist, patients may experience painful sensations in other median nerve innervated fingers, even years after the repair [6].
Different factors are involved in the misdirection of regenerating axons. Moreover, different biological mechanisms have been shown to exist that can later correct for this misdirection. In this Chapter, these factors and mechanisms are discussed. In addition, several recently developed methods are reviewed that have provided valuable insight into the process of regeneration.

THE COURSE OF THE REGENERATING AXON

After nerve injury and repair, the course of the regenerating axon starts at the *coaptation site*. At this site, multiple cellular events have taken place after the injury, including clearance of the debris of the distal axonal bodies by macrophages and Schwann cells, a process called Wallerian degeneration. The proximal axon extends its course across this injury site by sending out multiple sprouts (Figure 1). At the tip of these sprouts are growth cones that continuously create cell protrusions called filopodia and lamellipodia. Growth cones act as antennae for neurotrophic signals. These signals can attract regenerating axons in a certain direction by stimulating actin dynamics inside the growth cone, which leads to axonal elongation [7]. Different neurotrophic factors have been identified including, for

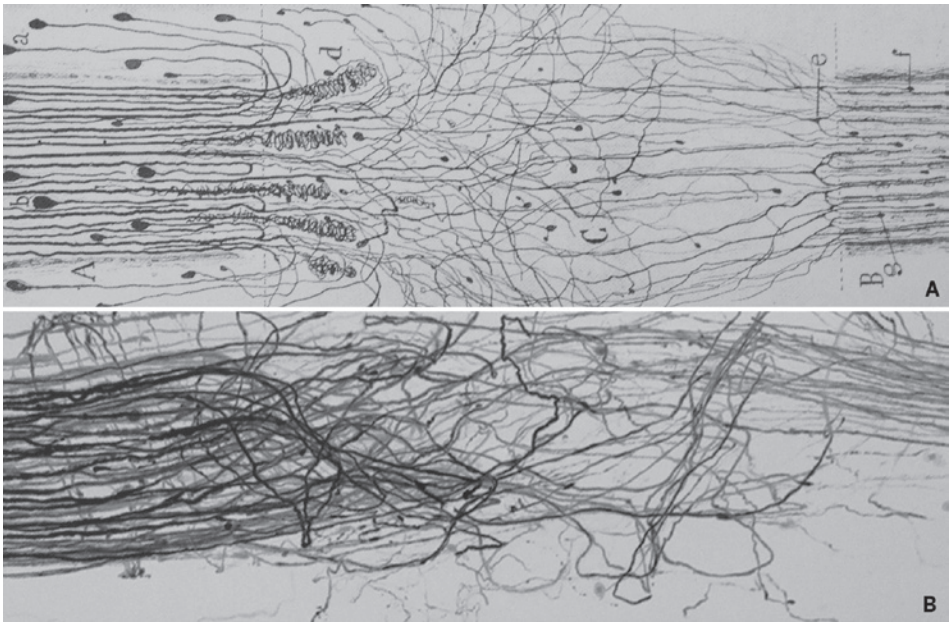

Figure 2

(A) silver staining of Ramon y Cajal demonstrating 'choatic' regeneration across the injury site, (B) similar image obtained using transgenic fluorescent mice. (Figure obtained with permission from article by Pan et al. [55]) In both images the proximal nerve stump is presented left to the injury site and the distal nerve stump right to the injury site.

example, nerve growth factor (NGF), brain-derived neutrophic factor (BDNF) [8] and glial cell-line-derived neurotrophic factor (GDNF) [9]. These factors are produced and secreted by Schwann cells that remain inside the distal basal lamina tubes after Wallerian degeneration. In this way axons are attracted to regenerate towards the distal nerve stump, an effect which has been called *neurotropism* [10]. Besides attractive stimuli, repulsive factors exist that might divert regenerating axons or induce growth cone collapse (for example, semaphorins [11]). In addition, axons might be physically guided. After nerve injury and repair a collagen matrix is formed between the nerve ends. Schwann cells from the proximal and distal nerve stump migrate along this matrix and present specific cell adhesion molecules to guide regenerating axons [12].

In an ideal situation this combination of factors results in a straight course of the regenerating axon back towards its original basal lamina tube (as illustrated in Figure 1). In reality however, it has been shown that axons frequently travel laterally before choosing a distal pathway (Figure 2) [13]. This dispersion of axonal regeneration may lead to inappropriate target reinnervation, despite surgically correct alignment of the fascicles during nerve repair, because once the axon has entered

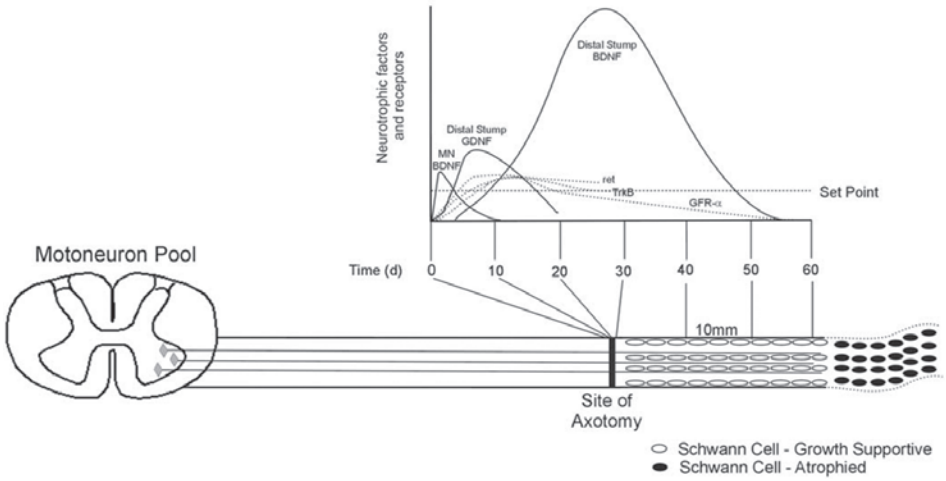

Figure 3

Up-regulation and decline in the expression of growth factors (GDNF and BDNF) and receptors (trkB, ret GFR-α) by motoneurons and in the distal nerve stump 0-60 days after nerve injury. (Figure obtained with permission from article by Furey et al. [56]).

a distal basal lamina tube, the rest of the course is determined by the original pathway of that endoneural tube. Whether or not the axon will eventually also reach the end of the basal lamina tube may still depend on several factors. An important factor is the amount of neurotrophic support, which is again determined by the Schwann cells in the distal nerve stump. As recently demonstrated, Schwann cells only produce these neurotrophic factors for a certain period of time (Figure 3). In addition, the profile of growth factor expression might differ for Schwann cells inside motor versus sensory nerves [14]. Another factor that might determine successful regeneration of the axon across the basal lamina tube is the interaction of the growth cone with specific cell adhesion molecules. Examples of such factors are L2 and HNK-1 [15, 16] and PSA-NCAM [17].

Finally, the regenerating axon has to make a functional reconnection with the target at the end of the basal lamina tube. This last step has mainly been investigated for motor axon reinnervation of the motor endplate. Also in this process selection may occur. After nerve injury and repair, it has been shown that motor endplates are initially polyinnervated, but that later the motor axon to endplate ratio again returns to a normal 1:1 innervation [18-20]. This initial poly- or hyperinnervation may be a mechanism for improving the accuracy of reinnervation. Feedback mechanisms such as tread-mill exercise [21] and manual stimulation may influence this selection process [22].

METHODS TO INVESTIGATE ACCURACY OF REGENERATION

A number of different methods have been developed to investigate accuracy of regeneration and reinnervation. The experiments by Ramon y Cajal at the beginning of the 20th century are legendary [23] (Figure 2A). His silver staining of regenerated nerve fibers already provided us with most of the insight we have today on the accuracy of regeneration across the coaptation site. Also of historical interest are the experiments on the attractive effect of the distal stump (*neurotropism)*, in which Y-shaped tubes were used with different types of tissue in the distal forks. Based on these experiments, the theory of neurotropism was first rejected by Weiss and Taylor [24], because in their experiment no preference for axonal regeneration to different types of tissue was found. However, later the experiment was repeated by others [25-29], who did find a preference for axons to regenerate towards the outlet containing nerve. Since then this theory has been generally accepted. In this review we will not discuss the results of these experiments in detail. Rather, we present more recently developed methods that in our opinion have provided valuable insight into specificity and accuracy of regeneration, including the use of fluorescent transgenic animal models, retrograde tracing techniques, and functional methods based on motion analysis.

Fluorescent transgenic animal models

An exciting, relatively new evaluation method in research on peripheral nerve regeneration is the development of a fluorescent transgenic animal model (in the beginning only fluorescent mice were use, but more recently a transgenic rat model has been developed [30]). In these transgenic animals, a thy1 promotor construct is used to direct the expression of green fluorescent protein (GFP), or a yellow variant (YFP), selectively in neuronal cells (and not in other cell types such as, for example, Schwann cells, fibroblasts, and muscle fibers).[31]. Subsequently, selection of an transgenic animal line, in which the expression of this fluorescent protein is limited to only a subset of axons, has made it possible to visualize the pathway of an individual regenerating axon *in vivo*. This live imaging can be performed at multiple time intervals, before and after the nerve injury. In this way the accuracy of axon regeneration can be determined. *In vivo* analysis of regeneration towards the platysma muscle (that can easily be accessed and viewed) has, for example, shown that the accuracy of regeneration is high after crush injury, with individual regenerating axons entering their original path and reestablishing branches at nearly every original branching point. This specificity is completely lost after transection injury and repair [32]. In addition, this technique can be used to investigate the accuracy of regeneration at the coaptation site and to investigate reinnervation of the motor endplate at the neuromuscular junction by simultaneous labeling of the acetylcholine receptors (AChRs) with α-bungarotoxin (Btx) [31] (Figure 4). Up to now, experiments using these transgenic animal models have mainly confirmed previous observations, including the relatively chaotic process of

axon regeneration across a coaptation site (as demonstrated by Cajal, Figure 2A) and hyperreinnervation at the motor endplate [20]. In the future, these animals may also be employed to investigate new strategies to improve axonal regeneration and target reinnervation *in vivo*, providing an additional advantage that the same animals could be used for analysis with other evaluation methods (such as those mentioned below).

Retrograde tracing techniques

Retrograde tracing techniques are also useful for analyzing the specificity of regeneration, especially because these methods can be applied to *quantify* the accuracy of regeneration. Retrograde tracing is based on the uptake of a fluorescent dye that is retrogradely transported to the nucleus and/or cell body of the neuron (located in the anterior horn in case of motoneurons, or dorsal root ganglion in case of sensory neurons). This label can be applied anywhere along the course of the nerve or directly into the target muscle, by tracer injection or by cup application to the proximal nerve end (after nerve transection, the proximal end of the nerve is placed in a cup containing the tracer). Different technical issues must be considered in the use of retrograde tracers, including labeling efficiency, possible fading of the tracer, dye interactions (when using multiple tracers), potential toxicity [33] and persistence of the tracer, when multiple tracers are used as in sequential tracing [34]. Sequential tracing is an especially useful technique for investigating the accuracy of regeneration towards a specific nerve branch by application of the first tracer before injury to label the original neuronal pool, and the second tracer at a certain interval after the injury (and possibly repair) to label the neurons from which axons have regenerated towards this branch. In **Chapter 4** we used this technique to investigate the accuracy of regeneration after different types of nerve injury and repair (crush, direct coaptation and autograft repair) in the rat sciatic nerve model.

Another possibility of retrograde tracing is to apply multiple tracers at the same time to different nerve branches. This technique has also been used in different animal models including the sciatic nerve, femoral nerve and facial nerve model. In the femoral nerve model simultaneous retrograde tracing has been used to investigate accuracy of motor versus sensory regeneration by applying different tracers to the distal cutaneous and motor branches. Experiments using this model have shown that motor axons initially grow equally into both branches, with similar numbers of retrogradely labeled motoneurons at 2 weeks and also a large number of axons innervating both branches. With time (at 3 and 8 weeks) increasingly more motoneurons projected to the motor branch and fewer motoneurons to the cutaneous branch or both branches [35], a phenomenon which was termed *preferential motor reinnervation* (PMR). Several mechanisms may explain this phenomenon of PMR [36], including the *pruning* of misdirected axon collaterals in favor of correctly directed ones.

In the sciatic and facial nerve model, simultaneous tracing has been used to investigate dispersion of axonal collaterals originating from the same motoneuron to different branches [37]. As mentioned above, a regenerating axon may send out multiple sprouts across the coaptation site. These sprouts may often travel laterally before choosing a distal pathway. Sprouts originating from the same motoneuron may, therefore, end up in different distal target branches. Especially after facial nerve repair, a high percentage of multiple projections to the zygomatic, buccal and marginal mandibular branches has been found (15%) [38, 39], compared with 2.2% double projections after sciatic nerve repair [37]. In **Chapter 7 and 8** we used simultaneous retrograde tracing to compare axonal dispersion across single lumen and multichannel nerve tubes for the percentage of motoneurons with double projections. In **Chapter 9** we used simultaneous tracing to investigate preferential regeneration of motor axons towards the peroneal nerve after injection of a lentiviral vector encoding for glial cell line-derived neurotrophic factor (GDNF).
An important advantage of retrograde tracing techniques is the possibility of quantifying accuracy of regeneration. Care should be taken however when interpreting the results of retrograde tracing not only because of the factors mentioned above, but also because it does not evaluate the final step of motor endplate reinnervation.

Motion analysis

Different methods have been applied to investigate accuracy of reinnervation related to function including selective tension contraction measurements [40], selective recordings of compound muscle action potential amplitude (CMAPs) [41] and walking track analysis [42-44]. All these approaches have been used in the rat sciatic nerve lesion model. Although these methods have provided important insight in the recovery of function after nerve injury and repair, they also have several shortcomings, particularly in the analysis of the impact of misdirection on the recovery of function. Muscle contraction measurements and CMAP recordings for example do not account for co-contractions, nor do they measure the actual recovery of function. The most commonly used functional evaluation method, walking track analysis, only looks at the recovery of distal intrinsic foot muscles that often do not recover as well as the more proximally located muscles (such as the gastrocnemius and anterior tibialis muscles), especially after transection injury and repair. Foot print analysis is also limited due to contractures [45] and autotomy [46]. Other gait parameters have therefore been investigated, including analysis of the ankle angle [47-51]. Advantage of ankle motion analysis is that it can also be used to investigate accuracy of reinnervation of muscles involved in ankle plantar (tibial nerve function) and dorsiflexion (peroneal nerve function) [52], especially if used simultaneously with electromyography (EMG) recordings in the tibialis anterior and gastrocnemius muscles [53]. In **Chapter 3** we present a novel evaluation method that we developed to investigate the recovery of ankle motion after different types of sciatic nerve injury and repair (crush injury, direct coaptation and

autograft repair), called *2D digital video ankle motion analysis*. Advantage of this method is that tibial and peroneal nerve function can be determined separately from ankle plantar and dorsiflexion, respectively.

SUMMARY

Several factors can explain the poor recovery of function often observed after nerve injury and surgical repair, such as the interval between nerve injury and repair, the type of injury and possibilities for repair, age of the patient, and, as discussed in this Chapter, misdirection of regenerating axons. As already stated by Sir Sydney Sunderland '*the core of the problem is not promoting axon regeneration, but in getting them back to where they belong*' [4].

REFERENCES

1. Fu, S.Y. and T. Gordon, *Contributing factors to poor functional recovery after delayed nerve repair: prolonged denervation.* J Neurosci, 1995. **15**(5 Pt 2): p. 3886-95.
2. Fu, S.Y. and T. Gordon, *Contributing factors to poor functional recovery after delayed nerve repair: prolonged axotomy.* J Neurosci, 1995. **15**(5 Pt 2): p. 3876-85.
3. Giannini, C. and P.J. Dyck, *The fate of Schwann cell basement membranes in permanently transected nerves.* J Neuropathol Exp Neurol, 1990. **49**(6): p. 550-63.
4. Sunderland, S., *Nerve injuries and their repair: A critical appraisal.* . 1991, Melbourne: Churchill Livingstone.
5. de Ruiter, G.C., et al., *Misdirection of regenerating motor axons after nerve injury and repair in the rat sciatic nerve model.* Exp Neurol, 2008. **211**(2): p. 339-50.
6. Dyck, P.J., et al., *Assessment of nerve regeneration and adaptation after median nerve reconnection and digital neurovascular flap transfer.* Neurology, 1988. **38**(10): p. 1586-91.
7. Lykissas, M.G., et al., *The role of neurotrophins in axonal growth, guidance, and regeneration.* Current Neurovascular Research, 2007. **4**: p. 143-151.
8. Paves, H. and M. Saarma, *Neurotrophins as in vitro growth cone guidance molecules for embryonic sensory neurons.* Cell Tissue Res, 1997. **290**: p. 285-297.
9. Boyd, J.G. and T. Gordon, *Neurotrophic factors and their receptors in axonal regeneration and functional recovery after peripheral nerve injury.* Mol Neurobiol., 2003. **27**(3): p. 277-324.
10. Forssman, J., *Uber den Ursachen, welche die Wachstumrichtung der Peripheren Nerven fasern bei der Regeneration bestimmen.* Beitr. Pathol. Anat., 1898: p. 24-55.
11. Tannemaat, M.R., et al., *Human neuroma contains increased levels of semaphorin 3A, which surrounds nerve fibers and reduces neurite extension in*

vitro. J Neurosci, 2007. **27**(52): p. 14260-4.
12. Son, Y.S. and W.J. Thompson, *Schwann cell processes guide regeneration of peripheral axons.* Neuron, 1995. **14**: p. 125-132.
13. Witzel, C., C. Rohde, and T.M. Brushart, *Pathway sampling by regenerating peripheral axons.* J Comp Neurol, 2005. **485**(3): p. 183-90.
14. Hoke, A., et al., *Schwann cells express motor and sensory phenotypes that regulate axon regeneration.* J Neurosci, 2006. **26**(38): p. 9646-55.
15. Martini, R., M. Schachner, and T.M. Brushart, *The L2/HNK-1 carbohydrate is preferentially expressed by previously motor axon-associated Schwann cells in reinnervated peripheral nerves.* J Neurosci, 1994. **14**(11 Pt 2): p. 7180-91.
16. Martini, R., et al., *The L2/HNK-1 Carbohydrate Epitope is Involved in the Preferential Outgrowth of Motor Neurons on Ventral Roots and Motor Nerves.* Eur J Neurosci, 1992. **4**(7): p. 628-639.
17. Franz, C.K., U. Rutishauser, and V.F. Rafuse, *Polysialylated neural cell adhesion molecule is necessary for selective targeting of regenerating motor neurons.* J Neurosci, 2005. **25**(8): p. 2081-91.
18. Gorio, A., et al., *Muscle reinnervation--II. Sprouting, synapse formation and repression.* Neuroscience, 1983. **8**(3): p. 403-16.
19. Ijkema-Paassen, J., M.F. Meek, and A. Gramsbergen, *Reinnervation of muscles after transection of the sciatic nerve in adult rats.* Muscle Nerve, 2002. **25**(6): p. 891-7.
20. Magill, C.K., et al., *Reinnervation of the tibialis anterior following sciatic nerve crush injury: a confocal microscopic study in transgenic mice.* Exp Neurology, 2007. **207**(1): p. 64-74.
21. Udina, E., et al., *Effects of activity-dependent strategies on regeneration and plasticity after peripheral nerve injuries.* Annals of Anatomy, 2011. **193**: p. 347-353.
22. Sinis, N., et al., *Chapter 23: Manual stimulation of target muscles has different impact on functional recovery after injury of pure motor or mixed nerves.* In Rev Neurobiol., 2009. **87**: p. 417-32.
23. Cajal, S., *Degeneration and regeneration of the nervous system.* London: Oxford University Press, 1928.
24. Weiss, P. and A. Taylor, *Further experimental evidence against "neurotropism" in nerve regeneration.* J. Exp. Zool., 1944. **95**: p. 233-257.
25. Mackinnon, S.E., et al., *A study of neurotrophism in a primate model.* J Hand Surg [Am], 1986. **11**(6): p. 888-94.
26. Brunelli, G., *Chemotactic arrangement of axons inside and distal to a venous graft.* J Reconstr Microsurg, 1987. **4**(1): p. 75.
27. Abernethy, D.A., A. Rud, and P.K. Thomas, *Neurotropic influence of the distal stump of transected peripheral nerve on axonal regeneration: absence of topographic specificity in adult nerve.* J Anat, 1992. **180 (Pt 3)**: p. 395-400.
28. Chiu, D.T., et al., *Neurotropism revisited.* Neurol Res, 2004. **26**(4): p. 381-7.
29. Politis, M.J., K. Ederle, and P.S. Spencer, *Tropism in nerve regeneration in vivo. Attraction of regenerating axons by diffusible factors derived from cells in distal nerve stumps of transected peripheral nerves.* Brain Res, 1982. **253**(1-2): p. 1-12.
30. Moore, A.M., et al., *A transgenic rat expressing green fluorescent protein (GFP) in peripheral nerves provides a*

new hindlimb model for the study of nerve injury and regeneration J Neurosci Methods, 2012. **204**(1): p. 19-27.
31. Lichtman, J.F. and J.R. Sanes, *Watching the neuromuscular junction.* J of Neurocytology, 2003. **32**: p. 767-775.
32. Nguyen, Q.T., J.R. Sanes, and J.W. Lichtman, *Pre-existing pathways promote precise projection patterns.* Nat Neurosci, 2002. **5**(9): p. 861-7.
33. Puigdellivol-Sanchez, A., et al., *On the use of fast blue, fluoro-gold and diamidino yellow for retrograde tracing after peripheral nerve injury: uptake, fading, dye interactions, and toxicity.* J Neurosci Methods, 2002. **115**(2): p. 115-27.
34. Puigdellivol-Sanchez, A., et al., *Persistence of tracer in the application site--a potential confounding factor in nerve regeneration studies.* J Neurosci Methods, 2003. **127**(1): p. 105-10.
35. Brushart, T.M., *Motor axons preferentially reinnervate motor pathways.* J Neurosci, 1993. **13**(6): p. 2730-8.
36. Madison, R.D., G.A. Robinson, and S.R. Chadaram, *The specificity of motor neurone regeneration (preferential reinnervation).* Acta Physiol (Oxf), 2007. **189**(2): p. 201-6.
37. Valero-Cabre, A., et al., *Peripheral and spinal motor reorganization after nerve injury and repair.* J Neurotrauma, 2004. **21**(1): p. 95-108.
38. Guntinas-Lichius, O., et al., *Impact of different types of facial nerve reconstruction on the recovery of motor function: an experimental study in adult rats.* Neurosurgery, 2007. **61**(6): p. 1276-83; discussion 1283-5.
39. Hizay, A., et al., *Use of Y-tube-conduit following facial nerve injury reduces collateral axonal branching at the lesion site but neither reduces polyinnervation of motor endplates nor improves functional recovery.* Neurosurgery, 2012. **Epub ahead of print**.
40. Zhao, Q., et al., *Specificity of muscle reinnervation following repair of the transected sciatic nerve. A comparative study of different repair techniques in the rat.* J Hand Surg [Br], 1992. **17**(3): p. 257-61.
41. Evans, P.J., et al., *Selective reinnervation: a comparison of recovery following microsuture and conduit nerve repair.* Brain Res, 1991. **559**(2): p. 315-21.
42. De Medinaceli, L., *Use of sciatic function index and walking track assessment.* Microsurgery, 1990. **11**: p. 191-192.
43. de Medinaceli, L., Freed, WJ, Wyatt, RJ, *An index of the functional condition of rat sciatic nerve based on measurements made from walking tracks.* Exp Neurol, 1982. **77**: p. 634-643.
44. Bain, J.R., S.E. Mackinnon, and D.A. Hunter, *Functional evaluation of complete sciatic, peroneal, and posterior tibial nerve lesions in the rat.* Plast Reconstr Surg, 1989. **83**(1): p. 129-38.
45. Dellon, A.L. and S.E. Mackinnon, *Sciatic nerve regeneration in the rat. Validity of walking track assessment in the presence of chronic contractures.* Microsurgery, 1989. **10**(3): p. 220-5.
46. Weber, R.A., et al., *Autotomy and the sciatic functional index.* Microsurgery, 1993. **14**(5): p. 323-7.
47. Santos, P.M., S.L. Williams, and S.S. Thomas, *Neuromuscular evaluation using rat gait analysis.* J Neurosci Methods, 1995. **61**(1-2): p. 79-84.
48. Lin, F.M., et al., *Ankle stance angle: a functional index for the evaluation of sciatic nerve recovery after complete transection.* J Reconstr Microsurg, 1996. **12**(3): p. 173-7.

49. Yu, P., et al., *Gait analysis in rats with peripheral nerve injury.* Muscle Nerve, 2001. **24**(2): p. 231-9.
50. Varejao, A.S., et al., *Motion of the foot and ankle during the stance phase in rats.* Muscle Nerve, 2002. **26**(5): p. 630-5.
51. Varejao, A.S., et al., *Ankle kinematics to evaluate functional recovery in crushed rat sciatic nerve.* Muscle Nerve, 2003. **27**(6): p. 706-14.
52. de Ruiter, G.C., et al., *Two-dimensional digital video ankle motion analysis for assessment of function in the rat sciatic nerve model.* J Peripher Nerv Syst, 2007. **12**(3): p. 216-22.
53. Gramsbergen, A., I.J.-P. J, and M.F. Meek, *Sciatic nerve transection in the adult rat: abnormal EMG patterns during locomotion by aberrant innervation of hindleg muscles.* Exp Neurol, 2000. **161**(1): p. 183-93.
54. Lundborg, G., *A 25-year perspective of peripheral nerve surgery: evolving neuroscientific concepts and clinical significance.* J Hand Surg [Am], 2000. **25**(3): p. 391-414.
55. Pan, Y.A., et al., *Effects of neurotoxic and neuroprotective agents on peripheral nerve regeneration assayed by time-lapse imaging in vivo.* J Neurosci, 2003. **23**(36): p. 11479-11488.
56. Furey, M.J., et al., *Prolonged target deprivation reduces the capacity of injured motoneurons to regenerate.* Neurosurgery, 2007. **60**(4): p. 723-733.

CHAPTER 3

2D-digital video ankle motion analysis for assessment of function in the rat sciatic nerve model

Godard CW de Ruiter [1,2,5], Robert J Spinner [2], Awad O Alaid [1,2], Anthony Koch [1], Huan Wang [1,2], Martijn JA Malessy [5], Bradford L Currier [3], Michael J Yaszemski [3], Kenton R Kaufman [4], Anthony J Windebank [1]

[1] Laboratory for Molecular Neuroscience, Mayo Clinic, Rochester MN, USA
[2] Departments of Neurologic Surgery, Mayo Clinic, Rochester MN, USA
[3] Department of Orthopedic Surgery, Mayo Clinic, Rochester MN, USA
[4] Laboratory for Motion analysis, Mayo Clinic, Rochester MN, USA
[5] Department of Neurosurgery, Leiden University Medical Center, The Netherlands

Published in Journal of Peripheral Nervous System, 2007, Volume 12; 216-222

ABSTRACT

Background Ankle motion analysis may provide a better method to assess function in the rat sciatic nerve model than the standard method, the sciatic function index (SFI), but it is not widely used in experiments on nerve regeneration, possibly because of complicated analysis.
Methods In this study, we investigated the practical use of a 2D digital video motion analysis system. Reproducibility was investigated in normal rats. Recovery of ankle motion was analyzed after sciatic, tibial, and peroneal nerve crush injury. Results were compared with scores for the SFI.
Results 2D digital video motion analysis proved to be reproducible with no significant difference in results from animal to animal and day to day. Interobserver variability was also small. In the analysis of recovery after separate nerve crush injuries, subtle differences in ankle plantar flexion and dorsiflexion could be detected. The method was also more sensitive that the SFI: whereas scores for the SFI had returned to normal 4 weeks after sciatic nerve crush injury, the ankle angle at mid stance was still significantly different from that in sham-operated animals 6 weeks after the injury.
Conclusion 2D digital video ankle motion analysis is a practical method to assess function in the rat sciatic nerve model that is more sensitive than the standard method of the SFI.

INTRODUCTION

The rat sciatic nerve model is the most commonly used model in experiments on nerve regeneration. Several methods can be used to evaluate the results of regeneration, including electrophysiology and nerve and muscle morphometry [1]. These methods are useful for evaluating different aspects of the regeneration and reinnervation process, but results do not necessarily correlate with the recovery of nerve function [2-6]. Functional analysis eventually may be the most important evaluation method before introducing experimental treatments of nerve repair techniques into patients.
At present, the standard method of analyzing recovery of function in the rat sciatic nerve model is the sciatic function index (SFI) [7]. Introduced in 1982 by de Medinaceli et al [8] and later modified by Bain et al [9], the SFI is based on the measurement of footprints in walking tracks for different parameters of print length, toe spread and intermediate toe spread (Figure 1A). Footprints have been acquired using paper and paint, radiographic film, and photographic paper [7]. A disadvantage is that footprints sometimes can not be measured because of contractures [10], autotomy [11] or smearing. Therefore, video-based footprint analysis techniques have been developed [12-14]. Rats are thereby filmed in a transparent runway that has a mirror placed below the track at a 45° degree angle [12], or rats at

rest are filmed from below in a transparent box to determine the static sciatic index [14]. Although these video-based methods have increased the number of measurable footprints, problems of contractures and autotomy of the foot still remain [7, 10, 11, 15].

Alternative methods to assess function in the rat sciatic nerve model have been investigated, including, analysis of the ankle angle during the stance and swing phases [16-19]. Ankle motion analysis has not been widely adopted in experiments on nerve regeneration possibly because of technical difficulties in acquiring images and analysis of the ankle angle from these images. We investigated the use of two-dimensional (2D) digital video motion analysis to assess ankle kinematics in the rat. The same system is in use in the evaluation of patients with neurologic deficits [20]. In this study we investigated the ease and reproducibility of the method in normal rats. We also determined its sensitivity to detect suble differences in ankle plantar and dorsiflexion after sciatic, tibial, and peroneal nerve crush injuries. Results were compared with scores for the SFI, the tibial functional index (TFI), and the peroneal functional index (PFI) [9] obtained from the same videos using a mirror placed below the track.

MATERIAL AND METHODS

Ankle motion analysis in normal animals

Ankle motion in rats (female Sprague-Dawley rats, 250 g) was analyzed to determine animal-to-animal and day-to-day variability. The minimum number of trials needed to obtain consistent measurements was determined from the range in results for an increasing number of trails. The mean results for this number of trails were compared for the analysis of three and six normal animals to determine the minimum number of animals needed for consistent measurements. Animal-to-animal variability was determined by comparing means for this number of trails and animals (one-way analysis of variance). Day-to-day variability was determined from comparing results for the same animals on two different days (paired analysis). Interobserver variability was determined for the same trials by two independent observers. Coefficient of repeatability was calculated [21]. Linear correlations (Pearson) between animal speed and ankle motion were investigated.

Sciatic, tibial, and peroneal nerve crush injury

Deficit and recovery of ankle motion after crush injury were analyzed in 12 rats assigned to one of four experimental groups: sham operation or sciatic, tibial, or peroneal crush (three per group).

To apply nerve crush injury, the sciatic nerve was exposed through a 1-cm incision in the buttock, with blunt spreading and retraction of the gluteus maximus muscle. The sciatic, tibial, or peroneal nerve was crushed for 5 s using smooth-tipped forceps. The fascia of the gluteus maximus muscle was closed using a continuous

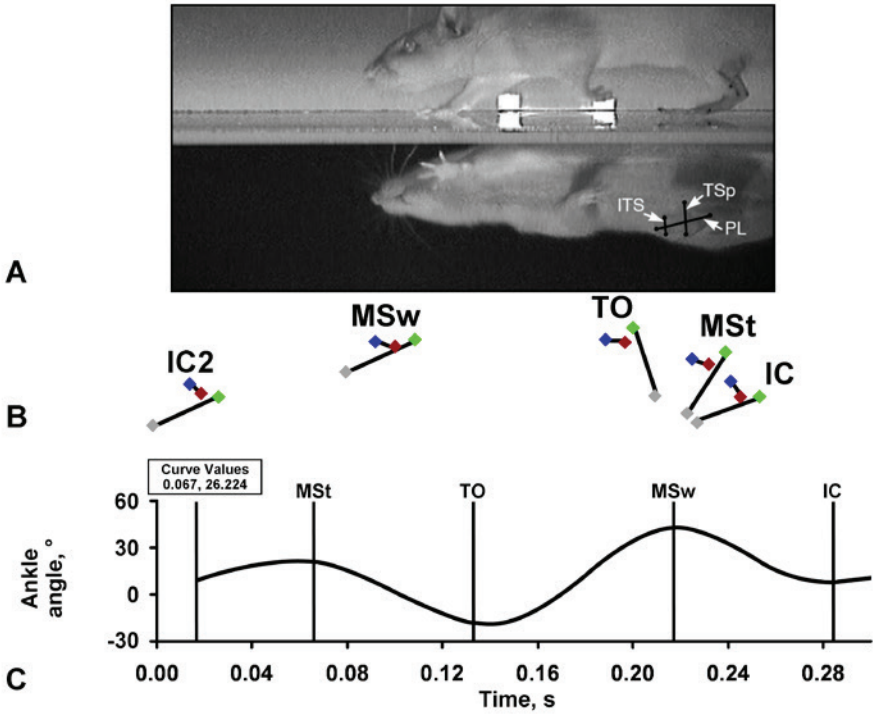

Figure 1

(A) Example of a frame from a digital video showing the rat in the transparent runway with markers on the tibia, lateral malleolus, calcaneus, and fifth metatarsal to create a two-dimensional ankle model. It also shows the mirror that was placed below the transparent track at a 45° angle to analyze the footprints for the print length (PL), toe-spread (TSp), and intermediate toe-spread (ITS) in the same trial. (B) Colored stick figures show the position of the ankle model at the different moments of initial contact (IC), mid-stance (MSt), toe off (TO), mid-swing (MSw), and a second IC. (C) Results for the change in ankle angle after automatic tracking of the markers and filtering (Butterworth filter set to 6 Hz) presented in a report by the Vicon Peak analysis system. A line (in this figure positioned at MSt) can be scrolled along the curve to obtain the value of the ankle angle at any time in the step cycle, as shown in the "Curve Values" box.

3.0 polyglactin 910 suture. Skin was closed with wound clips. The same surgical procedure was used for the sham operation but without nerve crush.

All rats were filmed 1 week before injury and weekly after injury for 6 weeks. Animals were housed in separate cages with a 12-h light-dark cycle. To prevent contractures, a wire mesh was placed in the cage [22]. The left foot was treated daily with Chew-Guard (Butler Animal Health Supply LLC) to prevent autotomy. All procedures were approved by the Mayo Clinic Institutional Animal Care and Use Committee.

Mean results for ankle motion after sciatic, tibial, and peroneal crush were compared with means in sham-operated animals using the Student's *t* test.

2D digital motion ankle analysis

Before filming, rats were briefly anesthetized using isoflurane inhalation (IsoFlo, Abbott Animal Health, UK). The left lower limb was shaved. Black dot markers were placed on bony landmarks with a permanent marker. The proximal point of the lower third of the tibia, the lateral malleolus, the calcaneus and the fifth metatarsal were marked (always with the ankle fixed in a 90º angle) to create a 2D biomechanical model of the ankle (Figure 1A) [19]. Black dots were also placed on the undersides of the toe tips for digital footprint analysis (Figure 1A).

Filming was performed in a darkened room by two observers using the Vicon Peak motion analysis system. Animals were placed in a transparent runway (120cm long, 12cm wide, 30cm tall with a 45° angled mirror below the track). Rats were trained to run to a dark box at the end of the runway. Images were acquired with a 60-Hz digital camera (Dinion^{XF}, Bosch Security Systems) placed 1 m from and perpendicular to the runway to prevent optical distortion. Only trails with acquisition of one complete step cycle (from the moment the left foot touches the floor of the runway at the beginning of the stance phase until it touches the floor again at the end of the following swing phase) and a left and right footprint were used (Figure 1B). Trials were selected for gait speed based on a step cycle duration of 0.25-0.50s. Trials in which the rats were galloping (both feet in the air) were excluded.

Trials were processed using software (PeakMotus 8, Vicon Peak) that tracked the marker dots in all frames of the video. Marker placement was manually corrected as needed. The frequency of the step cycle was 2-4 Hz (0.25-0.50 s). Therefore, data were filtered using a Butterworth filter set to 6 Hz. Results were presented as the ankle angle in degrees as a function of gait cycle (Figure 1C). From the continuous curve, ankle angle was recorded at different even times during the gait cycle (Figure 1):

- *Initial contact (IC)*: the moment the left foot touches the ground
- *Mid stance (MSt)*: the moment the right foot in the air crosses the left foot bearing the animal's weight.
- *Toe off (TO)*: the moment the left foot comes off the runway, the moment of maximum plantar flexion
- *Mid-swing (Msw)*: the moment the left foot crosses the right foot in the stance, the moment of maximum dorsiflexion.

Ankle angles were reported in degrees from the neutral position with dorsiflexion being positive and plantar flexion being negative. Gait speed was calculated by dividing the horizontal displacement of the marker on the fifth metatarsal from IC to IC by duration of the step cycle.

SFI, TFI, and PFI

Footprint analysis was performed in the same trials using the motion analysis software. Measurements were taken from footprint images in the frame before heel rise by manually identifying all toes. The most posterior point of the heel still in

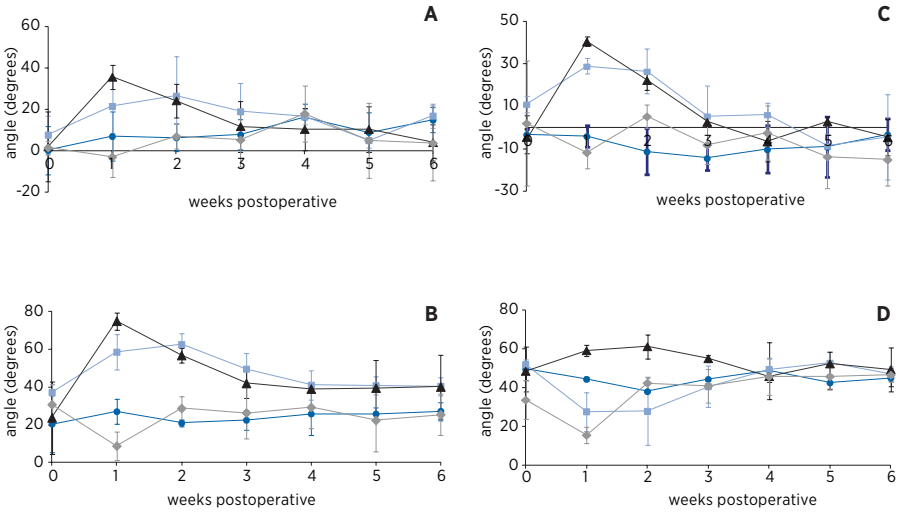

Figure 2

Recovery of the ankle angle over time at (A) initial contact, (B) mid-stance, (C) toe off, and (D) mid-swing after sham operation (○) or sciatic (■), tibial (Δ), or peroneal (◆) nerve crush injury (three animals per group).

contact with the runway was determined from both the next frame (showing heel rise) and the side view of the ankle. Measurements for print length (from tip of third toe to heel), toe spread (from tip of first toe to tip of the fifth toe) and intermediate toe spread (tip of the second toe to tip of the fourth toe) were digitally acquired (Figure 1A). Scores for the SFI, TFI, and PFI were calculated using the following formulas (modified by Bain et al [9], used with permission):

SFI = -38.3 (EPL-NPL)/(NPL) + 109.5 (ETS-NTS)/(NTS) + 13.3(EIT-NIT)/(NIT) – 8.8

TFI = -37.2 (EPL-NPL)/(NPL) + 104.4 (ETS-NTS)/(NTS) + 45.6(EIT-NIT)/(NIT) – 8.8

PFI = 174.9 (EPL-NPL)/(NPL) + 80.3 (ETS-NTS)/(NTS) -13.4

where EPL = experimental print length, NPL = normal print length, ETS = experimental toe spread, NTS = normal toe spread, EIT = experimental intermediate toe spread, NIT = normal intermediate toe spread.

Table 1
Ankle motion in normal rats

Measurement	Mean±SD (n=6)	Mean±SD (n=3)	P value		CR (n=3)
			Animal-to-animal variability*	Day-to-day variability†	
Ankle angle, °					
IC	2.8 ± 9.0	1.2 ± 11.2	0.02	0.50	19.6
MSt	32.6 ± 17.0	31.2 ± 8.7	0.45	0.78	5.4
TO	3.9 ± 8.3	0.4 ± 6.1	0.28	0.05	5.8
MSw	50.9 ± 7.7	53.7 ± 5.8	0.18	0.17	5.5
Gait speed, cm/s	62.9 ± 18.4	57.9 ± 3.3	0.52	0.21	

CR, coefficient of repeatability; IC, initial contact; MSt, mid stance; MSw, mid swing; TO, toe off.
*Difference in values for different animals (n=3) filmed on the same day.
†Difference in values for the same animals filmed on different days (3 rats, 4 or 10 trials/rat).

RESULTS

Ankle motion analysis in normal animals

Ankle angle in normal animals approximated to a sinusoidal form (Figure 1C). The maximum angle of plantar flexion was reached at TO and the maximum angle of dorsiflexion at MSw. Analysis of the range in results for an increasing number of trials showed that after four trials the range did not increase. We therefore obtained four trials per rat for analysis of ankle motion. Filming and selection of four trials on average took 5 min and tracking of markers about 5 min per trial; therefore, a total of 25 min were needed for analysis of one animal.

Mean results for different ankle angles were not significantly different for the analysis of three or six animals ($P > 0.05$). We therefore determined animal-to-animal, day-to-day, and interobserver variability of ankle motion in three animals. Results were not significantly different from animal to animal and day to day (Table 1). Interobserver variability, for the coefficient of repeatability, was small. There was no significant correlation between the speed of the animal and the different ankle angles (IC, P =0.51; MSt, P >0.99; TS, P =0.50; MSw, P =0.16).

Deficit and recovery of ankle motion after sciatic, tibial or peroneal nerve crush injury

During follow-up, no autotomy or foot ulcers occurred, and ankle motion was not limited by contractures. The mean weight of the animals increased from 250 ± 9 to 268 ± 10 g after 6 weeks.

Table 2
Deficit in ankle motion 1 week after nerve crush injury

	Ankle angle, degrees (°)*				
Crush injury	**IC**	**MSt**	**TO**	**MSw**	**SFI/TFI/PFI scores**
Sham operation	7.1 ± 12.0	27.0 ± 6.6	−4.0 ± 5.2	44.5 ± 1.2	SFI, −3.19 ± 9.11 TFI, 11.3 ± 8.5 PFI, 2.3 ± 19.3
Sciatic nerve	21.6 ± 13.0	58.5 ± 9.5†	28.8 ± 3.6†	27.8 ± 9.9†	SFI, −78.40 ± 3.29†
Tibial nerve	35.7 ± 5.9†	74.9 ± 4.5†	40.4 ± 2.2†	59.2 ± 3.0†	TFI, −79.5 ± 1.9‡
Peroneal nerve	−2.8 ± 9.7	8.8 ± 7.4†	−11.6 ± 7.6	15.7 ± 4.3†	PFI, −54.6 ± 1.6§

IC, initial contact; MSt, mid stance; MSw, mid swing; PFI, peroneal functional index; SFI, sciatic functional index; TFI, tibial functional index; TO, toe off.
*Data are presented as mean±SD.
†Results were significantly different from those of sham-operated animals (P<.05).
‡Results were significantly different from those of sham-operated animals (P<.001).
§Results were significantly different from those of sham-operated animals (P=.007)

Gait speed significantly decreased after sciatic crush (37.2 ± 2.7 cm/s) compared with sham-operated animals (57.7 ± 10.5 cm/s). Gait speed did not change after tibial (57.4 ± 11.4 cm/s) and peroneal crush (54.1 ± 6.8 cm/s). Ankle angles significantly changed compared with angles in sham-operated animals (Table 2). After sciatic crush, the maximum angle of plantar flexion and dorsiflexion were decreased (P < 0.001 and P =0.04, respectively), and the angle at MSt showed a decreased plantar flexion (P = 0.009). After tibial crush, there was decreased plantar flexion for the angles at TO and MSt (both P < 0.001). The angle at MSw showed increased dorsiflexion (P =0.01). After peroneal crush, the maximum angle of dorsiflexion at MSw was decreased (P < 0.001). All other angles showed increased plantar flexion (but only significantly for the angle at MSt, P = 0.03).
All angles recovered to normal (sham-operated) values within 2-4 weeks after sciatic, tibial, or peroneal crush injury (Figure 2) except for the angle at MSt (Figure 2B). This angle reached a plateau 4 weeks after sciatic and tibial crush and was still significantly different from the angle in sham-operated animals 6 weeks after sciatic crush (P = 0.03) (after tibial crush, P = 0.27).

SFI, TFI, and PFI

Scores fro the SFI, TFI, and PFI were significantly decreased compared with the scores for these indices in sham-operated animals after sciatic (-78.4 ± 3.3), tibial (-79.5 ± 1.9), and peroneal crush injury (-54.6 ± 1.6) (Table 2). Scores returned to normal 2 weeks after tibial and peroneal crush and 3 weeks after sciatic crush.

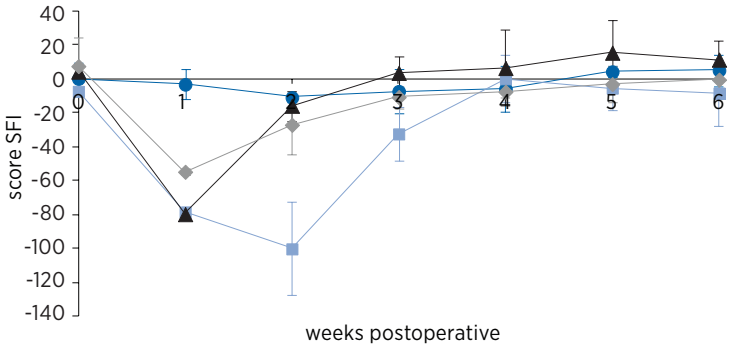

Figure 3

Recovery of sciatic, tibial, and peroneal functional index (SFI, TFI, PFI) scores over time after sham operation (○, SFI score) or sciatic (■, SFI), tibial (Δ, TFI), or peroneal (◆, PFI) nerve crush injury (three animals per group). (SFI could only de determined in two of three animals 1 week after sciatic crush injury because of exorotation of the foot in one animal).

DISCUSSION

Functional analysis is the most important evaluation method for translating experimental treatments for nerve repair into patients. We investigated the use of a 2D digital video motion analysis tot assess function in the rat sciatic nerve model. This method was found to reliable. Results for different ankle angles were not significantly different from animal to animal or day to day except for angle at IC. Interobserver variability for the analysis of the same trials was relatively small. The system was easy to use; analysis of one animal took about 25 min and could be performed by personnel not specifically trained in gait analysis. We took significant measures to reduce variability. Santos et al [16] reported that animal-to-animal variability might be caused by difference in speed. We controlled this by training the animals in the runway before filming and by filming the animals at the same time of day (with a 12-h light cycle, animals were found to be more active during the morning than later in the day). Trials were also selected based on a total duration of step cycle of 0.25-0.50 s. No significant correlations between speed and different ankle angles were found. Future technical refinements may further reduce variability. For instance, tattooed markers may reduce day-to-day variability. More accurate marker placement (e.g. by visualizing bony landmarks with radiography) may improve animal-to-animal variability. Higher camera recording speed may further reduce variability. The maximum angle at TO sometimes occurred between frames (Figure 1C). Finally, other factors such as weight of the animal and laboratory settings may influence results. Therefore, an age-matched control group should be included.

2D digital video ankle motion analysis was found to be a more sensitive method to assess function in the rat sciatic nerve model than the SFI. At the end of the experiment (6 weeks after sciatic nerve crush injury), the angle at MSt was still significantly different from that in sham-operated animals, whereas the SFI had returned to normal at 4 weeks after injury. This sensitivity to detect subtle deficit after nerve crush injury demonstrates that it can be used in longitudinal studies to assess subtle differences in recovery after experimental treatments. In addition, ankle motion analysis is not limited by exorotation, contractures, or autotomy, and it evaluates function of more proximally located muscles, which are reinnervated earlier than distal foot muscles.

The results after separate sciatic, tibial and peroneal nerve crush injury showed that 2D digital video ankle motion analysis can be used to detect subtle differences in plantar flexion and dorsiflexion. After sciatic crush, both the angle of maximum plantar flexion, and after peroneal crush only the angle of maximum dorsiflexion, confirming results by Yu et al. [18]. In addition, in our study, the maximum angle of dorsiflexion was increased after tibial crush, as was the maximum angle of plantar flexion after peroneal crush, as a result of the unopposed function of antagonistic muscles.

2D digital video ankle motion analysis is a reliable and sensitive method to assess function in the rat sciatic nerve model. It opens opportunities to evaluate subtle differences in peripheral nerve regeneration in experimental models with different paradigms.

REFERENCES:

1. Dellon, A.L. and S.E. Mackinnon, *Selection of the appropriate parameter to measure neural regeneration.* Ann Plast Surg, 1989. **23**(3): p. 197-202.
2. Shenaq, J.M., S.M. Shenaq, and M. Spira, *Reliability of sciatic function index in assessing nerve regeneration across a 1 cm gap.* Microsurgery, 1989. **10**(3): p. 214-9.
3. De Medinaceli, L., *Use of sciatic function index and walking track assessment.* Microsurgery, 1990. **11**: p. 191-192.
4. Kanaya, F., J.C. Firrell, and W.C. Breidenbach, *Sciatic function index, nerve conduction tests, muscle contraction, and axon morphometry as indicators of regeneration.* Plast Reconstr Surg, 1996. **98**(7): p. 1264-71, discussion 1272-4.
5. Mackinnon, S.E., *Sciatic function index, nerve conduction tests, muscle contraction, and axon morphometry as indicators of regeneration.* Plast Reconstr Surg, 1996. **98**: p. 1272-1274.
6. Munro, C.A., et al., *Lack of association between outcome measures of nerve regeneration.* Muscle Nerve, 1998. **21**(8): p. 1095-7.
7. Varejao, A.S., et al., *Functional evaluation of peripheral nerve regeneration in the rat: walking track analysis.* J Neurosci Methods, 2001. **108**(1): p. 1-9.

8. de Medinaceli, L., Freed, WJ, Wyatt, RJ, *An index of the functional condition of rat sciatic nerve based on measurements made from walking tracks.* Exp Neurol, 1982. **77**: p. 634-643.
9. Bain, J.R., S.E. Mackinnon, and D.A. Hunter, *Functional evaluation of complete sciatic, peroneal, and posterior tibial nerve lesions in the rat.* Plast Reconstr Surg, 1989. **83**(1): p. 129-38.
10. Dellon, A.L. and S.E. Mackinnon, *Sciatic nerve regeneration in the rat. Validity of walking track assessment in the presence of chronic contractures.* Microsurgery, 1989. **10**(3): p. 220-5.
11. Weber, R.A., et al., *Autotomy and the sciatic functional index.* Microsurgery, 1993. **14**(5): p. 323-7.
12. Dijkstra, J.R., et al., *Methods to evaluate functional nerve recovery in adult rats: walking track analysis, video analysis and the withdrawal reflex.* J Neurosci Methods, 2000. **96**(2): p. 89-96.
13. Walker, J.L., et al., *Enhancement of functional recovery following a crush lesion to the rat sciatic nerve by exposure to pulsed electromagnetic fields.* Exp Neurol, 1994. **125**(2): p. 302-5.
14. Bervar, M., *Video analysis of standing--an alternative footprint analysis to assess functional loss following injury to the rat sciatic nerve.* J Neurosci Methods, 2000. **102**(2): p. 109-16.
15. Smit, X., et al., *Static footprint analysis: a time-saving functional evaluation of nerve repair in rats.* Scand J Plast Reconstr Surg Hand Surg, 2004. **38**(6): p. 321-5.
16. Santos, P.M., S.L. Williams, and S.S. Thomas, *Neuromuscular evaluation using rat gait analysis.* J Neurosci Methods, 1995. **61**(1-2): p. 79-84.
17. Lin, F.M., et al., *Ankle stance angle: a functional index for the evaluation of sciatic nerve recovery after complete transection.* J Reconstr Microsurg, 1996. **12**(3): p. 173-7.
18. Yu, P., et al., *Gait analysis in rats with peripheral nerve injury.* Muscle Nerve, 2001. **24**(2): p. 231-9.
19. Varejao, A.S., et al., *Motion of the foot and ankle during the stance phase in rats.* Muscle Nerve, 2002. **26**(5): p. 630-5.
20. Kaufman, K.R., W.J. Shaughnessy, and J.H. Noseworthy, *Use of motion analysis for quantifying movement disorders.* Adv Neurol, 2001. **87**: p. 71-81.
21. Bland, J.M. and D.G. Altman, *Statistical methods for assessing agreement between two methods of clinical measurement.* Lancet, 1986. **1**(8476): p. 307-10.
22. Strasberg, S.R., et al., *Wire mesh as a post-operative physiotherapy assistive device following peripheral nerve graft repair in the rat.* J Peripher Nerv Syst, 1996. **1**(1): p. 73-6.

CHAPTER 4

Misdirection of regenerating motor axons after nerve injury and repair in the rat sciatic nerve model

Godard C.W. de Ruiter [1,2,3], Martijn J.A. Malessy [3], Awad O Alaid [1], Robert J. Spinner [2], JaNean K Engelstad [4], Eric J. Sorenson [5], Kenton R. Kaufman [6], Peter J. Dyck [4], Anthony J. Windebank [1]

[1] Laboratory for Molecular Neuroscience, Mayo Clinic, Rochester MN, USA
[2] Department of Neurologic Surgery, Mayo Clinic Rochester MN, USA
[3] Department of Neurosurgery, Leiden University Medical Center, the Netherlands
[4] Laboratory for Peripheral Nerve Research, Mayo Clinic, Rochester MN, USA
[5] Department of Clinical Neurophysiology, Mayo Clinic, Rochester MN, USA
[6] Laboratory for Motion analysis, Mayo Clinic, Rochester MN, USA

Published in Experimental Neurology
2008, Volume 211(2); 339-350

ABSTRACT

Background Misdirection of regenerating axons is one of the factors that can explain the poor results often found after nerve injury and repair. Little is known however about the exact impact of misdirection. In this study, we quantified the degree of misdirection and the effect on recovery of function after different types of nerve injury and repair in the rat sciatic nerve model; crush injury, direct coaptation, and autologous nerve graft repair.

Methods Sequential tracing with retrograde labeling of the peroneal nerve before and 8 weeks after nerve injury and repair was performed to quantify the accuracy of motor axon regeneration. Digital video analysis of ankle motion was used to investigate the recovery of function. In addition, serial compound action potential recordings and nerve and muscle morphometry were performed.

Results In our study, accuracy of motor axon regeneration was found to be limited; only 71% (±4.9%) of the peroneal motoneurons were correctly directed 2 months after sciatic crush injury, 42% (±4.2%) after direct suture, and 25% (±6.6%) after autograft repair. Recovery of ankle motion was incomplete after all types of nerve injury and repair and demonstrated a disturbed balance of ankle plantar and dorsiflexion. The number of motoneurons from which axons had regenerated was not significantly different from normal. The number of myelinated axons was significantly increased distal to the site of injury.

Conclusion Misdirection of regenerating motor axons is a major factor in the poor recovery of nerves that innervate different muscles. The results of this study can be used as basis for developing new nerve repair techniques that may improve accuracy of regeneration.

INTRODUCTION

Functional results after nerve injury and repair are often disappointing [1]. Several factors that influence the results of regeneration have been identified, including the type of injury (sharp or blunt trauma or traction), location of the injury, time between the injury and surgery [2, 3], and the age of the patient. Misdirection of regenerating axons is also a factor that may explain poor functional recovery [4]. After repair of motor nerves, misdirection may lead to cocontraction of muscles or synkinesis. After repair of a sensory nerve, misdirection may lead to disturbed sensory function even years after the injury [5].

Misdirection has been investigated experimentally with different tools and techniques, including Y-shaped tubes [6, 7], selective muscle contraction measurements [8, 9], and compound muscle action potentials [10]. Different retrograde tracing techniques have also been used to investigate the accuracy of motor and sensory regeneration, including single labeling [11-13], simultaneous double labeling [14-16] and sequential double labeling [17, 18], and recently, a new technique that uses mice

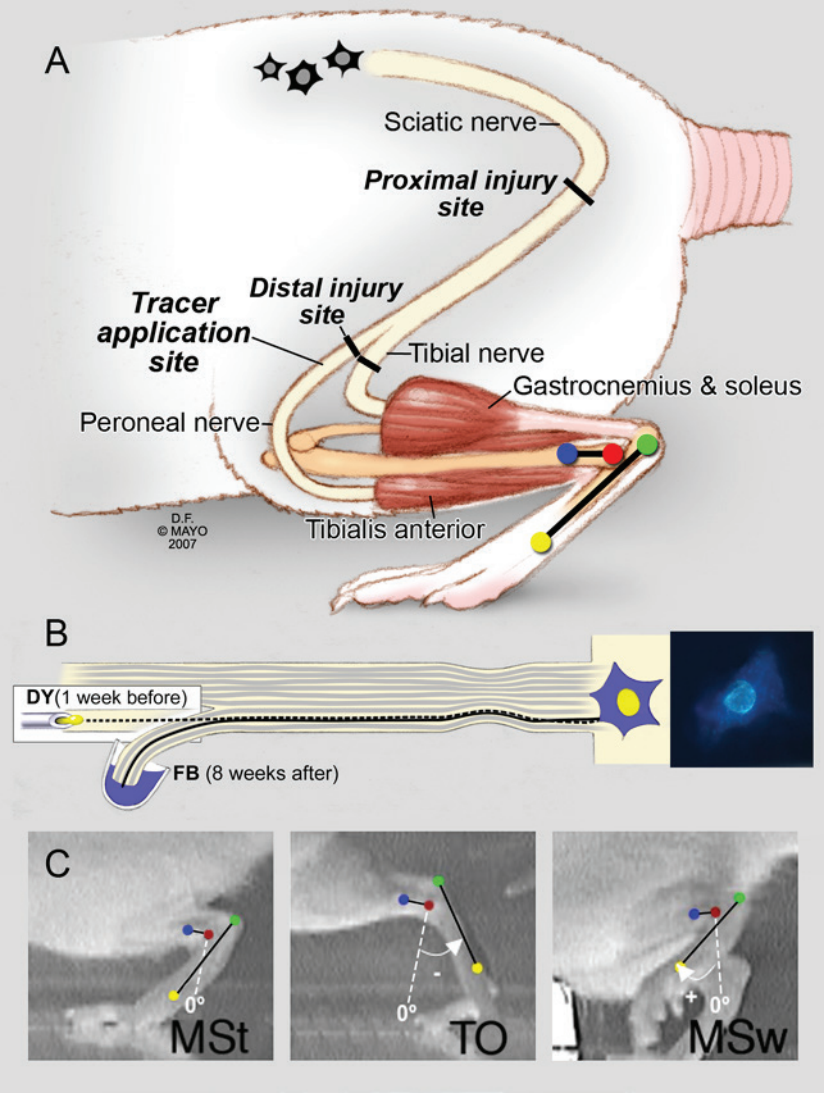

Figure 1

A, The rat sciatic nerve model with distal tibial and peroneal nerve branches that respectively innervate the gastrocnemic-soleus and anterior tibial muscles for ankle plantar and dorsiflexion. The proximal site of injury for all types of nerve injury and repair, the distal site of injury for autograft repair, and the site of tracer application are shown. B, Sequential retrograde tracing technique with injection of the first tracer (diamidino yellow [DY] into the peroneal nerve 1 week before nerve injury and the second tracer (fast blue [FB]) 8 weeks after nerve injury and repair. C, 2D digital video analysis of the ankle angles at midstance (MSt), toe-off (TO), and midswing (MSw), reported in degrees from neutral position, with plantar flexion being negative and dorsiflexion being positive.

with a fluorescent marker in a subset of their axons, has been introduced [19, 20]. The results of these studies all suggest that accuracy of regeneration is limited. However, little is known about the extent of misdirection and the effect on the recovery of function, especially in the repair of motor nerves innervating different distal target muscles. This becomes of more interest as new repair techniques that may more accurately guide regeneration become available (e.g. selective nerve growth factors and nerve guides with a more complex microarchitecture).

In this study we investigated misdirection in the rat sciatic nerve model after different types of nerve injury; crush injury vs transection injury, and repair techniques; direct coaptation vs autograft repair (in clinical practice, direct coaptation repair is always attempted first in case of a transection injury; in case a nerve graft is needed to bridge a defect, the autograft is still the gold standard of repair). Two recently introduced methods were used to evaluate results: sequential retrograde tracing [21-24] and digital video ankle motion analysis [25] (**Chapter 3**). Sequential retrograde tracing was performed to quantify the accuracy of motor axons for regeneration to the original target nerve (Figure 1). Ankle motion was analyzed to investigate the effect of misdirection on the recovery of function. Markers placed on the leg of the rat were automatically tracked for the change in ankle angle (Figure 1). Ankle motion analysis is sensitive in detecting differences in effect on ankle plantar flexion and dorsiflexion after separate sciatic, tibial, and peroneal nerve crush injuries [25]. Also, it is a more sensitive method than the sciatic function index, currently the standard method for assessment of function in the rat sciatic nerve model. In addition, compound muscle action potential (CMAP) recordings were made every other week, nerve and muscle morphometry were performed at the end of the experiment, and correlations between results of the different evaluation methods were investigated.

The results presented in this study can be used as a baseline for future experiments that focus on the improvement of regeneration after nerve injury and repair.

MATERIAL AND METHODS

Experimental groups

All animals (*n*=34), Sprague-Dawley rats (250-275 g), were randomly assigned to one of the experimental groups of crush injury, direct coaptation, or autograft repair. In the sequential tracing experiment, 4 animals per group were used. In 4 animals, the efficacy of the tracing method was determined on the contralateral side. In the motion analysis experiment, 5 animals per group were used and normal ankle motion was analyzed in 3 control animals. CAMP recordings and nerve and muscle morphometry were performed in the animals used in the motion analysis experiment (except for the control values that were obtained from a different experiment, **Chapter 7** [26]). All procedures were approved by the Institutional Ani-

mal Care and Use Committee and performed according to the animal care guidelines of the Mayo Foundation.

Surgical procedures and post-operative care

Animals were anesthetized by intraperitoneal injection of a mixture of 80 mg/kg ketamine and 2.5mg/kg xylazine. The sciatic nerve was exposed through a dorsal gluteal-splitting approach with the aid of a Zeiss operating microscope. The nerve was either crushed by applying maximal force with a smooth forceps for 5 seconds or transected with sharp microscissors 2mm distally from the white line formed by the fascia of the paraspinal muscles. The transection injury was repaired immediately with 4 10-0 monofilament sutures (Ethicon, Inc, Somerville, New Jersey). For the autograft repair, in addition to the proximal transection injury site, a second transection injury site was made 1 cm distally by transection of the tibial and peroneal branches (Figure 1A). Both injury sites were repaired microsurgically. For the distal repair site, the tibial and peroneal nerves were repaired separately with 4 and 2 10-0 sutures, respectively. The wound was closed in layers. Buprenorphine hydrochloride (Reckitt Benckiser Healthcare, Slough, United Kingdom) was administered subcutaneously just before and 12 hours after the repair for prevention of pain. During follow-up period, animals were housed separately in cages, with a 12-hour light-dark cycle. Water and food were available *ad libitum*. The hindlimbs that were operated on were sprayed daily with Chewguard (Butler Corporation, Greensboro, North Carolina) to prevent autotomy. A wire mesh was placed inside the cages for cage exercise enrichment and to prevent contractures [27]. In addition, manual physiotherapy (by passively moving the ankle) was performed once a week.

Sequential retrograde tracing

One week before injury, 1µl of 5% diamidino yellow (DY) solution (EMS-Chemie, GRoß-Umstadt, Germany) was injected, with a 25-gauge needle attached to a scaled Hamilton syringe, into the peroneal nerve (15 mm from the intended injury site) (Figure 1B). Eight weeks after injury, the peroneal nerve was transected proximal to the injection site of DY tracer, and the proximal end was placed in 1.5µl of 5% fast blue (FB) solution (EMS-Chemie) for 30 min. After the application of FB, the nerve stump was cleaned with 0.9% saline and sutured into surrounding fat tissue to prevent leakage of the tracer. (The method of preventing tracer leakage was validated in normal animals, after which no double-labeled profiles were found). The same procedures and time intervals were used to determine the labeling efficiency in control animals. Six days after application of FB tracer, the animals were perfused with phosphate-buffered saline (PBS) and 4% paraformaldehyde in 10% sucrose solution. Spinal cord segments L1-6 were removed and post-fixed overnight in a solution of 15% sucrose in PBS. Tissue was embedded in Tissue Freezing medium (TFM; TBS, Durham, North Carolina) and stored at -80ºC until sectioning.

Longitudinal 30-μm-thick sections were cut on a cryostat at -20 ºC. Slides were evaluated immediately with a fluorescent microscope (Axioplan 2, Carl Zeiss, Inc. Oberkochen, Germany) with a DAPI filter set (360/400-nm band-pass excitation filter, 440 nm long-pass emission filter, and 400-nm dichroic beam splitter) at x20 magnification with a Plan Apochromat 20x/0.75 objective (Carl Zeiss, Inc). Neuronal profiles were counted in every section by an observer blinded to the experimental groups. Only profiles with a visible nucleus were counted. Profiles with blue cytoplasm and dark nuclei were counted as FB-labeled cells, and those with yellow nuclei and dark cytoplasm as DY-labeled cells. Profiles with blue cytoplasm and yellow nuclei were counted as double-labeled FB-DY cells (Figure 1). No corrections were made for lost caps of motoneuron nuclei or double counting of split motoneuron nuclei. The total number of regenerated profiles was calculated by adding the number of single FB-labeled and double FB-DY-labeled profiles. The percentage correctly directed peroneal motoneurons was calculated by dividing the number of double-labeled profiles by the total number of DY-labeled profiles (single- and double-labeled DY). Labeling efficiency was determined from the percentage double labeling in normal animals. Spinal distributions of profiles (rostrocaudal and anteroposterior) were microscopically analyzed in all sections.

2D digital video ankle motion analysis

Ankle motion was analyzed 1 week after nerve injury and repair every other week starting 2 weeks after sciatic nerve crush injury and 4 weeks after direct coaptation and autograft repair. For the analysis of ankle motion, rats were briefly anesthetized with isoflurane inhalation (Abbott Animal Health, North Chicago, Illinois). The left leg was shaved. Black dot markers (Sharpie, Sanford Manufacturing, Chicago, Illinois) were placed on bony landmarks of the tibia, lateral malleolus, calcaneus, and fifth metatarsal to create a 2D biomechanical model of the ankle (Figure 1). For detailed description of ankle motion analysis see **Chapter 3**.

In short: Animals were placed in a transparent runway (120cm long, 12cm wide, 30cm high) and filmed using a 60-Hz digital camera (Dinion ^{XF} CCD Camera; Bosch Security Systems) that was positioned on a tripod 1 m perpendicular to the runway. Rats were trained to walk inside the runway by shifting a black box from one end to the other. Trials of the rat running from the right to the left side were selected because of the presence of 1 complete step cycle and a total duration of the step cycle of 0.25 to 0.50 s. After filming, the digital videos were processed using motion analysis software (Vicon Peak, Centennial, Colorado) that automatically tracks the markers on the leg of the rat in each frame of the video. The data were filtered with a Butterworth filter set at 6 Hz recorded with Vicon software. The results of ankle motion after crush injury, direct coaptation, and autograft repair were compared for the value of the ankle angle at different moments during the step cycle: midstance (MSt), the moment the right foot in the air crosses the left foot in the stance (that bears the weight); toe off (TO), the moment the left foot comes off the runway (in normal animals, the moment of maximum plantar

flexion); and midswing (MSw), the moment the left foot crosses the right foot in the stance (in normal animals, the moment of maximum dorsiflexion). Data for the ankle angles were reported in degrees from the neutral position of the ankle angel (the plantar surface of the foot perpendicular to the tibia, with dorsiflexion being positive and plantar flexion being negative (Figure 1C).

Compound muscle action potential recording

After the animals were filmed, they were (again) briefly anesthetized with ketamine and xylazine. CMAPs were recorded in the tibial- and peroneal nerve-innervated foot muscles using a Nicolet Viking IV EMG machine (Viasys NeuroCare, Madison, Wisconsin). Fine needle electrodes were placed in the injured/operated leg of the rat; recording electrodes were placed directly posterior to the tibia, with approximately 5 mm between the distal cathode and proximal anode. The simulating electrodes were adjusted locally to produce maximal CMAP amplitude. The stimulus was increased incrementally to produce a supramaximal response.

Nerve morphometry

At the end of the follow-up period (16 weeks), the sciatic nerve was reexposed and fixed in situ with 2.5% glutaraldehyde in PBS for 30 min [28]. A 1-mm nerve segment was transected/selected 2 mm distal to the site of injury. The nerve specimen was immersed (immediately) in glutaraldehyde overnight and postfixed in 1% osmium tetroxide and embedded in spur resin. Semithin (1 μm) sections were cut on a ultramicrotome with a glass knife and stained with 1% *p*-phenylenediamine. Sections were analyzed with the imaging system for nerve morphometry [28] for the total number of myelinated fibers/nerve, mean size and size distribution of myelinated fibers, and mean myelin thickness [28].

Muscle morphometry

For analysis of the total muscle fiber surface area and mean muscle fiber size after nerve injury and repair, the soleus muscle was resected from the left limb and imbedded in tissue freezing medium (TBS) using isopentane and liquid nitrogen. Transverse 10-μm-thick sections were cut on a cryostat (at -20 °C) from the midbelly of the muscle and were stained for myofibrillar ATPase (at pH 9.4) according to the method described by Brooke and Kaiser [29], which stains slow (type I) fibers light and fast (type II) fibers dark. The total muscle fiber surface area (without areas of fibrosis or vessels) was determined with the KS400 system (Zeiss, Version 3.0) [30]. The number of type I and type II fibers was counted in every section. The mean muscle fiber size was calculated from the muscle fiber surface area and the total number of muscle fibers.

Statistical Analysis

All results are reported as the mean ± SD, unless stated otherwise. The 2-tailed Student *t* test was used for comparisons between 2 groups, with the assumption

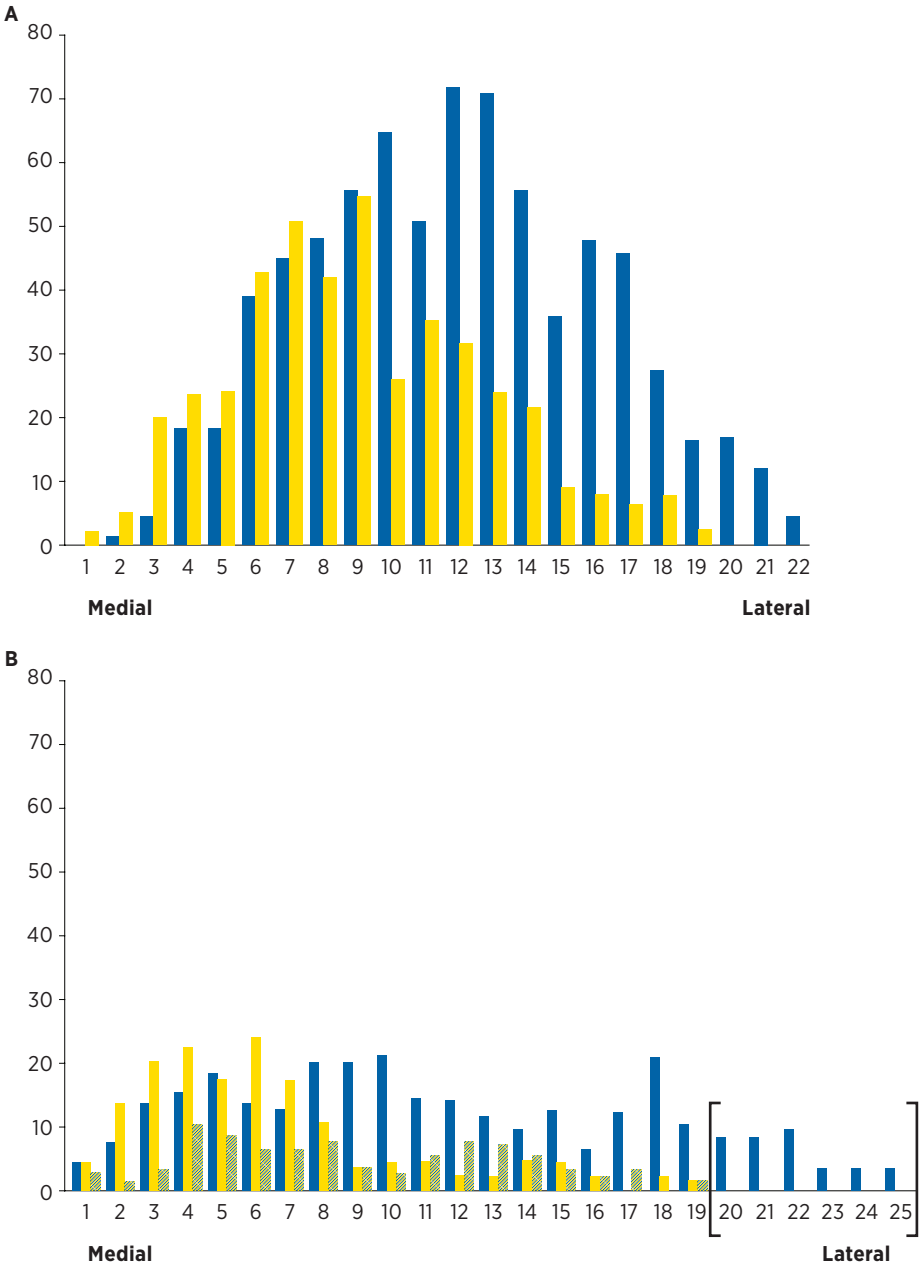

Figure 2

Distribution of differently labeled profiles (diamidino yellow [DY], fast blue [FB], and FB-DY) for the number of profiles per longitudinal section taken from medial to lateral through the anterior horn. A, Normal distribution of tibial (blue) and peroneal (yellow) motoneurons after simultaneous tracing, with FB and DY application tot the tibial and peroneal nerve branches, respectively. B, Distribution of profiles labeled by sequential tracing 8 weeks after autograft repair. In this case there were no signs of reuptake of persistent DY tracer because no double-labeled profiles were found in the area of the anterior horn normally exclusively occupied by tibial motoneurons (indicated by brackets, compare to A).

Table 1

Comparison of single-labeled FB and DY and double-Labeled FB-DY profiles in normal animals, and after crush injury, direct coaptation, and autograft repair

	profiles, mean no. ± SD				labeling efficacy, mean % (±SD)	percentage of correctly directed profiles,† mean % (±SD)
group*	FB	DY	FB-DY	Total		
normal	12 ± 13	25 ± 10	389 ± 49	427 ± 54	91.3 (±2.4)	..
crush injury	95 ± 115	120 ± 79	281 ± 36	376 ± 69	..	71.4 (±4.9)
direct coaptation repair	92 ± 54	338 ± 48	250 ± 73	342 ± 92	..	42.0 (±4.2)
autograft repair	99 ± 14	230 ± 74	73 ± 8	372 ± 17	..	25.1 (±6.6)

DY, diamidino yellow; FB, fast blue.

*each group included 4 animals.

†The percentage of correctly directed profiles was calculated for the total number of double-labeled (FB-DY) profiles divided by the total number of DY-labeled profiles: FB–DY/(FB–DY + DY).

that the data were normally distributed. Repeated measures ANOVA was used for comparison of 3 or more groups.

Linear correlations (Pearson) were investigated between the mean percentages of correctly directed peroneal motoneurons and the mean ankle angles at 8 and 16 weeks after crush injury, direct coaptation, and autograft repair. Linear correlations were also investigated between the mean quantitative results of regeneration and the mean ankle angle at 16 weeks.

RESULTS

Sequential retrograde tracing

The distribution of retrogradely labeled profiles within the anterior horn of the spinal cord after sequential tracing of the peroneal nerve was changed after nerve injury and repair compared with the normal distribution of peroneal motoneurons in control animals; single-labeled FB profiles were also present or found in an area that normally is occupied exclusively by tibial motoneurons, suggesting misdirection of regenerating axons originating from the tibial motoneuron pool into the peroneal nerve branch (Figure 2). This area was also used to exclude extreme cases of DY tracer reuptake; the presence of double-labeled FB-DY profiles in this area would indicate re-uptake of persistent DY tracer by misdirected axons from the tibial motoneurons. In no case were double labeled FB-DY profiles found in this area.

The number of FB, DY, and FB-DY profiles counted after crush injury, direct coaptation repair, and autograft repair is listed in Table 1. The number of single-labeled

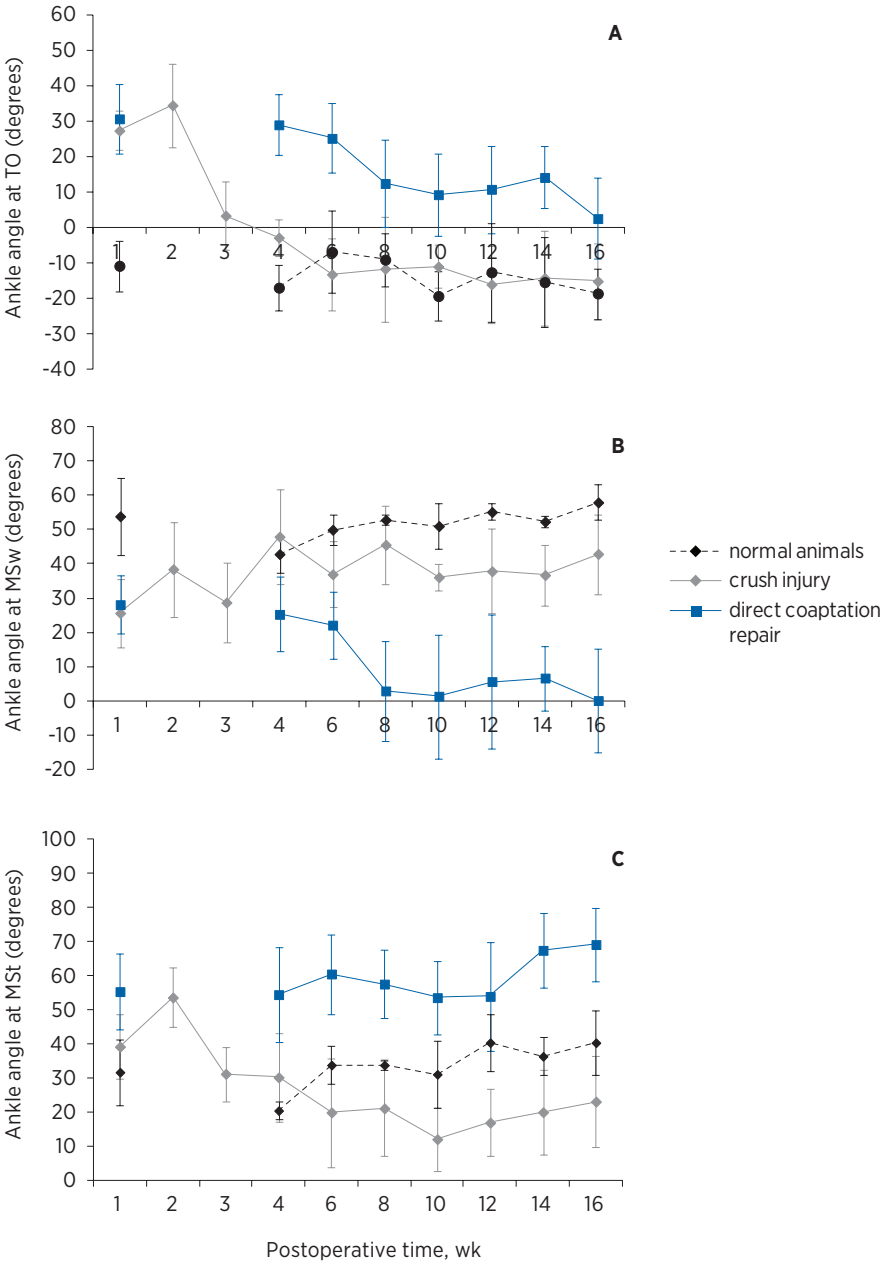

Figure 3

Recovery of ankle angles at toe-off (TO) (A), midswing (MSw) (B), and midstance (MSt) (C) after sciatic nerve crush injury and direct coaptation repair. REsutls for the recovery of ankle angles after autograft repair are not shown because these were not different from the results after direct coaptation repair except the results were more variable after autograft repair (larger SD).

FB profiles represents the total number of tibial motoneurons from which axons had regenerated to the peroneal nerve after injury and repair. Correction for incomplete labeling of peroneal motoneurons by the first DY injection was not necessary because of the high labeling efficacy in normal animals (91% ± 2.4%) The number of single-labeled DY profiles represents the total number of peroneal motoneurons from which axons had regenerated to the tibial nerve branch. No corrections were made for inclusion of nonregenerated peroneal motoneurons because of the high number of profiles from which axons had regenerated to the peroneal nerve: crush injury (401 ± 227), direct suture (342 ± 92) and autograft repair (372 ± 17) (numbers not significantly different from the normal number of peroneal profiles (427 ± 54, ANOVA, P=0.36). The number of double-labeled FB-DY profiles represents the number of correctly directed peroneal motoneurons. Thus, the percentages of correctly directed peroneal motoneurons, calculated for the number of correctly directed profiles (FB-DY) divided by the total number of profiles that was labeled before injury with DY (DY and FB-DY), were 71% ± 4.9% after crush injury, 42% ± 4.2% after direct coaptation repair, and 25% ± 6.6% after autograft repair (P<0.001).

An interesting difference was found in the distribution of differently labeled profiles after crush injury versus transection injury and repair. After crush injury, single-labeled FB and double-labeled FB-DY profiles were more segregated, whereas after direct coaptation and autograft repair, profiles were all intermingled.

2D digital video ankle motion analysis

No contractures of the ankle were present after sciatic crush injury, direct coaptation, or autograft repair. Autotomy was not observed after sciatic crush injury but was seen in 1 animal after direct coaptation and in 2 animals after autograft repair. All ankle angles decreased after sciatic crush injury, direct coaptation, and autograft repair. The angle at TO showed decreased plantar flexion (Figure 3A). The angle at MSw showed decreased dorsiflexion (Figure 3B). The angle at MSt showed decreased ability to support the body weight (Figure 3C).

After sciatic crush injury all angles had recovered to normal values 4 weeks after injury (TO, P=0.45; MSw, P=0.27; MSt, P=0.26). However, after that, the angles at MSt and MSw showed increased plantar flexion compared with normal (P=0.47 and 0.04, respectively, at 14 weeks (Figure 3B and C), but not quite significant at 16 weeks, P=0.09 and P=0.08).

Recovery of the different ankle angles after direct coaptation and autograft repair was incomplete. At the end of the experiment (16 weeks) the angles at TO, MSw, and MSt were still significantly different from normal (direct coaptation repair: TO, P=0.04; MSw, P=0.007; MSt, P=0.25; autograft repair: TO, P=0.01; MSw, P=0.08; MSt, P=0.002). The best recovery was observed for the angle at TO (Figure 3A). Sixteen weeks after direct coaptation repair, the angle had recovered to about 67% of normal (angle TO in normal animals, -15.0°; 1 week after direct coaptation repair, 30°; and 16 weeks after repair, 0°; P=0.003). For the angle at TO, recovery after

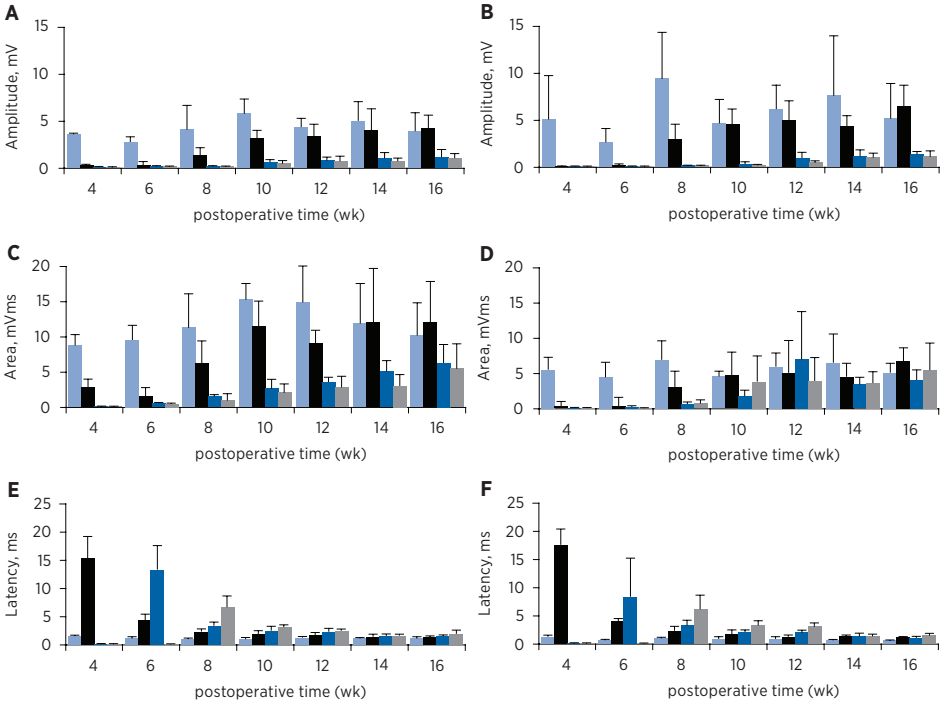

Figure 4

Recovery of compound muscle action potential (CMAP) amplitude (A,B), area (C,D), and latency (E,F) in the plantar (A,C,E) and dorsal foot muscles (B,D,F). Light blue, results for normal animals; black bars, results after crush injury; dark blue bars, results after direct coaptation repair; gray bars, results after autograft repair.

autograft repair was poor (27%; angle at 16 weeks, 17.5°) and not significantly different from that after 1 week (P=0.25).

The angle at MSw decreased further after direct coaptation and autograft repair (Figure 3B); 8 weeks after direct coaptation repair, the angle had decreased even more (-0.83°) compared with the angle 1 week after transection of the nerve (24.7°, P=0.047). Also 8 weeks after autograft repair, the angle had decreased further (17.8°, compared with 28.9° after 1 week), but not significantly (P=0.42). After 8 weeks, the angle at MSt did not change; 16 weeks after direct coaptation repair, the angle (-2.83°) was still significantly different from that at 1 week (P=0.04).

The angle at MSt did not recover significantly over time (Figure 3C): 16 weeks after direct coaptation and autograft repair, the angles (68.6° and 62.3°, respectively) were not significantly different from the angles after 1 week (56.8° and 57.1°, P=0.07 and 0.32)

Compound muscle action potentials

No CMAPs were recorded in the plantar and dorsal foot muscles 1 week after sciatic crush injury, direct coaptation, and autograft repair (Figure 4). The first CMAPs were recorded 4 week after sciatic nerve crush injury and 6 weeks after direct coaptation and autograft repair. The CMAP amplitude in the plantar foot muscles had recovered y 12 weeks after sciatic crush injury (P=0.02 at 10 weeks and P=0.28 at 12 weeks) (Figure 4A). After direct coaptation and autograft repair, CMAP amplitude recovered only slightly, and at the end of the experiment (at 16 weeks) it was still significantly different from that of normal animals (P=0.02 and 0.002, respectively). Similar results were found for CMAP amplitudes recorded in dorsal foot muscles (Figure 4B) and the CMAP areas (Figure 4C and D). The CMAP latency (Figure 4E and F) was increased compared with normal after all types of injury and repair. It decreased again to normal values 12 weeks after sciatic crush injury and 14 weeks after direct coaptation repair (although at the end of the experiment, there still small differences after all types of nerve injury and repair compared with results in normal animals).

Nerve morphometry

After crush injury, the number of myelinated fibers was increased slightly compared with normal (Table 2), but they were also smaller and less myelinated (Figure 5). After direct coaptation and autograft repair, there were more myelinated fibers than after crush injury (direct coaptation repair, P=0.02, but not significantly after autograft repair, P=0.68). These myelinated fibers were also smaller (P<0.001 for crush injury and autograft repair) and less myelinated (although not significantly, P=0.08, and 0.49, respectively).

Table 2

Results for nerve morphometry

	distal to the injury or repair site, mean±SD			
group*	**fascicle area, mm²**	**no. of MF/ fascicle**	**mean MF diameter, mm**	**myelin thickness, mm**
normal†	0.73 ± 0.09	7,650 ± 464	8.02 ± 0.46	1.20 ± 0.09
crush injury	0.486 ± 0.03	9,642 ± 1,184	4.971 ± 0.323	0.737 ± 0.154
direct coaptation repair	0.472 ± 0.051	13,079 ± 1,166	3.729 ± 0.189	0.591 ± 0.056
autograft repair	0.601 ± 0.332	10,058 ± 1,725	3.816 ± 0.199	0.672 ± 0.103

MF, myelinated fiber.

*all groups contained 5 animals.

† results for normal animals are also presented in **Chapter 7**

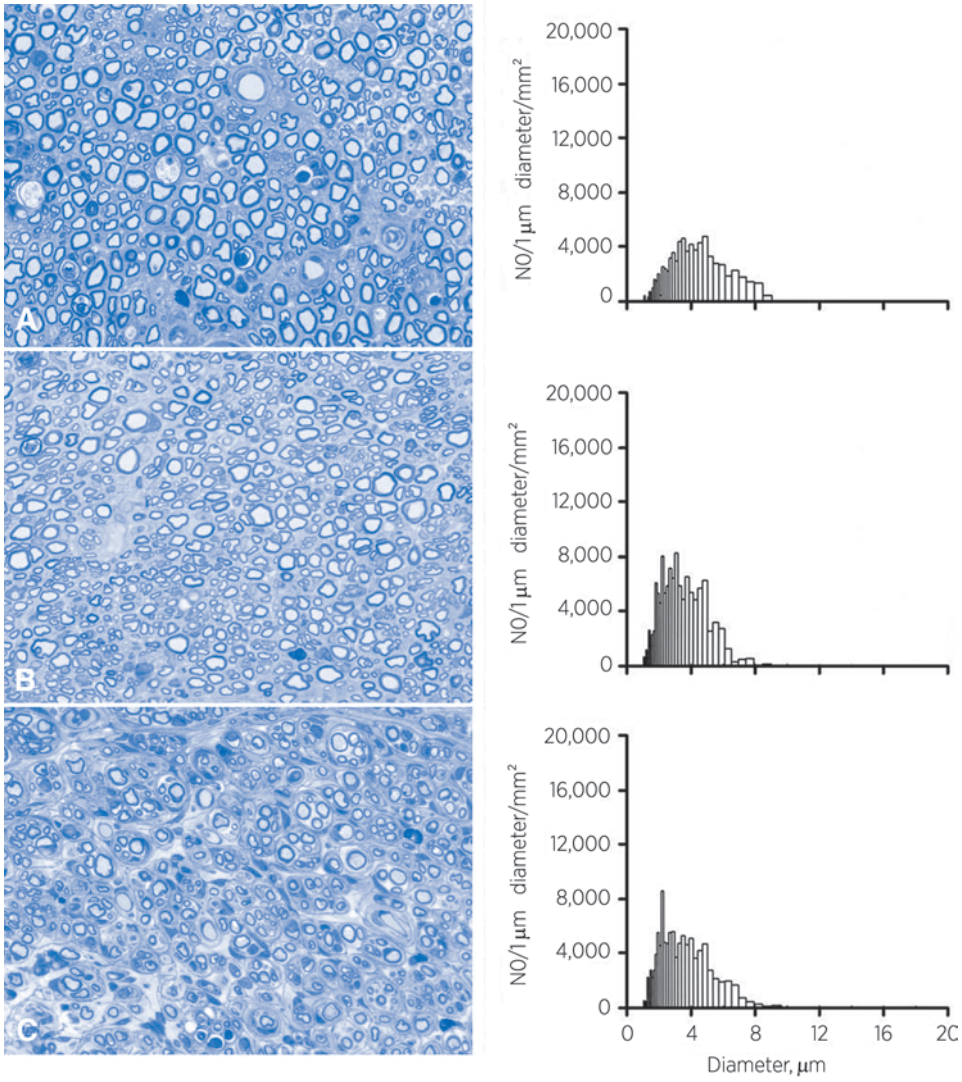

Figure 5
Size distribution of myelinated fibers (MF) after crush injury (A), direct coaptation (B), and autograft repair (C).

Muscle morphometry

After crush injury, the total muscle fiber surface area and mean muscle fiber size were slightly decreased compared with normal (Table 3). After direct coaptation and autograft repair, the total muscle fiber surface area and mean muscle fiber size were even smaller than after crush injury, although not significantly ($P>0.05$ for both comparisons). The number of muscle fibers was similar to the normal number after all types of nerve injury and repair. The distribution of type I and type II fibers, however, had changed after direct coaptation and autograft repair

from predominantly type I in normal soleus muscles to more type II than type I in reinnervated soleus muscles.

Correlations

There were no significant correlations between the percentages of correctly directed peroneal motoneurons and the ankle angles after crush injury, direct coaptation, and autograft repair at 8 weeks (TO, P=0.05; MSw, P=0.49; MSt, P=0.51) or at 16 weeks (TO, P=0.09; MSw, P=0.62; MSt, P=0.33). Also, there were no significant correlations between the quantitative results of regeneration and the ankle angles at 16 weeks (Table 4), except for the mean myelinated diameter and the angle at MSt (r=0.9970 and P=0.0495) and the mean myelin thickness and the angle at MSw (r=0.9999 and P=0.007).

DISCUSSION

To improve functional results for patients with nerve injuries, it is important to investigate different factors that may contribute to recovery. One of these factors includes the number of axons that regenerate. Another important factor is the degree to which the original pathways are restored. In our study, the number of motoneurons whose axons had regenerated to the peroneal nerve after crush injury, direct coaptation, and autograft repair was not significantly different from the normal number of peroneal motoneurons. The number of myelinated fibers was increased after all type of nerve injury and repair. Although other factors (eg, time to reinnervation and quality of the axon) also have to be considered, our study of sequential tracing and ankle motion analysis shows that misdirection of regenerating axons is an important factor that may limit results after nerve injury and repair.

Accuracy of motor axons regeneration

The percentages of correctly directed peroneal motoneurons showed that the accuracy of motor axon regeneration is limited: only 71.4% of the peroneal motoneurons were correctly directed 2 months after the crush injury, 42.0% after direct coaptation repair, and 25.1% after autograft repair. These percentages of correct direction were surprisingly low.

The percentage after crush injury (71%) was low considering that clinical recovery after crush injury is often complete [1]. Also experimentally, scores for the sciatic function index return to normal 4 weeks after a crush injury [31]. This complete recovery of function after crush injury has been explained by guidance of regenerating axons through their original basal lamina tubes [19, 32]. Thus, in our study, misdirection may have been caused damage to the basal lamina tubes by the applied crush technique [33, Varejao, 2004 #143]. Others, however, have also found indications for the presence of some misdirection after crush injury [17, 19, 34].

The percentages after direct coaptation (42.0%) and autograft repair (25%) were low even after maximal attempt to correct fascicular alignment. On the basis of the size of the peroneal motoneuron pool (31% of the rat sciatic nerve [35]) this suggests that regeneration after transection of the nerve occurs at random. Although this finding supports earlier studies that indicated that reinnervation of muscles is nonspecific [7, 8, 11, 36-38] some studies have reported specificity [6, 10, 24]. This discrepancy among different studies may be explained by several factors, including the size of the nerve and technical factors, as discussed below. The mechanism for misdirection, even with correct fascicular alignment, may be explained by dispersion of regenerating axons at the coaptation site, as demonstrated earlier by Ramón y Cajal (1928) (Figure 2A, **Chapter 2**) [39]. Witzel et al. [20] recently confirmed this finding using mice with a fluorescent marker in a subset of their axons and showed that regenerating axons have access to more than 100 basal lamina tubes.

Finally, the lowest percentage of correctly directed peroneal motoneurons after autograft repair can be explained by criss-crossing of regenerating axons at the distal tibial and peroneal coaptation sites, as recently demonstrated by Lutz [40].

Although these percentages provide insight to the accuracy of regeneration after nerve injury and repair and can be used as a baseline for further experiments, additional factors must be considered in the interpretation of the results. First, the size of the nerve must be considered. Puigdellivol-Sanchez et al. [24] recently found a much higher percentage of correctly directed tibial motoneurons (87%), using the same sequential tracing technique, animal model, and time points of evaluation as in our study. The difference (with 42% correctly directed peroneal motoneurons in our study) can be explained at least partly by the relatively larger size of the tibial nerve [35]. Using simultaneous tracing of the tibial (FB) and peroneal (DY) nerves, we found that the sciatic nerve consists of about 61% tibial motoneurons and 39% peroneal motoneurons [26].

Second the time point of evaluation must be considered. Pruning may later correct for misdirection [14, 15]. However, the relative importance of this mechanism in the repair of motor nerves that innervate different muscles has not been determined (see below). Third, the percentages of correctly directed motoneurons may also differ depending on the animal model and age of the animal [41].

Fourth, factors concerning the sequential tracing technique must be considered. We used a technique that was introduced by Puigdellivol-Sanchez et al. [21]. This technique has a high labeling efficiency (91% after 8 weeks in our study) and does not cause marked damage to the nerve; also, there is no significant fading of the first tracer (DY) or blockage of uptake of the second one (FB) [21, 23]. However, a potential problem of the technique might be persistence of DY tracer at the injection site, resulting in an overestimation of the percentage correct direction. Puigdellivol-Sanchez et al. [22] estimated that the last accounts for about 17% of the DY labeling after 8 weeks. Review of their data demonstrated that this was in part due to 1 outlier. After exclusion of this outlier, the percentage decreased to 6%. We grossly determined persistence of DY tracer by examining the distribution of

double-labeled profiles in an area of the anterior horn that is normally occupied exclusively by tibial motoneurons (Figure 2) and found no sign of persistence of tracer.

Another potential problem of this sequential tracing technique is that no distinction can be made between profiles only labeled by the second tracer (FB) as a result of misdirection of tibial axons versus correctly directed peroneal motoneurons not labeled by the first tracer (DY). The technique also cannot distinguish between profiles only labeled by the first tracer (DY) as a result of misdirection of peroneal axons vs peroneal motoneurons that had not regenerated. This was not a problem in our study because of the high labeling efficiency and high total number of regenerated profiles after all types of injury and repair, but is must be considered, for example, in the analysis of repair techniques with lower numbers of regenerated motoneurons. A third tracer applied simultaneously with the second tracer to the tibial nerve branch might solve this problem. Finally, it must be noted that in this study we used an ideal autograft (mixed nerve and size-matched). Results may be different for clinical repair of motor nerves with multiple sensory sural nerve grafts [42].

Recovery of function

Ankle motion analysis showed that misdirection may have an effect on recovery of function. After all 3 types of nerve injury and repair, the balance of ankle plantar and dorsiflexion was disturbed. Two months after crush injury, the angles of plantar flexion at MSt and MSw were increased, confirming previous results of Varejao et al. [43]. After direct coaptation and autograft repair, the maximum angle of dorsiflexion at MSw was decreased further compared with the angle 1 week after transection of the nerve (Figure 3B). This disturbed balance of plantar and dorsiflexion can be explained by the random regeneration of tibial and peroneal motoneurons resulting in a much higher percentage of correctly directed tibial motoneurons than of correctly directed peroneal motoneurons. The tibial motoneuron pool, as mentioned above, is significantly larger than the peroneal motoneuron pool. This random regeneration may even lead to more regenerated tibial than peroneal motoneurons into the peroneal nerve and, thus, to active plantar flexion during the swing phase. However, this was not investigated in our study with simultaneous CMAP recordings.

Ankle motion analysis also showed there probably is little adaptation for misdirected motoneurons; the angle at MSw did not change significantly from 8 to 16 weeks after direct coaptation repair, and at 16 weeks, the angle was still significantly decreased compared with the angle at 1 week after nerve transection. However, a longer period of follow-up may be needed [44]. A mechanism to later correct for misdirection might be initial polyinnervation of muscles by axonal branches from the same motoneuron, followed by pruning of misdirected axon collaterals [44, 45]. This mechanism would also explain the increased number of myelinated fibers after nerve injury and repair that has been found to subsequently decrease

to normal values after 1 year [46]. However, the percentage of motoneurons with multiple projections to different muscles after sciatic nerve injury and repair is low (5.6% 90 days after autograft repair [47]); thus the effect of this mechanism on the recovery of function is questionable.

Another mechanism that may later correct for misdirection is central adaptation. The role of this mechanism after injury and repair remains to be defined. Of note, we found that after sciatic nerve crush injury different labeled profiles were more organized in the anterior horn than they were after direct coaptation and autograft repair. This may have contributed to better functional recovery after crush injury. For example, central adaptation might be better for groups of motoneurons from which axons were misdirected to the same nerve branch than for intermingled motoneurons with correct and incorrect projections. This could also explain the closer to normal distribution of type I and type II muscle fibers after sciatic crush injury compared with more type II than type I fibers after direct coaptation and autograft repair.

Aside from accuracy of regeneration, other factors also contribute to the recovery of function after nerve injury and repair. In our study, CMAPs were recorded earlier after crush injury than after direct coaptation and autograft repair, probably as a result of staggered axonal regeneration across the coaptation site. A shorter period of denervation leads to better muscle [2] and functional recovery. Furthermore, myelinated fibers were smaller and less myelinated after direct coaptation and autograft repair than after crush injury (Figure 5). This combined effect of different factors on the recovery of function can explain that no significant correlations were found in our study between the percentages of correctly directed peroneal motoneurons and the different ankle angles. Nevertheless, this study demonstrates that misdirection of regenerating axons (in addition to the degree of regeneration) is a significant factor that can explain the poor outcome after nerve injury and repair. The results of this study can be used as the baseline for the evaluation of new techniques of nerve repair that may improve the accuracy of regeneration- for example, for nerve tubes with a more advance microarchitecture (multichannel nerve tube)- and the selective application of nerve growth factors.

ACKNOWLEDGEMENTS

We thank LouAnn Gross for her advice on embedding and staining techniques, Tony Koch for his excellent animal care, and Jane Meyer for her secretarial assistance.

REFERENCES

1. Sunderland, S., Nerve injuries and their repair: A critical appraisal. 1991, Melbourne: Churchill Livingstone.
2. Fu, S.Y. and T. Gordon, Contributing factors to poor functional recovery after delayed nerve repair: prolonged denervation. J Neurosci, 1995. 15(5 Pt 2): p. 3886-95.
3. Fu, S.Y. and T. Gordon, Contributing factors to poor functional recovery after delayed nerve repair: prolonged axotomy. J Neurosci, 1995. 15(5 Pt 2): p. 3876-85.
4. Brushart, T., The mechanical and humoral control of specificity in nerve repair. Operative nerve repair and reconstruction. 1991, Philadelphia: J.B. Lippincott. 215-230.
5. Dyck, P.J., et al., Assessment of nerve regeneration and adaptation after median nerve reconnection and digital neurovascular flap transfer. Neurology, 1988. 38(10): p. 1586-91.
6. Politis, M.J., Specificity in mammalian peripheral nerve regeneration at the level of the nerve trunk. Brain Res, 1985. 328(2): p. 271-6.
7. Abernethy, D.A., A. Rud, and P.K. Thomas, Neurotropic influence of the distal stump of transected peripheral nerve on axonal regeneration: absence of topographic specificity in adult nerve. J Anat, 1992. 180 (Pt 3): p. 395-400.
8. Bernstein, J.J. and L. Guth, Nonselectivity in establishment of neuromuscular connections following nerve regeneration in the rat. Exp Neurol, 1961. 4: p. 262-75.
9. Zhao, Q., et al., Specificity of muscle reinnervation following repair of the \ transected sciatic nerve. A comparative study of different repair techniques in the rat. J Hand Surg [Br], 1992. 17(3): p. 257-61.
10. Evans, P.J., et al., Selective reinnervation: a comparison of recovery following microsuture and conduit nerve repair. Brain Res, 1991. 559(2): p. 315-21.
11. Brushart TM, M.M., Alteration in connections between muscle and anterior horn motoneurons after peripheral nerve repair. Science, 1980. 208(9): p. 603-605.
12. Aldskogius, H., et al., Specific and nonspecific regeneration of motor axons after sciatic nerve injury and repair in the rat. J Neurol Sci, 1987. 80(2-3): p. 249-57.
13. Aldskogius, H. and L. Thomander, Selective reinnervation of somatotopically appropriate muscles after facial nerve transection and regeneration in the neonatal rat. Brain Res, 1986. 375(1): p. 126-34.
14. Brushart, T.M., Preferential reinnervation of motor nerves by regenerating motor axons. J Neurosci, 1988. 8(3): p. 1026-31.
15. Brushart, T.M., Motor axons preferentially reinnervate motor pathways. J Neurosci, 1993. 13(6): p. 2730-8.
16. Madison, R.D., S.J. Archibald, and T.M. Brushart, Reinnervation accuracy of the rat femoral nerve by motor and sensory neurons. J Neurosci, 1996. 16(18): p. 5698-703.
17. Bodine-Fowler, S.C., et al., Inaccurate projection of rat soleus motoneurons: a comparison of nerve repair

techniques. Muscle Nerve, 1997. 20(1): p. 29-37.
18. Rende, M., et al., Accuracy of reinnervation by peripheral nerve axons regenerating across a 10-mm gap within an impermeable chamber. Exp Neurol, 1991. 111(3): p. 332-9.
19. Nguyen, Q.T., J.R. Sanes, and J.W. Lichtman, Pre-existing pathways promote precise projection patterns. Nat Neurosci, 2002. 5(9): p. 861-7.
20. Witzel, C., C. Rohde, and T.M. Brushart, Pathway sampling by regenerating peripheral axons. J Comp Neurol, 2005. 485(3): p. 183-90.
21. Puigdellivol-Sanchez, A., et al., Fast blue and diamidino yellow as retrograde tracers in peripheral nerves: efficacy of combined nerve injection and capsule application to transected nerves in the adult rat. J Neurosci Methods, 2000. 95(2): p. 103-10.
22. Puigdellivol-Sanchez, A., et al., Persistence of tracer in the application site--a potential confounding factor in nerve regeneration studies. J Neurosci Methods, 2003. 127(1): p. 105-10.
23. Puigdellivol-Sanchez, A., et al., On the use of fast blue, fluoro-gold and diamidino yellow for retrograde tracing after peripheral nerve injury: uptake, fading, dye interactions, and toxicity. J Neurosci Methods, 2002. 115(2): p. 115-27.
24. Puigdellivol-Sanchez, A., A. Prats-Galino, and C. Molander, Estimations of topographically correct regeneration to nerve branches and skin after peripheral nerve injury and repair. Brain Res, 2006.
25. de Ruiter, G.C., et al., Two-dimensional digital video ankle motion analysis for assessment of function in the rat sciatic nerve model. J Peripher Nerv Syst, 2007. 12(3): p. 216-22.
26. de Ruiter, G.C., et al., Accuracy of motor axon regeneration across autograft, single-lumen, and multichannel poly(lactic-co-glycolic acid) nerve tubes. Neurosurgery, 2008. 63(1): p. 144-53; discussion 153-5.
27. Strasberg, S.R., et al., Wire mesh as a post-operative physiotherapy assistive device following peripheral nerve graft repair in the rat. J Peripher Nerv Syst, 1996. 1(1): p. 73-6.
28. Dyck, P.J., D. P.J.B., and J.K. Engelstad, Pathologic alterations of nerves. Peripheral Neuropathy, ed. D. P. and T. P.K. Vol. 1. 2005, Philadelphia: Elsevier. 733-829.
29. Brooke, M.H. and K.K. Kaiser, Some comments on the histochemical characeterization of muscle adenosine triphosphate. J Histoechem Cytochem, 1969. 17: p. 431-432.
30. Vleggeert-Lankamp, C.L., et al., Type grouping in skeletal muscles after experimental reinnervation: another explanation. Eur J Neurosci, 2005. 21(5): p. 1249-56.
31. Hare, G.M., et al., Walking track analysis: a long-term assessment of peripheral nerve recovery. Plast Reconstr Surg, 1992. 89(2): p. 251-8.
32. de Medinaceli, L., Functional consequences of experimental nerve lesions: effects of reinnervation blend. Exp Neurol, 1988. 100(1): p. 166-78.
33. Beer, G.M., J. Steurer, and V.E. Meyer, Standardizing nerve crushes with a non-serrated clamp. J Reconstr Microsurg, 2001. 17(7): p. 531-4.
34. Swett, J.E., C.Z. Hong, and P.G. Miller, All peroneal motoneurons of the rat survive crush injury but some fail to

reinnervate their original targets. J Comp Neurol, 1991. 304(2): p. 234-52.
35. Swett, J.E., et al., Motoneurons of the rat sciatic nerve. Exp Neurol, 1986. 93(1): p. 227-52.
36. Gillespie, M.J., T. Gordon, and P.R. Murphy, Reinnervation of the lateral gastrocnemius and soleus muscles in the rat by their common nerve. J Physiol, 1986. 372: p. 485-500.
37. Miledi, R. and E. Stefani, Non-selective re-innervation of slow and fast muscle fibres in the rat. Nature, 1969. 222(193): p. 569-71.
38. Weiss, P. and A. Taylor, Further experimental evidence against "neurotropism" in nerve regeneration. J. Exp. Zool., 1944. 95: p. 233-257.
39. Cajal, S., Degeneration and regeneration of the nervous system. London: Oxford University Press, 1928.
40. Lutz, B.S., The role of a barrier between two nerve fascicles in adjacency after transection and repair of a peripheral nerve trunk. Neurol Res, 2004. 26(4): p. 363-70.
41. Robinson, G.A. and R.D. Madison, Developmentally regulated changes in femoral nerve regeneration in the mouse and rat. Exp Neurol, 2006. 197(2): p. 341-6.
42. Sulaiman, O.A., et al., Chronic Schwann cell denervation and the presence of a sensory nerve reduce motor axonal regeneration. Exp Neurol, 2002. 176(2): p. 342-54.
43. Varejao, A.S., et al., Ankle kinematics to evaluate functional recovery in crushed rat sciatic nerve. Muscle Nerve, 2003. 27(6): p. 706-14.
44. Hennig, R. and E. Dietrichs, Transient reinnervation of antagonistic muscles by the same motoneuron. Exp Neurol, 1994. 130(2): p. 331-6.
45. Gorio, A., et al., Muscle reinnervation--II. Sprouting, synapse formation and repression. Neuroscience, 1983. 8(3): p. 403-16.
46. Mackinnon, S.E., A.L. Dellon, and J.P. O'Brien, Changes in nerve fiber numbers distal to a nerve repair in the rat sciatic nerve model. Muscle Nerve, 1991. 14(11): p. 1116-22.
47. Valero-Cabre, A., et al., Superior muscle reinnervation after autologous nerve graft or poly-L-lactide-epsilon-caprolactone (PLC) tube implantation in comparison to silicone tube repair. J Neurosci Res, 2001. 63(2): p. 214-23.

PART
TWO

GUIDANCE OF MOTOR AXON REGENERATION

CHAPTER 5

Review of the experimental and clinical literature on nerve tubes for peripheral nerve repair

Godard C.W. de Ruiter [1], Robert J. Spinner [2], Michael J. Yaszemski [3], Anthony J. Windebank [4] Martijn J.A. Malessy [1]

[1] Department of Neurosurgery, Leiden University Medical Center, the Netherlands
[2] Department of Neurologic Surgery, Mayo Clinic Rochester MN, USA
[3] Laboratory for Biomedical Engineering. Mayo Clinic Rochester MN, USA
[4] Laboratory for Molecular Neuroscience, Mayo Clinic Rochester MN, USA

Parts of this review were published in:

Nerve tubes for peripheral nerve repair
Neurosurgery Clinics of North America,
January 2009, Vol 20 (1): 91-105

Designing ideal conduits for peripheral nerve repair
Neurosurgical Focus, 2009, 26(2): E5

INTRODUCTION

At this moment, the gold standard for repair of nerve defects that cannot be directly restored without tension to the nerve ends still is the autologous nerve graft (figure 1A). Most commonly the sural nerve is used, taken from the leg of the patient. Obviously, repair with autografts has several disadvantages, such as the need for an extra incision, limited availability, mismatch in size of the damaged nerve and the donor nerve, and the chance for the development of a painful neuroma. Because of these disadvantages various alternatives have been developed for autograft repair, for instance repair with autogenous venous grafts [1], nerve allografts [2, 3], and nerve tubes, guides or conduits. Practical advantages of nerve tubes are the unlimited right off-the-shelf availability in different sizes that match the damaged nerve (figure 1B). Besides, functional recovery is often reduced after autograft repair compared with direct coaptation repair. Possible explanation for this is that axons need to cross 2 coaptation sites, which might decrease both the number of axons reaching the distal targets and lead to increased misdirection of regenerating axons [4]. An ideal alternative therefore will also lead to improved regeneration and functional results of nerve repair. In this review we give an overview of both the experimental and clinical data present on nerve tubes for peripheral nerve repair. In addition, different modifications to the common hollow or single lumen nerve tube are discussed that may improve the results of regeneration, including collagen/laminin-containing gels, internal frameworks, supportive cells, growth factors, and conductive polymers.

DEVELOPMENT OF NERVE TUBES

The concept of nerve tube repair

The first attempts of nerve tube repair date back to the end of the 19th century (for review see table 1 article by Weiss [5]). The results of these first attempts were disappointing and later viewed by Sunderland as only of historical interest [6]. The concept of the nerve tube was reintroduced in the 1980s, mainly as a tool to investigate the process of regeneration. In the beginning, mostly silicone tubes were used. Later, nerve tubes of also other synthetic non-biodegradable [7-11] and biodegradable materials (including polymers of glycolic acid [12], lactic acid [12, 13] and caprolactone) were developed. These first experiments with silicone nerve tubes by Lundborg et al. demonstrated that axons can successfully regenerate across a 1-cm gap in the rat sciatic nerve model [14]. No regeneration was observed in the absence of the distal nerve stump and across 15-mm defects. This was later explained by the accumulation of neurotrophic factors in the silicone chamber that probably only act over limited distance (neurotropism or chemotaxis). Another explanation might be that the formation of a fibrin matrix (Figure 2), which is essential in the process of regeneration [15], does not occur if the gap is too long [16].

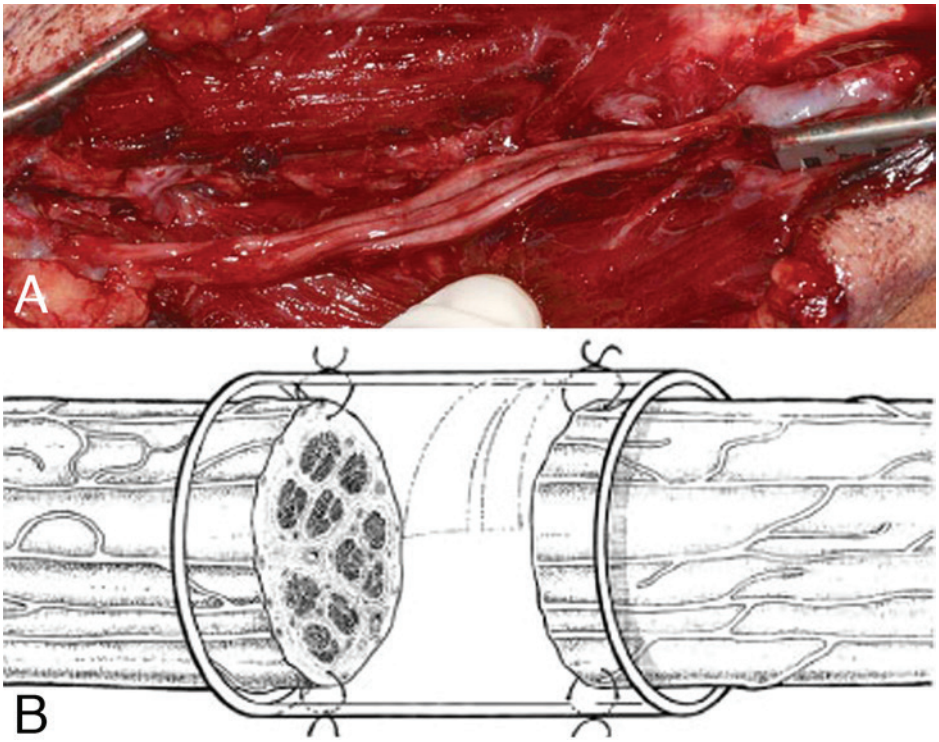

Figure 1

A: Repair of a radial nerve lesion (after a humerus fracture) with autologous sural nerve grafts.

B: Nerve tube repair. *From* Lundborg, G. A 25-year perspective of peripheral nerve surgery: evolving neuroscientific concepts and clinical significance. The Journal of Hand Surgery [Am] 2000; 25 (3): 391-414

Physical characteristics of the nerve tube

Other physical properties, including the dimensions of the nerve tube, prefiling with phosphate buffered saline (PBS) [17], and porosity [16] have also been shown to affect the formation of the fibrin matrix. Jenq and Coggeshall found that the addition of holes to silicone nerve tubes increased both the number of myelinated axons and the length of the gap that could be bridged [18, 19]. Possible explanations were that by adding holes, cells (for example macrophages and leucocytes) and molecules (for example fibrin and fibronectin) involved in the formation of the fibrin matrix could enter the site of regeneration. The importance of the permeability of the nerve tube was later confirmed in other experiments [20-24], although it still remains questionable what exactly is the ideal pore size (microporous or macroporous). Disadvantages of macropores might be that neurotrophic factors can diffuse out of the nerve tube and that the fibrin matrix might be disorganized (orientation perpendicular to the pores instead of longitudinal). It is important to note that permeability not only depends on pore size, but may also be affected by

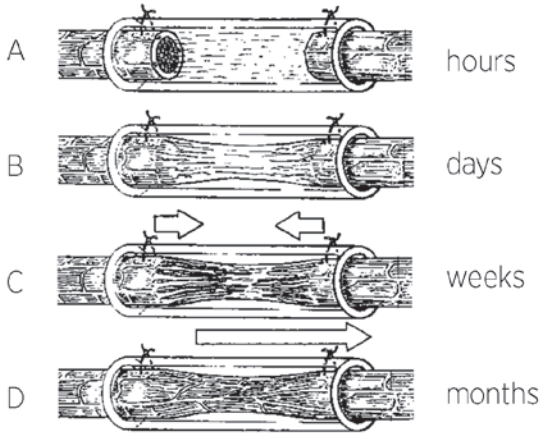

Figure 2
The different phases in the process of regeneration across the nerve tube. A: within hours after implantation the lumen fills with fluid containing neurotrophic factors and various inflammatory cells. B: within days a fibrin matrix is formed between the nerve stumps. C: in weeks Schwann cells, fibroblasts and microvessels migrate along the fibrin matrix from both proximal and distal nerve ends. D: in months axons regenerate from the proximal nerve stump into the matrix. *From* Dahlin and Lundborg. Use of tubes in peripheral nerve repair. Neurosurg Clin N Am 2001; 12 (2): 341 – 352

for example hydrophilic properties of the material. Next to porosity, the surface texture and dimensions of the nerve tube have been found to affect the formation of the fibrin matrix [8]; with smooth surfaces (for example in silicone nerve tubes) the longitudinal matrix coalesces and forms a free floating nerve cable, while with rough surfaces the tissue disperses and completely fills the lumen of the nerve tube [25].

With the potential use of nerve tubes for clinical nerve repair, especially biodegradable nerve tubes, other physical characteristics were also investigated, including swelling and degradation properties. Swelling of a nerve tube might primarily block the lumen for regeneration or secondarily lead to compression of the regenerated nerve. Degradation may cause swelling by the accumulation of degradation products that increase the osmotic value of the nerve tube [26, 27]. Besides, degradation products might be toxic or interfere with the process of regeneration. Degradation may also affect the porosity and tensile properties of the nerve tube. These tensile properties are important because a nerve tube should be flexible for implantation into mobile limbs, but at the same time the nerve tube should be resistant to deformation (elongation, breaking or kinking) and strong enough to hold a suture. Transparency is preferred for suturing and accurate positioning of the nerve stumps. In the end, nerve tubes must be sterilizable without compromising the physical properties mentioned above. In table 1 we have summarized the known physical properties of some of the frequently used nerve tubes. It must be

noted that physical properties of the nerve tube not only depend on the biomaterial, but also on other factors such as the dimensions of the nerve tube and fabrication technique. Not all nerve tubes that are now available for clinical use have been characterized extensively *in vitro* before clinical application.

Evaluation methods and animal models

Different evaluation methods and animal models have been used to investigate the process of regeneration across nerve tubes. Most experiments have been performed in the rat sciatic nerve model. Commonly used evaluation methods in this model include electrophysiology, nerve morphometry, and walking track analysis. The first most important observation however is the percentage successful regeneration across the nerve tube. Failures have been reported due to collaps, swelling, and suture pullout [12, 28-30]. The second most important observation is the quantity of regeneration across the nerve tube. This is mostly determined for the number of axons (myelinated and/or unmyelinated) at the middle part and/or distal to the nerve tube and is then preferably compared to both the numbers in normal nerve and after autograft repair. The numbers of axons that have been reported in the literature however differ [31]. Sometimes only the density of nerve fibers in a specified area is provided [32, 33] (table 1). This area may not be representative of the total cross-sectional area of the nerve. The total number of axons also is not the best parameter to quantify regeneration, because this number is increased early in the process of regeneration due to collateral sprouting or branching, and has been found to decrease later [34]. Different factors may stimulate the sprouting or branching of axons, for example the addition of Schwann cells [35-37] or neurotrophic factors (see part modified nerve tubes). Numbers may increase without an actual increase in the number of motoneurons and dorsal root ganglion cells from which axons have regenerated across the nerve tube. Quantification of regeneration across the nerve tube can therefore best be performed in our opinion with retrograde tracing to determine these numbers [38]. This technique with fluorescent dyes that are retrogradely transported to the motoneuron or dorsal root ganglion can also be used to analyze the accuracy of regeneration across the nerve tube. For example, different tracers can be applied sequentially to the same nerve branch before and after nerve repair to determine the direction of regenerating axons or simultaneously to different nerve branches (for instance the tibial and peroneal nerves) to determine the dispersion of regenerating axons across the nerve tube [39]. Although nerve tube repair is often suggested to lead to an improved orientation of regenerating nerve fibers, only a few studies have actually investigated the accuracy of regeneration across the nerve tube [38, 40-43]. These studies did not show an improved accuracy after nerve tube repair compared with direct coaptation or autograft repair. Brushart et al. found that regenerating axons might disperse across the tube and that this dispersion increases with gap length [44]. This dispersion of regenerating axons might lead to (1) misdirection of regenerating axons or (2) polyinnervation of different targets by axons originating from

Table 1
Experimental data

Nerve tube					Model			Evaluation		
Material	Permeability	Flexibility	Degradation	Swelling	Animal	Nerve	gap size	methods	control	follow-up
Natural										
collagen[1-3]	diffusion of molecules up to 215 Å			3x dry weight	monkeys	median	4, 5 mm	electrophysiology, number of axons	reversed autograft	up to 760 ds
					rats	sciatic	4 mm	electrophysiology	and normal, direct coaptation, and negative controls	4 and 12 wks
Synthetic										
Nonbiodegradable										
silicone [4]					rat	sciatic	6, 10, 15, 20 mm	nerve histology	absence distal nerve stump	1 mo
Biodegradable										
polyglycolic acid[5]					monkeys	ulnar	3 cm	electrophysiology, nerve fiber density	sural nerve grafts	1 yr
poly(L-lactic acid) [6]	83.5%, 12.1μm *1	*2 80 MPa, 1.0 MPa, 0.02 mm/mm	Mn 43% at 8 weeks		rats	sciatic	1 cm	SFI, gastrocnemius muscle weight, nerve fiber density	reversed isograft	16 wks
poly(DL-lactic co-glyclic acid) [7], 75:25	83%, 20μm *1	*2 8 MPa, 0.95 MPa, 0.02 mm/mm	Mn 38% at 8 weeks							

poly(L-lactide-co-6-caprolactone) [8, 9], 50:50	low and high *3	*4 3 MPa, 25 MPa, 490%	Mn 50% at 10 months		mice	sciatic	6 mm	electrophysiology, sweating tests, percentages successful reinnervation, number of axons	silicone Teflon, collagen, polysulfone	4, 5 mo
					rats	sciatic	8 mm	electrophysiology, simultaneous retrograde tracing, SFI	normal, autograft, silicone	90 ds
poly(DL-lactide-ε-caprolactone)[10-12], 50:50 (DL 85:15)		*5 2.5MPa	45% mass loss at 8 mo	300% vol increase at 3 mo	rats	sciatic	1 cm [11] 15mm [12]	nerve fiber density electrophysiology, video analysis	reversed autograft	10 wks 5 mo

* 1 porosity and mean pore size, measured by mercury porosimetry 7
* 2 modulus, tensile strength, and tensile strain 7, also tested during degradation in phosphate buffered saline (PBS) at 37ºC for up to 8 weeks
* 3 low prepared with fine powder of amylose (<10μm), high with glucose of around 10μm, permeability tested with UV spectrscopy
* 4 elasticity modulus, tensile strength, and percent elongation
* 5 tensile strength, rapid loss after 3 weeks 10

Abbreviations: ds =days, Mn = average molecular weight, mo = months, SFI = sciatic function index from walking track analysis (paper-paint or ink method), vol = volume, wks = weeks, yr = year

the same neuron. This compared to autograft repair that contains more regenerating branched axons inside the basal lamina tubes [45].

Functional analysis eventually is the most important method for translating results of nerve tube repair into patients. This type of analysis has not been frequently included in the evaluation of nerve tube repair. The reason for this might be that the most commonly used method, the sciatic function index (SFI), that is based on footprint analysis [46, 47], lacks sensitivity. This might be caused by contractures [48] and autotomy [49], but also because the SFI evaluates the distal foot muscles that often don't recover because of the prolonged time of denervation [50]. We developed a novel evaluation method, called 2D motion analysis, that can be used to measure recovery of more proximally located muscles from the ankle angles of maximum plantar and dorsiflexion during the stance and swing phases (**Chapter 3**). This method is more sensitive than the SFI and is currently being used by our laboratory for the functional analysis after different nerve repair techniques. Advantage of functional analysis in comparison to other evaluation methods also is that animals can be evaluated at multiple time points. Combined with electrophysiology this can provide insight in the time to reinnervation and recovery.

Electrophysiology is frequently included in the evaluation of results after nerve tube repair. Mostly compound muscle action potentials (CMAPs) are recorded and analyzed for the amplitude, area under the curve, or latency [31]. This method is not as time-consuming as most other evaluation methods, but it is important to note that it should not be used instead of functional evaluation. CMAP recovery after nerve repair may be relatively better than functional recovery due to distal sprouting that results in larger motor units, and due to misdirected axons that contribute to the CMAP, but probably not to recovery of function [51].

Different animal models have also been used for the analysis of nerve tube repair, including mice, rabbits, and monkeys (table 1). Disadvantage of this use of larger animal models is that it makes it difficult to compare the results between studies, especially for the extrapolation of the size of the nerve gap [52]. Obvious advantage of larger animals is the closer to human comparison, especially for the primate model. Both the polyglycolic acid (PGA) and collagen nerve tube (that are now available for clinical use, see below) have first been investigated experimentally in monkeys [33, 53, 54]. Dellon and Mackinnon in 1988 published the first study in which they compared repair of a 3-cm gap in the ulnar nerve (proximal to the elbow) in adult male *Macca cynomolgus* monkeys with sural nerve grafts, solid and mesh PGA tubes (8 repairs per group) [33]. After 1-year of follow-up nerve fiber densities did not differ from normal after the different repair techniques. Unfortunately, absolute numbers were not provided. Electromyography demonstrated recovery in 19 out of 28 (68%) of the intrinsic muscles studied in the solid and mesh tube groups (2 muscles per repair, 7 repairs per group). Recovery after autograft repair

was not reported because the Martin-Gruber anastomosis in this group had not been divided. Electromyography results were reported for 7 tube repairs, because in one case of solid tube repair there was no continuity (the reason for exclusion of one of the mesh tubes was not reported). In 3 out of 7 solid and 4 out of 8 mesh tubes some scar tissue was observed in the center of the tube. Later, the same authors published another study performed in monkeys, in which regeneration across 2 and 5-cm nerve gaps in radial sensory and ulnar nerves was compared for crimped and mesh glycolide trimethylene carbonate (Maxon) and collagen nerve tubes [55]. Poor regeneration was found across 5-cm nerve gaps.
Archibald et al. compared repair of 4 mm gaps with collagen nerve tubes and autografts (reversed segments) in rats (sciatic nerve) and *Macaca fasicularis* monkeys (median nerve, 2cm above the wrist) [53]. This study showed that collagen nerve tube repair was as effective as autograft repair in terms of physiological responses from target muscle and sensory nerves. Later they reported a second study on collagen nerve tube repair of 5-mm median nerve lesions (again 2cm above the wrist) in monkeys, which included 3 years of electrophysiologic assessment and nerve morphometry [54]. In this study a significantly increased number of axons distal to the repair site (1.2-2x) was found after both collagen nerve tube and autograft repair.

CLINICAL USE OF NERVE TUBES FOR PERIPHERAL NERVE REPAIR

Currently, various nerve tubes are available for clinical nerve repair: *Neurotube* (polyglycolic acid), *Neuragen* (collagen), *Neurolac* (polycaprolactone), *NeuroMatrix* and *Neuroflex* (both collagen), and *SaluBridge* (hydrogel, non-biodegradable) [57]. These nerve tubes are mainly used in the repair of small nerve gaps (<3cm) in small sensory nerves, such as digital nerve lesions, but they are also increasingly used in lesions of larger nerves [13]. In addition, recently a processed allograft (*Avance* from *AxoGen*) has become available for clinical use. Below we only discuss the results of the large series and randomized studies that have been reported on the clinical use of the silicone, polyglycolic acid (PGA), and poly(DL-lactide-e-caprolactone) (PLC) nerve tubes (summarized in table 2). In addition, series have been reported on the use of non-biodegradable polytetrafluoroethylene (PTFE) nerve tubes (Gore-Tex or Teflon) for median and ulnar nerve [56] and inferior alveolar/lingual nerve lesions[57, 58], a small series on the use of collagen (*Neuragen*) nerve tubes in the repair of obstetrical brachial plexus injuries [59], and a number of cases on the use of PGA nerve tubes (for the repair of the inferior alveolar nerve [60], medial plantar nerve [61], zygomatic and buccinatory branches of the facial nerve[62], the spinal accessory nerve [63], for nerve reconstruction after a hallux-to-thumb transfer [64], and for interfascicular median nerve repair with multiple PGA tubes [65]). Combinations of PGA tubes with collagen sponges [66, 67] and an interposed nerve segment [68] have also been used in patients, and a chitosan tube with internal oriented filaments of PGA [69] (see part modifications to the common hollow nerve tube).

Table 2
Clinical series and randomized controlled trials (RCT)

Nerve tube							Evaluation			
Material	First author (year)	Study type	Number(s)	Patient age (yrs)	Nerve(s), location	Gap size	Methods	Control	Interval	Follow-up period
Synthetic										
Nonbiodegradable										
Silicone	Lundborg (1997)	RCT	11 patients, 8 controls	12 – 72, mean 29	median and ulnar, <10cm proximal to wrist	3 – 4 mm	tactilometry for perception vibration, Semmes-Weinsteins monofilaments, s2PD and m2PD (Moberg's method), neuroma/ hyperesthesia,/ coldintolerance strength abduction dig I or II with intrinsicmeter	direct repair	no	1 year
	Lundborg (2004)	RCT	17 patients, 13 controls	12 – 72, mean 32		3 – 5 mm	Model Instrument for Outcome after Nerve Repair, neurophysiology			5 years

Biodegradable										
Polyglycolic acid	Mackinnon (1990)	series	15 patients, 16 repairs	30.5 (SD 7.6)	digital	0.5 – 3.0 cm, mean 1.7	s2PD and m2PD: excellent **: ≤6mm and ≤3mm good: 7-15mm and 4-7mm poor: ≥15mm and ≥7mm	no	none placed acutely	11 – 32 mo, mean 22.4
	Weber (2000)	RCMT	62 repairs, 74 controls	17 – 65, mean 35	digital, distal to wrist	7.0 mm *, control 4.3		gap <8 mm direct repair gap >8 mm nerve graft	50 <72 hrs 5 4-20 days 7 > 20 days	mean 9.4 mo, control 8.1
	Battiston (2005)	series	19	15 – 67, mean 40	digital	1.0 – 4.0 cm, mean 2.0	s2PD and m2PD, MRC, quick-DASH	muscle-vein combined conduits	primary - 16 months	6 – 74 mo, mean 30
poly(DL lactide-ε-caprolactone)	Bertleff (2005	RCMT	21, 13 controls	mean 43	digital, distal to wrist	up to 2.0 cm	s2PD and m2PD	direct repair	not provided	1 year

* a gap of 5 mm was left intentionally, even in defects of 0 - 4 mm

** in Weber study outcome was defined for the lower of the s2PD or m2PD, as defined in the study by Mackinnon and Dellon, except that excellent outcome was defined for m2PD ≤ 4 mm.

Abbreviations: s2PD and m2PD = static and moving two-point discrimination , MRC = strength for British Medical Research Council Scale, RCMT = randomized controlled multicenter trial, , quick-DASH (disabilities of the arm, shoulder, and hand), mo = months, EP = electrophysiology

Silicone nerve tubes

In 1997 Lundborg et al. published their first results with 1-year follow-up of a prospective randomized study, in which small defects (3-4 mm) after fresh and complete clean-cut transection of the ulnar and median nerves proximal to the wrist (up to 10 cm) were repaired with silicone nerve tubes (11 patients) or conventional microsurgical direct coaptation repair (8 patients) [70]. A number of tests were used to evaluate the results (table 2). In general, no significant differences were found between the two types of repair. Also for the 5-year follow-up (2004) no significant difference in outcome was found, except that there was significantly less cold intolerance after silicone nerve tube repair [71]. The use of silicone nerve tubes however has been heavily criticized [72, 73], mainly because of the potential late compression of the nerve by the non-biodegradable tube. Critics often refer to a study by Merle et al. [74], in which silicone tube (1 patient) and sheath repair (2 patients) resulted in chronic nerve compression. Later also a study by Braga-Silva was reported on silicone nerve tube repair of median and ulnar nerve lesions (up to 3cm) in which 7 out of 26 patients requested removal of the nerve tube because of local discomfort [75]. Dahlin and Lundborg themselves performed a re-exploration surgery in 7 patients, as an ethically permitted part of their prospective study (4 patients complained of local discomfort), but found no signs of neuroma and only a mild microscopic foreign body reaction in 2 cases [76]. After removal of the silicone nerve tube, there was no new impairment of nerve function. They emphasized that in their studies silicone nerve tubes were used with a diameter exceeding the diameter of the nerve by at least 30%. Nevertheless, they acknowledged that a biodegradable nerve tube would be better, provided that it degrades with minimal tissue reaction and without impairment of nerve regeneration [77].

Polyglycolic acid (PGA) nerve tubes

In 2000 Weber et al presented the results of the first multicenter randomized study on the repair of digital nerves with gaps up to 3cm using glycolic acid (PGA) nerve tubes. Ten years before that Mackinnon and Dellon had already presented a series of 15 patients in which they had also used polyglycolic acid (PGA) nerve tubes to repair digital nerve defects up to 3 cm [78]. In that study excellent results were reported for 5 patients (33%), good results for 8 patients (53%) and poor results for 2 patients (14%). In the randomized study by Weber et al., PGA nerve tube repair was compared with standard repair (direct coaptation for gaps <8 mm and nerve graft repair for gaps >8 mm). The overall results at 1-year follow-up showed no significant difference between the two groups with excellent and good outcome in respectively 44% and 30% of the repairs with PGA nerve tubes compared to 43% of both excellent and good outcome after standard repairs. The authors subsequently performed a subgroup analysis for different gap lengths (≤ 4 mm, 5 to 7 mm, and 8 mm to 3 cm) that demonstrated excellent results for gaps ≤ 4 mm for moving 2-point discrimination (m2PD) in 91% of PGA nerve tube repairs compared to 49% of standard repairs (p=0.02). As commented by Lund-

borg in the discussion on this article, the statistics of this study are difficult to interpret because of the heterogeneous data (for example different levels of injury and mechanisms of injury were included). Also, the numbers per group of PGA nerve tube and standard repair for subgroup analysis were not provided. It is not clear also why separate subgroup analysis was performed for gaps ≤4 mm. Although the authors mention that it is generally accepted that 4 mm is the maximum gap length for digital nerves to be repaired with minimal tension by the end-to-end method, in the standard repair group all gaps of 5-7mm were repaired by direct coaptation. In the 5-7mm gap group excellent results were obtained in only 17% of the PGA nerve tube repairs and 57% of the standard repairs (p=0.06). Noteworthy, the technique that was used to measure two-point discrimination that was not based on the Moberg approach [79] with application of very light pressure (just enough to blanch the skin), but with increasing pressure until the stimulus was perceived by the patient (see discussion by Lundborg).

Another large series on PGA nerve tube repairs of 19 digital nerves in 17 patients with gaps up to 4 cm was published in 2005 by Battiston et al.[80]. In this study very good results (S3+ and S4, defined for static 2-point discrimination (s2PD) up to 15 mm, were reported for 13 patients (76.5%) and good results in 3 patients (17.7%). Analysis of the data however shows that in only 2 patients S4 (s2PD 2–6 mm) was obtained and that there were no excellent results for m2PD (≤ 3 mm, by the definition used in the studies by Mackinnon [78] and Weber [81], see table 2), and good results were obtained (m2PD 4 – 7 mm) in only 4 out of 19 repairs.

In conclusion, PGA nerve tubes might lead to comparable results as conventional nerve repair in the repair of small gaps in digital nerve lesions, but care should be taken with the interpretation of the data and the wide application to the repair of other nerve lesions based on these results.

Poly(DL-lactide-ε-caprolactone) (PLC) nerve tubes

In 2003 Bertleff et al. presented the results of a multicenter trial in which digital nerve repair for gaps up to 2 cm was compared for polylactide caprolactone (PLC) nerve tube and standard repair, which were all direct coaptation repairs (with the finger flexed to reduce tension) [82]. Randomization was performed separately for gaps ≤ 4 mm, 4–8 mms, and 8–20 mms. Sensory recovery was evaluated at 3, 6, 9 and 12 months for the s2PD and m2PD measured with the Pressure-Specified Sensory Device [83]. There were no significant differences in two-point discrimination for PLC and direct coaptation repair of gaps up to 2 cm, but unfortunately results for subgroup analysis were not provided. The pressure, which was applied (to feel the stimulus), seemed larger in the PLC nerve tube repair group than in the direct repair group (figure 6, no statistics provided). More wound healing problems were observed after PLC nerve tube repair than after direct coaptation. In a recent review Meek et al. also commented that small fragments of biomaterial in

experiments with PLC nerve tubes were still found 24 months after implantation and that PLC nerve tubes are normally stiff and only flexible after putting in warm saline before implantation [84]. A more extensive report on the use of PLC nerve tubes (according to the authors) will soon be published [84]. So far there is ample evidence to support the clinical use of PLC tubes.

In conclusion, in our opinion at this moment care should be taken with the wide use of tubes in peripheral nerve repair, not only because of the concerns that are mentioned above, but also because of the following reasons. First, little is still known about the accuracy of regeneration across nerve tubes. In the repair of larger mixed or motor nerves dispersion of regenerating axons across the nerve tube may lead to misdirection and polyinnervation (see part on development of nerve tubes) and result in impaired functional recovery due to for example co-contraction or synkinesis. It must be noted also that in most experimental studies on nerve tube repair accuracy of regeneration and functional analysis were not included. Finally, it must be noted that not all nerve tubes that are now available for clinical use have been characterized extensively *in vitro* and that long-term effects of biodegradable nerve tubes have not (yet) been reported (table 2, follow-up studies 1-2 years).

MODIFICATIONS TO THE SINGLE LUMEN NERVE TUBE

Different modifications to the common hollow or single lumen nerve tube have been investigated to enhance regeneration and extend the gap that can be bridged (figure 3 on page 77). Pre-filling of the nerve tubes with phosphate buffered saline (PBS) and the addition of pores have already been mentioned in the section on the development of nerve tubes. Below we discuss the addition of different extracellular molecules (collagen and laminin), internal frameworks, supportive cells, and nerve growth factors.

Collagen and laminin containing gels

Collagen and laminin are involved in the process of regeneration by forming a substrate for the migration of nonneuronal cells. Filling of silicone nerve tubes with collagen and laminin-containing gels has been shown to increase both the rate of regeneration [11] and the gap that can be bridged (up to 15-20 mm) [85]. This effect however depends on several factors including the concentration [86] and the permeability of the nerve tube [87]. Alignment of the collagen (gravitational or magnetically) may also further enhance regeneration [88]. Currently, different collagen and laminin containing gels (for example BD Matrigel ™) are being used for the incorporation of supportive cells and growth factors [37, 89, 90]. Also, oligopeptides derived from lamini-integrin active sites (such as YIGSR, IKVAV and RGD) are being investigated for potential role in guidance of regenerating axons [91].

Internal framework

An internal framework may also enhance regeneration and increase the gap that can be bridged due to stabilization of the fibrin matrix that is formed inside the nerve tube. Different internal structures have been investigated including polyamide filaments [92], laminin-coated fibers [93], PGA filaments [94] and collagen sponges [93, 95]. The combinations PGA tube - collagen sponge and chitosan tube - PGA filaments have already been used clinically, although there is little information on the effect of these internal structures on the accuracy of regeneration. Different tissues have also been added to the nerve tube, for example interposed nerve segments [96] (the stepping-stone procedure) and denatured muscle [97]. In addition, nerve tubes with a modified microarchitecture have been developed. Yoshii et al. developed a scaffold of longitudinally orientated collagen filaments that has been shown to lead to successful regeneration across gaps of 20 mm [98] and even 30 mm in rats [99]. Another example of a modification to the common single lumen nerve tube structure is the multichannel nerve tube structure [27, 100-103]. This structure has several advantages: it provides more surface area for cell attachment and controlled-release of incorporated growth factors, and may reduce dispersion by containment of axonal branches as in the autografts consisting of multiple basal lamina tubes [39].

Supportive cells

The addition of Schwann cells to the nerve tube has also been found to enhance regeneration in small gaps [36, 37, 89] and to extend the gap that can be bridged to about 2 cm [35, 90], although remarkably, autograft repair in most of these studies still was found to be superior [37, 89, 90, 104, 105]. Schwann cells possibly stimulate regeneration by the production of a range of growth factors, extracellular molecules (laminin), and may play a mechanical role by forming a cable bridging the gap [37]. Schwann cells can also be genetically modified to overexpress certain growth factors and selectively guide different types of axons. A disadvantage of the addition of Schwann is that it still requires the explantation of a donor nerve, to isolate autologous Schwann cells weeks before reconstruction. This may be overcome in the future by the differentiation of for example bone marrow stem cells into Schwann cells [106].

Growth factors

The addition of different growth factors to the nerve tube, including nerve growth factor (NGF), glial cell derived neurotrophic factor (GDNF), brain-derived neurotrophic factor (BDNF), and fibroblast growth factor (FGF), has also been shown to enhance regeneration and increase the nerve gap that can be bridged (to 15 mm). Growth factors can be added directly to the tube (into a solution) [107] or can be released after absorption to fibronectin mats [108, 109], collagen matrices [30], bovine serum albumin or from delivery systems such as subcutaneous minipumps[110] or microspheres that are incorporated during the fabrication pro-

cess of the nerve tube [111, 112]. The advantage of growth factors in comparison to Schwann cells is that no extra procedure is needed. The advantage of delivery of growth factors from microspheres is the potential for controlled release over an extended period of time without leakage from the tube.

Conductive polymers

Finally, conductive polymers may also enhance regeneration across the nerve tube. Aebischer et al. found significantly increased numbers of myelinated axons after repair with poled versus unpoled polyvinylidene fluoride (PVDF) tubes [113] possibly by accelerated axonal elongation on the charged surface. Schmidt et al. found an almost twofold neurite outgrowth *in vitro* on conductive polypyrrole films after electrical stimulation [114].

CONCLUSION

In this review we provided an overview of the experimental and clinical data currently available on nerve tubes for peripheral nerve repair. At present there is no sound scientific proof of the superiority of the empty hollow biodegradable nerve tubes that are now clinically used as compared to direct coaptation or autograft repair. The repair of all sorts of nerve lesions may lead to unnecessary failures and again a discontinuation of interest in the concept of the nerve tube. The extensions of the applications, especially in the repair of larger mixed or motor nerves, should be carefully evaluated. Also, although the autologous nerve graft has several practical disadvantages, it is important to realize that it still has a number of advantages, such as the presence of Schwann cells that secrete growth factors and basal lamina tubes that contain regenerating axons, besides the favorable properties of natural strength and flexibility of the nerve, and the fact that it is immunocompatible. Eventually, different modifications to the single lumen nerve tube might lead to a nerve tube that is a better alternative than autologous nerve graft repair.

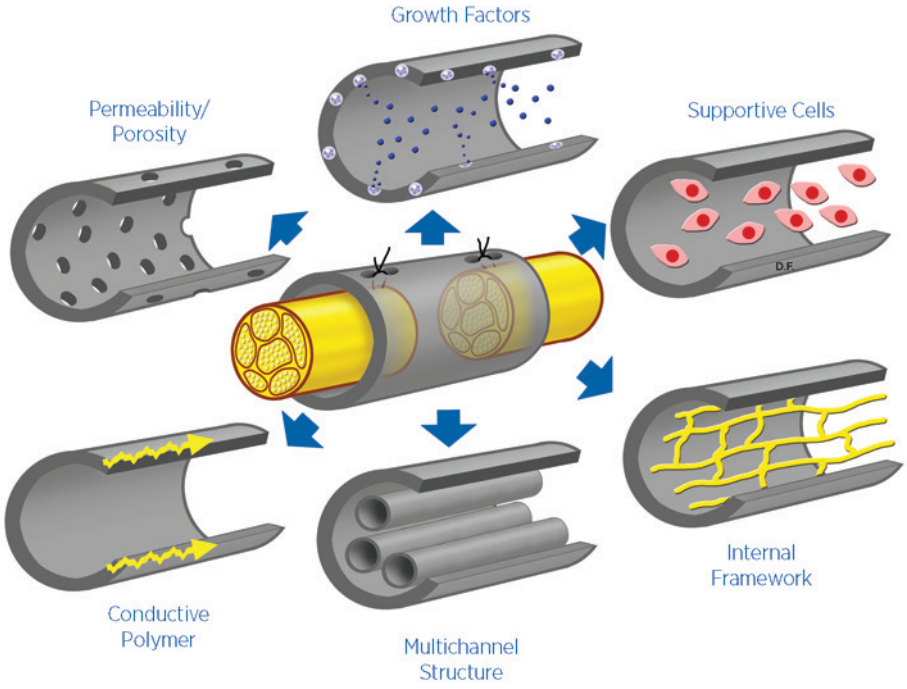

Figure 3

Modifications to the single lumen nerve tube. *Modified from* Hudson TW, Evans, GR, Schmidt, CE. Engineering strategies for peripheral nerve repair. Clin Plast Surg 1999; 26: 617 – 62

Table 3

Modifications to the single lumen nerve tube

Collagen and laminin-containing gels/ solutions										
	First author (yr)	Nerve tube	Gel/ solution	Animal	Nerve	Gap size (mm)	Methods	Groups/ controls	Follow-up	Most important result(s)
laminin	Madison (1985)	poly-D,L-lactates	Matrigel *	mice	sciatic	4 to 5	HRP-labeling	empty tubes	2 weeks	labeled neurons in all animals with laminin containing gels, none in empty
collagen, laminin	Valentini (1987)	semiperme-able PVC		mice	mouse	4	NM	semipermeable tubes with saline	12 weeks	fewer axons in gel-filled semipermeable tubes
collagen	Madison (1988)	silicone	Vitrogen *, laminin-gel,	rat	sciatic	15, 20	HRP-labeling, distance regen-eration	empty tubes	16 weeks	2x increase in maximum distance of axonal elongation
collagen, laminin	Labrador (1998)	silicone	Vitrogen *, Matrigel **	mouse	sciatic	4, 6	sweating test, pinprick, CMAP, CNAP	diff con, PBS, hyaluronate gel, plasma	up to 4 months	higher levels of target reinnervation with diluted gels
aligned colla-gen, laminin	Verdu (2000)	silicone	Vitrogen *, Matrigel **	mouse	sciatic	6	sweating test, pinprick, CMAP, CNAP	horizontal/ vertical polymerization, magnetic***	up to 4 months	higher number of MF for magnetically aligned gels
laminin-fibronectin coated fibers	Tong (1994)	collagen	collagen fibers	rat	sciatic	10	NM, NAP	uncoated collagen fibers	2 months	more MF and UMF in laminin-fibronectin coated fiber tubes

* Matrigel: solubilized basement membrane preparation containing laminin, type IV collagen, heparane sulfate proteoglycans, entactin, nidogen, and trace amounts of growth factors (12mg/ml), obtained from EHS sarcoma

* Vitrogen: solution of purified bovine dermal collagen, containing 95-98% type I collagen,

*** magnetic induction by placement of filled tubes with longitudinal axis perpendicular to a 9 Tesla magnetic field for 2 hours at 37 ^{0}C

Abbreviation: CMAP = compound muscle action potentials, CNAP = compound nerve action potentials, conc = concentrations, diff = different, HRP = horseradish peroxidase, NAP = nerve action potential, NM = nerve morphometry, MAP = muscle action potential, MF = myelinated fibers, no = number, PBS = phosphate buffered saline, PGA = polyglycolic acid, PLA = poly-D,L-lactic acid, PVC = polyvinylchloride acrylic copolymer

Intrinsic frameworks										
	First author (yr)	Nerve tube	material frame-work, number	Animal	Nerve	Gap size (mm)	Methods	Groups/ controls	Follow-up	Most important result(s)
filaments	Lundborg (1996, 1997)	silicone tubes	polyamide, 8	rat	sciatic	10, 15	NM, NF staining, pinch reflex	empty tubes, no repair	4 weeks	response to pinch and positive staining for NF distal to tube in all cases filaments, none in empty tube
filaments	Yoshii (2003)	no tube	collagen, 2000, 4000	rat	sciatic	20, 30	NM, presence ankle flexion	autograft, collagen tube	8 and 12 weeks	regeneration across 20 and 30mm gaps, more MF for 4000 filaments
sponge	Nakamura (2004)	PGA tube	collagen sponge	dog	peroneal	15	MEP, CNAP	autograft	up to 6 months	shorter latency, larger peak voltage and larger MF for PGA-collagen tubes
muscle tissue	Meek (2001)	PLC	denatured muscle	rat	sciatic	15	NM	non-operated side	up to 12 weeks	regeneration across 15mm gap in all cases
multichannel	de Ruiter (2008)	75:25 PLGA	7	rat	sciatic	10	NM, CMAP, muscle fiber size and type, sim and seq tracing	single lumen tubes, autograft, normal	8 and 12 weeks	tendency to reduce dispersion no MN and MF not significantly different from single lumen nerve tubes

Abbreviations: CMAP = compound muscle action potentials, CNAP = compound nerve action potentials, MEP = muscle-evoked potentials, MF = myelinated fibers, MN = motoneuron, NF = neurofilament, no = number, PGA = polyglycolic acid, PLC = poly(DL-lactide-ε-caprolactone, PLGA = poly(lactic co-glycolic acid), sim = simultaneous, seq = sequential

Schwann cells (SC) *										
	First author (yr)	Nerve tube	Suspension	Animal	Nerve	Gap size (mm)	Methods	Groups/ controls	Follow-up	Most important result(s)
syngeneic (F), heterologous (CD) adult	Guénard (1992)	PAN/PVC, permeable	Matrigel	rat	sciatic	8	NM	different dens: (F) 40, 80, 120 x10^6, (CD) 80 x 10^6, Matrigel, empty, autografts	3 wks	more MF for high dens SC more MF for syngeneic than for heterologous SC
syngeneic adult	Ansselin (1997)	collagen	RPMI 1640 **	rat	sciatic	18	NM, SFI, CMAP	different densities: >or< 5 x 10^5, PBS	6 months	more MF for high dens SC
Fluoro-gold labeled, syngeneic	Kim (1994)	collagen	collagen gel	rat	sciatic	10	NAP	collagen gel alone, sural nerve grafts	60 and 120 days	NAP and no MF equal for SC and sural grafts, but lower for collagen alone
syngeneic, isogeneic, autologous adult	Rodriguez (2000)	PLC, permeable	Matrigel	mouse	sciatic	6	NM, CMAP, CNAP, sweating, pinprick	syngeneic, isogeneic, autologous SC, autograft	4 months	best results for autologous SC

allogeneic neonatal	Evans (2002)	PLLA, permeable	collagen (Vitrogen)	rat	sciatic	10	NM, SFI, gastroc muscle weight	diff dens: 10^4, 10^6, isograft, collagen, silicone	4 months	MF density in distal nerve in all groups lower than for isografts
syngeneic/ isogeneic neonatal	Sinis (2005)	TMC/CL, permeable	Matrigel	rat	median	20	grasping test, FDS muscle weight, CMAP	normal, autograft, empty	9 months	regeneration only after repair with autograft or nerve tube with SC
isogeneic	Sinis (2007)	TMC/CL, permeable	Matrigel	rat	median (cross-chest)	40	Idem above	non-operated, autograft	12 months	no regeneration across nerve tubes with SC

* syngeneic = from the same strain, isogeneic = from the same litter, allogeneic = same species, but genetically different (although in study by Evans et al Schwann cells were harvested from Sprague-Dwaley rats and implanted into Lewis rats), heterologous = from different species, autologous = from the same animal

** RPMI 1640 medium containing 1.25 U Dispase/ml, 0.05% (wt/vol) collagenase, and 0.1% hyaluronidase

Abbreviations: CD = outbred Sprague Dawley rats, CMAP = compound muscle action potential, dens = density (SC/ml), F = inbred Fisher rats, FDS = flexor digitorum superficialis, gastroc = gastrocnemius, MF = myelinated fibers, NAP = nerve action potential, NM = nerve morphometry, no = number, PAN/PVC = acrylonitrile vinylchloride, PLC = poly(lactide-co-ε-caprolactone), PLGA = poly(lactic co-glycolic acid), PLLA = poly(L-lactic acid), subcut = subcutaneous, SC = Schwann cells, TMC/CL = trimethylenecarbonate-co-epsilon-caprolactone

Growth factors										
	First author (yr)	Nerve tube	carrier/ delivery system	Animal	Nerve	Gap size (mm)	Methods	Groups/ controls	Follow-up	Most important result(s)
NGF	Hollowell (1990)	silicone	saline solution	rat	sciatic	8	NM, HRP-labeling	solution cyt C	10 weeks	no MN and DRG not significantly different
	Derby (1993)	silicone and semiperme-able polysulfone	solution	rat	sciatic	7-8 and 12-13	NM (MF and UMF), behavorial tests	solution cyt C	10mm: 3, 4, 8 wks 15mm: 6 months	'head start': at 3 wks 3x more MF, at 4 wks no difference
	Whitworth (1996)	no tube, rolling of mat	fibronectin mats	rat	sciatic	10	immunostaining, NM	plain mats	up to 60 days	increased penetration distance, slightly greater no MF in distal nerve at 60 days
	Santos (1998)		subcutaneous minipump							
	Lee (2003)	silicone	fibrin-based	rat	sciatic	13	NM	diff conc (5, 20, 50ng/ml), empty, fibrin, isograft	6 weeks	no MF mid and distal to tube not sign diff from isograft for 20 and 50 ng/ml
	Xu (2003)	PPE	microspheres	rat	sciatic	10	NM, reflex response	silicone, saline, BSA microspheres	3 months	more MF in the distal nerve compared to all repair groups
GDNF and NGF	Fine (2002)	EVA	BSA	rat	sciatic	15	NM, FG labeling	BSA alone	47 days, 42 days	no MF: GDNF 4942, NGF 1199, BSA 5 no MN: GDNF 98.1, NGF 20.0, BSA 0 no DRG: GDNF 22.7, NGF 3.3, BSA 0

GDNF and NT-3	Barras (2002)	EVA	BSA	rat	facial	8	NM, FG labeling	BSA alone	6 weeks	no MN: GDNF 981, NT-3 53, BSA 0
BDNF, NGF, and NT-3	Bloch (2001)	EVA	BSA	rat	dorsal root	4	NM (MF and UMF)	BSA alone	4 weeks	no MF (mid tube): BDNF 863, NGF 1843, NT-3 1495, control BSA 293
BDNF and NT-4	Simon (2003)	no tube, rolling of mat	fibronectin mats	rat	sciatic	10	soleus and EDL muscle weight and fiber type	plain mats	120 days	NT-4 reversed soleus mass loss by restoring type I muscle fiber proportion and diameters
NT-3	Sterne (1997)	no tube, rolling of mat	fibronectin mats	rat	sciatic	10	immunostaining, NM	plain mats	up to 8 months	max effect at 15 days with increased penetration distance, greater no MF in distal nerve at 8 months
FGF	Midha (2003)	PHEMA-MMA	collagen gel*	rat	sciatic	10	NM	autograft, collagen gel, empty	8 weeks	no MF in distal nerve comparable to autograft and higher than other groups

* Vitrogel (see collagen and laminin-containing gels)

Abbreviations: BSA = bovine serum albumin, conc = concentrations, Cyt = cytochrome, diff= different, DRG = dorsal root ganglion cells, EDL = extensor digitorum longus, EVA = ethylene-vinyl acetate copolymer, FG = fluorogold, MF = myelinated fibers, MN = motoneurons, PHEMA-MMA = poly(2-hydroxyethyl methacrylate-co-methyl methacrylate), sign = significantly, UMF = unmyelinated fibers

Conductive polymers									
	First author (yr)	Nerve tube	Animal	Nerve	Gap size (mm)	Methods	Groups/ controls	Follow-up	Most important result(s)
PVDF	Aebischer (1987)	poled PVDF	mouse	sciatic	4	NM	unpoled	4, 12 weeks	more MF in poled vs unpoled tubes

Abbreviation: MF = myelinated fibers PDVF = polyvinylidene fluoride

REFERENCES

1. Chiu, D.T., et al., *Autogenous vein graft as a conduit for nerve regeneration.* Surgery, 1982. **91**(2): p. 226-33.
2. Mackinnon, S.E., et al., *Clinical outcome following nerve allograft transplantation.* Plast Reconstr Surg, 2001. **107**(6): p. 1419-29.
3. Siemionow, M. and E. Sonmez, *Nerve Allograft Transplantation: A Review.* J Reconstr Microsurg, 2008.
4. de Ruiter, G.C., et al., *Misdirection of regenerating motor axons after nerve injury and repair in the rat sciatic nerve model.* Exp Neurol, 2008.
5. Weiss, P., *The technology of nerve regeneration: a review. Sutureless tubulation and related methods fo nerve repair.* J Neurosurgey, 1944. **1**: p. 400-450.
6. Sunderland, S., *Nerve grafting.* Nerves and nerve injuries, ed. S. Sunderland. 1978, Edinburgh, London, New York: Churchill, Livingstone.
7. Uzman, B.G. and G.M. Villegas, *Mouse sciatic nerve regeneration through semipermeable tubes: a quantitative model.* J Neurosci Res, 1983. **9**(3): p. 325-38.
8. Aebischer, P., V. Guenard, and R.F. Valentini, *The morphology of regenerating peripheral nerves is modulated by the surface microgeometry of polymeric guidance channels.* Brain Res, 1990. **531**(1-2): p. 211-8.
9. Scaravilli, F., *Regeneration of the perineurium across a surgically induced gap in a nerve encased in a plastic tube.* J Anat, 1984. **139 (Pt 3)**: p. 411-24.
10. Young, B.L., et al., *An effective sleeving technique in nerve repair.* J Neurosci Methods, 1984. **10**(1): p. 51-8.
11. Madison, R.D., et al., *Peripheral nerve regeneration with entubulation repair: comparison of biodegradeable nerve guides versus polyethylene tubes and the effects of a laminin-containing gel.* Exp Neurol, 1987. **95**(2): p. 378-90.
12. Henry, E.W., et al., *Nerve regeneration through biodegradable polyester tubes.* Exp Neurol, 1985. **90**(3): p. 652-76.
13. Seckel, B.R., et al., *Nerve regeneration through synthetic biodegradable nerve guides: regulation by the target organ.* Plast Reconstr Surg, 1984. **74**(2): p. 173-81.
14. Lundborg, G., et al., *Nerve regeneration in silicone chambers: influence of gap length and of distal stump components.* Exp Neurol, 1982. **76**(2): p. 361-75.
15. Williams, L.R., et al., *Spatial-temporal progress of peripheral nerve regeneration within a silicone chamber: parameters for a bioassay.* J Comp Neurol, 1983. **218**(4): p. 460-70.
16. Zhao, Q., Dahlin, LB, Kanje, M, Lundborg, G, *Repair of the transected rat sciatic nerve: matrix formation within implanted silicone tubes.* Restor Neurol Neurosci, 1993. **5**: p. 197-204.
17. Williams, L.R. and S. Varon, *Modification of fibrin matrix formation in situ enhances nerve regeneration in silicone chambers.* J Comp Neurol, 1985. **231**(2): p. 209-20.
18. Jenq, C.B. and R.E. Coggeshall, *Nerve regeneration through holey silicone tubes.* Brain Res, 1985. **361**(1-2): p. 233-41.

19. Jenq, C.B. and R.E. Coggeshall, *Permeable tubes increase the length of the gap that regenerating axons can span.* Brain Res, 1987. **408**(1-2): p. 239-42.
20. Vleggeert-Lankamp, C.L., et al., *Pores in synthetic nerve conduits are beneficial to regeneration.* J Biomed Mater Res A, 2007. **80**(4): p. 965-82.
21. Rodriguez, F.J., et al., *Highly permeable polylactide-caprolactone nerve guides enhance peripheral nerve regeneration through long gaps.* Biomaterials, 1999. **20**(16): p. 1489-500.
22. Kim, D.H., et al., *Comparison of macropore, semipermeable, and nonpermeable collagen conduits in nerve repair.* J Reconstr Microsurg, 1993. **9**(6): p. 415-20.
23. Jenq, C.B., L.L. Jenq, and R.E. Coggeshall, *Nerve regeneration changes with filters of different pore size.* Exp Neurol, 1987. **97**(3): p. 662-71.
24. Aebischer, P., V. Guenard, and S. Brace, *Peripheral nerve regeneration through blind-ended semipermeable guidance channels: effect of the molecular weight cutoff.* J Neurosci, 1989. **9**(10): p. 3590-5.
25. Guenard, V., R.F. Valentini, and P. Aebischer, *Influence of surface texture of polymeric sheets on peripheral nerve regeneration in a two-compartment guidance system.* Biomaterials, 1991. **12**(2): p. 259-63.
26. den Dunnen, W., van der Lei, B, Robinson PH, Holwerda, A, Pennings, AJ, Schakenraad, JM, *Biological performance of a degradable poly(lactic acid-ε-caprolactone) nerve guide: influence of tube dimensions.* J Biomed Mater Res A, 1995. **29**: p. 757-766.
27. de Ruiter, G.C., et al., *Methods for in vitro characterization of multichannel nerve tubes.* J Biomed Mater Res A, 2007.
28. Evans, G.B., K. Widmer, M. Gürlek, A. Savel, T. Gupta, P. Lohman, R. Williams, J. Hodges, J. Nabawi, A. Patrick, C. Mikos, AG., *Tissue engineered conduits: the use of biodegradable poly-DL-lactic-co-glycolic acid (PLGA) scaffolds in peripheral nerve regeneration.* Biological matrices and tissue reconstruction., ed. H.R. Stark GE, Tanczos E. 1998, Berlin: Springer. 225-35.
29. Belkas, J.S., et al., *Peripheral nerve regeneration through a synthetic hydrogel nerve tube.* Restor Neurol Neurosci, 2005. **23**(1): p. 19-29.
30. Midha, R., et al., *Growth factor enhancement of peripheral nerve regeneration through a novel synthetic hydrogel tube.* J Neurosurg, 2003. **99**(3): p. 555-65.
31. Vleggeert-Lankamp, C.L., *The role of evaluation methods in the assessment of peripheral nerve regeneration through synthetic conduits: a systematic review. Laboratory investigation.* J Neurosurg, 2007. **107**(6): p. 1168-89.
32. den Dunnen, W.F., et al., *Poly(DL-lactide-epsilon-caprolactone) nerve guides perform better than autologous nerve grafts.* Microsurgery, 1996. **17**(7): p. 348-57.
33. Dellon, A.L. and S.E. Mackinnon, *An alternative to the classical nerve graft for the management of the short nerve gap.* Plast Reconstr Surg, 1988. **82**(5): p. 849-56.
34. Mackinnon, S.E., A.L. Dellon, and J.P. O'Brien, *Changes in nerve fiber numbers distal to a nerve repair in the*

rat sciatic nerve model. Muscle Nerve, 1991. **14**(11): p. 1116-22.
35. Ansselin, A.D., T. Fink, and D.F. Davey, *Peripheral nerve regeneration through nerve guides seeded with adult Schwann cells.* Neuropathol Appl Neurobiol, 1997. **23**(5): p. 387-98.
36. Kim, D.H., et al., *Labeled Schwann cell transplants versus sural nerve grafts in nerve repair.* J Neurosurg, 1994. **80**(2): p. 254-60.
37. Guenard, V., et al., *Syngeneic Schwann cells derived from adult nerves seeded in semipermeable guidance channels enhance peripheral nerve regeneration.* J Neurosci, 1992. **12**(9): p. 3310-20.
38. Valero-Cabre, A., et al., *Superior muscle reinnervation after autologous nerve graft or poly-L-lactide-epsilon-caprolactone (PLC) tube implantation in comparison to silicone tube repair.* J Neurosci Res, 2001. **63**(2): p. 214-23.
39. de Ruiter, G.C., Spinner, R.J., Malessy, M.J.A., Moore, M.J., Sorenson, E.J., Currier, B.L., Yaszemski, M.J., Windebank, A.J., *Accuracy of motor axon regeneration across autograft, single lumen, and multichannel poly(lactic-co-glycolic acid) (PLGA) nerve tubes.* Neurosurgery, in press, 2008.
40. Bodine-Fowler, S.C., et al., *Inaccurate projection of rat soleus motoneurons: a comparison of nerve repair techniques.* Muscle Nerve, 1997. **20**(1): p. 29-37.
41. Evans, P.J., et al., *Selective reinnervation: a comparison of recovery following microsuture and conduit nerve repair.* Brain Res, 1991. **559**(2): p. 315-21.
42. Rende, M., et al., *Accuracy of reinnervation by peripheral nerve axons regenerating across a 10-mm gap within an impermeable chamber.* Exp Neurol, 1991. **111**(3): p. 332-9.
43. Zhao, Q., et al., *Specificity of muscle reinnervation following repair of the transected sciatic nerve. A comparative study of different repair techniques in the rat.* J Hand Surg [Br], 1992. **17**(3): p. 257-61.
44. Brushart, T.M., et al., *Joseph H. Boyes Award. Dispersion of regenerating axons across enclosed neural gaps.* J Hand Surg [Am], 1995. **20**(4): p. 557-64.
45. Vleggeert-Lankamp, C.L., et al., *Type grouping in skeletal muscles after experimental reinnervation: another explanation.* Eur J Neurosci, 2005. **21**(5): p. 1249-56.
46. de Medinaceli, L., Freed, WJ, Wyatt, RJ, *An index of the functional condition of rat sciatic nerve based on measurements made from walking tracks.* Exp Neurol, 1982. **77**: p. 634-643.
47. Bain, J.R., S.E. Mackinnon, and D.A. Hunter, *Functional evaluation of complete sciatic, peroneal, and posterior tibial nerve lesions in the rat.* Plast Reconstr Surg, 1989. **83**(1): p. 129-38.
48. Dellon, A.L. and S.E. Mackinnon, *Sciatic nerve regeneration in the rat. Validity of walking track assessment in the presence of chronic contractures.* Microsurgery, 1989. **10**(3): p. 220-5.
49. Weber, R.A., et al., *Autotomy and the sciatic functional index.* Microsurgery, 1993. **14**(5): p. 323-7.
50. Fu, S.Y. and T. Gordon, *Contributing factors to poor functional recovery after delayed nerve repair: prolonged denervation.* J Neurosci, 1995. **15**(5 Pt 2): p. 3886-95.

51. de Ruiter, G.C., Malessy, M.J.A., Alaid, A.O., Spinner, R.J., Engelstad, J.K., Sorenson, E.J., Kaufman, K.R., Dyck, P.J., Windebank, A.J., *Misdirection of regenerating motor axons after nerve injury and repair in the rat sciatic nerve model.* Exp Neurol, 2008. **accepted for publication**.
52. Yannas, I.V. and B.J. Hill, *Selection of biomaterials for peripheral nerve regeneration using data from the nerve chamber model.* Biomaterials, 2004. **25**(9): p. 1593-600.
53. Archibald, S.J., et al., *A collagen-based nerve guide conduit for peripheral nerve repair: an electrophysiological study of nerve regeneration in rodents and nonhuman primates.* J Comp Neurol, 1991. **306**(4): p. 685-96.
54. Archibald, S.J., et al., *Monkey median nerve repaired by nerve graft or collagen nerve guide tube.* J Neurosci, 1995. **15**(5 Pt 2): p. 4109-23.
55. Mackinnon, S.E. and A.L. Dellon, *A study of nerve regeneration across synthetic (Maxon) and biologic (collagen) nerve conduits for nerve gaps up to 5 cm in the primate.* J Reconstr Microsurg, 1990. **6**(2): p. 117-21.
56. Stanec, S. and Z. Stanec, *Reconstruction of upper-extremity peripheral-nerve injuries with ePTFE conduits.* J Reconstr Microsurg, 1998. **14**(4): p. 227-32.
57. Pitta, M.C., et al., *Use of Gore-Tex tubing as a conduit for inferior alveolar and lingual nerve repair: experience with 6 cases.* J Oral Maxillofac Surg, 2001. **59**(5): p. 493-6; discussion 497.
58. Pogrel, M.A., A.R. McDonald, and L.B. Kaban, *Gore-Tex tubing as a conduit for repair of lingual and inferior alveolar nerve continuity defects: a preliminary report.* J Oral Maxillofac Surg, 1998. **56**(3): p. 319-21; discussion 321-2.
59. Ashley, W.W., Jr., T. Weatherly, and T.S. Park, *Collagen nerve guides for surgical repair of brachial plexus birth injury.* J Neurosurg, 2006. **105**(6 Suppl): p. 452-6.
60. Crawley, W.A. and A.L. Dellon, *Inferior alveolar nerve reconstruction with a polyglycolic acid bioabsorbable nerve conduit.* Plast Reconstr Surg, 1992. **90**(2): p. 300-2.
61. Kim, J. and A.L. Dellon, *Reconstruction of a painful post-traumatic medial plantar neuroma with a bioabsorbable nerve conduit: a case report.* J Foot Ankle Surg, 2001. **40**(5): p. 318-23.
62. Navissano, M., et al., *Neurotube for facial nerve repair.* Microsurgery, 2005. **25**(4): p. 268-71.
63. Ducic, I., C.T. Maloney, Jr., and A.L. Dellon, *Reconstruction of the spinal accessory nerve with autograft or neurotube? Two case reports.* J Reconstr Microsurg, 2005. **21**(1): p. 29-33; discussion 34.
64. Dellon, A.L. and C.T. Maloney, Jr., *Salvage of sensation in a hallux-to-thumb transfer by nerve tube reconstruction.* J Hand Surg [Am], 2006. **31**(9): p. 1495-8.
65. Donoghoe, N., G.D. Rosson, and A.L. Dellon, *Reconstruction of the human median nerve in the forearm with the Neurotube.* Microsurgery, 2007. **27**(7): p. 595-600.
66. Inada, Y., et al., *Regeneration of peripheral motor nerve gaps with a polyglycolic acid-collagen tube: technical case report.* Neurosurgery, 2007. **61**(5): p. E1105-7; discussion E1107.

67. Inada, Y., et al., *Regeneration of peripheral nerve gaps with a polyglycolic acid-collagen tube.* Neurosurgery, 2004. **55**(3): p. 640-6; discussion 646-8.
68. Hung, V. and A.L. Dellon, *Reconstruction of a 4-cm Human Median Nerve Gap by Including an Autogenous Nerve Slice in a Bioabsorbable Nerve Conduit: Case Report.* J Hand Surg [Am], 2008. **33**(3): p. 313-5.
69. Fan, W., et al., *Repairing a 35-mm-long median nerve defect with a chitosan/PGA artificial nerve graft in the human: a case study.* Microsurgery, 2008. **28**(4): p. 238-42.
70. Lundborg, G., et al., *Tubular versus conventional repair of median and ulnar nerves in the human forearm: early results from a prospective, randomized, clinical study.* J Hand Surg [Am], 1997. **22**(1): p. 99-106.
71. Lundborg, G., et al., *Tubular repair of the median or ulnar nerve in the human forearm: a 5-year follow-up.* J Hand Surg [Br], 2004. **29**(2): p. 100-7.
72. Dellon, A.L., *Use of a silicone tube for the reconstruction of a nerve injury.* J Hand Surg [Br], 1994. **19**(3): p. 271-2.
73. Meek, M.F., et al., *The use of silicone tubing in the late repair of the median and ulnar nerves in the forearm.* J Hand Surg [Br], 2000. **25**(4): p. 408-9.
74. Merle, M., et al., *Complications from silicon-polymer intubulation of nerves.* Microsurgery, 1989. **10**(2): p. 130-3.
75. Braga-Silva, J., *The use of silicone tubing in the late repair of the median and ulnar nerves in the forearm.* J Hand Surg [Br], 1999. **24**(6): p. 703-6.
76. Dahlin, L.B., L. Anagnostaki, and G. Lundborg, *Tissue response to silicone tubes used to repair human median and ulnar nerves.* Scand J Plast Reconstr Surg Hand Surg, 2001. **35**(1): p. 29-34.
77. Dahlin, L. and G. Lundborg, *The use of silicone tubing in the late repair of the median and ulnar nerves in the forearm.* J Hand Surg [Br], 2001. **26**(4): p. 393-4.
78. Mackinnon, S.E. and A.L. Dellon, *Clinical nerve reconstruction with a bioabsorbable polyglycolic acid tube.* Plast Reconstr Surg, 1990. **85**(3): p. 419-24.
79. Moberg, E., *Two-point discrimination test. A valuable part of hand surgical rehabilitation, e.g. in tetraplegia.* Scand J Rehabil Med, 1990. **22**(3): p. 127-34.
80. Battiston, B., et al., *Nerve repair by means of tubulization: literature review and personal clinical experience comparing biological and synthetic conduits for sensory nerve repair.* Microsurgery, 2005. **25**(4): p. 258-67.
81. Weber, R.A., et al., *A randomized prospective study of polyglycolic acid conduits for digital nerve reconstruction in humans.* Plast Reconstr Surg, 2000. **106**(5): p. 1036-45; discussion 1046-8.
82. Bertleff, M.J., M.F. Meek, and J.P. Nicolai, *A prospective clinical evaluation of biodegradable neurolac nerve guides for sensory nerve repair in the hand.* J Hand Surg [Am], 2005. **30**(3): p. 513-8.
83. Dellon, E.S., et al., *Validation of cutaneous pressure threshold measurements for the evaluation of hand function.* Ann Plast Surg, 1997. **38**(5): p. 485-92.
84. Meek, M.F. and J.H. Coert, *US Food and Drug Administration/Conformit Europe-approved absorbable nerve conduits for clinical repair of peripheral and cranial nerves.* Ann Plast Surg, 2008. **60**(1): p. 110-6.

85. Madison, R.D., C.F. Da Silva, and P. Dikkes, *Entubulation repair with protein additives increases the maximum nerve gap distance successfully bridged with tubular prostheses.* Brain Res, 1988. **447**(2): p. 325-34.
86. Labrador, R.O., M. Buti, and X. Navarro, *Influence of collagen and laminin gels concentration on nerve regeneration after resection and tube repair.* Exp Neurol, 1998. **149**(1): p. 243-52.
87. Valentini, R.F., et al., *Collagen- and laminin-containing gels impede peripheral nerve regeneration through semipermeable nerve guidance channels.* Exp Neurol, 1987. **98**(2): p. 350-6.
88. Verdu, E., et al., *Alignment of collagen and laminin-containing gels improve nerve regeneration within silicone tubes.* Restor Neurol Neurosci, 2002. **20**(5): p. 169-79.
89. Rodriguez, F.J., et al., *Nerve guides seeded with autologous schwann cells improve nerve regeneration.* Exp Neurol, 2000. **161**(2): p. 571-84.
90. Sinis, N., et al., *Nerve regeneration across a 2-cm gap in the rat median nerve using a resorbable nerve conduit filled with Schwann cells.* J Neurosurg, 2005. **103**(6): p. 1067-76.
91. Luo, Y. and M.S. Shoichet, *A photolabile hydrogel for guided three-dimensional cell growth and migration.* Nat Mater, 2004. **3**(4): p. 249-53.
92. Lundborg, G., et al., *A new type of "bioartificial" nerve graft for bridging extended defects in nerves.* J Hand Surg [Br], 1997. **22**(3): p. 299-303.
93. Matsumoto, K., et al., *Peripheral nerve regeneration across an 80-mm gap bridged by a polyglycolic acid (PGA)-collagen tube filled with laminin-coated collagen fibers: a histological and electrophysiological evaluation of regenerated nerves.* Brain Res, 2000. **868**(2): p. 315-28.
94. Wang, X., et al., *Dog sciatic nerve regeneration across a 30-mm defect bridged by a chitosan/PGA artificial nerve graft.* Brain, 2005. **128**(Pt 8): p. 1897-910.
95. Nakamura, T., et al., *Experimental study on the regeneration of peripheral nerve gaps through a polyglycolic acid-collagen (PGA-collagen) tube.* Brain Res, 2004. **1027**(1-2): p. 18-29.
96. Francel, P.C., et al., *Enhancing nerve regeneration across a silicone tube conduit by using interposed short-segment nerve grafts.* J Neurosurg, 1997. **87**(6): p. 887-92.
97. Meek, M.F., et al., *Evaluation of functional nerve recovery after reconstruction with a poly (DL-lactide-epsilon-caprolactone) nerve guide, filled with modified denatured muscle tissue.* Microsurgery, 1996. **17**(10): p. 555-61.
98. Yoshii, S. and M. Oka, *Peripheral nerve regeneration along collagen filaments.* Brain Res, 2001. **888**(1): p. 158-162.
99. Yoshii, S., et al., *Bridging a 30-mm nerve defect using collagen filaments.* J Biomed Mater Res, 2003. **67A**(2): p. 467-74.
100. Sundback, C., et al., *Manufacture of porous polymer nerve conduits by a novel low-pressure injection molding process.* Biomaterials, 2003. **24**(5): p. 819-30.
101. Hadlock, T., et al., *A polymer foam conduit seeded with Schwann cells promotes guided peripheral nerve regeneration.* Tissue Eng, 2000. **6**(2): p. 119-27.

102. Bender, M.D., et al., *Multi-channeled biodegradable polymer/CultiSpher composite nerve guides.* Biomaterials, 2004. **25**(7-8): p. 1269-78.
103. Yang, Y., et al., *Neurotrophin releasing single and multiple lumen nerve conduits.* J Control Release, 2005. **104**(3): p. 433-46.
104. Sinis, N., et al., *Long nerve gaps limit the regenerative potential of bioartificial nerve conduits filled with Schwann cells.* Restor Neurol Neurosci, 2007. **25**(2): p. 131-41.
105. Evans, G.R., et al., *Bioactive poly(L-lactic acid) conduits seeded with Schwann cells for peripheral nerve regeneration.* Biomaterials, 2002. **23**(3): p. 841-8.
106. Mimura, T., et al., *Peripheral nerve regeneration by transplantation of bone marrow stromal cell-derived Schwann cells in adult rats.* J Neurosurg, 2004. **101**(5): p. 806-12.
107. Rich, K.M., et al., *Nerve growth factor enhances regeneration through silicone chambers.* Exp Neurol, 1989. **105**(2): p. 162-70.
108. Whitworth, I.H., et al., *Nerve growth factor enhances nerve regeneration through fibronectin grafts.* J Hand Surg [Br], 1996. **21**(4): p. 514-22.
109. Sterne, G.D., et al., *Neurotrophin-3 delivered locally via fibronectin mats enhances peripheral nerve regeneration.* Eur J Neurosci, 1997. **9**(7): p. 1388-96.
110. Santos, X., et al., *Evaluation of peripheral nerve regeneration by nerve growth factor locally administered with a novel system.* J Neurosci Methods, 1998. **85**(1): p. 119-27.
111. Goraltchouk, A., et al., *Incorporation of protein-eluting microspheres into biodegradable nerve guidance channels for controlled release.* J Control Release, 2006. **110**(2): p. 400-7.
112. Piotrowicz, A. and M.S. Shoichet, *Nerve guidance channels as drug delivery vehicles.* Biomaterials, 2006. **27**(9): p. 2018-27.
113. Aebischer, P., et al., *Piezoelectric guidance channels enhance regeneration in the mouse sciatic nerve after axotomy.* Brain Res, 1987. **436**(1): p. 165-8.
114. Schmidt, C.E., et al., *Stimulation of neurite outgrowth using an electrically conducting polymer.* Proc Natl Acad Sci U S A, 1997. **94**(17): p. 8948-53.

CHAPTER 6

Methods for *in vitro* characterization of multichannel nerve tubes

Godard C.W. de Ruiter [1,2,4], Irene Onyeneho [1], Ellen T. Liang [1], Michael J.Moore [3], Andrew Knight [1], Martijn J.A. Malessy [4], Robert J. Spinner [2], Lichun Lu [3], Bradford L. Currier [3], Michael J. Yaszemski [3], Anthony J. Windebank [1]

[1] Laboratory for Molecular Neuroscience, Mayo Clinic, Rochester MN, USA
[2] Department of Neurologic Surgery, Mayo Clinic, Rochester MN, USA
[3] Laboratory for Biomedical Engineering, Mayo Clinic, Rochester MN, USA
[4] Department of Neurosu-rgery, Leiden University Medical Center, The Netherlands

Published in Journal of Biomedical Materials Research Part A, 2008; Volume 84(3): 643-651

ABSTRACT

Background Multichannel conduits have been developed for both experimental peripheral nerve and spinal cord repair. We present a series of methods to characterize multichannel nerve tubes for properties of bending, deformation, swelling, and degradation and introduce a new method to test the permeability of multichannel nerve tubes from the rate of diffusion of different-sized fluorescent dextran molecules (10, 40, and 70 kDa).
Methods First, single lumen nerve tubes made with different poly(lactic co-glycolic acid) (PLGA) ratios (50:50, 75:25 and 85:15) were compared. One ratio (75:25 PLGA) was subsequently used to compare single lumen and multichannel nerve tubes.
Results Nerve tubes made with lower ratios were found to be more flexible than nerve tubes made with a higher PLGA ratio. For lower ratios, however, swelling was also greater as a result of a faster degradation. Multichannel structure did not interfere with the permeability of the tube; the rate of diffusion into multichannel 75:25 PLGA nerve tubes appeared to be even higher than that into single lumen ones, but this was only significant for 70-kDa molecules. Also, multichannel 75:25 PLGA nerve tubes were more flexible and, at the same time, more resistant to deformation. However, swelling significantly decreased the total cross-sectional lumen area, especially in multichannel 75:25 PLGA nerve tubes.
Conclusion Permeability, bending, deformation, swelling and degradation are important properties to characterize in the development of multichannel nerve tubes. The methods presented in this study can be used as a basis for optimizing these properties for possible future clinical application.

INTRODUCTION

Biodegradable single lumen or hollow nerve tubes have been developed as an alternative for autologous nerve graft repair (for review see **Chapter 5**). The disadvantages of using an autograft include donor-site morbidity, limited availability and size mismatch with the injured nerve. In comparison, nerve tubes are available off the shelf in different sizes.
Multichannel conduits have been developed for experimental peripheral nerve [1, 2] and spinal cord repair [3-7]. The multichannel structure provides more surface area for cell attachment and local release of incorporated growth factors. Also, the multichannel structure may better support regeneration across larger gaps by stabilizing the fibrin matrix [8, 9], and may better guide regenerating axons (**Chapter 7** and **8**).
However, the extra internal structure of multichannel conduits may also interfere with important physical properties of nerve tubes, including permeability, bending and deformation properties, swelling, and degradation. Permeability of a nerve

tube has been shown to influence the results of regeneration [10-13], and is needed for the survival of cells inside the channel before the graft is vascularized. Bending properties are important because the nerve tube may be implanted into a mobile limb. The nerve tube should be flexible, but, at the same time, resistant to permanent deformation and kinking. These properties are also important if the tube is used to repair a large nerve gap. Swelling and degradation are important because swelling of the internal structure may compress regenerated nerve fibers. The rate of degradation may affect swelling properties through the formation of small degradation products that increase the osmotic pressure of the tube [14].

In this study, we compared important physical properties of single lumen and multichannel nerve tubes made from different ratios poly(lactic-co-glycolic acid) (PLGA) (50:50, 75:25, 85:15). This biomaterial is approved by the US Food and Drug Administration (FDA), is used clinically in sutures (polyglactin 910) and has been used previously to fabricate nerve tubes [2, 15]. Because the physical characteristics of PLGA may vary depending on the ratio of lactic to glycolic acid [16], we first tested single lumen nerve tubes made with different PLGA ratios (50:50, 75:25, 85:15) for the properties of bending, deformation, swelling and degradation. One ratio (75:25 PLGA) was subsequently used to compare these properties and the permeability of single lumen and multichannel nerve tubes.

MATERIALS AND METHODS

COMPARISON OF SINGLE-LUMEN NERVE TUBES MADE WITH DIFFERENT PLGA RATIOS

Single-lumen 50:50, 75:25, and 85:15 PLGA nerve tubes were compared for different properties of bending, deformation, swelling, and degradation.

Fabrication of single lumen nerve tubes

Single lumen nerve tubes were fabricated using an injection-molding-solvent-evaporation technique [4]. The polytef (Teflon) mold consisted of cylindrical space (2.1mm in diameter) with endcaps through which a single stainless steel wire (1.6mm in diameter) was inserted (Figure 1A). The dimensions of the wire were based on the diameter of a transected rat sciatic nerve (1.6mm with mushrooming effect, unpublished results). A solution of PLGA polymer (for PLGA ratios 50:50, 75:25, and 85:15; Fisher Scientific, Birmingham, AL, molecular weights 58.8, 92, and 120kDa respectively) in methylene chloride (450μl/300mg PLGA) was injected into the mold. The mold was placed overnight in an airtight chamber attached to a high-vacuum pump (VP 190; Savant Instruments, Holbrook, NY) to create porous nerve tubes with semi-permeable outside and inside layers[7].

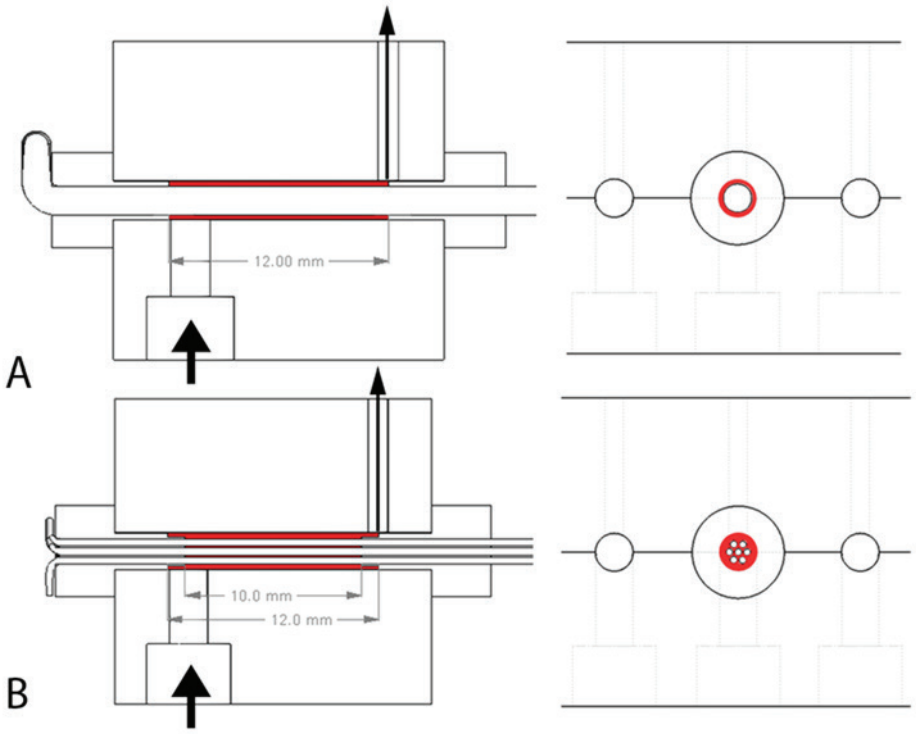

Figure 1

Side views (left) and cross-sectional views (right) of the mold with different assemblies for the fabrication of single lumen (A) and multichannel (B) nerve tubes. The mold consists of cylindrical spaces (2.1mm in diameter) with Teflon endcaps that can hold either (a) one stainless steel wire (1.6mm in diameter, Microparts) for the fabrication of single lumen nerve tubes or (B) seven 400-μm wires for the fabrication of multichannel nerve tubes. Large arrow, polymer injection site; small arrow, polymer evaporation site.

Bending and deformation properties

The bending and deformation properties of 50:50, 75:25, and 85:15 single-lumen PLGA nerve tubes were analyzed by 3-point-bending on a dynamical mechanical analyzer (DMA, 2980, TA instruments, New Castle, DE). Intact 12-mm tubes were placed on the holder at two points 1 cm apart. The third point was lowered from above in between these two points with increasing force. The displacement was measured and displayed graphically as function of the force (Figure 3A). From these graphs, stiffness could be calculated from a straight line drawn through the bending part of the graph, as shown in Figure 3 (A). The start of deformation of the tube was analyzed at the end of the bending part, the yield point. At this point, the minimal force need to deform the tube was noted and the maximum angle of bending was calculated from the displacement and length of the tube (Figure 3B). Five tubes per group were tested.

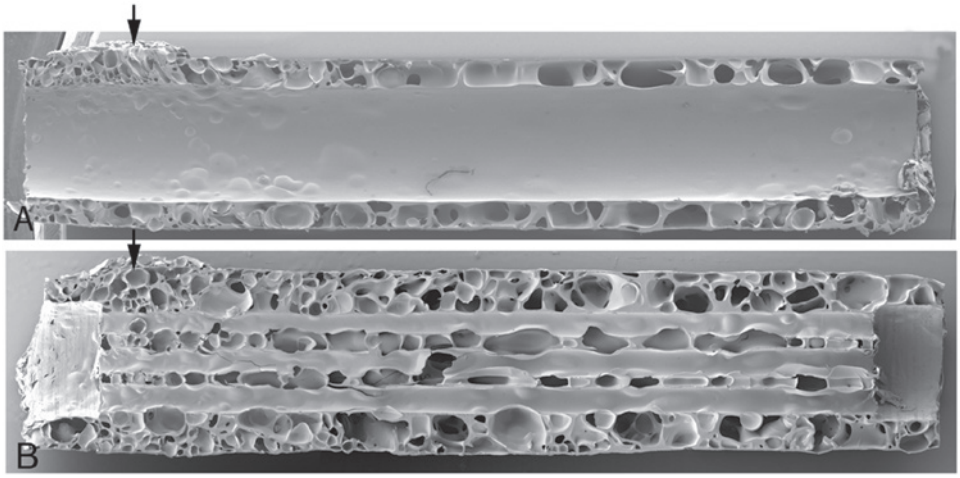

Figure 2
Scanning electron micrograph reconstructions (25xmagnification) of single lumen (A) and multi-channel (B) nerve tubes. Black arrows, polymer injection sites. White arrowheads, internal structure of the multichannel 75:25 nerve tube consists of smaller pores that appear to be more interconnected than the pores inside the single lumen 75:25 nerve tube.

Swelling and degradation

In vitro swelling and degradation of 50:50, 75:25, and 85:15 single lumen PLGA nerve tubes were tested in phosphate-buffered saline (PBS). Samples of a tube (3mm from the mid part) were placed in separate test tubes containing 1.5ml of PBS (Ph 7.4) with 2% sodium azide (to prevent contamination). Before placement, all sample were prehydrated in a series of ethanol concentrations (30 min in 100% ethanol, 20 min in 50% ethanol, and 20 min in 10% ethanol) and water (20 min) and weighed [17]. Test tubes were placed on a shaker in an incubator at 37°C. PBS was replaced every 3 or 4 days for the first 2 weeks and every 2 weeks thereafter to maintain a constant pH. Four samples per group were evaluated at each time point (day 0, day 3, week 1, 2, 4, 6, 8, 10, and 12). Samples were analyzed for residual weight (wet and dry), nerve tube dimensions, and mean molecular weight.
Nerve tube dimensions were determined for the total lumen cross-sectional area and total tube cross-sectional area (total cross-sectional area minus total lumen cross-sectional area). These areas were measured from digital pictures (Nikon Coolpixel 5700) taken through an inverted microscope with KS400 program (version 3.0 Zeiss) (Figure 4A-D). The mass swelling ratio was calculated from the wet and dry residual tube weights using the formula:

$$\textit{Mass swelling ratio} = \frac{(W_{wet} - W_{dry})}{W_{dry}}$$

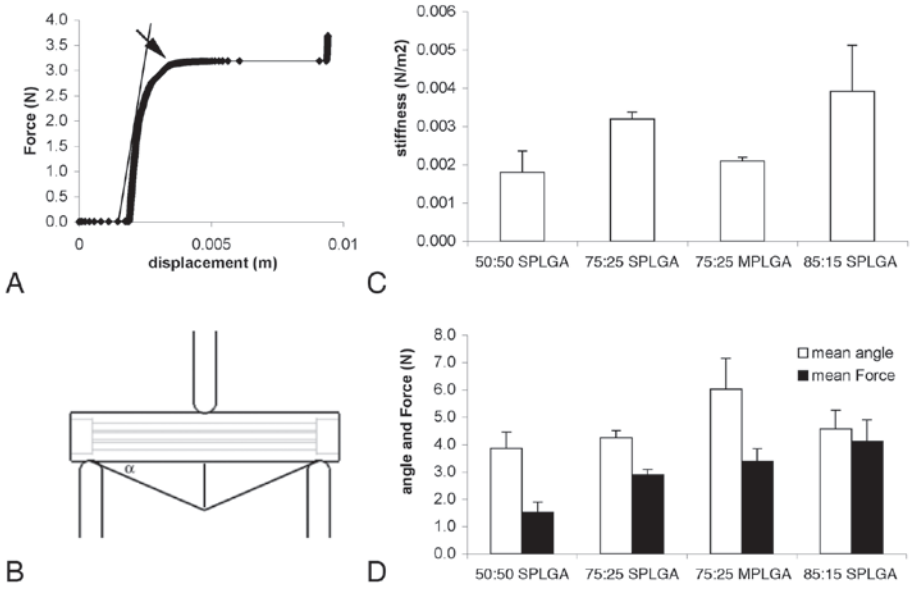

Figure 3

In vitro flexibility. A: An example of a 3-point-bending trial for a single lumen 75:25 PLGA tube. The line represents calculation of the stiffness from the bending trial. The arrow points at the yield point, the start of deformation. B: Diagram of 3-point bending and measurement of the angle (α) at yield point. C: Stiffness of single lumen 50:50, 75:25, 85:15 PLGA tubes (SPLGA) and multichannel 75:25 PLGA (MPLGA) tubes; single lumen nerve tubes made of lower PLGA ratios (85:15 > 75:25 > 50:50) were more flexible or less stiff; multichannel 75:25 PLGA nerve tubes were more flexible or less stiff than single lumen PLGA tubes. D: Angle and force at yield point (movement the tubes started to deform). Data on point on the graphs are the mean ± SD for the four nerve tube samples per group.

The mean molecular weight of the residual tubes was analyzed using gel permeation chromatography (Waters 717 Plus Autosampler, Milford, MA). The results were compared with a calibration curve obtained from monodisperse polystyrene standards (Polysciences, Warrington, PA) [7].

COMPARISON OF SINGLE LUMEN AND MULTICHANNEL 75:25 PLGA NERVE TUBES

One ratio, 75:25 PLGA, was used to compare single lumen and multichannel nerve tubes for the properties of permeability, bending, deformation swelling and degradation. The same analysis as described above for single lumen nerve tubes was used for multichannel nerve tubes, except for the analysis of permeability (see later). In addition, scanning electron microscopy was performed to observe the

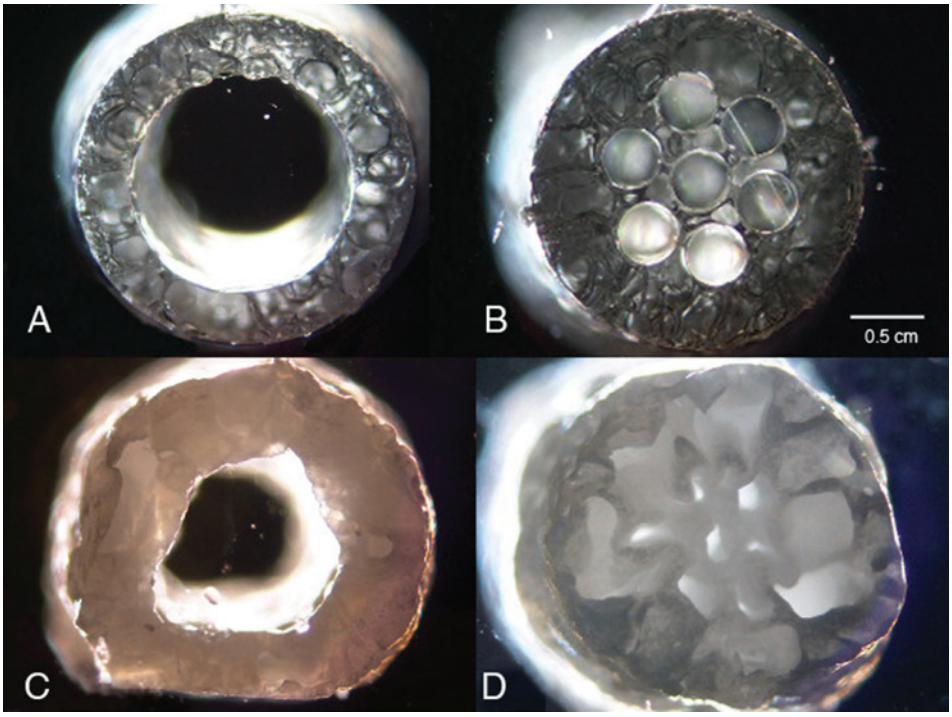

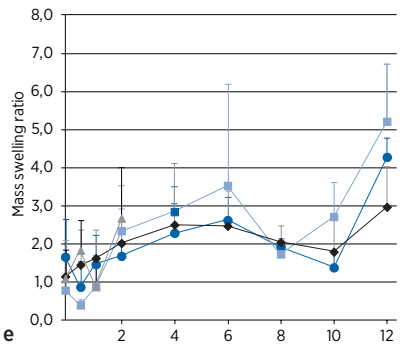

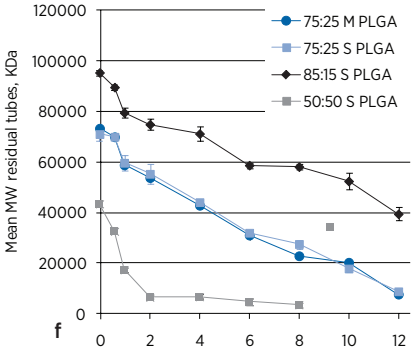

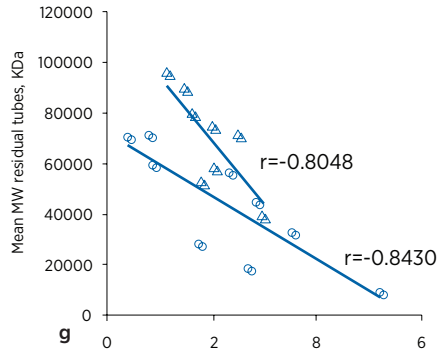

Figure 4

In vitro swelling and degradation. A: Single lumen 75:25 PLGA tube at day 0 dry. B: Multichannel 75:25 PLGA tube at day 0 dry. C: Single lumen 75:25 PLGA tube after 12 weeks in PBS. D: Multichannel 75:25 PLGA tube after 12 weeks in PBS. E: Mass swelling ratio measured for 12 weeks for single lumen 50:50, 75:25, 85:15 PLGA and 75:25 multichannel PLGA (MPLGA) tubes. Swelling ratios for 50:50 single lumen PLGA (SPLGA) tubes could not be measured after 2 weeks. F: Mean molecular weight (MW) of the residual PLGA nerve tubes analyzed over 12 weeks with gel permeation chromatography. G: Correlation between mass swelling ratio and mean molecular weight of the residual tubes for single lumen 75:25 and 85:15 PLGA.

porous structure of the tube and to analyze the surface texture of the lumen and channels.

FABRICATION TECHNIQUE OF MULTICHANNEL NERVE TUBES

Multichannel nerve tubes were fabricated with the same injection-molding technique as described earlier for the fabrication of single lumen nerve tubes. The same mold was also used, only with a different mold assembly (Figure 1). For multichannel nerve tubes, seven 0.4-mm diameter wires were inserted through endcaps. This was the optimal size and number of channels that could be fitted in the available cross-sectional lumen area of 1.6mm in diameter, with the minimal interchannel distance of 0.1mm that was needed to drill the holes in the endcaps. From the center line: 0.1mm + 0.4mm (channel) + 0.1mm + 0.4mm (channel) + 0.1mm + 0.4mm (channel) + 0.1mm = 1.6mm.

Scanning electron microscopy

Single lumen and multi-channel 75:25 PLGA tubes were cut longitudinally into halves and sputter coated (with Bio-Rad/Polaron E5400 High Resolution Sputter Coater). Pore structure was observed under a scanning electron microscope (Hitachi S-4700 Cold Field Emission Scanning Electron Microscope) at 25x magnification. Tiled pictures were taken and reconstructed in Adobe Photoshop (Adobe). The surface area of the lumen and channels was analyzed at 4,000 and 11,000x.

Permeability

The permeability of single lumen and multi-channel 75:25 PLGA tubes was tested by determining the rates at which molecules of fluorescein-isothiocyanate-dextran (FITC-D, Sigma, St. Louis, MO) with a range of molecular weights (10, 40 and 70kDa) diffused into the lumen and channels, respectively, of the tube. The rate of diffusion was determined from the fluorescence intensity inside the lumen or channels at different times.

Samples of tubes (5-mm samples from the mid-part) were placed vertically on a tissue culture dish. The bottom was sealed with a drop of paraffin. The dish was filled to a depth of 4 mm with a 10-mg/mL solution of FITC-D and placed on a modified fluorescence lighting stage (Microlite FL 1000 ultraviolet lamp, Three Rivers, MA) of a dissecting microscope (Carl Zeiss). Images were captured with a digital camera (Nikon Coolpixel 5700) through the objective of the microscope (Figure 5A). The concentration of FITC-D in the lumen or channels was determined from the fluorescent intensity. The intensity inside a channel was compared with the intensity of the known concentration outside the channel. Digital images were inverted and analyzed for color intensity in Adobe Photoshop (Figure 5B). For each tube, the measured concentration was displayed graphically as a function of time (Figure 5c). For multichannel tubes, this analysis was performed separately for

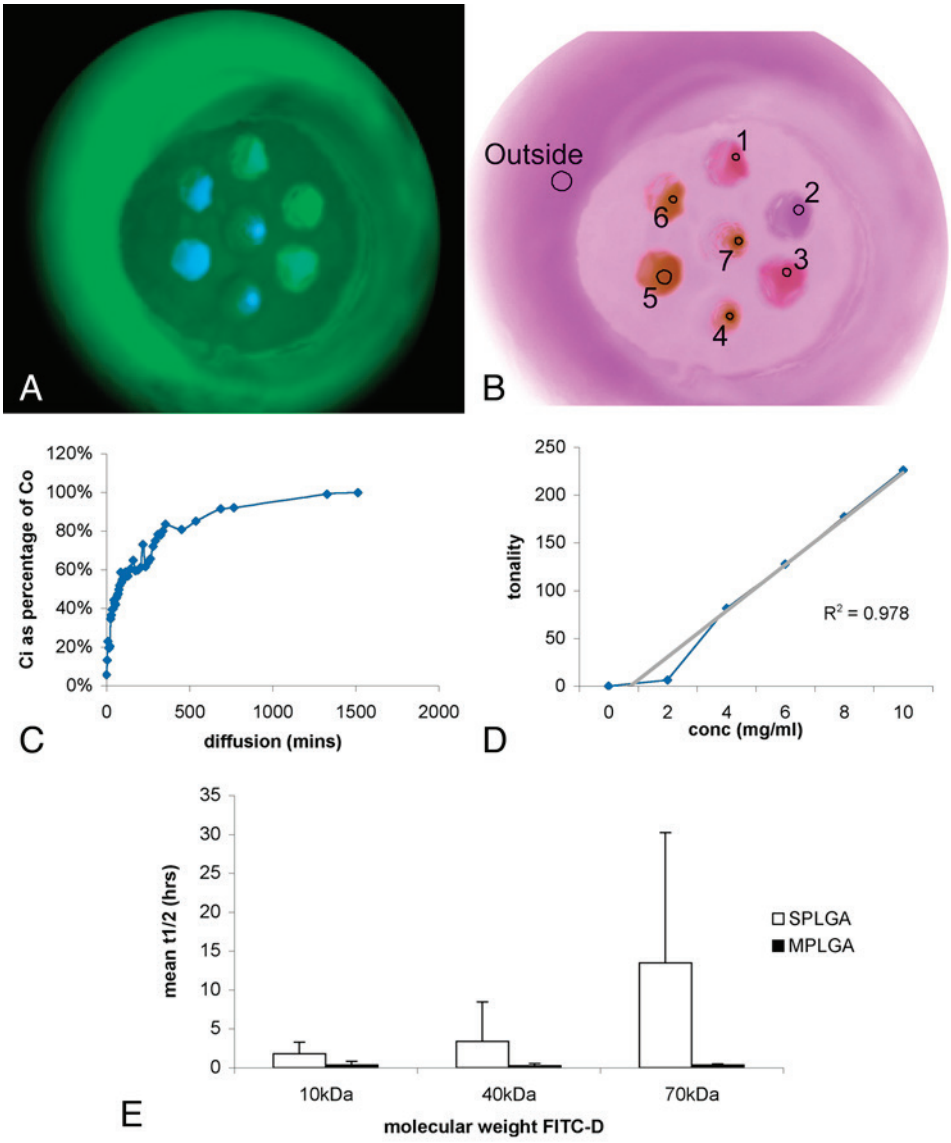

Figure 5

In vitro permeability. A: Digital image of a typical diffusion study with fluorescein isthiocyanate-dextran (FITC-D) molecules (taken through the objective of a microscope). B: Inverted images in Adobe Photoshop for measurements of color intensities: comparison of the inside of the channels with the known concentration of FITC-D outside the channels. In the electronic image, a representative sampling area was chosen outside the tube. Care was taken to avoid sampling heterogeneous color areas over the wax base. Similar areas were measured from each channel. Channels were consistently numbered 1-7. C: First-order kinetics of diffusion into a single lumen tube. $t_{1/2}$ was the time needed for the inside concentration (C_i) to be equal to 50% of the outside concentration (C_o). D: Linear correlation between known concentration and picture tonality

measured in Adobe Photoshop. The best correlation was found the blue color channel ($R^2 > 0.95$). Analysis of the intensity for longer periods also showed that there was no notable fading or change in outside concentration during the course of the experiment (unpublished data). E: Rate of diffusion for the different FITC-D molecule sizes (10, 40, and 70 kDa). Data points on the graphs are the mean ± SD for the four nerve tube samples per group. Multichannel 75:25 PLGA nerve tubes was not significant (for all molecular weights, $P > 0.05$). For multichannel nerve tube, the mean rate of diffusion was independent of the molecular size. For single lumen nerve tubes, the mean rate of diffusion tended to decrease with molecular weight (10 < 40 < 70 kDa), but this was not significant.

each channel. The rate of diffusion was presented for $t_{1/2}$, that is, the time at which the concentration in the lumen or channel was equal to 50% of the concentration outside. Four samples of tube were used per group. Before analysis, samples were prehydrated (same procedure as described earlier). Samples from multichannel tubes were always placed with the same orientation of numbered channels to investigate the influence of channel position with respect to the mold during fabrication. Channels were numbered according to their position in the mold (Figure 5B): 12 o'clock, number 1; 2 o'clock, number 2; 4 o'clock, number 3; 6 o'clock, umber 4; 8 o'clock, number 5; 10 o'clock, number 6; and center, number 7. The method was validated for a sequence of known concentrations. Linear regressions were calculated for the different color channels (original, gray, red, green, and blue).

Statistics

Statistical analysis was performed with the Student *t*-test (unpaired, 2-tailed *p* value) for comparison of two groups when the data were normally distributed. For comparison in which the data violated the assumptions of normality, a Mann-Whitney test was performed. For comparison of three groups or more, one-way analysis of the variance (ANOVA) was performed with a Bonferroni posttest. Linear correlations were investigated using Pearson analysis.

RESULTS

COMPARISON OF SINGLE LUMEN TUBES MADE WITH DIFFERENT PLGA RATIOS

Comparison of single lumen nerve tubes made with different PLGA ratios showed that the stiffness of the tubes was greater for higher PLGA ratios (85:15>75:25>50:50, $P < 0.05$, four samples were lost during the experiment) (Figure 3C). The difference however, was only significant for 50:50 versus 85:15 PLGA (posttest $P < 0.05$). The force needed to deform the nerve tube was also greater for higher PLGA ratios ($P < 0.05$) (Figure 3D), but again only significantly for 50:50 vs 85:15 (posttest $P < 0.001$). Swelling was greater for lower PLGA ratios (50:50 > 75:25 > 85:15) (Figure 4E). At 12 weeks, mass swelling ratios for single lumen 75:25 and 85:15 PLGA nerve

tubes were 5.2 and 3.0, respectively, but this difference was not statistically significant. The results for 50:50 single lumen PLGA nerve tubes could not be analyzed after 2 weeks because the tubes had completely lost their structural integrity. Also, the rate of degradation was greater for lower PLGA ratios (Figure 4F). There was a linear correlation between the results for the mass swelling ratio (Figure 4E) and mean molecular weight of the residual tubes in time (Figure 4F) (75:25 PLGA r = -0.8430, 85:15 PLGA r = -0.8048) (Figure 4G). The same bimodal distribution that was observed for the mass swelling ratios (Figure 4E) was also observed (although less obvious) for mean molecular weight of the residual tubes (Figure 4F). Results for the change in nerve tube dimensions showed that swelling significantly reduced the cross-sectional lumen or channel area of the tube (Figure 6).

Because of the increased swelling for the lower PLGA ratio (50:50) and decreased flexibility for higher ratio (85:15), we chose to use the 75:25 PLGA ratio, to compare single lumen and multichannel nerve tubes.

COMPARISON OF SINGLE LUMEN AND MULTICHANNEL 75:25 PLGA NERVE TUBES

Comparison of the permeability of single lumen and multichannel 75:25 PLGA nerve tubes showed that there was no difference in rate of diffusion of FITC-D molecules into lumen or channels of the tubes (Figure 5); multichannel nerve tubes appeared to be even more permeable, although this difference was only significant for 70-kDa FITC-D ($P < 0.05$) (Figure 5E). The $t_{1/2}$ for the individual channels of the multichannel tube was averaged because no difference was found for the rate of diffusion into the separate channels, including the most central one.

Scanning electron micrographs showed that both single lumen and multichannel 75:25 nerve tubes consisted of a highly porous internal structure surrounded by a continuous inside and outside polymer layer (Figure 2). At higher magnification, these layers were seen to be smooth and nonporous. The internal structure of the multichannel 75:25 PLGA nerve tube consisted of smaller pores when compared with the internal structure of single lumen 75:25 PLGA nerve tubes that appeared to be more interconnected (Figure 2, arrowheads).

Results for 3-point-bending showed that multichannel 75:25 PLGA nerve tube were less stiff or more flexible than single lumen 75:25 PLGA tubes (P <0.001), and at the same time more force was needed to deform multichannel 75:25 PLGA tubes (although not significantly) with a significantly larger angle at yield point (P <0.05) (Figure 3D).

Swelling was similar for single lumen and multichannel nerve tubes, but it had a significantly greater impact on the total cross-sectional channel area for multichannel 75:25 PLGA nerve tubes (43%) than on the total cross-sectional lumen area of single lumen 75:25 PLGA nerve tubes (at 10 weeks, 43 and 23%, respectively).

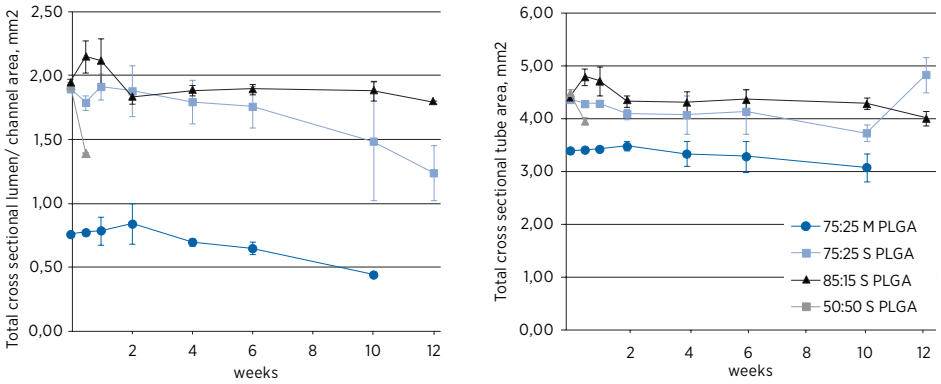

Figure 6

A: Change in tube dimensions for 12 weeks for the total cross-sectional nerve tube lumen/channel area. Dimensions for 75:25 MPLGA tubes could not be measured at 12 weeks. B: Change in tube dimensions for 12 weeks for the total cross-sectional tube area (including the total cross-sectional lumen/channel area). Data points on the graphs are the mean ± SD for the four nerve tube samples per time point per group.

DISCUSSION

The physical characteristics of a conduit may determine its ability to support regeneration [10-12, 18]. Therefore, *in vitro* characterization of different physical properties is important in the development of a nerve tube. Physical properties not only depend on the biomaterial that is used to fabricate the nerve tube, but also on the technique of fabrication, and different modifications to the common single lumen nerve tube [19], as in our study, multichannel nerve tube structure. In this study, we introduced a series of methods that can be used to characterize the physical properties of nerve tubes and especially that of conduits with more complex internal structures, including a novel method to test permeability.

Permeability

The fluorescence diffusion-intensity method introduced in our study was found to be a useful method to test the permeability of multichannel nerve tubes. There was a linear response with a high correlation coefficient between a sequence of known concentrations and color intensities. Multiple channels could be analyzed in time without direct sampling. Also analysis can be performed for a range of fluorescent dextran molecules comparable to the size of growth factors. Other methods can be used to measure the porosity of nerve tubes, including mercury intrusion porosimetry [15] or microcomputed tomography [20], but these methods do not necessarily correlate with effective diffusion that may also depend on the hydrophobic properties of the material and other properties.

Multichannel 75:25 PLGA tubes tended to be more permeable than single lumen 75:25 PLGA tubes. This difference can be explained by more interconnected pores in multichannel nerve tubes (Figure 2), although this was not quantified using, for example, microcomputed tomography [20]. Other techniques have been used to create porous nerve tube structures by cutting holes into the wall of the tube [11], by rolling of meshes [21, 22], by fiber spinning [23] or by adding salt or sugar crystals to a polymer suspension during fabrication and leaching them out afterward [15] or sugar [12]. The advantage of the solvent-evaporation technique is that porous nerve tubes can be created that have semipermeable inside and outside layers.

Bending and deformation properties

Testing of bending and deformation properties on a dynamic mechanical analyzer by 3-point-bending was useful in characterizing multichannel nerve tubes. Multichannel 75:25 PLGA tubes were more flexible than single lumen tubes but also more resistant to permanent deformation. Overall however, nerve tubes made from PLGA were stiff and easy to deform, with irreversible collapse of shape (with a mean angle at yield point of ~4° for single lumen 75:25 PLGA tubes and ~6° for multichannel 75:25 PLGA tubes). In addition to the tests performed in this study, dynamic mechanical analysis can be performed under different conditions, for example in PBS solution at 37°C. Repetitive bending can also be performed to test chronic wear. Although it is difficult to mimic exactly the *in vivo* conditions [24], 3-point bending is a useful test in the initial stages of the development of a nerve tube.

Swelling and degradation

As our study shows, swelling is also an important property to characterize in the development of a multichannel nerve tube. Swelling has a greater effect on the total cross-sectional lumen area of a multichannel tube than on a single lumen tube and initially is more than two times smaller (0.88 and 2.0 mm^2, respectively, calculated on the basis of the radius channel/lumen). Swelling can be explained by the formation of small degradation products that increase the osmotic value of the tube; the degradation of PLGA is an autocatalytic process that results in a faster rate of degradation on the inside than on the outside because of the accumulation of small degradation products on the inside (the outside forms a crust) [16, 25, 26]. This heterogeneous degradation of PLGA can also explain the bimodal distribution of mass swelling ratios in time. Finally, the faster rate of degradation for lower PLGA ratios explains the increased mass swelling for these ratios.

CONCLUSIONS

We present a series of methods to analyze important nerve tube properties that can also be applied for conduits with more complex structures (e.g. multichan-

nel nerve tubes). In our study, multichannel structure did not reduce permeability, and multichannel conduits were more flexible than single lumen ones made from the same biomaterial (75:25 PLGA) using the same fabrication technique. Overall however, nerve tubes made of PLGA were stiff and easily deformed. Swelling significantly reduced the total cross-sectional lumen area, especially in multichannel nerve tubes, which might explain the limited results we found for *in vivo* regeneration across single lumen and multichannel 75:25 PLGA nerve tubes [27] (**Chapter 7**). For future clinical application, more flexible multichannel nerve tubes are needed: ones that are permeable and do not swell. The methods for analysis of tube properties presented in this study can be used to optimize the development of multichannel nerve tubes.

ACKNOWLEDGEMENTS

We thank Frederick M. Schultz for the design and fabrication of the molds, Mark E Zobitz and Qingshan (Frank) Chen for their advice on the flexibility studies, Scott I. Gamb for his assistance with SEM analysis, Geraldine K. Bernard and Peggy L. Chihak for the graphic design.

REFERENCES

1. Bender, M.D., et al., *Multi-channeled biodegradable polymer/CultiSpher composite nerve guides.* Biomaterials, 2004. **25**(7-8): p. 1269-78.
2. Sundback, C., et al., *Manufacture of porous polymer nerve conduits by a novel low-pressure injection molding process.* Biomaterials, 2003. **24**(5): p. 819-30.
3. Stokols, S. and M.H. Tuszynski, *The fabrication and characterization of linearly oriented nerve guidance scaffolds for spinal cord injury.* Biomaterials, 2004. **25**(27): p. 5839-46.
4. Moore, M.J., et al., *Multiple-channel scaffolds to promote spinal cord axon regeneration.* Biomaterials, 2005.
5. Friedman, J.A., et al., *Biodegradable polymer grafts for surgical repair of the injured spinal cord.* Neurosurgery, 2002. **51**(3): p. 742-51; discussion 751-2.
6. Chen, B.K., et al., *Axon regeneration through scaffold into distal spinal cord after transection.* J Neurotrauma, 2009. **26**(10): p. 1759-71.
7. Moore, M.J., et al., *Multiple-channel scaffolds to promote spinal cord axon regeneration.* Biomaterials, 2006. **27**(3): p. 419-29.
8. Williams, L.R., et al., *Spatial-temporal progress of peripheral nerve regeneration within a silicone chamber: parameters for a bioassay.* J Comp Neurol, 1983. **218**(4): p. 460-70.
9. Lundborg, G., et al., *A new type of "bioartificial" nerve graft for bridging extended defects in nerves.* J Hand Surg [Br], 1997. **22**(3): p. 299-303.
10. Jenq, C.B. and R.E. Coggeshall, *Nerve regeneration through holey silicone tubes.* Brain Res, 1985. **361**(1-2): p. 233-41.

11. Jenq, C.B. and R.E. Coggeshall, *Permeable tubes increase the length of the gap that regenerating axons can span.* Brain Res, 1987. **408**(1-2): p. 239-42.
12. Rodriguez, F.J., et al., *Highly permeable polylactide-caprolactone nerve guides enhance peripheral nerve regeneration through long gaps.* Biomaterials, 1999. **20**(16): p. 1489-500.
13. Kim, D.H., et al., *Comparison of macropore, semipermeable, and nonpermeable collagen conduits in nerve repair.* J Reconstr Microsurg, 1993. **9**(6): p. 415-20.
14. den Dunnen, W., van der Lei, B, Robinson PH, Holwerda, A, Pennings, AJ, Schakenraad, JM, *Biological performance of a degradable poly(lactic acid-ε-caprolactone) nerve guide: influence of tube dimensions.* J Biomed Mater Res A, 1995. **29**: p. 757-766.
15. Widmer, M.S., et al., *Manufacture of porous biodegradable polymer conduits by an extrusion process for guided tissue regeneration.* Biomaterials, 1998. **19**(21): p. 1945-55.
16. Li, S., *Hydrolytic degradation characteristics of aliphatic polyesters derived from lactic and glycolic acids.* J Biomed Mater Res, 1999. **48**(3): p. 342-53.
17. Mikos, A.G., et al., *Wetting of poly(L-lactic acid) and poly(DL-lactic-co-glycolic acid) foams for tissue culture.* Biomaterials, 1994. **15**(1): p. 55-8.
18. Hudson, T.W., G.R. Evans, and C.E. Schmidt, *Engineering strategies for peripheral nerve repair.* Clin Plast Surg, 1999. **26**(4): p. 617-28, ix.
19. de Ruiter, G.C., et al., *Designing ideal conduits for peripheral nerve repair.* Neurosurg Focus, 2009. **26**(2): p. E5.
20. Moore, M.J., et al., *Quantitative analysis of interconnectivity of porous biodegradable scaffolds with micro-computed tomography.* J Biomed Mater Res A, 2004. **71**(2): p. 258-67.
21. Molander, H., et al., *Regeneration of peripheral nerve through a polyglactin tube.* Muscle Nerve, 1982. **5**(1): p. 54-7.
22. Dellon, A.L. and S.E. Mackinnon, *An alternative to the classical nerve graft for the management of the short nerve gap.* Plast Reconstr Surg, 1988. **82**(5): p. 849-56.
23. Aebischer, P., V. Guenard, and R.F. Valentini, *The morphology of regenerating peripheral nerves is modulated by the surface microgeometry of polymeric guidance channels.* Brain Res, 1990. **531**(1-2): p. 211-8.
24. Belkas, J.S., et al., *Long-term in vivo biomechanical properties and biocompatibility of poly(2-hydroxyethyl methacrylate-co-methyl methacrylate) nerve conduits.* Biomaterials, 2005. **26**(14): p. 1741-9.
25. Lu, L., C.A. Garcia, and A.G. Mikos, *In vitro degradation of thin poly(DL-lactic-co-glycolic acid) films.* J Biomed Mater Res, 1999. **46**(2): p. 236-44.
26. Lu, L., et al., *In vitro and in vivo degradation of porous poly(DL-lactic-co-glycolic acid) foams.* Biomaterials, 2000. **21**(18): p. 1837-45.
27. de Ruiter, G.C., et al., *Accuracy of motor axon regeneration across autograft, single-lumen, and multichannel poly(lactic-co-glycolic acid) nerve tubes.* Neurosurgery, 2008. **63**(1): p. 144-53; discussion 153-5.

CHAPTER 7

Accuracy of motor axon regeneration across autograft, single lumen and multichannel poly(lactic-co-glycolic acid) (PLGA) nerve tubes

Godard C.W. de Ruiter [1,3,5], Michael J. Moore [2], Martijn J.A. Malessy [5], Robert J. Spinner [3], Eric J. Sorenson [4], Bradford L. Currier [2], Michael J. Yaszemski [2], Anthony J. Windebank [1]

[1] Laboratory for Molecular Neuroscience, Mayo Clinic, Rochester MN, USA
[2] Laboratory for Biomedical Engineering, Mayo Clinic, Rochester MN, USA
[3] Department of Neurologic Surgery, Mayo Clinic, Rochester MN, USA
[4] Department of Clinical Neurophysiology, Mayo Clinic, Rochester MN, USA
[5] Department of Neurosurgery, Leiden University Medical Center, the Netherlands

Published in Neurosurgery, July 2008, Volume 63 (1); 144-153 (comments 153-155)

ABSTRACT

Background The accuracy of motor axon regeneration becomes an important issue in the development of a nerve tube for motor nerve repair. Dispersion of regeneration across the nerve tube may lead to misdirection and polyinnervation. In this study, we present a series of methods to investigate the accuracy of regeneration, which we used to compare regeneration across autografts and single lumen poly(lactic-co glycolic acid) (PLGA) nerve tubes. We also present the concept of the multichannel nerve tube that may limit dispersion by separately guiding groups of regenerating axons.

Methods Accuracy of motor axon regeneration across autograft, single lumen and multichannel poly(lactic co-glycolic acid) (PLGA) nerve tubes was investigated in a 1-cm gap of the rat sciatic nerve model 8 weeks after repair with simultaneous and sequential retrograde tracing. Simultaneous tracing of the tibial and peroneal nerve was performed to quantify axonal dispersion. Sequential tracing of the peroneal nerve was performed to quantify the percentage correctly directed peroneal motoneurons. In addition, quantitative results of regeneration were determined from compound muscle action potential recordings, nerve and muscle morphometry.

Results More motoneurons were found to have double projections to both the tibial and peroneal nerve after single lumen PLGA nerve tube (21.4%) than after autograft repair (5.9%). Multichannel PLGA nerve tube repair slightly reduced this percentage (16.9%), although not significantly. The direction of regeneration was nonspecific after all types of repair. Quantitative results of regeneration were similar after single lumen and multi-channel PLGA nerve tube repair, despite the smaller total cross-sectional channel area for multichannel nerve tubes. Overall quantitative results of regeneration were superior after autograft repair.

Conclusions Dispersion of regenerating axons across single lumen nerve tubes may limit the results in the repair of motor nerves innervating different distal targets. Multichannel nerve tubes proved to be a promising alternative, but need to be further optimized for possible future clinical application.

INTRODUCTION

Single lumen or hollow nerve tubes have been developed as alternative to nerve gap repair with an autologous nerve graft (**Chapter 5**). The advantage of repair with a nerve tube is the unlimited, right-of-the-shelf availability in a range of sizes without additional donor-site morbidity. The first biodegradable nerve tubes are now available for clinical use [1]. These nerve tubes are mainly used in the repair of small sensory nerves, such as digital nerve lesions with gaps up to 3 cm [2], and have recently been used in the repair of larger motor nerves [3, 4]. Single lumen nerve tube repair, however, may lead to inappropriate target reinnervation by the dispersion of regenerating axons across the graft [5]. This dispersion may result

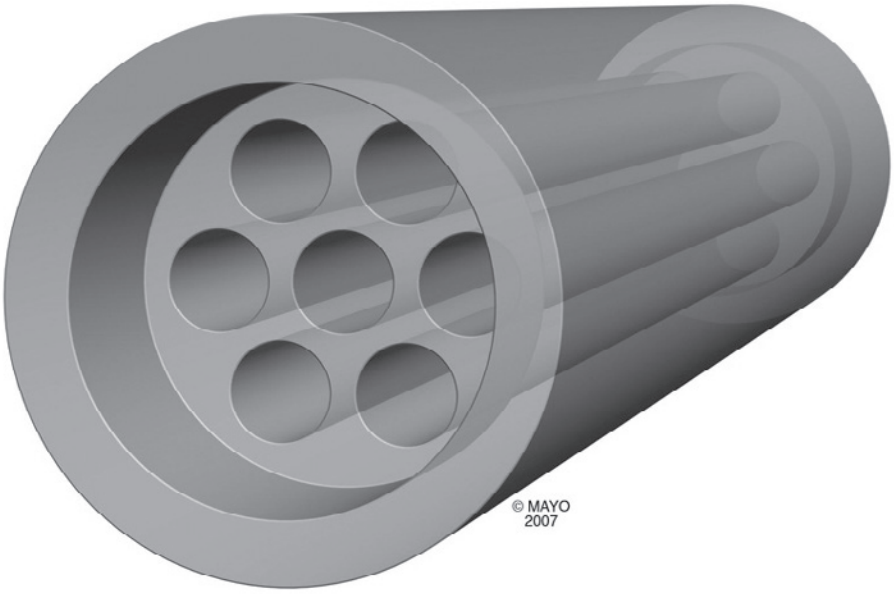

Figure 1
Drawing of a multichannel nerve tube with seven channels (400 μm in diameter) and sleeves on both ends for implantation.

in: 1) misdirection of regenerating axons, or 2) polyinnervation of different targets by dispersion of axonal branches originating from the same motoneuron. Dispersion probably occurs less after autograft repair by separate guidance of axonal branches inside the basal tubes, resulting in more grouped muscle fiber reinnervation [6]. Multichannel conduits (Figure 1), which have been developed for both experimental peripheral nerve repair [7-9] and spinal cord repair [10-12], may also limit this dispersion by separately guiding groups of regenerating axons inside the channels.

In this study, we used simultaneous and sequential tracing techniques to investigate the accuracy of motor axon regeneration across autograft, single lumen, and multichannel pol(lactic-*co*-glycolic acid) (PLGA) nerve tubes in a 1-cm gap of the rat sciatic nerve model. Simultaneous tracing of the tibial and peroneal nerves with fast blue (FB) and diamidino yellow (DY), respectively, was performed to quantify axonal dispersion for the percentage of motoneurons with double projections to both branches (Figure 2). Sequential tracing of the peroneal nerve with DY injection before repair and FB application 8 weeks after repair was used to quantify the percentage of peroneal motoneurons correctly directed to the peroneal nerve branch (Figure 3). In addition, quantitative results of regeneration were analyzed with compound muscle action potential (CMAP) recordings and nerve and muscle morphometry.

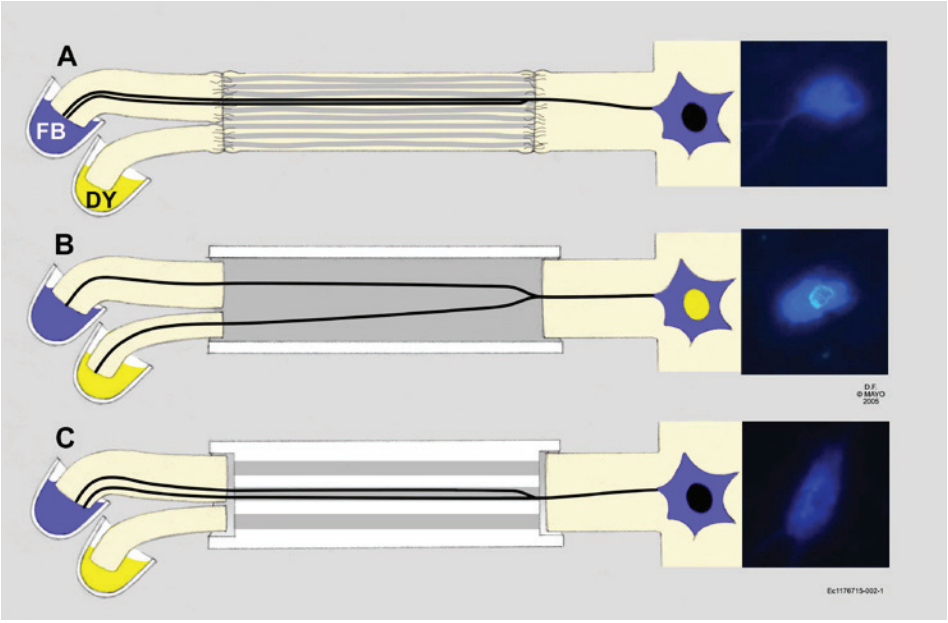

Figure 2
Technique of simultaneous retrograde tracing and concepts for the dispersion of regenerating motor axons after autograft, single lumen, and multichannel nerve tube repair. Simultaneous tracing: fast blue (FB) and diamidino yellow (DY) are applied to the tibial and peroneal nerve branches, respectively, 8 weeks after implantation. FB is transported retrograde to the cell body of the motoneuron and DY to the nucleus. A, after autograft repair, regenerating axons originating from the same motoneuron are contained by the basal lamina tubes, and both end up in the same (tibial) nerve branch. B, after single lumen nerve tube repair, axons originating from the same motoneuron disperse and end up separately in the tibial and peroneal nerve branches. C, after multi-channel nerve tube repair, axons originating from the same motoneuron are contained to the inside of a channel and end up in the same (tibial) nerve branch.

MATERIAL AND METHODS

Experimental groups

Sprague-Dawley rats weighing between 250 and 275 g were randomly assigned to one of the experimental groups for autograft (n = 17), single lumen (n = 30) or multi-channel (n = 30) (PLGA) nerve tube repair. For autograft repair, seven animals were used for simultaneous tracing, and six animals were for CMAP recording and nerve and muscle morphometry. Results for sequential tracing (n = 4) were obtained from another study [13] (**Chapter 4**). For single lumen and multichannel nerve tube repair, 12 animals were used for simultaneous tracing, 12 animals for sequential tracing, and 6 animals for CMAP recording and nerve and muscle morphometry. Control animals were included for simultaneous tracing (n = 4) and for CMAP recording and nerve and muscle morphometry (n = 4). All procedures were

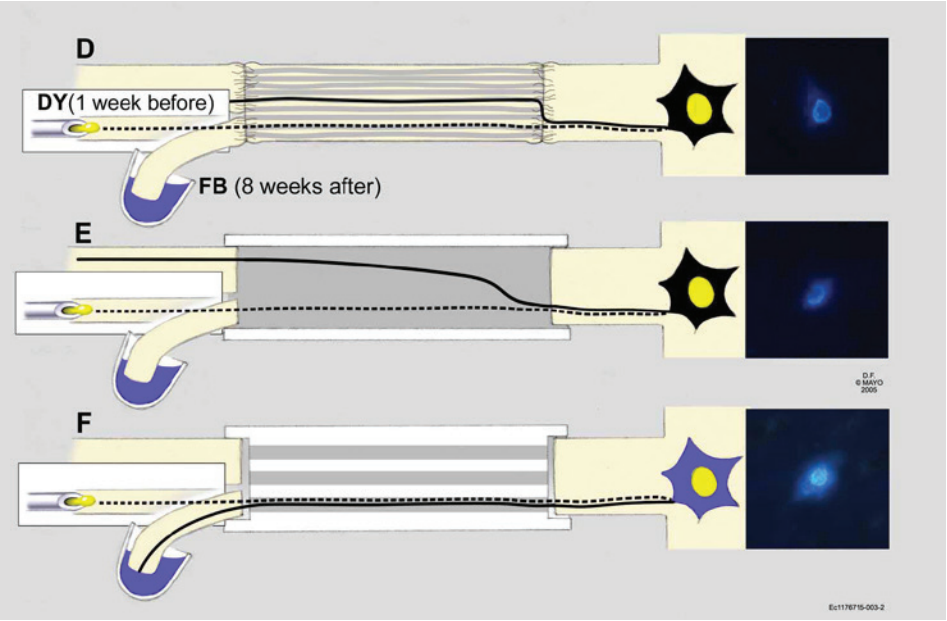

Figure 3

Technique of sequential retrograde tracing and concepts for misdirection of regenerating motor axons after autograft, single lumen, and multichannel nerve tube repair. Sequential tracing: the first tracer, DY, is injected into the peroneal nerve branch before nerve injury and is transported retrogradely to the motoneuron nucleus (dashed line). The second tracer, FB, is applied to the peroneal nerve branch 8 weeks after repair and is transported retrograde to the motoneuron cell body (continuous line). A, after autograft repair, regenerating axons are misdirected as a result of tension and/or fibrosis at the coaptation site. B, after single lumen nerve tube repair, there is no tension/fibrosis at the coaptation site, but axons may disperse. C, after multi-channel nerve tube repair, there is again no tension/fibrosis at the coaptation site and also no dispersion of regenerating axons. The dashed line illustrates the course of the original axon, and the continuous line illustrates the course of the regenerated axon form the same motoneuron.

approved by and performed according to the animal care guidelines of the Mayo Foundation Institutional Animal Care and Use Committee.

Single lumen and multichannel nerve tube fabrication

Single lumen and multichannel PLGA nerve tubes were fabricated through an injection-molding solvent evaporation technique [14] (**Chapter 6**) with the use of the same Teflon mold for the fabrication of single lumen and multichannel nerve tubes, except with different mold assemblies. The mold consisted of cylindrical spaces (2.1mm in diameter) with caps on both ends, through which either one stainless-steel wire (1.6mm in diameter), for the fabrication of single lumen nerve tubes, or seven stainless-steel wires (400μm in diameter), for the fabrication of multi-channel nerve tubes, were inserted (wires from Small Parts, Inc., Miami

Lakes, FL; mold designed and produced at Mayo Clinic). The caps for the fabrication of a multichannel nerve tube provided for an extra 1-mm sleeve on each end for implantation (Figure 1).
A solution of PLGA (copolymer ratio: lactic acid: glycolic acid, 75:25; 92kD, Fisher Scientific, Hampton, NH) in methylene chloride (300mg/450μl) was injected into the mold. The mold was placed in a vacuum for rapid solvent evaporation, thus creating a highly porous tube structure [14] (**Chapter 6**). Nerve tubes were sterilized in ethanol and pre-wetted in sterile phosphate-buffered saline before implantation.

Surgical techniques and animal care

Animals were deeply anesthetized with a mixture of ketamine (80 mg/kg) and xylazine (2.5 mg/kg), injected intraperitoneally. The sciatic nerve was exposed through a dorsal gluteal splitting approach with the aid of an operating microscope (Carl Zeiss, Inc., Oberkochen, Germany). For autograft repair, the nerve was transected at 2 sites, 1 cm apart, and immediately repaired with fascicular alignment by the use of 10-0 sutures (Ethilon; Ethicon, Inc., Piscataway, NJ; proximal 4 sutures, distal 3-4 sutures for the tibial branch and 2-3 for the peroneal branch).
For single lumen and multichannel nerve tube repair, the nerve was also transected at the same 2 sites. First, the proximal end was pulled 1mm into a 12-mm nerve tube (with a single 10-0 suture) while the original alignment was preserved; then the same procedure was performed distally for insertion of the tibial and peroneal branches separately, resulting in the creation of a 1-cm gap. Fibrin glue (Tisseel VH fibrin sealant; Baxter, Deerfield, IL) was applied to both ends of the tube to seal the lumen and sleeve. Multichannel nerve tubes were always implanted with the same orientation of the channels in relation to the nerve. The wound was closed in layers. The animals received buprenorphine hydrochloride (Reckitt Benckiser Healthcare, Slough, England) to control pain.
Postoperatively, animals were housed in individual cages with a 12-hour light-dark cycle, and water and food were available ad libitum. The operated limb was sprayed daily with Chewguard (Butler Corporation, Greensboro, NC) to prevent autotomy. A wire mesh was placed inside the cage to prevent contractures of the foot and ankle [15].

Simultaneous and sequential tracing

In the simultaneous tracing experiment, fast blue (FB) and diamidino yellow (DY) tracers (both from EMS-Chemie, Mannedorf, Switzerland) were applied to the tibial and peroneal nerve branches, respectively, 8 weeks after implantation (Figure 2). First, the tibial nerve was transected and placed in a cup containing 1.5μl of 5% FB solution for 30 minutes, followed by peroneal nerve transection and capsule application with 1.5μl of 5% DY solution for 30 minutes. The nerve ends were cleaned with 0.9% saline and sutured into surrounding fat tissue to prevent tracer leakage and cross-contamination.

In the sequential tracing experiment, 1µl of 5% DY solution was injected into the peroneal branch 1 week before implantation with the use of a scaled glass syringe (Hamilton Co., Reno, NV) with a 25-gauge needle (Figure 3). Eight weeks after implantation, the sciatic nerve was re-exposed, and the peroneal nerve was transected proximal to the previous injection site, and placed in a cup containing 1.5µl 5% FB solution for 30 minutes. Again, the nerve end was cleaned with 0.9% saline and sutured into surrounding fat tissue to prevent tracer leakage.
Animals were allowed to survive for 6 days after tracer application and then were perfused with phosphate-buffered salline and 4% paraformaldehyde and 10% sucrose. Spinal cord segments L1 to L6 were removed and post-fixed overnight. Tissue was embedded in tissue-freezing medium (Triangle Biomedical Services, Inc., Durham, NC) and stored at -80ºC until sectioning. Sagittal longitudinal 30-micron thick sections were cut on a cryostate at -20 ºC. Slides were immediately evaluated under a fluorescent microscope (Axioplan 2, Carl Zeiss, Inc. Oberkochen, Germany) with a DAPI filterset (360/400-nm bandpass excitation filter, 440-nm-long pass emission filter, and a 400nm dichroic beamsplitter) at magnification 20x with a planapochromatically corrected microscope 20x/0.75 objective (Plan Apochromat; Carl Zeiss, Inc.).
Neuronal profiles were counted in every section by one and the same observer that was blinded for the different experimental groups. Only profiles with a visible nucleus were counted. Profiles with blue cytoplasm and a dark nucleus were counted as FB-labeled, profiles with a yellow nucleus and dark cytoplasm as DY-labeled, and profiles with a yellow nucleus and blue cytoplasm as FB-DY double labeled. Profiles were counted in all sections. No corrections were made for the possibility of counting split motoneurons. Persistence of tracer in the sequential tracing experiment was analyzed from the distribution of double labeled profiles. If double labeled profiles were present in an area of the anterior horn that was normally exclusively occupied by tibial motoneurons (determined in normal animals in the simultaneous tracing experiment), the case was excluded. In the simultaneous tracing experiment, the percentage of double labeling for motoneurons with double projections was calculated by dividing the total number of double labeled profiles by the total number of labeled profiles. In the sequential tracing experiment, the percentage of correctly routed peroneal motoneurons was calculated by dividing the total number of double labeled FB-DY profiles by the total number of initially with DY labeled profiles (single labeled DY and double labeled FB-DY).

Compound muscle action potential recording

In the experiment on CMAP recording and nerve and muscle morphometry, CMAPs were recorded at 4, 6, 8, 10 and 12 weeks after implantation. CMAPs were recorded with the use of electromyography (Nicolet Viking IV; Viasys Healthcare, Inc., Conshohocken, PA) in the tibial and peroneal nerve-innervated footmuscles of the operated limb. Needle recording electrodes were placed in the plantar or dorsal footmuscles referenced to needle electrodes placed distally in the foot dig-

its. Needle-stimulating electrodes were placed directly posterior to the tibia with approximately 5 mm between the distal cathode and proximal anode. The stimulating electrodes were adjusted locally to produce the maximal CMAP amplitude. The stimulus was increased incrementally to produce a supramaximal response. CMAPs were recorded and analyzed for the amplitude, the area under the curve, and the latency of the action potential.

Nerve morphometry

The graft was reexposed 12 weeks after autograft, single lumen and multichannel nerve tube repair and fixed in situ with a 2.5% glutaraldehyde solution in phosphate-buffered saline for 30 minutes [16]. The graft was resected and placed in the same fixative overnight. Specimens (1 mm) were selected 2 mm proximal, at the mid, and 2 mm distal to the graft and embedded in spur resin for post-fixation in 1% osmium tetraoxide. Sections (1 μm) were cut with a glass knife on an ultramicrotome and stained with 1% phenylenediamine. The number of myelinated axons and mean size were analyzed at all three levels using the imaging system for nerve morphometry (Peripheral Nerve Laboratory of Dr Peter J. Dyck, Mayo Clinic Rochester). Between 500 and 600 myelinated axons were randomly selected in the slide and analyzed at 63x magnification [16].

Muscle morphometry

After resection of the graft, the soleus muscle was resected, placed in a plastic cup containing tissue-freezing medium, frozen with isopentane and liquid nitrogen, and stored at -80ºC until sectioning. Transverse 10 μm sections were cut on the cryostate at -20ºC. Sections taken from the mid-belly of the muscle were stained for myofibrillar ATPase at pH 9.4 according to the method described by Brook and Kaiser [17] staining slow (type I) fibers light and fast (type II) fibers dark. The total muscle fiber surface area was determined with an image analysis system (KS400 system, version 3.0; Zeiss, **Chapter 4**) [6]. The number of type I and type II fibers were counted. The mean muscle fiber size was calculated by dividing the total muscle fiber surface area by the total number of muscle fibers (type I and II).

Statistical analysis

Statistical analysis was performed by one-way analysis of variance with post-hoc Bonferroni tests. *P* values less than 0.05 were considered significant.

RESULTS

Number of analyzed animals per experimental group

Successful regeneration across the nerve graft (determined from the presence of FB-, DY-, or FB-DY-labeled profiles in the anterior horn after simultaneous tracing; the presence of FB-labeled profiles after sequential tracing; or the presence

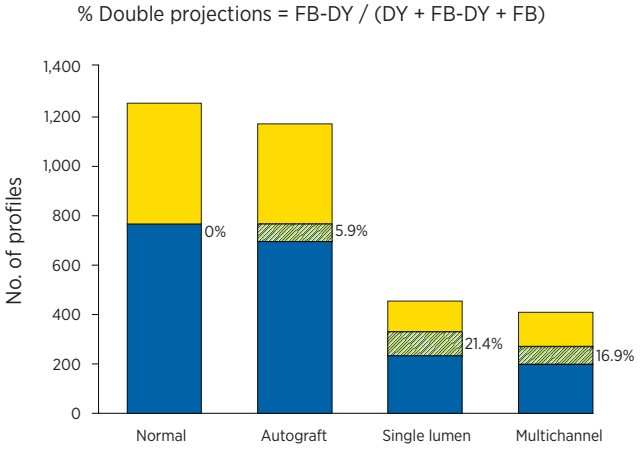

Figure 4

Bar graphs showing the results of simultaneous tracing for the mean number of FB-, DY- and FB-DY-labeled profiles and the percentages of double-projecting motoneurons in normal animals (n = 4), and after autograft repair (n = 7), single lumen (n = 4), and multichannel (n = 6) nerve tube repair. FB-labeled profiles (blue bars) represent motoneurons with exclusive projections to the tibial nerve. DY-labeled profiles (yellow bars) represent motoneurons with exclusive projections to the peroneal nerve. FB-DY-labeled profiles (striped bars) represent motoneurons with projections to both tibial and peroneal branch. No corrections were made for counting split cells (see material and methods). The percentages of double projections were calculated by dividing the number FB-DY-labeled profiles by the total number of profiles.

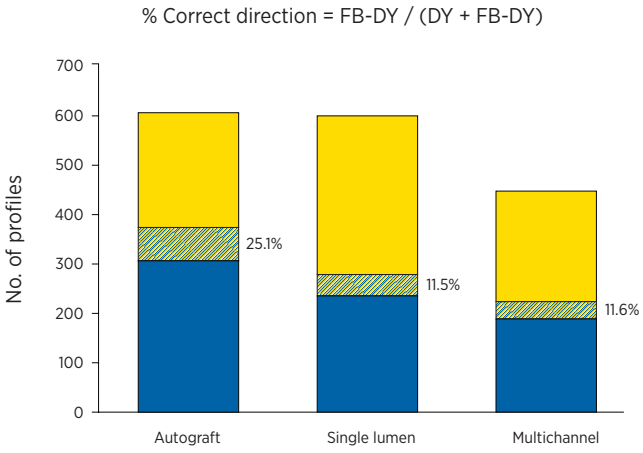

Figure 5

Bar graphs showing the results of sequential tracing for the mean number of FB-, DY-, and FB-DY-labeled profiles, and the percentages of correctly directed peroneal motoneurons after autograft (n = 4), single lumen (n = 5), and multichannel (n = 2) nerve tube repair. FB-labeled profiles (blue bars) represent misdirected tibial motoneurons. DY-labeled profiles (yellow bars) represent both misdirected and nonregenerated motoneurons. FB-DY-labeled profiles (striped bars) represent the number of correctly directed peroneal motoneurons. The percentages of correctly directed motoneurons were calculated by dividing the number of FB-DY-labeled profiles by the total number of DY-labeled profiles (DY and FB-DY).

of CMAPs and myelinated axons distal to the graft) was found in 17 (100%) of 17 animals after autograft repair, in only 16 (53.3%) of 30 animals after single lumen nerve tube repair, and in 13 (43.3%) of 30 animals after multichannel nerve tube repair. Animals that had no signs of regeneration across the nerve tube were excluded from further analysis because of the confounding effect on the results for the cases with successful regeneration (for example, including the cases with no signs of regeneration would lead to low percentages of double-projecting motoneurons because of 0% double-labeling in these cases). In addition, in the simultaneous tracing experiment, two cases of single lumen PLGA nerve tube repair were excluded from further analysis because of exclusive regeneration to the tibial branch (presence of only FB-labeled profiles). In the sequential tracing experiment, one case of single lumen nerve tube repair was excluded from further analysis because of persistence of the DY tracer, and one case of multichannel nerve tube repair was excluded because of failure to label the original peroneal motoneuron pool.

Simultaneous tracing

Spinal organization of single-labeled FB and DY profiles in control animals demonstrated that the tibial and peroneal motoneuron pool are normally present in two separate, nonintermingling spinal nuclei in the anterior horn at the levels L2 to L6. After autograft, single lumen and multichannel nerve tube repair, this spinal organization was disturbed, and FB-, DY- and FB-DY-labeled motoneurons were found intermingled.

The percentages of double projections were significantly different after autograft repair and for the cases with successful regeneration after single lumen and multichannel PLGA nerve tubes repair (F[2,14] = 16.5; P = 0.0002) (Figure 4). After single lumen nerve tube repair, more motoneurons had double projections to both the tibial and peroneal nerve branches (21.4 ± 4.9%) than after autograft repair (5.9 ± 2.9%; P-value <0.001 for posttest). The percentage after multi-channel tube was slightly lower (16.9 +/- 6.0%) compared with single lumen tube repair, but this difference was not significant. The total number of motoneurons from which axons had regenerated into in the tibial and/or peroneal nerve branch were significantly different from the normal number of motoneurons (1246 ± 43) (F[3.17] = 48.3; P < 0.0001), except after autograft repair (1140 ± 179). The total numbers after single lumen (448 ± 108) and multichannel (406 ± 156) nerve tube repair were not significantly different.

Sequential tracing

Differently labeled profiles (FB, DY, or FB-DY) were also found to be intermingled in the anterior horn after sequential tracing and autograft, single lumen, and multichannel tube repair. The size of the nucleus of profiles was variable, especially for DY profiles (ranging from 10 to 20 μm in diameter). Therefore, no corrections were made for the profiles counts based on the size of profile nucleus [18].

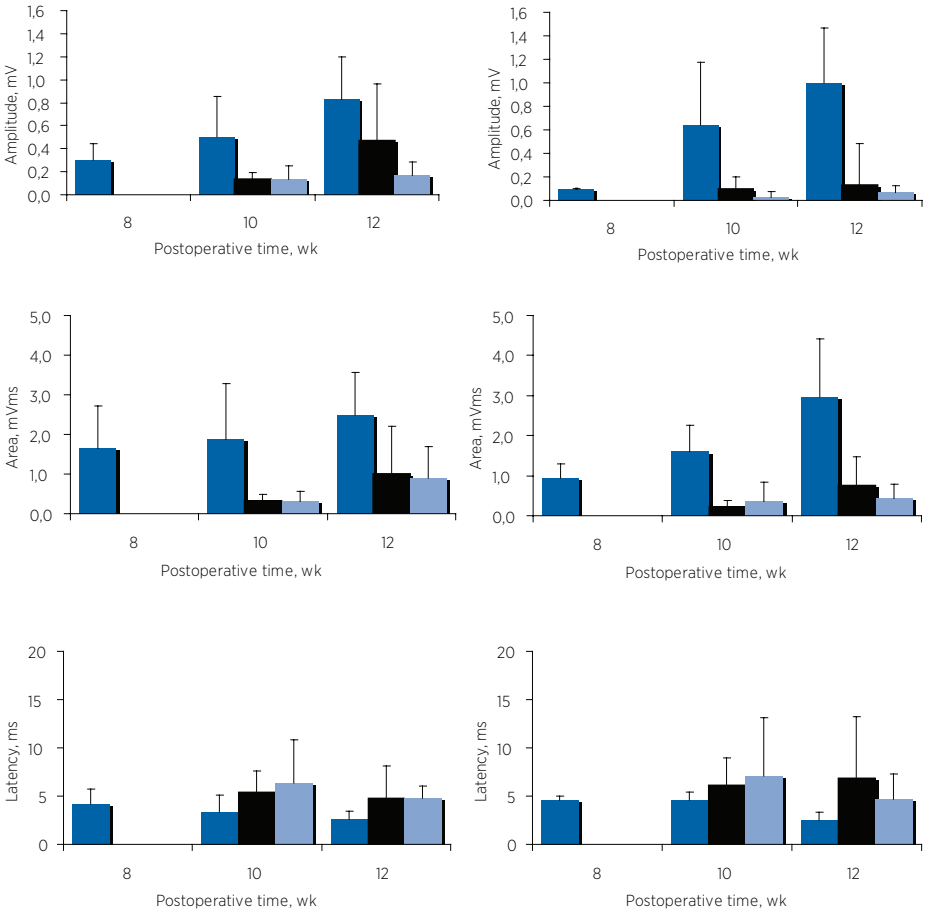

Figure 6

Results of compound muscle action potential recordings for the amplitude (A and B), area (C and D) and latency (E and F) recorded in the plantar (A, C, and E) and dorsal (B, D, and F) foot muscles 8, 10 and 12 weeks after autograft (blue), single lumen (black), and multichannel (light blue) nerve tube repair. Results are presented as means and standard deviations.

The percentages of correct direction were significantly different after autograft repair and for the cases of successful regeneration, after single lumen and multichannel PLGA nerve tube repair ($F[2,8] = 9.4$; $P = 0.008$) (Figure 5). The percentage after autograft repair (25.1 ± 6.6%) was significantly greater than with single lumen (11.5 ± 3.8%) and multichannel (11.6 ± 3.7%) nerve tubes ($P < 0.05$ for both posttests); however, these percentages were probably underestimated because of the decreased number of regenerated motoneurons after single lumen and multichannel nerve tube repair, resulting in a relatively high number of single DY-labeled

Table 1

Number and mean size of myelinated axons in normal rats, proximal to, at the middle of, and distal to the graft 12 weeks after autograft, single lumen, and multichannel nerve tube repair [a]

	Proximal to the graft		Middle of the graft		Distal to the graft	
Group	**No.**	**Size, mm**	**No.**	**Size, mm**	**No.**	**Size, mm**
Normal (*n*=4)						
mean	8,320	7.74	7,726	8.04	7,650	8.02
SD	533	0.33	378	0.39	464	0.46
Autograft repair (*n*=6)						
mean	11,958	4.66	14,459	3.43	11,578	3.74
SD	1,545	0.70	1,052	0.19	1,216	0.03
Single lumen nerve tube (*n*=4)						
mean	12,012	4.13	3,024	3.80	3,336	3.82
SD	3,404	0.63	1,094	0.34	2,205	0.04
Multichannel nerve tube (*n*=2)						
mean	10,650	3.81	2,929	4.01	3,320	4.04
SD	---[b]	---[b]	2,534	0.36	1,547	0.18

[a] SD, standard deviation.

[b] SD was incalculable because 1 sample was embedded longitudinally and therefore was lost.

profiles. After correction for the number of regenerated profiles found with simultaneous tracing, the percentages of correctly directed peroneal motoneurons are similar (27.4% for autograft, 32.0% for single lumen, and 35.6% for multichannel nerve tube repair). Considering the sizes of the peroneal and tibial motoneuron pool found with simultaneous tracing (487[39%] and 760[61%] motoneurons, respectively), theses percentages indicate that regeneration was non specific after all types of repair.

Compound muscle action potentials

The first CMAPs were detected at 8 weeks after autograft repair, compared with 10 weeks in the cases of successful regeneration after single lumen and multichannel PLGA nerve tube repair (Figure 6A and B). The CMAP amplitude and area recorded at 12 weeks were only significantly different in the dorsal foot muscles (F[2,9] = 9.7; P = 0.0057 and F[2,9] = 6.2; P = 0.0199, respectively); they were not significantly different in the plantar foot muscles (F[2,9] = 4.1; P = 0.05 and F[2,9] = 3.3; P = 0.08, respectively) (Figure 6A-D), with a significantly larger CMAP amplitude and area after autograft repair than with single lumen and multichannel nerve tube repair (P < 0.05 for both posttests, except for the comparison of the

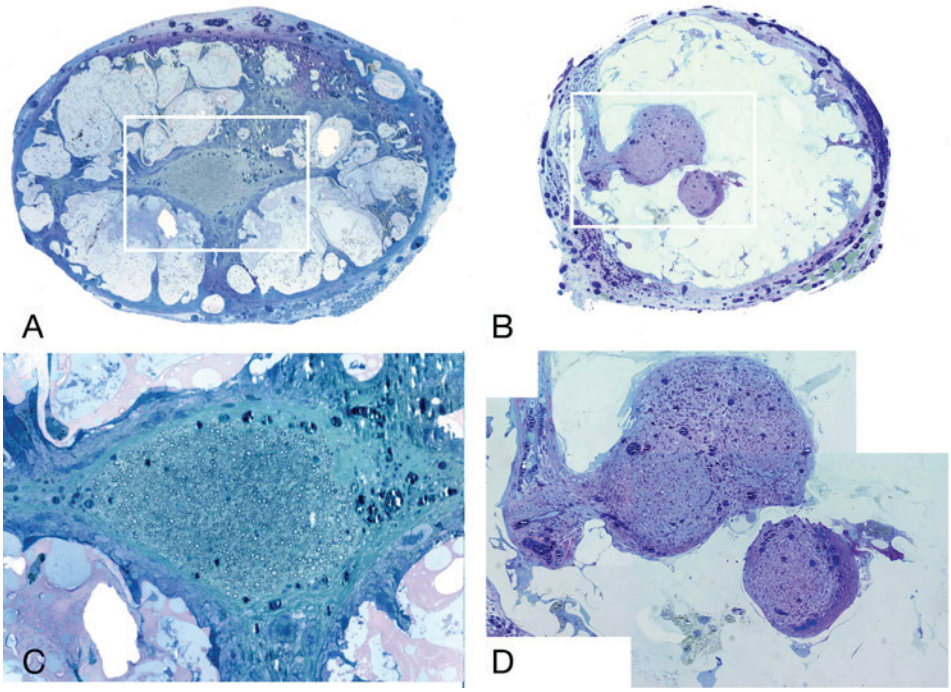

Figure 7

Microscopic sections from the middle of single lumen (A and C) and multichannel (B and D) nerve tubes 3 months after implantation. Toluidine blue for myelinated axons; original magnifications, x40 (A and B) and x160 (C and D). Note that after multichannel nerve tube repair, only 3 out of 7 channels were filled with myelinated axons. The original shape and orientation of the lumen/channels were lost, possibly because of swelling, degradation, and tapering or bundling of the channels towards the middle of the nerve tube.

CMAP area after autograft and single lumen nerve tube repair). The CMAP latency decreased with time after all repair techniques (Figure 6E and F).

Nerve morphometry

The number of myelinated axons at the midpoint and distal to the graft was significantly different from normal after autograft and after single lumen and multichannel PLGA nerve tube repair ($F[3,11] = 88.6$; $P < 0.001$ and $F[3,8] = 23.9$; $P = 0.0002$); four samples were lost because of longitudinal embedding (Table 1). After autograft repair, these numbers were significantly increased ($P < 0.001$ and $P < 0.05$, respectively). In the cases with successful regeneration after single lumen and multichannel PLGA nerve tube repair, these numbers were significantly decreased ($P < 0.001$ and $P < 0.05$ at the midpoint; and $P < 0.01$ and $P < 0.05$ distal to the graft, respectively).

Table 2

Mean muscle fiber size and distributions of type I and type II fibers in normal rats and 12 weeks after autograft, single lumen, and multichannel nerve tube repair

	Muscle morphometry	Muscle fiber types, no (%)	
Group	Mean muscle fiber size, x103 μm2	type I	type II
Normal (*n*=4)			
mean	6.60	648 (91)	69 (9)
SD	1.33	79 (4)	44 (4)
Autograft repair (*n*=5*)			
mean	4.50	307 (40)	447 (60)
SD	0.43	151 (10)	166 (10)
Single lumen nerve tube (*n*=3)			
mean	2.80	239 (40)	360 (60)
SD	0.48	22 (4)	58 (4)
Multichannel nerve tube (*n*=2)			
mean	4.00	536 (74)	197 (26)
SD	0.42	499 (1)	187 (1)

SD, standard deviation, *one soleus muscle was lost.

There was no significant difference for single lumen and multichannel PLGA nerve tube repair, despite the more than twofold smaller cross sectional lumen area available for regeneration in the multichannel nerve tube compared with the single lumen nerve tube (0.8 mm^2 for seven channels 400um in diameter, compared with 2.0 mm^2 for a single lumen nerve tube with a lumen diameter of 1.6mm), and the fact that only 3 out of 7 channels were filled with myelinated axons (Figure 7). The number of myelinated axons proximal to the graft was increased after all types of repair, although not significantly. The mean size of myelinated axons was significantly decreased compared with normal after all types of repair (proximal to the graft, $F[2,9] = 31.4$, $P < 0.0001$; mid, $F[3,11] = 190.2$, $P < 0.0001$; and distal, $F[3,8] = 257.0$, $P < 0.0001$), with no significant difference for autograft, single lumen, and multichannel nerve tube repair ($P > 0.05$ for all posttests, except for the comparison of single lumen and multichannel nerve tubes distal to the graft [$P < 0.05$]).

Muscle morphology

The number of muscle fibers was not significantly different in normal animals, after autograft, and in the cases with successful regeneration after single lumen and multichannel PLGA nerve tube repair (Table 2). The mean size of the muscle fib-

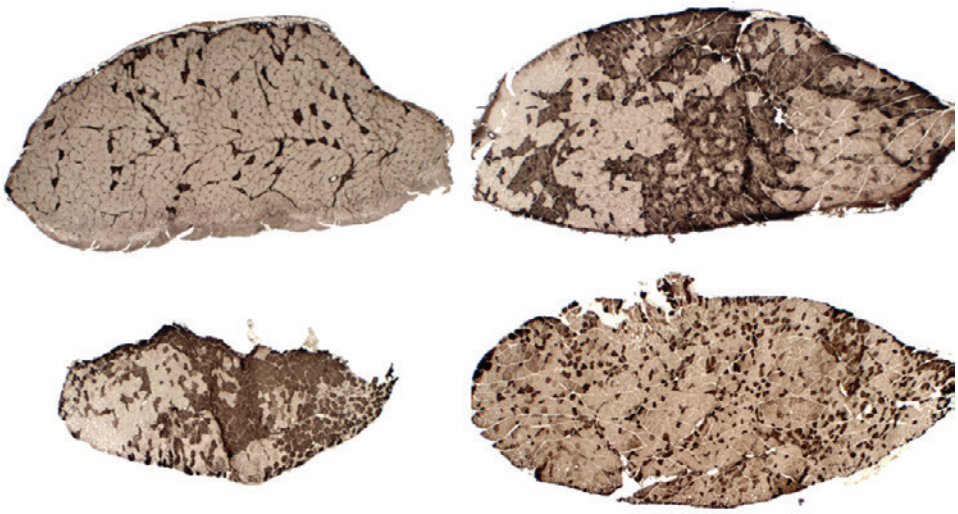

Figure 8

Microscopic sections taken from the mid-muscle belly of a normal soleus muscle (A) and after autograft repair (B), single lumen nerve tube repair (C), and multichannel nerve tube repair (D). Distribution of type I (light) and type II (dark) fibers changed from predominantly type I in normal muscle (A) to more type II than type I fibers after autograft repair (B) and single lumen nerve tube repair (C), but it was more equal to normal after multi-channel nerve tube repair (D).

ers was significantly different from normal after all types of repair (F[3,10] = 13.2; P = 0.0008), with no significant difference after autograft, single lumen, and multichannel PLGA nerve tube repair. The distribution of type I and type II muscle fibers had changed from more type I than type II in a normal soleus muscles (10:1) to more type II than type I after autograft and single lumen nerve tube repair (F[3,10] = 30.8; P < 0.0001, with P < 0.001 for both posttests) (Figure 8). For the successful cases of multichannel nerve tube repair, this distribution (3:1 ratio) was not significantly different from normal.

DISCUSSION

Accuracy of regeneration, ie, the event in which axons find their original or related end organ, is essential to obtain functional recovery when a nerve gap has to be bridged. Autografts are routinely used. In recent years, different single lumen nerve tubes have been introduced to serve as guidance for axonal outgrowth [1]. Little is known about the potential effect of single lumen nerve tube structure on the accuracy of regeneration as compared with the autograft [6], and even less is known about the effect of more complex structures, such as the multichannel nerve tube. In this study, we used simultaneous and sequential retrograde tracing techniques to compare the accuracy of motor axon regeneration across autograft,

single lumen and multichannel PLGA nerve tube repair in a 1-cm gap of the rat sciatic nerve model.

Single lumen nerve tube versus autograft repair

Simultaneous tracing in our study showed increased dispersion of regenerating axons in the cases in which there was successful regeneration across the single lumen nerve tube, with more double projecting motoneurons (21.4%) than after autograft repair (5.9%). Sequential tracing showed no difference in the direction of regenerating axons, with similar percentages of correctly directed peroneal motoneurons (after correction for the decreased number of regenerated profiles). Although various methods have been used to investigate the accuracy of reinnervation after single lumen nerve tube repair [19-23], this is, to our knowledge, the first study that compares the accuracy of regeneration across single lumen nerve tubes and autografts using simultaneous and sequential tracing.

Technical note

Numerous factors have to be considered in the interpretation of our results from tracing, including the size of the nerve gap, time point of evaluation, technique of tracing, and physical properties of the nerve tube. Dispersion has been found to increase with gap length [5]. Also, the number of double-projecting motoneurons has been found to decrease again with time [24]. Axonal branching with polyinnervation, followed by pruning, may therefore actually be a mechanism to correct for misdirection. This can explain the lower percentages of multiple-projecting motoneurons that were found by Valero-Cabré et al. 90 days after repair of 8-mm nerve gaps with single lumen poly-L-lactid-ε-caprolactone (6.0%) and silicone nerve tubes (10%) (compared with 5.6% after autograft repair) [22]. More research is needed to further investigate the influence of nerve gap size and the effect of the time point of evaluation in the analysis of the accuracy of regeneration across nerve tubes.

Factors concerning the techniques of tracing must also be considered. In this study, we used FB and DY tracers for both simultaneous and sequential tracing. This combination of tracers has been investigated in detail by Puigdellivol-Sánchez et al. [25-27]. The practical advantage of this technique is that both tracers can be visualized with the same filter. The sequential tracing technique with DY injection followed by FB application 8 weeks after repair has a high labeling efficiency (86.9% Puigdellivol et al. [25] and 91.3% **Chapter 4**) that is higher than the technique of tracer muscle injection [28], which has been used previously to investigate the accuracy of muscle reinnervation after nerve tube repair [19, 21]. There is also no significant fading of the first tracer (DY) or blockage of uptake of the second one (FB) [27]. Problems of the nerve injection technique, however, are: 1) persistence of DY tracer that may lead to overestimation of the percentage correctly directed motoneurons [26], and 2) damage to the nerve before nerve injury and repair that may affect regeneration to the peroneal nerve branch. In our study, only

one case of significant persistence of tracer was found. The number of motoneurons from which axons had regenerated into the peroneal branch did not appear to be different after simultaneous and sequential tracing (compare the number of DY- plus FB-DY-labeled motoneurons in Figure 5). In addition, the size of the nerve used for sequential tracing must be considered. Recently, Puigdellivol-Sánchez et al. [29] found a much higher percentage of correctly directed tibial motoneurons after direct coaptation repair (87%) by using the same technique and time point of evaluation. The difference with our results might be explained by the difference in repair techniques (direct coaptation vs graft repair [13], **Chapter 3**) and by the larger size of the tibial motoneuron pool.

Different physical properties of the nerve tube may also affect results. In our study, nerve tubes were made of PLGA using an injection-molding solvent evaporation technique [14] (**Chapter 6**). This biomaterial has been approved by the United States Food and Drug Administration (FDA); is biodegradable, biocompatible, and sterilizable; can be used for sustained-release drug delivery; and has been used previously to fabricate both single lumen and multichannel nerve tubes [8, 30, 31]. We recently found in vitro, however, that PLGA nerve tubes swell extensively, especially for lower lactic acid-to-glycolic acid ratios [14] (**Chapter 6**). Swelling may block the lumen or channels for regeneration or compress regenerated axons. In addition, acidic products formed during the degradation process may interfere with regeneration, and PLGA nerve tubes may elongate and collapse [30, 32]. These factors can explain the disappointing results found after PLGA nerve tube repair in our study, with successful regeneration across the nerve tube in only approximately 50% of the cases and, in these cases, with significantly decreased numbers of motoneurons from which axons had regenerated across the nerve tube, compared with normal and autograft repair.

Currently, we are investigating the use of novel biomaterials, for example, poly(caprolactone fumarate), which self-cross-links and can, therefore, also be used for the injection-molding technique of fabrication [33]. Another physical property that may affect the accuracy of regeneration is the permeability of the nerve tube, which may control the exchange of external and internal neurotrophic factors and molecules involved in the formation of the fibrin matrix inside the nerve tube [23]. Both single lumen and multichannel PLGA nerve tubes used in this study were highly permeable because of the solvent evaporation technique of fabrication [14] (**Chapter 6**).

Finally, it must be noted that we used an optimized technique for autografting with an immediate direct repair of matched size nerve stumps in this study. Results might differ from clinical nerve repair with interposition of multiple sural nerve grafts after a time delay. Moreover, in clinical nerve repair, it is not always possible to accurately determine and reconstruct the fascicular architecture of the nerve.

Although different factors must thus be considered in the interpretation of results, our study demonstrates that simultaneous and sequential tracing techniques provide new insights into the accuracy of regeneration across nerve tubes. Of course,

conventional evaluation methods (including CMAP recording and nerve and muscle morphometry) and functional analysis will still have to be performed, especially in the development of a nerve tube for possible clinical application.

Single lumen versus multi-channel nerve tube repair

To reduce dispersion, we designed a multichannel nerve tube and compared it with a single lumen nerve tube made of the same material using the same fabrication technique. Ih this study, no significant difference between single lumen and multichannel PGLA nerve tubes were found. In our opinion, however, the concept of a multichannel nerve tube that might limit dispersion remains appealing for the following reasons.

The only slight reduction in dispersion after multichannel nerve tube repair in this study might be explained by the findings that: 1) some axons had probably already branches before entering the channel (as can be concluded from the increased number of axons proximal to the nerve graft); 2) results for the number of axons FB- and DY-labeled profiles were variable (in some cases, even exclusive regeneration to the tibial branch was found); and 3) only three of seven channels were filled with myelinated axons 3 months after multichannel PLGA nerve tube repair (compared with the large number of basal lamina tubes in an autograft, approximately 1000 in the sciatic nerve in mice) [34]. Different modifications to the multichannel nerve tube, including more channels and different channel fillings, might further reduce dispersion. A total of seven channels (400 μm in diameter) was the maximum number that fit into a tube with a 1.6-mm inner diameter, because of the minimal distance of 100 μm needed to drill holes in the end caps through which wires were inserted. Currently, we are investigating the use of 3D-printing. With this fabrication technique, nerve tubes with any shape can be built in a layer-by-layer fashion. In the future, it might even be possible with this technique to reconstruct the fascicular architecture of the nerve, which often does not consist of longitudinally aligned fascicles, but instead forms an intraneural plexus [35].

Different channel fillings, including surface coatings, growth factors, and Schwann cells, may increase both the number of axons that regenerate and the number of channels across which axons regenerate. An additional advantage of the multichannel nerve tube, therefore, is that it provides more luminal surface area than single lumen nerve tubes for cell attachment and local release of incorporated growth factors. The finding that quantitative results of regeneration in this study were similar to repair with empty single lumen and multichannel nerve tubes (despite the more than twofold smaller cross sectional lumen area for multichannel nerve tubes) encourages us to investigate further the use of different channel fillings, including neurotrophic factors that might also be of interest to guide regenerating axons, which often wander at the suture site [36], straight into the channels [37].

Finally, of interest in this study was the distribution of type I and type II fibers that was closer to normal (10:1) after multi-channel tube repair (3:1) than after both single lumen tube and autograft repair (both 2:3) (Figure 8). Although this may be

explained by various factors, it may indicate more accurate muscle reinnervation after multichannel nerve tube repair. Both the small slow soleus muscle and large fast gastrocnemic muscle [38] are innervated by the lateral gastrocnemic nerve [39] and after nerve injury and repair, the fiber type distribution in soleus muscle may change as a result of misdirection [19, 40, 41]. Despite similar changes of correct direction, multichannel nerve tube repair may therefore lead to improved muscle reinnervation, for example, by a more organized distribution of regenerated motoneurons in the anterior horn. In the present study, differences in spinal organization could not be analyzed because of the small number of regenerated profiles. More research is needed to investigate this finding further.

CONCLUSIONS

Retrograde tracing in this study demonstrated the importance of investigating the accuracy of motor axon regeneration in the development of a nerve tube for motor nerve repair. We also presented the concept of the multichannel nerve tube that might limit dispersion, although in this study no statistical difference in accuracy of regeneration across single lumen and multichannel nerve tubes was found.

ACKNOWLEDGEMENTS

We thank LouAnn Gross for advice on embedding and staining techniques, Dr. Peter J. Dyck and JaNean Engelstad for advice on nerve morphometry, and Tony Koch for excellent animal care. Baxter Healthcare Corp., Westlake Village CA, provided the fibrin glue.

REFERENCES:

1. Schlosshauer, B., et al., *Synthetic nerve guide implants in humans: a comprehensive survey.* Neurosurgery, 2006. **59**(4): p. 740-7; discussion 747-8.
2. Weber, R.A., et al., *A randomized prospective study of polyglycolic acid conduits for digital nerve reconstruction in humans.* Plast Reconstr Surg, 2000. **106**(5): p. 1036-45; discussion 1046-8.
3. Ducic, I., C.T. Maloney, Jr., and A.L. Dellon, *Reconstruction of the spinal accessory nerve with autograft or neurotube? Two case reports.* J Reconstr Microsurg, 2005. **21**(1): p. 29-33; discussion 34.
4. Navissano, M., et al., *Neurotube for facial nerve repair.* Microsurgery, 2005. **25**(4): p. 268-71.
5. Brushart, T.M., et al., *Joseph H. Boyes Award. Dispersion of regenerating axons across enclosed neural gaps.* J Hand Surg [Am], 1995. **20**(4): p. 557-64.

6. Vleggeert-Lankamp, C.L., et al., *Type grouping in skeletal muscles after experimental reinnervation: another explanation.* Eur J Neurosci, 2005. **21**(5): p. 1249-56.
7. Bender, M.D., et al., *Multi-channeled biodegradable polymer/CultiSpher composite nerve guides.* Biomaterials, 2004. **25**(7-8): p. 1269-78.
8. Sundback, C., et al., *Manufacture of porous polymer nerve conduits by a novel low-pressure injection molding process.* Biomaterials, 2003. **24**(5): p. 819-30.
9. Yang, Y., et al., *Neurotrophin releasing single and multiple lumen nerve conduits.* J Control Release, 2005. **104**(3): p. 433-46.
10. Friedman, J.A., et al., *Biodegradable polymer grafts for surgical repair of the injured spinal cord.* Neurosurgery, 2002. **51**(3): p. 742-51; discussion 751-2.
11. Moore, M.J., et al., *Multiple-channel scaffolds to promote spinal cord axon regeneration.* Biomaterials, 2006. **27**(3): p. 419-29.
12. Stokols, S. and M.H. Tuszynski, *The fabrication and characterization of linearly oriented nerve guidance scaffolds for spinal cord injury.* Biomaterials, 2004. **25**(27): p. 5839-46.
13. de Ruiter, G.C., et al., *Misdirection of regenerating motor axons after nerve injury and repair in the rat sciatic nerve model.* Exp Neurol, 2008. **211**(2): p. 339-50.
14. de Ruiter, G.C., et al., *Methods for in vitro characterization of multichannel nerve tubes.* J Biomed Mater Res A, 2008. **84**(3): p. 643-51.
15. Strasberg, S.R., et al., *Wire mesh as a post-operative physiotherapy assistive device following peripheral nerve graft repair in the rat.* J Peripher Nerv Syst, 1996. **1**(1): p. 73-6.
16. Dyck, P.J., D. P.J.B., and J.K. Engelstad, *Pathologic alterations of nerves*. Peripheral Neuropathy, ed. D. P. and T. P.K. Vol. 1. 2005, Philadelphia: Elsevier. 733-829.
17. Brooke, M.H. and K.K. Kaiser, *Some comments on the histochemical characeterization of muscle adenosine triphosphate.* J Histoechem Cytochem, 1969. **17**: p. 431-432.
18. Abercrombie, M., *Estimation of nuclear population from microtome sections.* Anat Rec, 1946. **94**: p. 239-247.
19. Bodine-Fowler, S.C., et al., *Inaccurate projection of rat soleus motoneurons: a comparison of nerve repair techniques.* Muscle Nerve, 1997. **20**(1): p. 29-37.
20. Evans, P.J., et al., *Selective reinnervation: a comparison of recovery following microsuture and conduit nerve repair.* Brain Res, 1991. **559**(2): p. 315-21.
21. Rende, M., et al., *Accuracy of reinnervation by peripheral nerve axons regenerating across a 10-mm gap within an impermeable chamber.* Exp Neurol, 1991. **111**(3): p. 332-9.
22. Valero-Cabre, A., et al., *Superior muscle reinnervation after autologous nerve graft or poly-L-lactide-epsilon-caprolactone (PLC) tube implantation in comparison to silicone tube repair.* J Neurosci Res, 2001. **63**(2): p. 214-23.
23. Zhao, Q., et al., *Specificity of muscle reinnervation following repair of the transected sciatic nerve. A comparative study of different repair techniques in the rat.* J Hand Surg [Br], 1992. **17**(3): p. 257-61.
24. Hennig, R. and E. Dietrichs, *Transient reinnervation of antagonistic muscles*

by the same motoneuron. Exp Neurol, 1994. **130**(2): p. 331-6.
25. Puigdellivol-Sanchez, A., et al., *Fast blue and diamidino yellow as retrograde tracers in peripheral nerves: efficacy of combined nerve injection and capsule application to transected nerves in the adult rat.* J Neurosci Methods, 2000. **95**(2): p. 103-10.
26. Puigdellivol-Sanchez, A., et al., *Persistence of tracer in the application site--a potential confounding factor in nerve regeneration studies.* J Neurosci Methods, 2003. **127**(1): p. 105-10.
27. Puigdellivol-Sanchez, A., et al., *On the use of fast blue, fluoro-gold and diamidino yellow for retrograde tracing after peripheral nerve injury: uptake, fading, dye interactions, and toxicity.* J Neurosci Methods, 2002. **115**(2): p. 115-27.
28. Haase, P. and J.N. Payne, *Comparison of the efficiencies of true blue and diamidino yellow as retrograde tracers in the peripheral motor system.* J Neurosci Methods, 1990. **35**(2): p. 175-83.
29. Puigdellivol-Sanchez, A., A. Prats-Galino, and C. Molander, *Estimations of topographically correct regeneration to nerve branches and skin after peripheral nerve injury and repair.* Brain Res, 2006.
30. Evans, G.B., K. Widmer, M. Gürlek, A. Savel, T. Gupta, P. Lohman, R. Williams, J. Hodges, J. Nabawi, A. Patrick, C. Mikos, AG., *Tissue engineered conduits: the use of biodegradable poly-DL-lactic-co-glycolic acid (PLGA) scaffolds in peripheral nerve regeneration.* Biological matrices and tissue reconstruction., ed. H.R. Stark GE, Tanczos E. 1998, Berlin: Springer. 225-35.
31. Widmer, M.S., et al., *Manufacture of porous biodegradable polymer conduits by an extrusion process for guided tissue regeneration.* Biomaterials, 1998. **19**(21): p. 1945-55.
32. Evans, G.R., et al., *In vivo evaluation of poly(L-lactic acid) porous conduits for peripheral nerve regeneration.* Biomaterials, 1999. **20**(12): p. 1109-15.
33. Jabbari, E., et al., *Synthesis, material properties, and biocompatibility of a novel self-cross-linkable poly(caprolactone fumarate) as an injectable tissue engineering scaffold.* Biomacromolecules, 2005. **6**(5): p. 2503-11.
34. Giannini, C. and P.J. Dyck, *The fate of Schwann cell basement membranes in permanently transected nerves.* J Neuropathol Exp Neurol, 1990. **49**(6): p. 550-63.
35. Sunderland, S., *Nerve injuries and their repair: A critical appraisal.* . 1991, Melbourne: Churchill Livingstone.
36. Witzel, C., C. Rohde, and T.M. Brushart, *Pathway sampling by regenerating peripheral axons.* J Comp Neurol, 2005. **485**(3): p. 183-90.
37. Moore, K., M. MacSween, and M. Shoichet, *Immobilized concentration gradients of neurotrophic factors guide neurite outgrowth of primary neurons in macroporous scaffolds.* Tissue Eng, 2006. **12**(2): p. 267-78.
38. Young, B.L., et al., *An effective sleeving technique in nerve repair.* J Neurosci Methods, 1984. **10**(1): p. 51-8.
39. Gillespie, M.J., T. Gordon, and P.R. Murphy, *Reinnervation of the lateral gastrocnemius and soleus muscles in the rat by their common nerve.* J Physiol, 1986. **372**: p. 485-500.

40. Gillespie, M.J., T. Gordon, and P.R. Murphy, *Motor units and histochemistry in rat lateral gastrocnemius and soleus muscles: evidence for dissociation of physiological and histochemical properties after reinnervation.* J Neurophysiol, 1987. **57**(4): p. 921-37.
41. Ijkema-Paassen, J., M.F. Meek, and A. Gramsbergen, *Muscle differentiation after sciatic nerve transection and reinnervation in adult rats.* Ann Anat, 2001. **183**(4): p. 369-77.

CHAPTER 8

Controlling dispersion of axonal regeneration using a multichannel collagen nerve conduit

Li Yao [1,2], Godard C.W. de Ruiter [3,5], Huan Wang [2], Andrew M. Knight [2], Robert J. Spinner [3], Michael J. Yaszemski [4], Anthony J. Windebank [2], Abhay Pandit [1]

[1] National Center for Biomedical Engineering Science, National University of Ireland Galway, Ireland
[2] Laboratory for Molecular Neuroscience, Mayo Clinic, Rochester, USA
[3] Department of Neurologic Surgery, Mayo Clinic, Rochester, USA
[4] Laboratory for Biomedical Engineering, Mayo Clinic, Rochester, USA
[5] Department of Neurosurgery, Leiden University Medical Center, The Netherlands

Adapted from publication in Biomaterials 31 (2010): 5789-5797

ABSTRACT

Background Single channel conduits are used clinically in nerve repair as an alternative to the autologous nerve graft. Axons regenerating across single channel tubes, however, may disperse resulting in inappropriate target reinnervation. This dispersion may be limited by multichannel nerve conduits as they resemble the structure of nerve multiple basal lamina tubes. In this study, we investigated the influence of channel number on axonal regeneration using a series of 1-, 2-, 4-, and 7-channel collagen conduits and commercial (Neuragen ®) single channel conduits.
Methods Nerve conduits were implanted in rats with a 1cm gap of sciatic nerve. After four months, quantitative results of regeneration were evaluated with nerve morphometry and the accuracy of regeneration was assessed using retrograde tracing: two tracers being applied simultaneously to the tibial and peroneal nerves to determine the percentage of motoneurons with double projections. Recovery of function was investigated with compound muscle action potential recordings and ankle motion analysis.
Results Simultaneous tracing showed a significantly lower percentage of motor neurons with double projections after 2- (2.7%) and 4-channel (2.4%) conduit repair compared with single channel (7.1%) conduit repair (both $P<0.05$). The number of myelinated fibers and motoneurons were not significantly different for all types of conduit repair. Overall however, quantitative results of regeneration were superior after autograft repair.
Conclusion This study shows the potential influence of multichannel guidance on limiting dispersion without decreasing quantitative results of regeneration.

INTRODUCTION

The first single lumen nerve tubes made from various synthetic and natural materials are already available for clinical use (**Chapter 5**). However, as we found in **Chapter 7**, axons regenerating across single lumen nerve tubes might disperse, resulting in inappropriate target reinnervation. Multichannel nerve tubes might limit this dispersion. In the previous Chapter we compared regeneration across single lumen and multichannel conduits made of 75:25 poly(lactic co-glycolic acid) (PLGA). Although in that study a trend towards reducing axonal dispersion after multichannel compared with single lumen PLGA nerve tube repair was found, quantitative results of regeneration were limited by extensive swelling of the conduits, possibly due to the accumulation of small degradation products that increased the osmotic value inside the conduit structure (**Chapter 6**).
We therefore developed a novel series of conduits with improved physical properties to again investigate the influence of multichannel nerve tube structure on axonal regeneration, consisting of 1-, 2-, 4-, and 7-channel conduits made from collagen using an innovative multistep molding technique (Figure 1). The fabrication

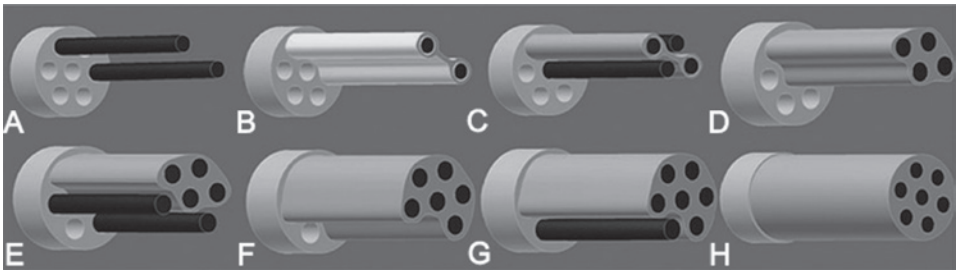

Figure 1

Multistep molding technique to create multichannel nerve tubes. (A) two stainless steel wires (black) were inserted through end caps (as described for the injection-molding technique, **Figure 1 Chapter 6**), (B) a collagen solution was allowed to self-assemble evenly on the wires and air-dried, (C) two additional wires were inserted into the two adjacent channels, (D) again, a collagen solution was allowed to self-assemble around the wires and air-dried, and so on for channel 5 - 7 (E-H). Obtained with permission from article Yao et al. (1).

technique and *in vitro* characterization of this series of collagen tubes have been reported separately [1].

Collagen is a naturally occurring protein that is ubiquitous among mammalian species. It is an important component of the nerve tissue matrix (epineurial, perineurial and endoneurial sheaths/ basal lamina tubes) and plays an important role in the regeneration process [2]. Collagen has been used before in the fabrication of nerve tubes [3], and there are also commercially available single channel collagen conduits (Neuragen®, Integra, NeuroMatrix® and Neuroflex®, both Stryker).

To investigate the influence of channel number on axonal regeneration we implanted the 1-, 2-, 4-, and 7-channel conduits in a 1cm gap of the rat sciatic nerve model. After 16 weeks of implantation, quantitative results of regeneration were analyzed with compound muscle action potential (CMAP) recordings and quantitative nerve morphometry. In a different experimental group qualitative restuls of regeneration were analyzed with simultaneous retrograde axonal tracing and ankle motion analysis. Finally, results were compared to repair with an autograft and repair with a commercially available conduit (Neuragen® from Integra).

MATERIALS AND METHODS

Fabrication of multichannel nerve conduits

1-, 2-, 4- and 7-channel collagen conduits were fabricated using a multistep molding technique (Figure 1). Similar mold assemblies to the ones used for the fabrication of multichannel PLGA nerve tubes (**Chapter 6**) were used (with wires inserted through endcaps), except that for 2- and 4-channel conduits wires of 530μm in diameter were used and for 7-channel conduits wires of 410μm in diameter. The distance between the 2 end caps was 1cm and the end-caps were layered to cre-

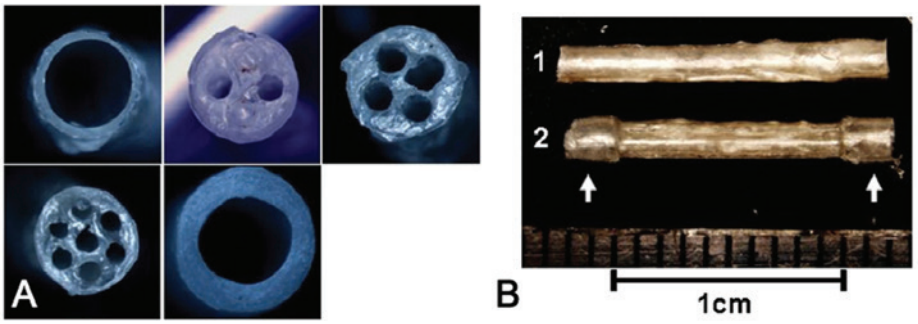

Figure 2
(A) transverse images of 1-, 2-, 4- and 7-channel collagen conduits and the NeuraGen ® (Integra) conduit, (B) longitudinal images of single channel and multichannel conduit with the sleeves at the end for nerve stump insertion.

ate a 1mm sleeve at the ends for insertion of the proximal and distal nerve ends. A solution of type I collagen (12mg/ml, in 10mM HCL, derived from bovine Achilles tendon by pepsin and acid extraction; purity 90%) was allowed to self-assemble around the wires in multiple steps (Figure 1) and was air dried. The collagen was then treated with a cross-linking solution of EDC (30mM) and NHS (10mM) in 2-morpholinoethanesulfonic acid solution (50mM; pH 5.5) overnight. After washing with NaH_2PO_4 (0.1M) and distilled water, the collagen was freeze-dried on the wires. Molds and wires were removed from the collagen conduits after freeze-drying. The same procedure was performed to fabricate 1-channel conduits, only a single stainless steel wire of 1.5mm in diameter was used. Samples of the different conduits are presented in Figure 2 A and B.

Animal procedures and experimental groups

In this study a total of 72 adult female Lewis rats, weighing between 190–220gr, were used. All experimental procedures were conducted according to animal care guidelines of the Mayo Foundation Institutional Animal Care and Use Committee. In the first experimental group, for the study of nerve morphometry and CMAP recording, 48 rats were randomly assigned to 6 subgroups: autograft, 1-, 2-, 4- and 7-channel collagen conduits, and commercial single channel conduit (Neuragen®, Integra Life Sciences Corporation, USA). In the second experimental group on simultaneous retrograde tracing and ankle motion analysis, 24 rats were randomly assigned to four subgroups: autograft, 1-, 2- and 4-channel conduits. In this latter group, treadmill training (running speed 15m/min, duration 10 min) was performed, one week post operation, and then 4 times per week for 8 weeks in total to prevent formation of contractures.

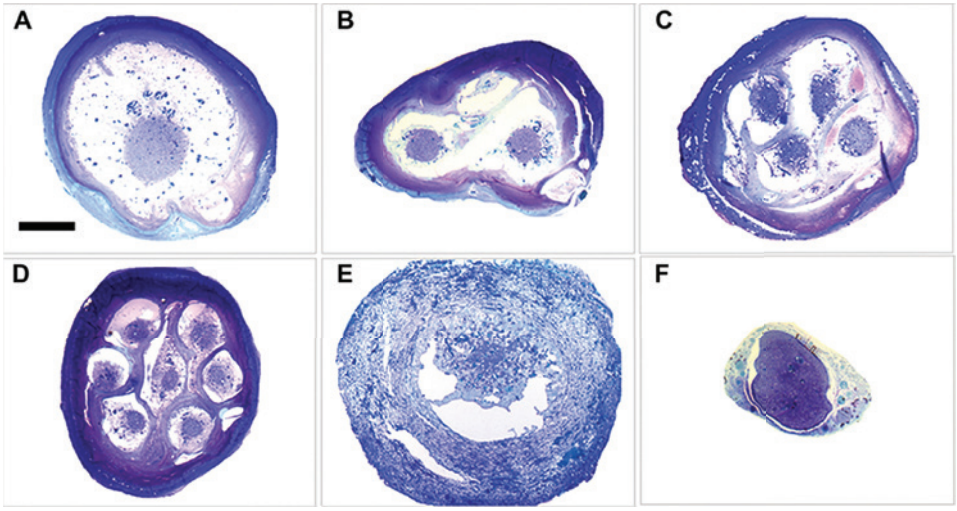

Figure 3

Microscopic images (5x magnification) of sections stained with toluidine blue taken through the middle of an (A) 1-channel, (B) 2-channel, (C) 4-channel, and (D) 7-channel collagen conduit, (E) a Neuragen® single channel conduit and (F) autograft. Scale bar, 500μm.

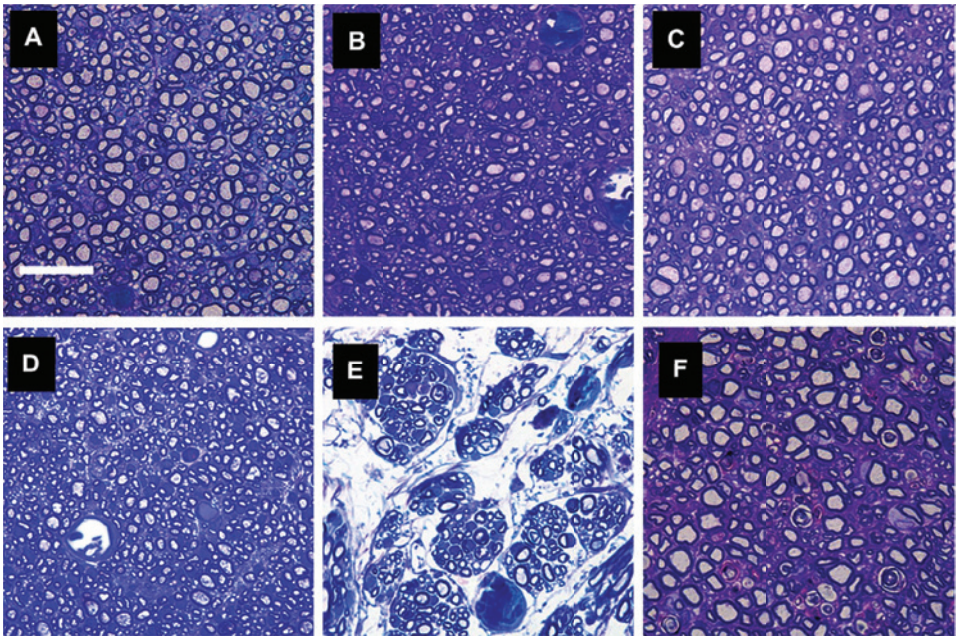

Figure 4

Microscopic images (40x magnification) of sections stained with toluidine blue taken through the middle of an (A) 1-channel, (B) 2-channel, (C) 4-channel, and (D) 7-channel collagen conduit, (E) a Neuragen® single channel conduit, and (F) autograft. Scale bar, 30μm.

Surgical procedure

Rats were anesthetized using 80mg/kg of ketamine and 5mg/kg of xylazine that were injected intraperitoneally. Dissection was performed with the aid of a Zeiss operating microscope (Carl Zeiss, Inc., Oberkochen, Germany). The left sciatic nerve was exposed and isolated at the midthigh level using a dorsal-lateral approach. A 5mm segment of the sciatic nerve was resected before the bifurcation of the nerve into the tibial and peroneal nerve branches. The proximal and distal nerve ends were inserted 1mm into the 12mm long tubes with 10-0 monofilament nylon sutures (Ethilon; Ethicon, Inc., Piscataway, NJ). The wound was subsequently closed in layers. The same procedure was performed for autologous nerve graft repair, except that a 1cm segment of sciatic nerve was transected and microsurgically repaired with 10-0 monofilament nylon sutures.

Nerve morphometry

After 16 weeks of implantation, in all animals of the first experimental group, the graft was re-exposed and fixed *in situ* with a Trump solution (4% formaldehyde and 1% glutaraldehyde in phosphate buffered solution) for 30 minutes [4]. The graft was resected and placed in the same fixative overnight. Specimens (2mm) at the midpoint of the graft were collected and embedded in spur resin. Sections (1μm) were cut with a glass knife on an ultramicrotome (Leica EMUC6 ultracut, Wetzlar, Germany). The sections of each specimen were stained with toluidine blue or 1% phenylenediamine for nerve morphometry. Nerve morphometry was performed on an image analysis system (see **Chapter 4** and **7** for more detailed description of the method). Briefly, the inner and outer borders of myelinated fibers was manually drawn for at least 500 myelinated fibers at 63x magnification in randomly selected areas in the slide to determine the number of myelinated fibers, the density of myelinated fibers, the mean diameter of myelinated fibers and the mean myelin thickness. SS

Compound muscle action potential recording

In all animals of both experimental groups, CMAPs were recorded before operation, 6, 8, 10, 12 and 16 weeks after nerve conduit implantation. Briefly, animals were first anesthetized with the procedure described above (surgical procedure), then CMAPs were recorded with an electromyography machine (Nicolet Viking IV; Viasys Healthcare, Inc., Conshohocken, PA) in the tibial and peroneal nerve-innervated foot muscles of the left limb (see **Chapter 4** and **7**). Needle recording electrodes were placed in the plantar or dorsal foot muscles referenced to needle electrodes placed distally in the foot digits. Needle-stimulating electrodes were placed directly posterior to the tibia with approximately 5mm between the distal cathode and proximal anode. The stimulating electrodes were adjusted locally to produce the maximal CMAP amplitude. The stimulus was increased incrementally to produce a supramaximal response. CMAPs were recorded and analyzed for the amplitude of the action potential.

Ankle motion analysis

In the second experimental group, ankle motion was analyzed before surgery, 1 week, 6 weeks, 12 weeks and 16 weeks after repair. The method as described in **Chapter 3** was applied only with the use of a different 2D ankle angle model. Three markers (instead of four) were placed on bony landmarks of the left leg: the tibia, the lateral malleolus, and the fifth metatarsal (the calcaneus as markation point was excluded in this model). Markers were tattooed to enhance the reproducibility of marker placement. Rats were filmed in a 1 meter long plexiglass runway with a black box on one end, which was alternately switched to the other end to get the rats to walk. The animal walking was filmed using a 60Hz digital camera (Dinion XF CCD Camera; Bosch Security Systems, Fairport, New York). After filming, the digital videos were processed using motion analysis software (Vicon Peak, Centennial, Colorado) that automatically tracks the markers on the leg of the rat in each frame of the video. The ankle joint motion was analyzed and the value of the ankle angle was compared at different moments during the step cycle: midstance (MSt), the moment the right foot in the air crosses the left foot in the stance (that bears the weight); terminal stance (TS), the moment the left foot comes off the runway (in normal animals, the moment of maximum plantar flexion); and midswing (MSw), the moment the left foot crosses the right foot in the stance (in normal animals, the moment of maximal dorsiflexion). Data for the ankle angles were reported in degrees of the intersection angle of the line connecting tibia and lateral malleolus and the line connecting lateral malleolus and fifth metatarsal.

Simultaneous retrograde tracing

In the second experimental group, after 16 weeks, all animals were anesthetized for simultaneous retrograde tracing (same method as described in **Chapter 7**). The nerve graft and distal tibial and peroneal nerve branches were exposed. First the peroneal nerve was transected and the proximal end was placed in a cup with 5% diamidino yellow (DY) (EMS-Chemie, Mannedorf, Switzerland) solution for 20 minutes. After that, the nerve end was cleaned, then sutured into and covered by surrounding fat tissue to prevent tracer leakage and cross-contamination. Then the tibial nerve was transected and the proximal nerve end was placed in a cup with 5% fast blue (FB) (EMS-Chemie, Mannedorf, Switzerland) solution for 20 minutes. Again, the nerve end was cleaned and then sutured into and covered by surrounding fat tissue. Six days after tracer application, the animals were transcardially perfused with 4% paraphomaldehyde and 10% sucrose in phosphate buffered solution (PBS). Spinal cord segments L1 to L6 were removed and post-fixed overnight. Sagittal longitudinal 30μm-thick sections were cut on a cryostat (LEICA Cryostat, CM3050S, Nussloch, Germany) at -20^{0}C. Slides were immediately evaluated under a fluorescent microscope (Axioplan 2; Carl Zeiss, Inc.). Neuronal profiles with blue cytoplasm and a dark nucleus were counted as FB-labeled, profiles with a yellow nucleus and dark cytoplasm as DY-labeled, and profiles with a yellow nucleus and blue cytoplasm as FB-DY-double-labeled profiles. All profiles in all sections

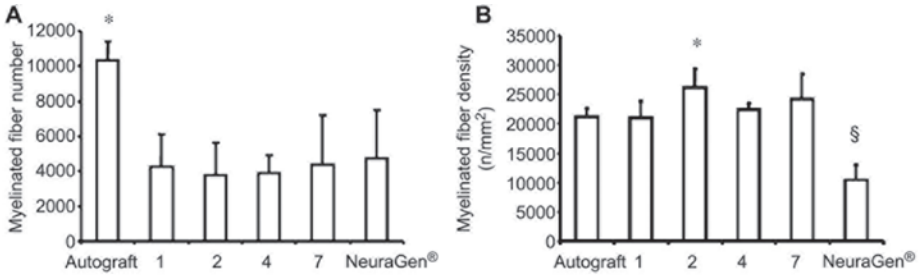

Figure 5

Results of nerve morphometry after autograft, 1-, 2-, 4-, 7-channel collagen conduit and Neuragen® single conduit repair for (A) the mean number of myelinated fibers (*, P<0.01, vs all the conduit groups) and (B) the mean myelinated fiber density (*, P< 0.05, vs the autograft, single channel and 4-channel tube graft groups; §, P<0.01, vs all the other groups).

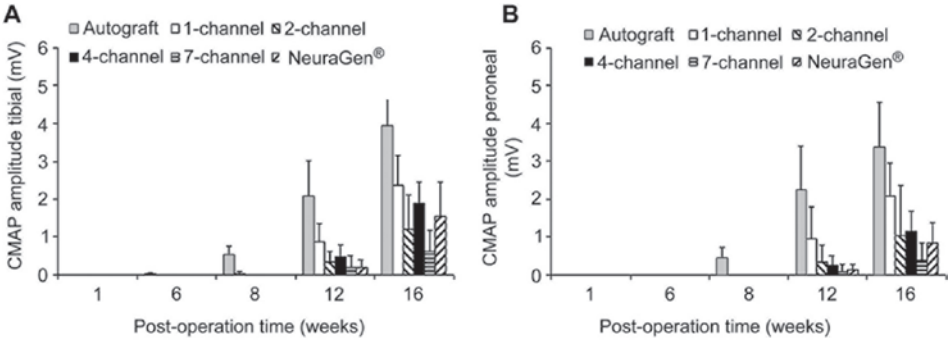

Figure 6

Results of the mean amplitude for compound muscle action potentials recorded in plantar and dorsal foot muscle respectively (A and B).

were counted. The percentage of double projections to both the tibial and peroneal nerve branch was calculated (as in **Chapter 7**) by dividing the total number of double-labeled neurons by the total number of neurons (single-labeled (DY and FB) and double-labeled neurons).

Statistics

The data were expressed as means ± SD and analyzed by using oneway ANOVA (post-hoc Bonferroni) with SPSS version 17.0 software package (SPSS Inc., Chicago, IL, USA). P values less than 0.05 were considered statistically significant.

RESULTS

Nerve morphometry

Successful regeneration (defined for the presence of myelinated axons at the mid of the conduit) was observed in 39 out of 40 cases of conduit repair (in one 2-channel conduit graft only fibrous tissue was present). Figures 3 and 4 show microscopic images (respectively taken at 5x and 40x magnification) of sections taken through the mid of all 6 types of grafts.

The mean number of fascicles (channels filled with myelinated axons) was one for the single channel conduits, 1.6 ± 0.8 for the 2-channel conduits, 3.75 ± 0.4 for the 4-channel conduits, and 6 ± 1 for the 7-channel conduits. The mean number of myelinated fibers was not significantly different between conduit groups (Figure 5A), but was significantly higher after autograft repair (10348 ± 1038, vs all conduit groups, $P<0.01$). The mean density of myelinated fibers (Figure 5B) was significantly higher for the 2-channel conduit group (vs autograft, 1-channel conduit, commercial conduit, $P<0.05$), and significantly lower for the commercial conduit group (vs all the other groups, $P<0.01$).

Compound muscle action potential recording

The first CMAPs were detected earlier after autograft repair compared with conduit repair (Figure 6) and the amplitudes at 12 weeks were significantly higher than for all other groups ($P<0.01$). At 16 weeks, the CMAP amplitudes of the 1- and 4-channel conduit groups were slightly larger than for 2- and 7-channel conduit groups, although not significantly different.

Simultaneous retrograde tracing

After autograft, 1-, 2- and 4-channel conduit repair, FB-, DY-, and FB-DY-labeled profiles in the anterior horn in the spinal cord were found intermingled, as reported in **Chapter 7**. The total number of labeled profiles was not significantly different after 1-, 2- and 4-channel conduit repair, but was significantly higher after autograft repair ($P<0.01$). Interestingly, the percentage of double-labeled neurons was significantly smaller after 2-channel (2.7% ± 2.9%) and 4-channel conduit (2.4% ± 1.5%) repair, compared with single channel conduit repair (7.1% ± 2.7%) (both $P<0.05$), indicating less axonal dispersion after multichannel nerve tube repair.

Ankle motion analysis

The ankle angle at terminal stance and midstance was significantly decreased one week after the surgery in all experimental groups (Figures 8B and 8C), and slowly recovered in time, but did not recover fully. The angle at midswing did not significantly change after surgery, but significantly increased in time. At 16 weeks there were no significant differences between all experimental groups for the different angles.

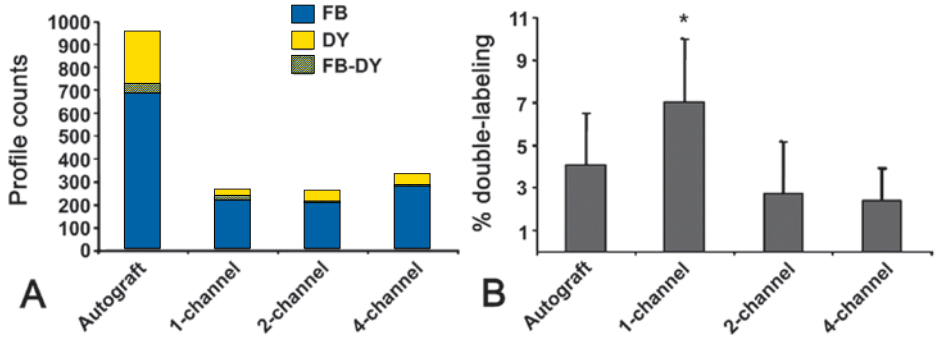

Figure 7

Results of simultaneous tracing for the mean number of FB-labeled, DY-lableed, and FB-DY double-labeled profiles (A) and percentages of double-labeled motoneurons (B) after autograft, 1-, 2-, and 4-channel conduit repair.

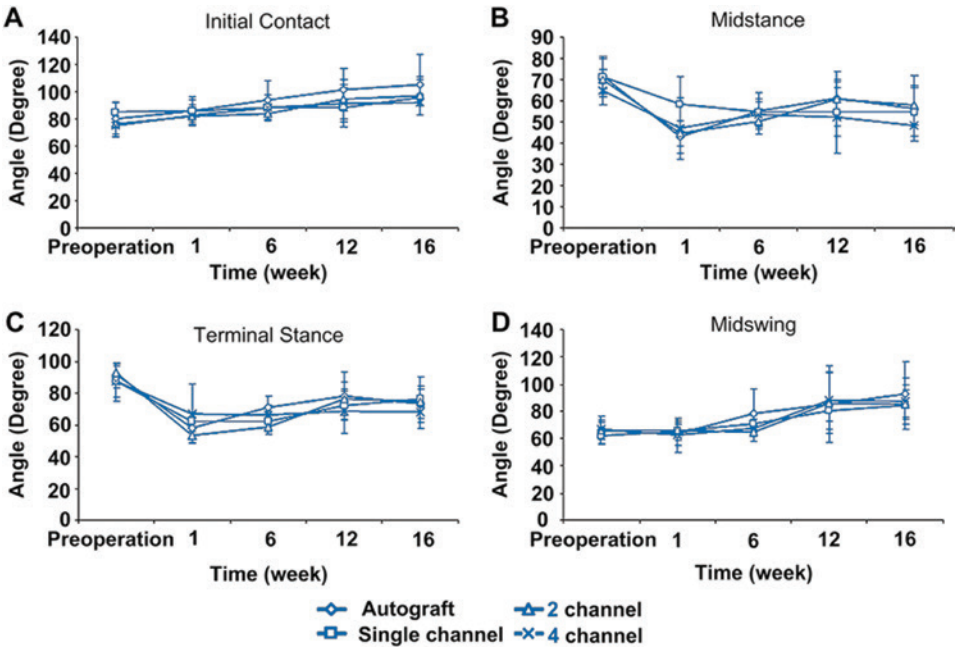

Figure 8

Recovery of ankle motion for the angles at (A) initial contact, (B) midstance, (C) terminal stance, and (D) mid-swing after autograft, 1-, 2-, 4- and 7-channel and Neuragen® conduit repair.

DISCUSSION

This study shows the influence of multichannel structure on limiting axonal dispersion without decreasing the quantitative results of regeneration. The numbers of regenerated myelinated axons and retrogradely labeled profiles were not significantly different for the different types of conduits despite the reduction in the total cross-sectional area for axons to grow into for multichannel nerve tubes (with ratios 1-channel versus 2-, 4- and 7-channel conduits of 4.1, 2.1 and 1.9, respectively). Also, almost all channels contained fascicles with myelinated fibers, contrary to our previous study (**Chapter 7**) in which only 3 out of 7 channels were filled with myelinated axons.

As for the limiting influence of multichannel structure on axonal dispersion; although the reduction might be small (with a 3x smaller percentage double projecting motoneurons after 4-channel conduit repair compared with single channel collagen conduit repair (2.4% vs 7.1%), it is important to realize that this percentage only indicates part of the axonal dispersion that occurs during regeneration across the conduit. In addition, there may be motoneurons with single projections that have dispersed and regenerated to the wrong target organ (See Figure 1, **Chapter 10**). This can be investigated for example with sequential retrograde tracing (**Chapter 7**). Also, the percentages double projections may have decreased in time due to pruning of misdirected collaterals in favor of correctly directed ones. The mechanism of pruning has been investigated in detail for motor versus sensory regeneration [5, 6], but may also affect the reinnervation of plantar and dorsiflexion muscles by tibial and peroneal motoneurons respectively. In our previous study (**Chapter 7**), in which the observation period was 8 weeks instead of 16 weeks, we also found much higher percentages of double projections (16.9% after multichannel nerve tube repair and 21.4% after single lumen nerve tube) compared with the percentages found in the present study. Pruning might thus be a mechanism to later correct for misdirection. Ideally however, initial targeting should be optimal. More channels will probably not completely solve the problem of misdirection, for as axons are also misdirected after autograft repair (**Chapter 4**), probably due to the dispersion of regenerating axons at the two coaptation sites [7], but modifying the multichannel conduit by for example adding supportive cells, growth factors in microspheres [8], and/or viral vectors expressing growth factors to attract axons into the distal pathways may overcome this problem of dispersion at the nerve-channel and channel-nerve junctions (for overview of different modifications, see **Chapter 5**). At the same time, these modifications can also increase the number of axons that regenerate into the conduit. An additional advantage of the multichannel conduit thereby is that it provides more internal lining for cell attachment and/or the controlled release of growth factors compared with single lumen conduits.

Finally, it should be noted that the quantitative results of regeneration in our study were still superior after autograft repair. Although this did not result in a better functional outcome, it is important to realize that an ideal alternative for the auto-

graft should perform better than the autograft. Only in selective cases of nerve graft repair, for example in the repair of small nerve defects (<3cm) in small nerves (for example digital nerves), the advantages of a conduit that is right-off-the-shelf available can outweigh the advantages of an autograft that consists of longitudinally orientated collagen tubes that contain Schwann cells.

CONCLUSION

This study clearly demonstrates the influence of multichannel guidance on limiting axonal dispersion without decreasing quantitative results of regeneration.

REFERENCES:

1. Yao, L., et al., *Multichanneled collagen conduits for peripheral nerve regeneration: design, fabrication, and characterization.* Tissue Engineering Part C, 2010. 16(6): p. 1585-1596.
2. Giannini, C. and P.J. Dyck, *The fate of Schwann cell basement membranes in permanently transected nerves.* J Neuropathol Exp Neurol, 1990. 49(6): p. 550-63.
3. Archibald, S.J., et al., *A collagen-based nerve guide conduit for peripheral nerve repair: an electrophysiological study of nerve regeneration in rodents and nonhuman primates.* J Comp Neurol, 1991. 306(4): p. 685-96.
4. Dyck, P.J., D. P.J.B., and J.K. Engelstad, *Pathologic alterations of nerves*. Peripheral Neuropathy, ed. D. P. and T. P.K. Vol. 1. 2005, Philadelphia: Elsevier. 733-829.
5. Brushart, T.M., *Preferential reinnervation of motor nerves by regenerating motor axons.* J Neurosci, 1988. 8(3): p. 1026-31.
6. Brushart, T.M., *Motor axons preferentially reinnervate motor pathways.* J Neurosci, 1993. 13(6): p. 2730-8.
7. Witzel, C., C. Rohde, and T.M. Brushart, *Pathway sampling by regenerating peripheral axons.* J Comp Neurol, 2005. 485(3): p. 183-90.
8. de Ruiter, G.C., et al., *Designing ideal conduits for peripheral nerve repair.* Neurosurg Focus, 2009. 26(2): p. E5.

CHAPTER 9

Directing regenerating motor axons to the peroneal division of the transected rat sciatic nerve by selective lentiviral vector-mediated overexpression of GDNF

Godard de Ruiter *[1,2], **MD, Stefan Hoyng** *[1,2], **MD, Ruben Eggers** [1,], **Martijn Tannemaat** [1,], **MD PhD, Joost Verhaagen, PhD** [1,] **Martijn Malessy**[1,2], **MD PhD**

* authors contributed equally

[1] Netherlands Institute for Neuroscience (NIN), Amsterdam, the Netherlands

[2] Department of Neurosurgery, Leiden University Medical Center, Leiden, The Netherlands

Background Misdirection of regenerating motor axons has a negative impact on the functional outcome following repair of peripheral nerves. The aim of this study was to direct regenerating motor axons using a lentiviral vector encoding for glial cell line-derived neurotrophic factor (LV-GDNF).
Methods LV-GDNF was selectively injected into the peroneal nerve in the rat sciatic nerve model, directly after transection and direct coaptation repair at the tibial-peroneal bifurcation. Results were evaluated after four weeks with simultaneous retrograde tracing of the tibial branch with fast blue (FB) and peroneal nerve branch with diamidino yellow (DY). Control groups consisted of LV-sGFP injection and direct coaptation repair without viral vector injection. In addition, nerve segments taken distally from the tracer application site were analyzed qualitatively for the presence of motor axons with ChAT immunohistochemistry.
Results After LV-GDNF injection, there was a doubling of the number of DY labelled motoneurons (from which axons had regenerated to the peroneal branch) compared to the control groups, with also a slight decrease in the number of FB labelled motoneurons (from which axons had regenerated to the tibial branch), although differences were only significant for the latter. Qualitative analysis of the nerves showed an increased presence of motor axons in the peroneal branch after LV-GDNF injection ($P<0.05$).
Discussion This study provides a first indication that LV-GDNF injection can be used to direct regenerating motor axons. Technical aspects of lentiviral vector injection and potential use in clinical nerve repair are discussed.

INTRODUCTION

Misdirection or misrouting of regenerating axons is one of the factors that can explain the disappointing functional recovery observed after nerve injury and repair [1]. For example, following repair of a motor nerve that is injured proximally to a branch point, regenerating motor axons may be directed to the wrong target branch and as a result reinnervate the inappropriate target muscle. This leads to co-contraction, because motoneurons that originate from the same moroneuron pool may have different target muscles. Co-contraction of different muscles may result in synkinesis (after facial nerve repair), mass movements (for example of shoulder and biceps muscles after repair of the upper trunk in brachial plexus injuries) or reduced motion (in case of reinnervation of antagonistic muscles).
In some patients it is possible to separately reconstruct nerve fascicles with different functions, but frequently, especially in more proximal injuries, this fascicular orientation may not be as well defined. In these cases misdirection at the coaptation site does occur, because axons do not always regenerate in a straight course to the distal nerve, but often first travel laterally at the coaptation site, before entering a distal endoneurial tube [2].

Little is still known about the impact of misdirection of regenerating motor axons on functional recovery, especially in motor nerve repair. Most research on specificity of regeneration has been performed in the femoral nerve that distally divides into the saphenous branch (SB), that is purely sensory, and a motor branch (MB) to the quadriceps muscle [3]. Experimental studies using this model have shown that motor axons preferentially regenerate towards the MB, which was termed *preferential motor reinnervation* [4, 5]. Although this phenomenon may be partially explained by *pruning* of misdirected collaterals [4] (that retract in favour of correctly directed axons), selective targeting of motor axons to the motor branch may be regulated by the expression of specific guidance molecules (e.g. L2 and HNK-1) [6, 7], by the expression of adhesion molecules (e.g. PSA-NCAM) by the regenerating motor axons [8], and/or the production of different growth factors by the Schwann cells in the MB [9].

In motor nerves innervating different distal target muscles, there are probably no such guiding cues or differences in growth factor expression between the different motor branches, for as many studies have shown limited specificity of regenerating axons for the different motor branches or target muscles [1, 10-15]. Most of these experiments on specificity of motor axon regeneration have been performed in the rat sciatic nerve model that distally branches into the tibial nerve (innervating muscles involved in plantar flexion) and peroneal nerve (innervating muscle involved in dorsiflexion). Recently, it was shown that following transection and surgical repair of the rat sciatic nerve only 42% of the peroneal motoneurons were correctly directed towards the peroneal nerve branch [1] (**Chapter 4**). Ankle motion analysis demonstrated that dorsiflexion function did not recover and that there were even signs for active plantar flexion during the swing phase (normally the moment of maximum dorsiflexion). This is probably due to the fact that the largest portion of peroneal motoneurons had regenerated towards the tibial nerve.

The goal of this study was to direct regenerating motor axons from the proximal stump selectively towards the peroneal nerve branch after transection of the sciatic nerve at the tibial-peroneal bifurcation by injection of a lentiviral vector encoding for GDNF into the peroneal nerve. Gene therapy is a new upcoming method in peripheral nerve regeneration that can also be applied to selectively guide regenerating axons by overexpression of certain growth factors [16-18]. In this study, GDNF was chosen because it is a potent neurotrophic factor for motor axons [19, 20]. The peroneal nerve was chosen, because of its relatively smaller size compared with the tibial nerve [1], which makes it is easier to detect a potential directing effect of LV-GDNF compared with injection into the larger tibial nerve. In addition, if possible to increase regeneration towards the peroneal branch, one of our future aims would be to investigate the impact on the recovery of dorsiflexion function). In the present study we first investigated the viral spread after LV-GDNF injection into the peroneal nerve using an ELISA set to detect the expression of GDNF at different levels in the sciatic, tibial and peroneal nerves. Second, the directing effect of LV-GDNF was analyzed four weeks after sciatic nerve injury and direct coaptation

repair at the bifurcation using simultaneous retrograde tracing with the tracers fast blue (FB) and diamidino yellow (DY) that were applied to respectively the tibial and peroneal nerve branches. ChAT immunohistochemistry was also performed to analyze the effect on the presence of motor axon branches in the distal nerves.

METHODS

Experimental groups

In all experiments adult female Wistar rats (Harlan, Horst, The Netherlands), weighing between 220 and 250g, were used. Animals were housed under standard conditions at a 12:12 h light/dark cycle with food and water ad libitum. All the experimental procedures were performed in accordance to the European directive for the care and use of laboratory animals (86/609/EEC) and were approved by the animal experimental committee of the Royal Netherlands Academy of Sciences. A total of 37 animals were used in this study. In 8 animals, the viral spread after LV-GDNF injection into the peroneal nerve was tested: in 4 animals the sciatic nerve was intact, in the other 4 animals the nerve was first transected and repaired at the tibial-peroneal bifurcation, after which the viral vector was injected. Simultaneous retrograde tracing and ChAT immunohistochemistry was performed in 8 animals 4 weeks after transection injury and repair, 8 animals after repair with LV-GDNF injection, and 8 animals after repair with LV-GFP injection. Five animals, in which the sciatic nerve was not transected, were used to obtain control values for simultaneous tracing.

Lentiviral vector preparation

The LV vectors encoding GDNF and stealth GFP have been described previously [21, 22]. The titers of the LV vector stocks were calculated by determining the p24 content (ng/μl) with an Elisa (zeptometrix, Buffalo, USA). Both vectors were titer matched to a viral titer of 6 ng/μl of p24 particles. All experiments were performed with the same viral stocks.

Surgical technique and animal care

Animals were deeply anesthetized with isoflurane (Isoflo, Abbotth, Hoofddorp, the Netherlands). The left sciatic nerve was exposed through a dorsal glutteal splitting approach with the aid of an operating microscope (OpMi-1, Zeiss, Sliedrecht, the Netherlands). The sciatic nerve was cut at the bifurcation into the tibial and peroneal nerve branches and these nerves were separately re-attached to the proximal sciatic nerve stump with 2-3 epineurial 10-0 nylon sutures for each branch (Ehtilon, Johnson& Johnson, Amersfoort, The Netherlands), while maintaining the correct fascicular orientation. In the viral vector groups subsequently, a 2 μl solution of 0.1M sodium buffered saline (pH 7.4) containing LV-GDNF or LV-GFP (total of 12 ng p24 particles) was injected into the peroneal nerve 5mm distal to the coaptation

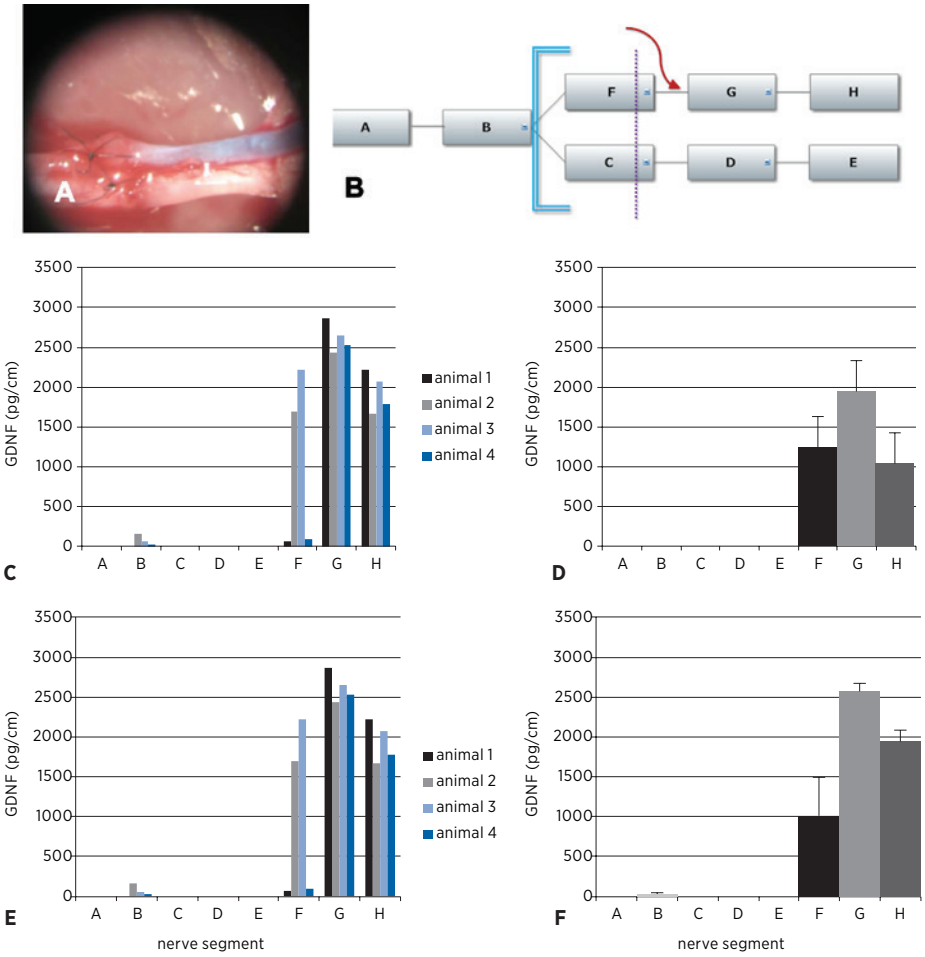

Figure 1

A: Example of LV-GDNF injection with viral spread (blue) in the peroneal nerve up to the repaired bifurcation. B: Schematic model of nerve segments (A-H) analyzed in ELISA experiment; blue line represents transection and repair site, purple line represents sites of tracer application, and red arrow site of viral vector injection. C: separate values for GDNF concentrations in different segments in unlesioned group, D: mean values (and SEM) for GDNF concentrations in different segments in unlesioned group, E: separate values for GDNF concentrations in different segments in the transection-coaptation repair group, D: mean values for GDNF concentrations in different segments in the transection-coaptation group.

site using a glass capillary with an 80 µm diameter tip attached to a 10 µl Hamilton syringe (Hamilton Company, Reno, USA) was added 0.1% Fast Green (Sigma, Zwijndrecht, the Netherlands) to the vector solution to visualize vector spread during injection. The needle was inserted through the epineurium into the peroneal fascicle and then was further inserted (1-2 mms) in a distal direction, parallel to

the nerve, before injection. Subsequently 2 μl of viral vector solution was slowly injected. Pictures of the viral spread were taken in all cases through the objective of the microscope. The needle was carefully removed to prevent leakage of vector solution. The skin was closed. Animals received buprenorphine (Schering-Plough B.V., Maarssen, the Netherlands) for postoperatieve analgesia and were kept at 37°C until recovery.

ELISA

Four weeks after injection of LV-GDNF, all animals in both groups (with and without transection injury and repair) were euthanized using Nembutal (sodium pentobarbital; 0.11ml/100g, Sanofi Sante, Maassluis, the Netherlands). The sciatic nerve was dissected into 0.5 cm segments starting proximal to the bifurcation (segment A and B) up to 1.5 distal to the bifurcation of the peroneal (segments F, G, and H) and tibial branch (segment C, D, and E) (Figure 1B). These segments were snap frozen on dry-ice. To quantify the amount of GDNF the nerve segments were homogenized in a mortar containing liquid nitrogen and resuspended in 250 μl lysis buffer (137 mM NaCl, 20 mM Tris/HCL, pH 8.0, Nonidet P40, 10% glycerol, 0.1% Polysorbate 20, 0.5 mM sodium othonovadate and 1 tablet / 50 ml of Roche total protease inhibitor).

The concentration of GDNF was measured with an ELISA kit (Emax #g7620, Promega, Madison, Wisconsin, USA) on high binding ELISA plates (Nunc-Immuno Maxisrop #439454). The procedure was performed following the manufacturer's instructions and the final GDNF concentration was expresses in pg/cm of nerve segment (A to H).

Simultaneous retrograde tracing

After four weeks simultaneous retrograde tracing was performed with FB and DY (both from EMS-Chemie, Mannedorf, Switzerland). First, the peroneal nerve was transected about 2 to 3mm from the coaptation site (proximal to the previous site of injection). The proximal end of the nerve was placed in a cup containing 1.5 μl of 5% DY solution for 30 minutes. After that the nerve end was cleaned with 0.9% saline and sutured in surrounding tissue to prevent tracer leakage and cross-contamination. Subsequently the same procedure was performed for the tibial nerve branch (also transection 2-3mm from the bifurcation site) except the nerve was placed in a cup containing 1.5 μl of 5% FB tracer. After one week of survival for retrograde transport of the tracer, the animals were perfused with phosphate-buffered saline and a solution containing 4% paraformaldehyde and 10% sucrose. Lumbar sections of the spinal cords were removed, postfixed overnight, and then cryoprotected for one day in 25% sucrose in o.1M sodium phosphate-buffered saline pH 7.4 (PBS). After that the tissue was embedded in tissue-freezing medium (OCT Compound 4583, Tissue-Tek, Sakura, Zoeterwoude, the Netherlands) by snap-freezing in 2-methylbutane and stored at -80°C until sectioning. Saggital longitudinal 30-μm-thick sections were cut on a cryostat at -20°C. Slides were immediately evaluated

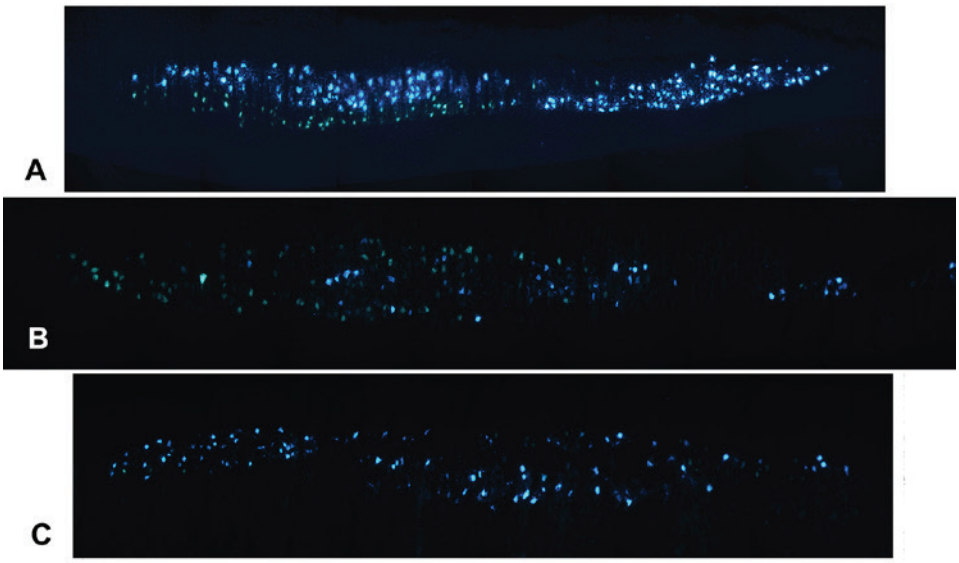

Figure 2

Microscopic images of examples of the distribution of FB- and DY-labeled motoneurons in the anterior horn of the spinal cord in a normal animal (A), and in animals after LV-GDNF (B) and LV-sGFP injection (C). FB-labeled motoneurons have blue cytoplasm. DY-labeled motoneurons have yellow nuclei. In the normal animal the DY- and FB-labeled motoneurons are grouped in two separate pools, respectively the peroneal and tibial motoneuronpool. In the case of LV-GDNF injection (B) there are clearly more DY-labeled motoneurons present than in the case of LV-sGFP injection (C). The organisation of profiles is lost and DY-labelled motoneurons are also present in the area normally exclusively occupied by tibial motoneurons.

at x10 magnification with a fluorescent microscope (Axioplan 2 Zeiss, Sliedrecht, the Netherlands). Profiles with a yellow nucleus were counted as DY labelled, with blue cytoplasm and a dark nucleus as FB labelled, and with blue cytoplasm and yellow nucleus as double FB-DY labelled (see figure). All sections were counted by one observer (GCdR), who was blinded for the experimental groups. No correction were made for the possibility of counting split motoneurons.

ChAT immunohistochemistry

Right after transection of the peroneal and tibial branches for tracer application, a 2mm nerve segment distal to the transection sites of these nerves were removed in the 6 of LV-GDNF and 7 of the LV-sGFP injected animals and fixed in 4% paraformaldehyde (in the other animals there was not 2 mm of tibial and/or peroneal nerve left distal to the tracer application sites). Immunohistochemistry was performed for choline acetyl transferase (ChAT). Briefly, sections were submitted to antigen retrieval (0.01 mg/ml proteinase K, 0.1% Triton X-100 in PBS) for 7 min followed by 3 washes in PBS. Endogenous peroxidase was blocked for 30 min (5% H2O2, 10%

methanol in PBS). Subsequently, the tissue was blocked using blocking buffer for 30 min (5% fetal bovine serum, 0.3% Triton X-100 in PBS). Sections were incubated at 4°C overnight in blocking buffer containing the primary antibody 1:200 (ChAT, Ab144p, Chemican, Hampshire, UK). After 3 washes the tissue was incubated for 2 hours with blocking buffer containing the seconday antibody 1:200)biotinylated horse anti-goat, Vector Laboratories, Burlingame, US). The sections were washed 3 times and incubated for one hour with avidin-biotin-peroxidase complex 1:800 (Vectastain Elite AC kit, Vector, Laboratories, Burlingame, USA). After washing in PBS sections were stained with 3.3'-Diamidinobenzidine (DAB) in TBS containing o.o1%H2O2 and 0.2 mg/ml NiSO4(NH4)2SO4 (nickel ammonium sulphate) resulting in a dark precipitate. Sections were dehydrated and embedded in Entalian.
Qualitative analysis of the slides for the presence of ChAT positive fibers was performed by 5 blinded observers who scored each slide as – (no ChAT positive fibers), +, ++, or +++, for increasing presence of ChaT fibers (Figure 2) . The scores of all observers for the same slide were added and mean scores per group were calculated.

Statistics

For all comparisons of values for different experimental groups an ANOVA test was used with posthoc Bonferroni test. For the qualitative analysis of motor axons branches (ChAT immunohistochemistry) by 5 blinded observers first the kappa value was calculated. *P*-values <0.05 were considered significant.

RESULTS

Transgene expression

Results of ELISA performed on 0.5 cm sections showed that the mean highest concentration GDNF was reached in the second segment (G) from the bifurcation (Figure 1D). The concentration of GDNF in the segment directly distal to the bifurcation (F) was slightly lower. Results were not significantly different after nerve transection and repair (Figure 1F), suggesting that transection and repair does not negatively influence the transfection of Schwann cells in the peroneal nerve branch. However, there were animal-to-animal variations (Figure 1C and E): in the group without lesion, there was one animal with a low concentration GDNF in segment F (<500 pg/cm) and in the group with transection injury and repair, there were 2 animals with concentrations <100 pg/cm. These animals did have increased levels of GDNF in next segment (G), but thus not in the segment adjacent to the transection and repair site. Further, in one animal in the unlesioned group and 3 animals in the transection and repair group, there was a slightly increased level of GDNF in the sciatic nerve segment proximal to the bifurcation (B). In the tibial nerve segments increase in GDNF concentrations did not occur, demonstrating

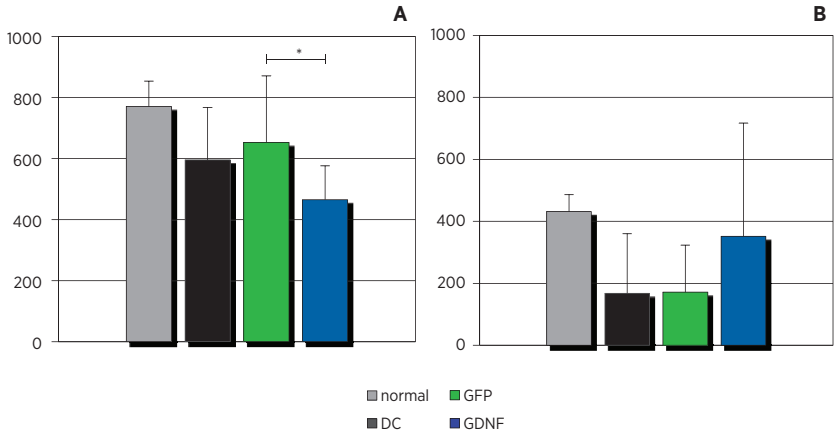

Figure 3

(A) FB and DY (B) profile counts (mean and SEM) for normal animals, direct coaptation repair (DC), and LV-GDNF and LV-sGFP injection groups. After LV-GDNF injection there is an increase in the number of DY-labeled profiles compared with the DC and LV-sGFP groups, although not significantly. The number of FB-labeled profiles is significantly decreased in the LV-GDNF group, compared with the LV-sGFP group (*).

that it is possible to selectively transduce the peroneal branch of the rat sciatic nerve using an LV-vector without cross-over to the tibial branch.

Simultaneous retrograde tracing

In all cases of direct coaptation repair (with or without viral vector injection) the distribution of DY- and FB-labelled profiles had shifted compared with normal animals. Examples are provided in Figure 2. Profiles counts (Figure 3) showed an increased number of DY labelled motoneurons (from which axons had regenerated to the peroneal branch) after LV-GDNF injection (352 ± 366) compared to the control groups (LV-GFP injection: 171 ± 152 and DC: 168 ± 192), although the difference in numbers of DY between the groups was not statistically significant (P = 0.15). There were variations in the numbers of DY-labeled motoneurons between the different animals especially in the LV-GDNF group (spread in number of DY-labelled profiles in the LV-GDNF group: 5 - 916, in the LV-GFP group: 3 - 448, and in the DC group: 9 - 424), with 2 animals in the LV-GDNF group that had respectively 916 and 876 DY-labelled profiles, and 486 and 409 FB-labelled profiles, resulting in a 2:1 DY to FB ratio, which is normally 1: 2 (normal animals: FB-labelled profiles 770 ± 83 and DY-labelled profiles 431 ± 55) (Figure 3). The number of FB-labelled profiles was slightly decreased after LV-GDNF injection (465 ± 111) compared with LV-GFP injection (653 ± 217) (P = 0.047), but not significantly compared with DC repair (595 ± 172) (P = 0.1102). Numbers of double-labelled (FB-DY) profiles were negligible (≤ 10 in all groups). The total numbers of regenerated motoneurons (FB and

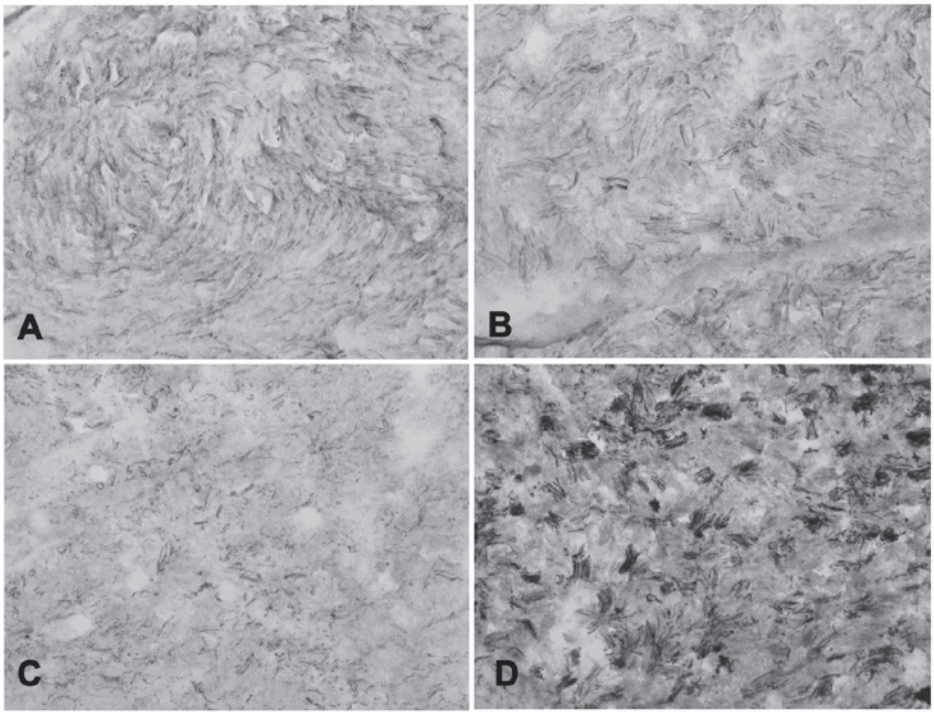

Figure 4

Microscopic images (x20 magnification) of examples of sections taken through the tibial (A and C) and peroneal nerve (B and D) after LV-sGFP (A and B) and LV-GDNF (C and D) injection analyzed with Chat immunohistochemistry. In Figure 4D there are clearly more motor axons than in the other sections (A-C). The motor axons are grouped, which could be explained by grouped/contained regeneration of axonal branches inside basal lamina tubes.

DY) were significantly decreased compared with normal (1202 ± 116) after DC (763 ± 196), LV-GDNF (817 ± 383) and LV-GFP (824 ± 234) (P = 0.0493).

Presence of motor axon branches in distal nerves

The cross-sectional area of the peroneal nerve after LV-GDNF injection was significantly enlarged compared with the LV-GFP control group (Figure 5B). ChAT immunohistochemistry also demonstrated an increased presence of motor axons in the peroneal nerve after LV-GDNF injection (Figure 4D) compared with the contralateral tibial nerve and compared with peroneal nerves in the LV-GFP group (Figure 4A-C); motor axons were grouped, and therefore difficult to quantify. Because of the latter, a semi-quantitative estimate of the slides by 5 blinded observers was performed, which showed a significantly increased presence of motor branches in the peroneal nerve in the LV-GDNF group compared with the LV-GFP group (P<0.05) (Figure 5C). There was a good correlation for the scoring between the

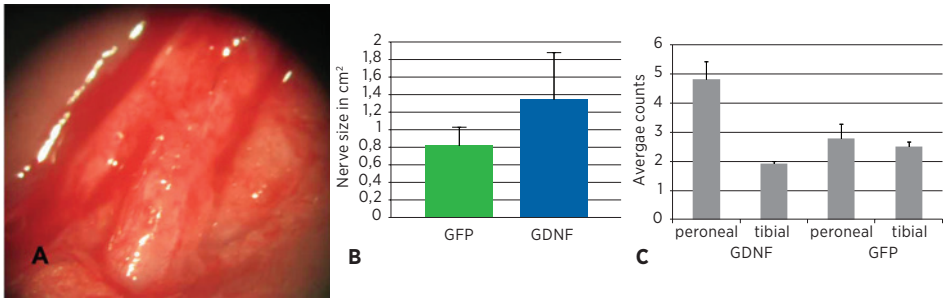

Figure 5

A: Example of image taken through the objective of the microscope at re-exploration after 4 weeks before tracer application. The peroneal nerve (on the right) is clearly enlarged compared with the tibial nerve and hyperaemic. B: Sizes of the tibial and peroneal nerves for sections obtained from the nerve segments taken distally from the tracer application sites in the LV-sGFP and LV-GDNF groups. C: Results for qualitative analysis of the sections of the tibial and peroneal nerves in the LV-sGFP and LV-GDNF groups.

different observers (kappa 0.64). Abundant fibers (as demonstrated in Figure 4D) were observed in 4 out of 6 LV-GDNF injection cases. Interestingly there was no correlation between the successful cases for simultaneous tracing (2) and ChAT immunohistochemistry (4); in only one case there was both an increase in number of DY-labeled profiles and number of ChAT positive fibers.

DISCUSSION

In this study we demonstrate that lentiviral vector-mediated gene transfer can be used to increase the expression of a neurotrophic factor to a specific branch of an intact and a transected and surgically repaired peripheral nerve. We used this approach to investigate whether it is possible to guide motor axons to a nerve branch that is expressing high levels of transgenic GDNF. Although the variability was high retrograde tracing revealed that there were on average more motoneurons from which axons had regenerated towards the peroneal branch that overexpressed GDNF than in the group with the control vector. In two animals an unusual high number of DY-labelled profiles was observed even reversing the normal peroneal : tibial motoneuron distribution (from 1:2 to 2:1), something that has not been reported before in other studies that have used the same simultaneous retrograde tracing technique to evaluate results after direct coaptation repair in the rat sciatic nerve model [1, 23] (**Chapter 4**). Moreover, in the animals that received an LV-GDNF injection into the peroneal branch significantly less motoneurons had projections towards the tibial nerve branch. Semi-quantitative estimate of the distal nerves with ChAT immunohistochemistry also showed an increased presence of motor axon branches in the distal peroneal nerve compared with the tibial nerve after

LV-GDNF injection. Overall these results thus indicate that viral vector mediated neurotrophic factor expression may be used to direct regenerating motor axons. However, the model used in this study was still limited by several technical aspects that are discussed below.

Technical aspects of the model

Different factors may explain the variation that was found in this study for the number of DY-labelled profiles in all groups. First of all, repair of the nerve at the bifurcation might have varied from animal to animal. We determined the branching point under the operating microscope, transected the nerve and subsequently sutured the tibial and peroneal nerves back to the proximal nerve, while maintaining correct fascicular alignment. The sciatic nerve, although optically divided at this point however may still consists of two large fascicles. In some cases therefore the tibial and peroneal nerves might have been repaired in continuity, and direction of tibial motoneurons towards the peroneal branch in these cases might have been limited (although cross-over in these cases may also occur [24]). A solution for this problem would be to use a Y-shaped conduit with proximal insertion of the sciatic nerve proximally and tibial and peroneal nerves distally, as has been used in earlier experiments on neurotropism [14, 25-28].

A second explanation for the variation in DY-labelled profiles, might be that the site of maximum number of motor axons may have varied relative to the site of tracer application due to difference in site of the so-called '*candy store*'. This site, at which motor axons are trapped due to a relatively higher concentration of neurotrophic factor compared to more distally in the nerve, may have varied from animal to animal, as can be concluded from the variation in concentration of GDNF at different levels in the peroneal nerve (Figure 1D and F). The site of the candy store may thus have varied relative to the site of retrograde tracing; in some cases the tracer may have been applied distal, and in others proximal to the candy store. From this we can also conclude that in the future in order to limit the effect of the candy store and to observe possible functional effects of directing regenerating motor axons the creation of a regulatable lentiviral construct will be essential.

Another explanation, for the observed variations, as can also be concluded from the ELISA results, is that there might have been variation in Schwann cell transduction efficiency after LV-GDNF injection. In two out four animals in the ELISA experiment we observed a very low concentration in the peroneal nerve segment just distally to the tibial-peroneal bifurcation (segment F). It could be that a certain treshold of GDNF had to be exceeded before motor axons were preferentially directed towards the peroneal nerve branch. This variation in GDNF expression could have been caused by a surgical variation in viral vector injection. When injecting, the needle has to be placed directly into a nerve fascicle and not into the perifascicular space. If not injected correctly, the viral solution may leak out of the nerve through the opening created in the perineurium. A solution for this potential problem of tracer leakage, might be to perform multiple injections at multiple

sites (as was done in a study by Hu et al [16], who injected the nerve 18 times at 3 different sites). However, we believe that for future potential clinical application, the number of injections should be preferably as low as possible, because injection may harm the architecture of the nerve by disrupting the orientation of basal lamina tubes or even by creating a separate dead-end channel inside the fascicle caused by the trajectory of the needle. More research is also needed on the spread of virus after injection into the nerve. Recently, White et al for example reported that the distribution of lentiviral vector after injection in the striatum may vary due to the size of the vector relative to the perivascular space [29]. We have found that our vector spreads more easily in the nerve after injection in proximal direction than in distal direction (unpublished observations). Therefore, in this experiment we injected into a distal direction, because in case of injection into a proximal direction the vector may have leaked out of the nerve at the coaptation site or even may have crossed over into the tibial nerve. This spread into proximal direction could explain the slight increase in GDNF concentration that was noted in the sciatic nerve proximal to the bifurcation site (B), although this might also be explained by the migration of transfected Schwann cells.

Finally, viral vector injection into the peroneal nerve might have interfered with retrograde tracing with DY. As illustrated in Figure 5A, at re-exploration the peroneal nerve in most cases had a swollen, hyperaemic aspect. During the 30 minutes of tracer application sometimes accumulation of blood inside the cup was observed, which might have limited DY tracer uptake. This could also explain the fact that abundant motor axons were observed in 4 out 6 cases with ChAT immunohistochemistry. Nevertheless, retrograde tracing in the analysis of the directing effect of viral vector injection on regenerating axons still is the most valuable evaluation method, because an increase in number of motor axons can also be explained by excessive branching inside the distal basal lamina tubes rather than increased regeneration towards the peroneal nerve.

Future potential clinical applications of lentiviral vector injection

Although some biosafety issues remain [30, 31], lentiviral vectors are already being used in clinical trials for Parkinson's disease, β-thalassemia, X-linked adrenoleukodystrophy (ALD), and AIDS [32] and many more clinical applications are currently being investigated. Also, in future clinical nerve repair lentiviral vector injections may play a role. Possible applications include: preventing atrophy and death of axotomised motoneurons; increasing the number and velocity of regenerating axons crossing coaptation sites and/or nerve grafts; preventing denervated muscle atrophy; to upgrade the results for autograft repair by the expression of different growth factors; and finally to direct/guide regenerating axons, which was the aim of the present study. The latter may be applied in the repair of mixed nerves, for example in median nerve repair at the wrist a viral vector encoding for a neurotrophic factor selectively enhancing motor axon regeneration (as for example GDNF) could be injected into the recurrent branch (innervating the muscles of

the thenar compartment) and a viral vector encoding for a neurotrophic factor selectively enhancing sensory axon regeneration (as for example NGF) into the digital cutaneous branches. For sensory regeneration Hu et al. [16] recently demonstrated using an adenoviral vector encoding for NGF that also sensory axons can be directed. In their study Ad-NGF injection into the saphenous branch 1 week after transection and direct coaptation repair of rat femoral nerve resulted a significantly increased ratio of DRG neurons regenerated towards the saphenous branch (SB/MB ~2) compared with injection of Ad-GFP (SB/MB~1) determined with simultaneous tracing 3 weeks after injury and repair. Most studies using adenoviral vectors in the peripheral nervous system however have been limited to the relatively short term, because of high immunogenicity of adenoviral vectors and the rapid humoral destruction of transduced cells [33].

To our knowledge the present study provides the first indication that viral vectors may be applied to direct regenerating motor axons. In this study we used a lentiviral vector encoding for GDNF, because this neurotrophic factor has been shown to improve motoneuron survival and regeneration after prolonged axotomy [34], and because motor neurons express receptors for GDNF (RET and GFRα-1) and upregulate these receptors after axotomy [35]. However, other molecules involved in guidance may also be used in gene therapy to either attract regenerating motor axons or divert them (for example by injecting a vector encoding for semaphoring 3A) [36-38]. The latter may be applied to prevent loss of axons towards a nerve branch that is of less interest (as for example the lateral antebrachial cutaneous nerve in repair of the musculocutaneous nerve).

CONCLUSIONS

Viral vectors may be applied in the future to direct regenerating motor axons to improve the results of motor nerve repair. More research is needed to improve the technique of viral vector injection and new vectors are currently also being developed (regulatable vectors and vectors expressing other molecules involved in axonal guidance). The results of this study can be used as basis for future research.

REFERENCES:

1. de Ruiter, G.C., et al., *Misdirection of regenerating motor axons after nerve injury and repair in the rat sciatic nerve model.* Exp Neurol, 2008. 211(2): p. 339-50.
2. Witzel, C., C. Rohde, and T.M. Brushart, *Pathway sampling by regenerating peripheral axons.* J Comp Neurol, 2005. 485(3): p. 183-90.
3. Madison, R.D., G.A. Robinson, and S.R. Chadaram, *The specificity of motor neurone regeneration (preferential reinnervation).* Acta Physiol (Oxf), 2007. 189(2): p. 201-6.

4. Brushart, T.M., *Motor axons preferentially reinnervate motor pathways.* J Neurosci, 1993. 13(6): p. 2730-8.
5. Brushart, T.M., *Preferential reinnervation of motor nerves by regenerating motor axons.* J Neurosci, 1988. 8(3): p. 1026-31.
6. Martini, R., M. Schachner, and T.M. Brushart, *The L2/HNK-1 carbohydrate is preferentially expressed by previously motor axon-associated Schwann cells in reinnervated peripheral nerves.* J Neurosci, 1994. 14(11 Pt 2): p. 7180-91.
7. Martini, R., et al., *The L2/HNK-1 Carbohydrate Epitope is Involved in the Preferential Outgrowth of Motor Neurons on Ventral Roots and Motor Nerves.* Eur J Neurosci, 1992. 4(7): p. 628-639.
8. Franz, C.K., U. Rutishauser, and V.F. Rafuse, *Polysialylated neural cell adhesion molecule is necessary for selective targeting of regenerating motor neurons.* J Neurosci, 2005. 25(8): p. 2081-91.
9. Hoke, A., et al., *Schwann cells express motor and sensory phenotypes that regulate axon regeneration.* J Neurosci, 2006. 26(38): p. 9646-55.
10. Gillespie, M.J., T. Gordon, and P.R. Murphy, *Reinnervation of the lateral gastrocnemius and soleus muscles in the rat by their common nerve.* J Physiol, 1986. 372: p. 485-500.
11. Bernstein, J.J. and L. Guth, *Nonselectivity in establishment of neuromuscular connections following nerve regeneration in the rat.* Exp Neurol, 1961. 4: p. 262-75.
12. Nguyen, Q.T., J.R. Sanes, and J.W. Lichtman, *Pre-existing pathways promote precise projection patterns.* Nat Neurosci, 2002. 5(9): p. 861-7.
13. Gramsbergen, A., I.J.-P. J, and M.F. Meek, *Sciatic nerve transection in the adult rat: abnormal EMG patterns during locomotion by aberrant innervation of hindleg muscles.* Exp Neurol, 2000. 161(1): p. 183-93.
14. Abernethy, D.A., A. Rud, and P.K. Thomas, *Neurotropic influence of the distal stump of transected peripheral nerve on axonal regeneration: absence of topographic specificity in adult nerve.* J Anat, 1992. 180 (Pt 3): p. 395-400.
15. Hamilton, S.K., et al., *Misdirection of regenerating axons and functional recovery following sciatic nerve injury in rats.* J Comp Neurol. 519(1): p. 21-33.
16. Hu, X., et al., *Sensory axon targeting is increased by NGF gene therapy within the lesioned adult femoral nerve.* Exp Neurol, 2010. 223(1): p. 153-65.
17. Tannemaat, M.R., et al., *Differential effects of lentiviral vector-mediated overexpression of nerve growth factor and glial cell line-derived neurotrophic factor on regenerating sensory and motor axons in the transected peripheral nerve.* Eur J Neurosci, 2008. 28(8): p. 1467-79.
18. Hoyng, S.A., et al., *Nerve surgery and gene therapy: a neurobiological and clinical perspective.* J Hand Surg (Eur), 2011. 36E(9): p. 735-746.
19. Yan, Q., C. Matheson, and O.T. Lopez, *In vivo neurotrophic effects of GDNF on neonatal and adult facial motor neurons.* Nature, 1995. 373(6512): p. 341-4.
20. Zurn, A.D., et al., *Glial cell line-derived neurotrophic factor (GDNF), a new neurotrophic factor for motoneurones.* Neuroreport, 1994. 6(1): p. 113-8.
21. Eggers, R., et al., *Neuroregenerative effects of lentiviral vector-mediated GDNF expression in reimplanted ventral*

roots. Mol Cell Neurosci, 2008. 39(1): p. 105-17.
22. Hendriks, W.T., et al., *Lentiviral vector-mediated reporter gene expression in avulsed spinal ventral root is short-term, but is prolonged using a immune "stealth" transgene.* Restor Neurol Neurosci, 2007. 25(5-6): p. 585-99.
23. Puigdellivol-Sanchez, A., A. Prats-Galino, and C. Molander, *Estimations of topographically correct regeneration to nerve branches and skin after peripheral nerve injury and repair.* Brain Res, 2006.
24. Lutz, B.S., *The role of a barrier between two nerve fascicles in adjacency after transection and repair of a peripheral nerve trunk.* Neurol Res, 2004. 26(4): p. 363-70.
25. Politis, M.J., K. Ederle, and P.S. Spencer, *Tropism in nerve regeneration in vivo. Attraction of regenerating axons by diffusible factors derived from cells in distal nerve stumps of transected peripheral nerves.* Brain Res, 1982. 253(1-2): p. 1-12.
26. Mackinnon, S.E., et al., *A study of neurotrophism in a primate model.* J Hand Surg [Am], 1986. 11(6): p. 888-94.
27. Brunelli, G., *Chemotactic arrangement of axons inside and distal to a venous graft.* J Reconstr Microsurg, 1987. 4(1): p. 75.
28. Chiu, D.T., et al., *Neurotropism revisited.* Neurol Res, 2004. 26(4): p. 381-7.
29. White, E.A., et al., *The Distribution Properties of Lentiviral Vectors Administered into the Striatum by Convection-Enhanced Delivery.* Hum Gene Ther.
30. Nayak, S. and R.W. Herzog, *Progress and prospects: immune responses to viral vectors.* Gene Ther. 17(3): p. 295-304.
31. Yi, Y., M.J. Noh, and K.H. Lee, *Current advances in retroviral gene therapy.* Curr Gene Ther. 11(3): p. 218-28.
32. Kumar, P. and C. Woon-Khiong, *Optimization of lentiviral vectors generation for biomedical and clinical research purposes: contemporary trends in technology development and applications.* Curr Gene Ther. 11(2): p. 144-53.
33. Mason, M.R., et al., *Gene therapy for the peripheral nervous system: a strategy to repair the injured nerve?* Curr Gene Ther. 11(2): p. 75-89.
34. Boyd, J.G. and T. Gordon, *Glial cell line-derived neurotrophic factor and brain-derived neurotrophic factor sustain the axonal regeneration of chronically axotomized motoneurons in vivo.* Exp Neurol, 2003. 183(2): p. 610-9.
35. Naveilhan, P., W.M. ElShamy, and P. Ernfors, *Differential regulation of mRNAs for GDNF and its receptors Ret and GDNFR alpha after sciatic nerve lesion in the mouse.* Eur J Neurosci, 1997. 9(7): p. 1450-60.
36. Charron, F. and M. Tessier-Lavigne, *The Hedgehog, TGF-beta/BMP and Wnt families of morphogens in axon guidance.* Adv Exp Med Biol, 2007. 621: p. 116-33.
37. Fradkin, L.G., J.M. Dura, and J.N. Noordermeer, *Ryks: new partners for Wnts in the developing and regenerating nervous system.* Trends Neurosci. 33(2): p. 84-92.
38. Tannemaat, M.R., et al., *Human neuroma contains increased levels of semaphorin 3A, which surrounds nerve fibers and reduces neurite extension in vitro.* J Neurosci, 2007. 27(52): p. 14260-4.

CHAPTER 10

General discussion and future directions

Misdirection of regenerating axons

Despite the capacity of the peripheral nervous system to regenerate, functional results after nerve injury and repair are often poor. Several factors can explain the disappointing recovery, including: delay in nerve repair, degree and level of the nerve injury, and age of the patient. In the first part of this thesis we demonstrate that misdirection or misrouting of regenerating axons also plays an important role. Using a sequential retrograde tracing technique in which the first tracer was injected into the peroneal nerve before the injury (DY) and the second tracer 8 weeks after repair (FB) (see illustration Figure 1, **Chapter 4**), we found that after crush injury of the rat sciatic nerve 71% of the peroneal motoneurons were correctly directed towards the peroneal nerve branch, and after transection of the sciatic nerve and direct coaptation repair, only 42%. This difference in percentage of correct direction after transection injury and repair compared with crush injury can be explained by disruption of the continuity of the basal lamina tubes. Apparently, axons that cross the coaptation site disperse and end up in different distal basal lamina tubes. After autograft repair, with two coaptation sites, the percentage correctly directed peroneal motoneurons was even lower: 25%.

Subsequently we studied the impact of misdirection on functional recovery. For this purpose, we developed a novel evaluation method, called *2D-digital video ankle motion analysis*. This method was first validated in normal animals and after sciatic, tibial, and peroneal nerve crush injury (**Chapter 3**). We compared this technique to the sciatic function index, which is the standard assessment technique in the rat sciatic nerve model. Our new method was more sensitive in the detection of functional recovery, especially in showing differences in the recovery of ankle plantar and dorsiflexion (tibial and peroneal nerve function, respectively). *2D-digital video ankle motion analysis* of function after transection injury and repair showed interesting effects with a negative impact on recovery: the ankle angle at midswing (normally the moment of maximum dorsiflexion/ peroneal nerve function) was reduced 1 week after nerve injury and repair, which was expected, but in time the angle decreased even further. This finding can be explained by misdirection of a significant portion of the peroneal motoneuronpool towards the tibial nerve branch. In our sequential tracing experiment only 42% of the peroneal motoneurons were correctly directed towards the peroneal nerve branch. Considering that the number of motoneurons from which axons had regenerated 8 weeks after autograft repair (Chapter 7) was not significantly different from normal, it is likely that the other peroneal motoneurons (remaining 58%) had regenerated towards the tibial nerve branch. This misdirection could thus result in active plantar flexion during the swing phase and therefore a further reduction in dorsiflexion angle. Also of interest is the work by Puigdellivol et al. [1], who used the same model, technique of sequential retrograde tracing and time point of evaluation, but instead investigated correct direction towards the tibial nerve branch. They found that about 1/3 of the motoneurons were labeled only by the second tracer (262.8 out of 877.6,

numbers obtained from Table 1 Puigdellivol et al. [1] multiplied by 4). Considering the sizes of the tibial and peroneal motoneuronpools (around 800 and 400 motoneurons, respectively, see Figure 4 **Chapter 7**), this means that also in their study more than 50% of the peroneal motoneurons (262.8 out of 400) were misdirected towards the tibial nerve branch. They concluded that 'epineurial suture repair leads to a high degree of topographically correct directional axon regeneration', because they found that 88% of the tibial motoneurons were correctly directed to the tibial nerve. One cannot, however, draw this conclusion if one considers the difference in size of the tibial and peroneal nerve branches.

In our experiment on motion analysis we did not see any signs of a mechanism that might correct for misdirection (**Chapter 2**). The further decrease in midswing ankle angle appeared 8 weeks after the nerve injury and repair and lasted for the entire follow-up period of 16 weeks. One might expect that pruning of misdirected axons in favor of correctly directed ones, which has been reported to occur between 3 and 8 weeks in the rat femoral nerve model [2], would already have taken place. Plastic changes, such as for example remodeling of spinal cord circuits, may, however, require more time [3]. Longer follow-up is, therefore, needed to investigate further whether this angle will improve in time. Preferably, this analysis should be combined with simultaneous recordings of compound muscle action potentials in the plantar and dorsiflexion muscles, which might show whether the reduced angle of dorsiflexion is caused by active plantar flexion during the swing phase. Another interesting future experiment would be to analyze the percentages correct direction at multiple time intervals after nerve injury and repair to investigate potential effects of pruning of misdirected collaterals. In the same experiment the organization of differently labeled motoneurons in the anterior horn could also be analyzed to see whether more grouping of motoneurons with the same label occurs in time compared with the disorganized distribution of differently retrogradely labeled motoneurons that we observed in our simultaneous tracing experiments (**Chapter 7 and 9**).

In conclusion, misdirection is an important factor that contributes to reduced functional recovery after nerve injury and repair, especially when we consider that other conditions in our experiment were optimal: immediate repair with reconstruction of the original fascicular orientation. In clinical nerve repair results may be poorer, because there is often a delay in repair and because the original fascicular orientation cannot be reconstructed. Another experiment that might be interesting for further study is the role of misdirection in delayed nerve repair, where the capacity of regeneration is decreased; this mimics the clinical situation more closely. Finally, functional analysis may be combined with other methods that also evaluate sensory recovery.

GUIDANCE OF REGENERATING AXONS

In the second part of this thesis, we investigated the use of two different strategies to guide nerve regeneration after injury and repair. The first strategy was *physical guidance* using a multichannel conduit. The second strategy was *biological guidance* using gene therapy. The results and future perspectives of both these tools will be discussed separately below.

MULTICHANNEL NERVE TUBE

Our hypothesis for axonal guidance through a multichannel nerve tube was that the internal structure would limit the axonal dispersion that is seen after single lumen nerve tube repair (Figure 1B and C). Multichannel conduits bear a closer resemblance to the structure of an autograft containing multiple basal lamina tubes (Figure 1A). To test this hypothesis, we developed a novel multichannel nerve tube made from poly(lactic co-glycolic acid) (PLGA) using a modified injection-molding technique (Figure 1, **Chapter 6**). The end caps that were used to align the wires inside the mold were provided with an extra top-layer to create a sleeve for insertion of the nerve stumps. The same injection-molding technique was used to fabricate single lumen nerve tubes with a single wire. Before *in vivo* implantation, single lumen PLGA nerve tubes made from different copolymer ratios (50:50, 75:25, and 85:15 PLGA) were first tested *in vitro* to determine optimal flexibility, swelling and degradation characteristics (important properties of nerve tubes for peripheral nerve repair). The middle ratio (75:25 PLGA) was chosen to fabricate multichannel nerve tubes, because of greater flexibility than the higher ratio (85:15) and less swelling than the lower ratio (50:50) as well as a slower rate of degradation. These 75:25 PLGA multichannel nerve tubes were also tested *in vitro* and the results were compared to the results for single lumen nerve tubes made from the same ratio of PLGA. In addition to the flexibility, swelling and degradation properties mentioned above, a new method was developed to compare *in vitro* permeability properties of the single lumen and multichannel nerve tubes. The results of this *in vitro* study showed that the multichannel structure did not negatively influence the permeability and flexibility properties of the conduit: 75:25 PLGA multichannel nerve tubes were even more permeable and flexible than the 75:25 PLGA single lumen ones. For these conduits, however, this can be explained by the injection-molding evaporation technique that leads to more interconnection of the pores in the wall in the multichannel nerve tubes compared with the single lumen ones (Figure 2, **Chapter 6**). Theoretically, one would expect multichannel tubes to be less permeable and less flexible. This unexpected finding demonstrates the importance of *in vitro* analysis of novel conduits before *in vivo* implantation, because adding internal guiding structures may not only have an impact on guidance of regenerating axons, but may also have an effect on regeneration by changing other physi-

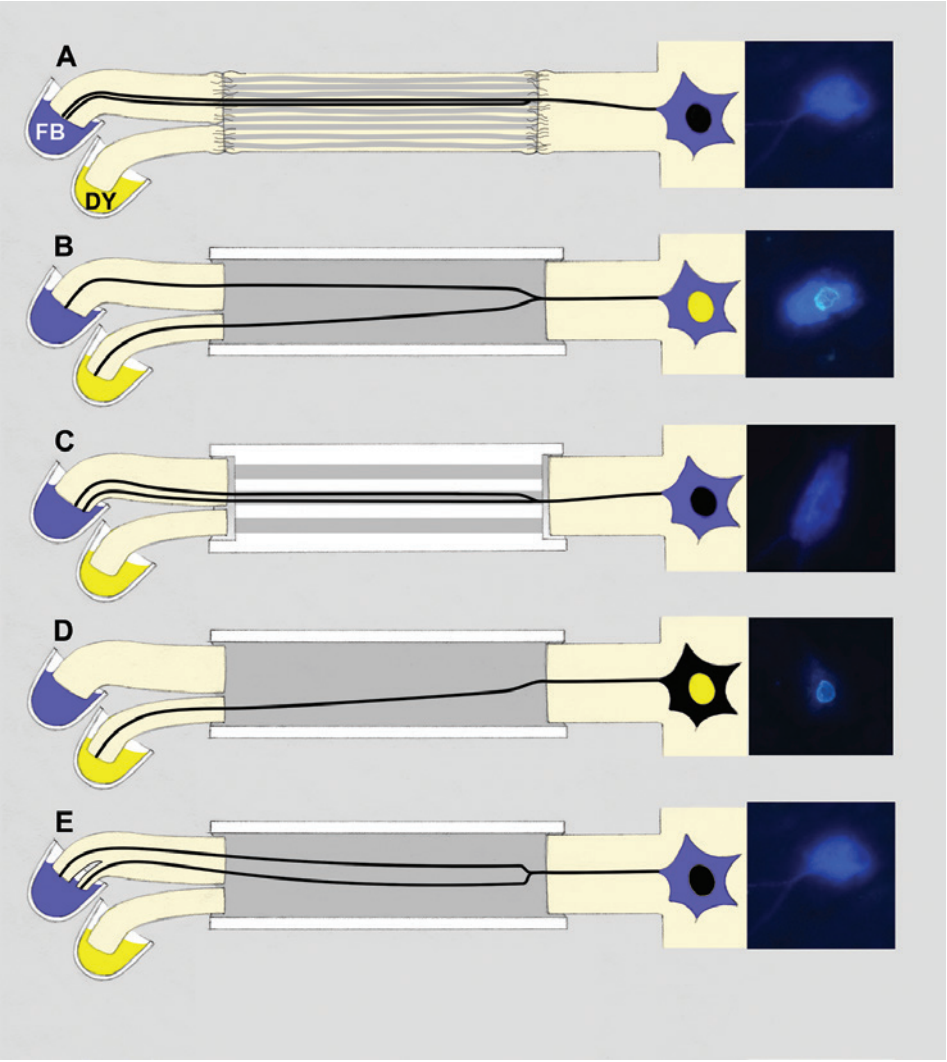

Figure 1

Concepts for the dispersion of regenerating motor axons after (A) autograft, (B) single lumen, and (C) multichannel nerve tube repair, and the technique of simultaneous tracing with fast blue (FB) and diamidino yellow (DY) tracers being applied to the tibial and peroneal nerve branches, respectively, 8 weeks after implantation. FB is transported retrograde to the cell body of the motoneuron and DY to the nucleus.

A: After autograft repair, regenerating axons originating from the same motoneuron are contained by the basal lamina tubes, and both end up in the same (tibial) nerve branch.

B: After single lumen nerve tube repair, axons originating from the same motoneuron disperse and end up separately in the tibial and peroneal nerve branches.

C: After multi-channel nerve tube repair, axons originating from the same motoneuron are contained on the inside of a channel and end up in the same (tibial) nerve branch.

D and E: other examples of dispersion across the single lumen nerve tube, which do not cause double labeling, such as dispersion of a single projection from a motoneuron (D), and double projections to the same branch but towards different fascicles inside this branch (E).

cal properties of the conduit (as for example permeability, flexibility, swelling and degradation characteristics). In addition, these properties are also important for potential future clinical application. The methods and results presented in **Chapter 6** can be used as a basis for the development of novel conduits with more complex internal structures.

After the *in vitro* analysis, the 75:25 PLGA single lumen and multichannel nerve tubes were implanted in a 1-cm gap in the rat sciatic nerve model to investigate the accuracy of regeneration across these conduits using simultaneous and sequential tracing techniques (**Chapter 7**). The results of this study showed that single lumen nerve tube repair indeed leads to a higher percentage of dispersion, with 21.4% double projecting motoneurons to both the tibial and peroneal nerve branch compared with 5.9% after autograft repair. Multichannel nerve tube repair showed a trend towards reducing this dispersion, although the percentage double projecting motoneurons (16.9%) was not significantly different from that after single lumen nerve tube repair. This can be explained by the finding that only 3 out of 7 channels were filled with myelinated axons. In addition, overall success rate in this study was small: regeneration across the conduits was found in 53% of the cases after single lumen nerve tube repair and 43% of the cases after multichannel nerve tube repair. A possible explanation for these disappointing results may be extensive swelling of the nerve tubes due to the accumulation of small degradation products that had increased the osmotic value of the tube (**Chapter 6**).

Following the experiment with the multichannel 75:25 PLGA nerve tubes, a novel series of multichannel nerve tubes (1-, 2-, 4- and 7-channel) was developed with different physical properties. The natural material collagen (type I) was used and a multiple step-molding technique was applied [4] (see Figure 1, page 131, **Chapter 8**). The results of this study showed that multichannel structure can limit axonal dispersion with 2.7% double projecting motoneurons after 2-channel and 2.4% after 4-channel collagen conduit repair compared with 7.1% after single channel collagen conduit repair. Although this reduction might appear to be small, it is important to realize that this percentage only indicates part of the axonal dispersion that occurs during regeneration across the conduit. In addition, single unbranched axons might disperse (Figure 1D). This cannot be detected with simultaneous tracing. Also, axonal branches originating from the same motoneuron might end up in the same nerve branch, but within different fascicles innervating different target muscles, for example the gastrocnemius and soleus muscles in the case of the tibial nerve (Figure 1E). Further, in the analysis of the results, it is important to consider the time-point of evaluation. The percentages double projections might have decreased in time due to pruning of misdirected collaterals. In our first study (**Chapter 7**), in which the observation period was 8 weeks instead of 16 weeks, we also found much higher percentages of double projecting motoneurons (16.9% after multichannel nerve tube repair and 21.4% after single lumen nerve tube)

compared with the percentages found in the second study, although the results of these two studies cannot be compared, because in the second study conduits with four channels were used (instead of seven, as in the first study) and conduits were made of different biomaterials using different techniques of fabrication. More research is, therefore, needed to investigate whether there is a decrease of double-projections with time.

Another interesting result of our second *in vivo* study on multichannel conduit repair was that the quantitative results of regeneration (for the numbers of regenerated myelinated axons and retrogradely labeled profiles) were again (as in the first study) not significantly decreased compared with single lumen tubes, despite the reduction in the total cross-sectional area for axons to grow into. Also, successful regeneration was found in 39 out of 40 cases of conduit repair and almost all channels contained fascicles with myelinated fibers. The first phase of successful regeneration across a single lumen nerve tube is the formation a fibrin matrix between the two nerve ends (Figure 2, **Chapter 5**). Possibly the formation of multiple fibrin cables to guide regeneration is also more advantageous. More research is needed to further investigate what happens in the initial stages of regeneration across multichannel nerve tubes.

Finally, as in the first study, quantitative results of regeneration were still superior after autograft repair. Although this did not result in a better functional outcome, it is important to realize that an ideal alternative for the autograft should perform better than the autograft.

FUTURE DIRECTION OF RESEARCH ON MULTICHANNEL NERVE TUBES

As demonstrated in this thesis, multichannel nerve tubes limit the dispersion of regenerating axons that occurs across single lumen nerve tubes, as they more closely resemble the structure of an autograft. Although the number of channels is now still limited by the size of the wires and space needed between the wires, novel fabrication techniques in the future may increase the number of channels that can be fitted into the tube. An ideal design would be a conduit with an internal honeycomb structure to reduce the amount of space between the channels and to increase the total cross-sectional surface area available for regeneration. Another future aim could be to build multichannel scaffolds with a 3D printing technique to resemble more closely the original architecture of the nerve that often (especially more proximally) consists of an intraneural plexus instead of parallel-aligned channels.

Besides multichannel nerve tube structure, other modifications to the common hollow or single nerve tube have been developed that may also be applied to guide regenerating axons, including the addition of collagen gels, filaments, supportive cells, and growth factors (see Table 3, Chapter 5). These modifications can be used in combination with the multichannel conduit structure. An additional advantage

of such a multichannel structure is that it provides a greater internal luminal surface area for cell attachment, and, the internal framework can be used for the controlled release of growth factors through microspheres. Adding these microspheres to the internal structure rather than to the lumen would provide the potential for more controlled release during the degradation process of the conduit to overcome the initial burst release that occurs with an 'in-lumen' delivery system [5]. In addition, growth factors could be used to attract regenerating axons into the distal pathways to prevent the dispersion/wandering of axons at the coaptation sites and/or preferentially attract different types of axons to regenerate into separate channels by the expression of different growth factors.

GENE THERAPY

In last part of this thesis we investigated the use of lentiviral vectors (LV) to selectively guide regenerating motor axons. The basis for this project was the observation in **Chapter 4** that peroneal motoneurons were misdirected due to the smaller size of this branch in comparison to the larger tibial nerve branch, which led to impaired recovery of peroneal nerve function. The aim of this project was, therefore, to increase the number of motoneurons regenerating to the peroneal nerve branch by selective injection of a lentiviral vector encoding for the neurotrophic factors GDNF (LV-GDNF). First, in a pilot study, we analyzed the distribution or spread of viral vector into the peroneal nerve after injection of LV-GDNF 0.5cm from the tibial-peroneal bifurcation (in intact animals and after transection and repair just proximal to this bifurcation). The expression levels of GDNF in 0.5cm segments of nerve were analyzed using an ELISA. Results showed that, with this technique, high concentrations of GDNF can be obtained selectively in the peroneal nerve distal to the bifurcation site, without increased levels in the tibial or sciatic nerve, although the levels of GDNF varied from animal to animal. Subsequently, in a larger study, the effect of LV-GDNF injection into the peroneal nerve after transection injury and repair of the sciatic nerve at the tibial-peroneal bifurcation was investigated with simultaneous retrograde tracing four weeks after sciatic nerve transection and repair. This study showed an increased number of motoneurons from which axons had regenerated towards the peroneal nerve branch after LV-GDNF injection compared with injection of a control vector encoding for green fluorescent protein (LV-sGFP). This effect was, however, not statistically significant. In two of the eight animals, the normal ratio of the motoneuronpoolsize, which is tibial: peroneal, 2:1, was completely reversed (1:2). In addition, ChAT immunohistochemistry showed an increased number of motor axons in the peroneal nerve after LV-GDNF injection. Although these results thus provided a first indication that it may be possible to guide regenerating motor axons with gene therapy, more research is needed. This should be focused on optimization of the injection technique to get constant levels of growth factor concentration. Besides, regulatable vectors are being developed

to turn off the elevated growth factor expression once the axons have reached the designated target branch to prevent trapping of axons at the site of highest concentration (phenomenon called the *candy store*). Future application of selective injection of a lentiviral vector encoding for GDNF could be to guide regenerating motor axons to a motor branch, for example after median nerve repair at the wrist. In addition, other potential future applications of gene therapy in peripheral nerve regeneration are to upgrade the autograft by selective overexpression of specific growth factors or to increase the speed of regeneration in more proximal nerve injuries to improve the recovery of, for example, hand function in brachial plexus repair [6]. Finally, combinations of the techniques mentioned above (for example, filling of multichannel nerve tubes with genetically modified Schwann cells) may ultimately be applied to improve the results of nerve repair.

REFERENCES:

1. Puigdellivol-Sanchez, A., A. Prats-Galino, and C. Molander, *Estimations of topographically correct regeneration to nerve branches and skin after peripheral nerve injury and repair.* Brain Res, 2006.
2. Brushart, T.M., *Motor axons preferentially reinnervate motor pathways.* J Neurosci, 1993. **13**(6): p. 2730-8.
3. Navarro, X., V. Meritxell, and A. Valero-Cabre, *Neural plasticity after peripheral nerve injury and regeneration.* Prog in Neurobiology, 2007. **82**: p. 163-201.
4. Yao, L., et al., *Multichanneled collagen conduits for peripheral nerve regeneration: design, fabrication, and characterization.* Tissue Engineering Part C, 2010. **16**(6): p. 1585-1596.
5. de Boer, R., et al., *Rat sciatic nerve repair with a poly-lactic-co-glycolic acid scaffold and nerve growth factor releasing microspheres.* Microsurgery, 2011. **31**(4): p. 293-302.
6. Pondaag, W. and M.J. Malessy, *Recovery of hand function following nerve grafting and transfer in obstetric brachial plexus lesions.* J Neurosurgery (Pediatrics), 2006. **105**(1 Suppl): p. 33-40.

Samenvatting en toekomstige richting van het onderzoek

MISDIRECTIE VAN ZENUWREGENERATIE

De functionele resultaten na chirurgisch herstel van perifere zenuwletsels zijn vaak teleurstellend. Verschillende factoren kunnen dit tegenvallende herstel verklaren zoals een tijdsverloop tussen het ontstaan van het letsel en chirurgisch herstel en de leeftijd van de patiënt. Een andere verklarende factor, die in dit proefschrift werd onderzocht, is de verkeerde uitgroei van zenuwvezels; genaamd *misdirectie*. Deze misdirectie treedt op doordat zenuwvezels niet altijd recht vooruit groeien naar het oorspronkelijke distale gedeelte van de zenuw, maar ter plaatse van de coaptatieplaats (de plek van beschadiging en chirurgisch herstel) kunnen afdwalen en terechtkomen in het verkeerde distale gedeelte van de zenuw (zie figuur 1, **hoofdstuk 2**). Dit kan vervolgens leiden tot een verminderd herstel van functie, bijvoorbeeld doordat de zenuwvezels uit één zenuw uitkomen in meerdere spieren met verschillende functies.

Kwantificatie van misdirectie

Hoewel het bovenbeschreven fenomeen van misdirectie als ontdekt is in het begin van de vorige eeuw [1], zijn er slechts enkele studies die deze misdirectie hebben gekwantificeerd (zie **hoofdstuk 2** voor een overzicht van deze studies). De meeste van deze studies hebben zich daarbij gericht op de nauwkeurigheid van motorische versus sensibele regeneratie naar respectievelijk spier en huid. Er is weinig bekend over de nauwkeurigheid van regeneratie van motorische zenuwvezels naar verschillende spieren en met name ook over het effect op functioneel herstel. In het eerste gedeelte van dit proefschrift onderzochten wij deze nauwkeurigheid van motor axon regeneratie in het nervus ischiadicus model in de rat. Deze zenuw splitst zich distaal in twee motorische takken, de nervus tibialis en de nervus peroneus, die verschillende spieren aansturen, respectievelijk betrokken bij plantair en dorsiflexie van de enkel (figuur 1, **hoofdstuk 4**). We kwantificeerden misdirectie in dit model met behulp van een *sequentiële retrograde tracing* techniek, waarbij de eerste tracer werd toegediend aan de nervus peroneus voor het aanbrengen van het letsel en de tweede tracer acht weken daarna. Vervolgens werd het percentage motoneuronen dat was gelabeld door beide tracers en dus juist was uitgegroeid, berekend door het aantal dubbel gelabelde motoneuronen te delen door het totale aantal motoneuronen dat voor het letsel was gelabeld. Dit onderzoek toonde dat 8 weken na een crush letsel 71% van de motoneuronen van de nervus peroneus correct was uitgegroeid naar de oorspronkelijk zenuw. Na doorsnijding van de zenuw en chirurgische coaptatie bedroeg het percentage correcte uitgroei slechts 42% en na herstel met een autologe donorzenuw zelfs maar 25%. Dit verschil in percentages correcte uitgroei na doorsnijding en herstel vergeleken met het crush letsel, kan worden verklaard door onderbreking van de continuïteit van de basale

lamina kokers na doorsnijding van de zenuw. Het nog lagere percentage na herstel met een autograft kan worden verklaard doordat axonen twee keer een coaptatie oversteken en daardoor meer kans hebben om af te dwalen en uiteindelijk terecht te komen in de verkeerde distale tak.

Effect van misdirectie op functioneel herstel

Voor de analyse van het effect van de *misdirectie* op functioneel herstel ontwikkelden wij een nieuwe methode, genoemd *2D-digital video ankle motion analysis*. Deze methode werd in eerste instantie gevalideerd in normale dieren en na crush letsels van de nervus ischiadicus, tibialis en peroneus (**hoofdstuk 3**). We vergeleken onze methode met de toen geldende standaard methode voor functionele analyse, genaamd de *sciatic function index*, waarbij de voetafdruk van de rat wordt geanalyseerd door bijvoorbeeld de poot in inkt te dopen en de rat vervolgens over een stuk papier te laten lopen [2]. Voor onze nieuwe methode maakten wij gebruik van een digitale camera en computersoftware om bewegingen van de enkel te analyseren. Deze apparatuur wordt ook gebruikt bij sporters, bijvoorbeeld om de slag van honkballers en de swing van golfers te analyseren. Wij toonden aan dat onze methode gevoeliger is voor de detectie van herstel dan de *sciatic function index*. Daarbij heeft onze methode het voordeel dat deze ook kan worden gebruikt voor de afzonderlijke analyse van herstel van functie van de nervus tibialis en nervus peroneus door bestudering van respectievelijk plantair- en dorsiflexie van de enkel.

In **hoofdstuk 4** gebruikten wij deze methode van *ankle motion analysis* om herstel te analyseren na verschillende typen zenuwletsel: crush letsel, doorsnijding en coaptatie en herstel met een autograft. De resultaten van deze studie toonden dat misdirectie inderdaad een negatief effect heeft op functioneel herstel. Zo was de hoek van de enkel tijdens de *midswing* fase (normaal het moment van maximale dorsiflexie) zoals verwacht na letsel en herstel afgenomen, maar in de loop van de tijd nam deze steeds verder af, in plaats van dat herstel optrad. Deze onverwachte uitkomst kan worden verklaard door een verkeerde uitgroei van een groot gedeelte van de motoneuronen van de nervus peroneus richting de nervus tibialis. Zoals aangetoond in ons experiment met *sequentiële tracing* was maar 42% van de peroneus motoneuronen correct uitgegroeid. Omdat het aantal motoneuronen dat was uitgegroeid niet verschilde van het aantal in controle dieren, kan worden aangenomen dat de rest van de peroneus motoneuronen (58%) was uitgegroeid naar de nervus tibialis. Deze verkeerde uitgroei kan dus leiden tot actieve plantairflexie tijdens de *swing* fase en daardoor een verminderde hoek van dorsiflexie.

Vergelijking met de literatuur

Onze studie uit **hoofdstuk 4** toont aan dat de uitgroei van motor axonen na doorsnijding onnauwkeurig is en dat dit de functionele resultaten van zenuwherstel beperkt. Er is één andere studie die de nauwkeurigheid van motor axon regene-

ratie heeft gekwantificeerd [3]. In deze studie werd gebruik gemaakt van hetzelfde model en dezelfde techniek van sequentiële tracing, alleen werd in die studie uitgroei naar de nervus tibialis in plaats van de nervus peroneus onderzocht. De auteurs vonden dat 88% van de tibialis motoneuronen correct was uitgegroeid 8 weken na doorsnijding en chirurgisch herstel en concludeerden op basis van deze resultaten dat coaptatie van een zenuw tot een hoog percentage van correctie uitgroei van axonen leidt. Echter, ook in die studie was ongeveer 1/3 van de motoneuronen dat alleen gelabeld was door de tweede tracer (tabel 1 artikel Puigdellivol), hetgeen wijst op misdirectie van >50% van de peroneus motoneuronen. Dit kan worden berekend op basis van de aantallen motoneuronen van de nervus tibialis en nervus peroneus (ongeveer 800 en 400 respectievelijk, figuur 4 Hoofdstuk 7). Het verschil in percentages (88% correcte uitgroei voor tibialis motoneuronen versus 42% correctie uitgroei voor peroneus motoneuronen) toont dus aan dat het belangrijk is rekening te houden met de grootte van de motoneuronpool.

Correctiemechanismen voor misdirectie

De resultaten van ons motion analysis experiment toonden geen aanwijzingen voor het optreden van correctiemechanismen voor misdirectie (zie **hoofdstuk 2** voor een overzicht van deze mechanismen). De verdere afname van de enkelhoek tijdens de midswing ontstond na acht weken en bleef verlaagd gedurende de gehele follow-up periode van zestien weken. Het mag worden verwacht, dat eventuele *pruning*, het verdwijnen van verkeerd uitgegroeide zenuwvezels, bij 16 weken zou hebben plaats gevonden, omdat dit fenomeen in het rat femoralis model optreedt na ongeveer drie tot acht weken [4]. Het is mogelijk dat andere mechanismen, zoals bijvoorbeeld plastische veranderingen (remodulatie van verbindingen in het ruggenmerg [5]), welke de effecten van misdirectie zouden kunnen reduceren, pas na 16 weken optreden. In toekomstige studies zou daarom voor een langere follow-up kunnen worden gekozen (zie hieronder).

Conclusie eerste deel proefschrift en toekomstig richting van het onderzoek

Op basis van de resultaten in het eerste gedeelte van het proefschrift kan worden geconcludeerd dat misdirectie inderdaad een belangrijke beperkende factor is welke het functioneel herstel na letsels van zenuwen die verschillende spieren aansturen beperkt zoals bijvoorbeeld de nervus ischiadicus [6], de nervus ulnaris [7] en de nervus suprascapularis [8]. De resultaten na klinisch zenuwherstel zijn waarschijnlijk vaak nog slechter doordat hierbij ook andere beperkende factoren een rol spelen, zoals een tijdsverloop tussen het optreden van het letsel en de operatie en een relatief hoge leeftijd van de patiënt. Daarbij kan in de praktijk de originele oriëntatie van de fascikels vaak niet worden hersteld, zoals in onze studie wel het geval was. Toekomstige experimenten zouden daarom de rol van misdirectie in een model van *delayed nerve repair* kunnen onderzoeken en/of herstel met verschillende fasciculaire oriëntaties. Ander onderzoek zou gericht kun-

nen zijn op eventueel herstel van functie op langere termijn door het optreden van correctiemechanismen. Deze mechanismen zouden verder kunnen worden onderzocht door het percentage correcte uitgroei te bepalen mbv sequentiële retrograde tracing op meerdere tijdstippen na het letsel en herstel. Daarbij zou in hetzelfde experiment gekeken kunnen worden naar de chaotische verdeling van de verschillende gelabelde motoneuronen in de voorhoorn van het ruggenmerg om te onderzoeken of er meer organisatie ontstaat (zie observaties van simultane retrograde tracing in **hoofdstuk 7** en **9**). Verder zouden bij de functionele analyse tegelijkertijd ook de compound muscle action potentials (CMAP) kunnen worden gemeten en zou sensibel herstel kunnen worden onderzocht.

TWEEDE DEEL PROEFSCHRIFT

GELEIDING VAN ZENUWREGENERATIE

In het tweede deel van dit proefschrift onderzochten wij de toepassing van twee verschillende strategieën om de correctie uitgroei van axonen tijdens zenuwregeneratie te verbeteren. De eerste strategie was fysische geleiding met behulp van een gefabriceerde zenuwbuis met meerdere kanalen (multichannel). De tweede strategie was biologische geleiding met behulp van gentherapie. De resultaten en toekomstige perspectieven van deze twee strategieën worden hieronder apart besproken.

Multichannel zenuwbuis

Holle zenuwbuizen worden op dit moment al veelvuldig toegepast als alternatief voor het autoloog zenuwtransplantaat in de overbrugging van defecten <3 cm in sensibele zenuwen, zoals bijvoorbeeld digitale zenuwen in de hand (voor overzicht zie **hoofdstuk 5**). Deze buizen worden maar weinig gebruikt in het herstel van motorische zenuwen. Een mogelijke reden hiervoor is dat herstel met holle buis kan leiden tot de afdwaling van regenererende axonen (zie figuur 1B, **hoofdstuk 10**). Dit in vergelijking met het autoloog zenuwtransplantaat dat bestaat uit meerdere basale lamina kokers waardoorheen de axonen uitgroeien (figuur 1A, **hoofdstuk 10**). De hypothese waarvoor wij de multichannel zenuwbuis ontwikkelden, was dan ook dat de interne structuur van deze buis de afdwaling die optreedt na herstel met holle buizen kan beperken door de aparte geleiding van groepen zenuwvezels in de kanalen (figuur 1C, **hoofdstuk 10**).

De ontwikkeling van de multichannel zenuwbuis

Om deze hypothese te testen, ontwikkelden wij een nieuwe multichannel zenuwbuis gemaakt van poly(lactic co-glycolic acid) (PLGA) met behulp van een gemodificeerde *injection-molding* techniek (figuur 1, **hoofdstuk 6**). Dezelfde injection-

molding techniek werd gebruikt voor de fabricatie van holle zenuwbuizen. Voor *in vivo* implantatie werden eerst holle zenuwbuizen van verschillende co-polymeer ratio's (50:50, 75:25, 85:15 PLGA) getest *in vitro* om de optimale co-polymeer eigenschappen te bepalen met als doel enerzijds flexibiliteit te maximaliseren en anderzijds zwelling te minimaliseren. Flexibiliteit van de buis is een belangrijke eigenschap voor zenuwherstel, omdat zenuwletsels kunnen optreden thv gewrichten (bijvoorbeeld letsels van de nervus ulnaris ter hoogte van de elleboog). Het minimaliseren van zwelling van de wand van de buis is belangrijk, omdat dit primair het lumen kan blokkeren of secundair compressie kan geven van uitgegroeide zenuwvezels. Op basis van dit *in vitro* experiment werd de ratio van 75:25 PLGA gekozen voor de fabricatie van de multichannel zenuwbuizen, omdat de flexibiliteit groter was dan voor de hogere ratio (85:15), er minder zwelling was vergeleken met de lagere ratio (50:50). Deze 75:25 multichannel zenuwbuizen werden ook getest *in vitro* en de resultaten werden vergeleken met de resultaten voor holle zenuwbuizen gemaakt van dezelfde ratio. Vervolgens werd een nieuwe methode ontwikkeld om *in vitro* permeabiliteit van holle en multichannel zenuwbuizen te vergelijken. Permeabiliteit van de buis is van belang voor de diffusie van nutriënten voor regeneratie. Uit de resultaten van deze *in vitro* studie bleek dat de structuur van de multichannel zenuwbuis geen negatief effect heeft op de eigenschappen voor permeabiliteit en flexibiliteit van de zenuwbuis. Multichannel zenuwbuizen gemaakt van 75:25 PLGA waren zelfs meer doorlaatbaar en flexibeler dan holle zenuwbuizen gemaakt van dezelfde ratio. Theoretisch zou men verwachten dat een multichannel zenuwbuis minder doorlaatbaar is en minder flexibel. Echter, mogelijk leidt de injection-molding techniek van fabricatie tot meer verbindingen tussen de poriën in de wand van de multichannel zenuwbuis vergeleken met de poriën in de wand van de holle buis (figuur 2, **hoofdstuk 6**). Dit toont het belang aan van *in vitro* analyse van een zenuwbuis, voordat deze *in vivo* wordt geïmplantateerd. De meeste van de holle zenuwbuizen die op dit moment klinisch worden toegepast zijn niet *in vitro* getest (zie **hoofdstuk 5**). De toevoeging van een interne structuur aan de buis beinvloedt niet alleen de geleiding van axonen, maar kan ook belangrijke fysische eigenschappen van de buis veranderen, zoals aangetoond in **hoofdstuk 6**. De methoden en resultaten van deze studie kunnen worden gebruikt als basis voor de ontwikkeling van buizen met een complexere interne structuur.

Analyse van zenuwregeneratie door de multichannel zenuwbuis

Na de *in vitro* analyse, werden de holle en multichannel zenuwbuizen gemaakt van 75:25 PLGA geïmplanteerd in een gap van 1 cm lang defect in de nervus ischiadicus van de rat om de nauwkeurigheid van motor axon regeneratie door deze buizen te onderzoeken met behulp van simultane en sequentiële tracing technieken (**hoofdstuk 7**). De resultaten van deze eerste studie toonden aan dat herstel met een holle zenuwbuis inderdaad leidt tot meer afdwaling; er was een hoger percentage motoneuronen met dubbele projecties naar de nervus tibialis en nervus peroneus (21,4%) vergeleken met herstel met een autograft (5,9%). Na herstel met een mul-

tichannel zenuwbuis was er een trend naar afname van afdwaling (16,9% van de motoneuronen had dubbele projecties), maar dit verschil was niet significant vergeleken met de afdwaling na herstel met een holle zenuwbuis. Het feit dat in deze eerste studie geen significante reductie van afdwaling werd gevonden kan worden verklaard doordat tijdens het regeneratie proces in de multichannel zenuwbuis maar drie van de zeven kanalen gevuld waren met gemyeliniseerde axonen. Daarbij was het succes percentage in deze studie laag: groei door de buis werd maar gevonden in 53% van de gevallen na herstel met een holle zenuwbuis en 43% na herstel met een multichannel zenuwbuis. Een mogelijke verklaring hiervoor kan zijn dat er toch te veel zwelling op was getreden van het 75:25 PLGA co-polymeer, waardoor zenuwregeneratie door de buizen werd belemmerd.

Na het experiment met de multichannel 75:25 zenuwbuis, werd een nieuwe serie van multichannel zenuwbuizen ontwikkeld met één, twee, vier en zeven kanalen [9]. Deze buizen werden gemaakt van het natuurlijk voorkomend materiaal collageen (type I) middels een *multiple step-molding* techniek (figuur 2, Hoofdstuk 10). De fysische eigenschappen van deze buis werd eerst getest *in vitro* volgens de methoden gepresenteerd in **hoofdstuk 6**.
De resultaten van de tweede *in vivo* studie toonden aan dat de multichannel structuur inderdaad de afdwaling van axonen kan reduceren (**hoofdstuk 8**). Na herstel met een 2 en 4 kanaals zenuwbuis hadden respectievelijk 2,7 en 2,4% van de motoneuronen dubbele projecties naar de nervus tibialis en nervus peroneus, vergeleken met 7,1% na herstel met een holle zenuwbuis. Alhoewel dit verschil misschien klein lijkt, is het belangrijk te realiseren dat dit percentage slechts een deel van de afdwaling betreft. Daarnaast kan er afdwaling zijn van enkele projecties (hetgeen niet kan worden aangetoond met simultane tracing, figuur 1D **hoofdstuk 10**) en kan afdwaling weliswaar leiden tot regeneratie naar dezelfde distale zenuw, maar naar verschillende fascikels in die zenuw (figuur 1E **hoofdstuk 10**). Verder is het belangrijk in de analyse van de resultaten rekening te houden met het tijdpunt van evaluatie. In onze eerste studie in **hoofdstuk 7** was de periode van observatie acht weken, terwijl in de tweede studie de resultaten na 16 weken werden geëvalueerd. We vonden bijvoorbeeld hogere percentages motoneuronen met dubbele projecties in de eerste studie (16,9% na herstel met een multichannel zenuwbuis en 21,4% na herstel met een holle zenuwbuis) dan in de tweede studie. De resultaten van deze twee studies kunnen echter niet worden vergeleken, omdat in de tweede studie buizen met twee en vier kanalen werden gebruikt (in plaats van zeven zoals in de eerste studie) en de buizen van verschillende materialen werden gemaakt. Meer onderzoek is daarom nodig om te onderzoeken of het percentage daalt in de loop van de tijd.

Kwantitatieve resultaten van zenuwregeneratie

De kwantitatieve resultaten van zenuwregeneratie (voor wat betreft het aantal gemyeliniseerde axonen en retrograad gelabelde motoneuronen) waren zowel

na herstel met een PLGA als na herstel met een collageen multichannel zenuwbuis niet significant verlaagd vergeleken met na herstel met een holle zenuwbuis gemaakt van hetzelfde materiaal. Dit ondanks het verminderde doorsnede oppervlak dat in een multichannel zenuwbuis beschikbaar is voor regeneratie. Daarnaast was het succespercentage na herstel met een collageen buis groter dan na herstel met een PLGA buis: in 39 van de 40 operaties waren bijna alle kanalen gevuld met regenererende fascikels met gemyeliniseerde axonen. De eerste fase van regeneratie door een buis is de vorming van een fibrine matrix tussen de zenuwuiteinden (figuur 2, **hoofdstuk 5**). Mogelijk voordeel van de multichannel zenuwbuis tov de holle buis is dat meerdere van dit soort kabels worden gevormd. Meer onderzoek is nodig voor verdere analyse van de eerste fases in regeneratie door multichannel zenuwbuizen.
Tenslotte waren de kwantitatieve resultaten van regeneratie in beide studies nog steeds het beste na herstel met een autograft. Alhoewel dit niet leidde tot betere functionele resultaten is het belangrijk te realiseren dat een ideaal alternatief voor de autograft het beter zou moeten doen, omdat zelfs na herstel met een autograft de klinische resultaten vaak teleurstellend zijn [10].

Conclusie en toekomstige richting van het onderzoek met multichannel zenuwbuizen

Zoals wij aantoonden in dit proefschrift kunnen multichannel zenuwbuizen dus de afdwaling van axonen die optreedt na herstel met een holle zenuwbuis voorkomen, doordat deze meer lijken op de structuur van een autograft. Opmerkelijk is dat het aantal kanalen dat in de buis kan worden gemaakt in ons geval werd beperkt door de fabricatietechniek. Wellicht kan het aantal kanalen in de multichannel zenuwbuizen met behulp van nieuwe fabricatietechnieken in de toekomst bij multichannel zenuwbuizen worden vergroot. De ideale structuur hierbij is die van een honingraat, omdat met deze opbouw de hoeveelheid biomateriaal tussen de kanalen kan worden verkleind en daarmee het doorsnede oppervlak dat beschikbaar is voor regeneratie kan worden vergroot. Een andere doel zou kunnen zijn om zenuwbuizen te bouwen, waarvan de interne structuur meer lijkt op die van de beschadigde zenuw die mn op het proximale niveau niet bestaat uit parallel verlopende kanalen maar uit een netwerk van fascikels die slingerend lopen, splitsen en fuseren. Deze zogenaamde intraneurale plexus structuur zou kunnen worden nagemaakt door gebruik te maken van 3D-printing technieken.

Naast de multichannel structuur, kunnen ook andere modificaties van de holle zenuwbuis worden onderzocht, zoals de toevoeging van gels met collageen, filamenten, cellen en groeifactoren (zie tabel 3, **hoofdstuk 5** voor een overzicht van deze factoren). Deze aanpassingen kunnen ook worden toegepast in combinatie met de multichannel structuur. Een additioneel voordeel van de multichannel zenuwbuis hierbij is dat deze meer oppervlak biedt voor de hechting van cellen en een intern framework biedt voor gecontroleerde afgifte van groeifactoren door

bijvoorbeeld gebruik te maken van microspheres. Door deze microspheres in te bouwen in de structuur is het mogelijk dat groeifactoren geleidelijk worden afgegeven. Bij losse microspheres ingebracht in het lumen van de zenuwbuis treedt direct na implantatie een hoge afgifte op [11]. Daarnaast zouden groeifactoren ook kunnen worden gebruikt om zenuwvezels aan te trekken richting de kanalen (om zo afdwaling bij de overgang van de zenuw naar de buis te voorkomen) en/of om verschillende typen axonen selectief te geleiden naar aparte kanalen door gebruik te maken van verschillende groeifactoren in de verschillende kanalen.

Gentherapie

In het laatste deel van dit proefschrift hebben wij de toepassing van lentivirale vectoren (LV) voor de selectieve geleiding van motor axonen onderzocht (**hoofdstuk 9**). De basis voor dit project was de observatie in **hoofdstuk 4** dat met name motoneuronen van de nervus peroneus terecht kwamen in de verkeerde distale tak doordat de nervus peroneus in doorsnede kleiner is dan de nervus tibialis. Dit leidde ook tot een verminderd herstel van functie van de nervus peroneus. Het doel van dit project was daarom om het aantal motoneuronen waarvan axonen uitgroeiden naar de nervus peroneus te vergroten. Dit werd nagestreefd door selectief een lentiviral vector coderend voor de neurotrofe factor GDNF (LV-GDNF) in de nervus peroneus te injecteren. Wij kozen hierbij voor de factor GDNF, omdat deze met name de uitgroei van motorische axonen stimuleert. De factor wordt na zenuwletsel voor een bepaalde periode geproduceerd door Schwann cellen in de distale zenuw. Injectie van LV-GDNF in de distale zenuw leidt tot een verhoogde expressie van GDNF. Dit werd aangetoond in een pilot studie, waarin het virus distaal van de bifurcatie naar de nervus peroneus en tibialis werd geïnjecteerd. De expressie van GDNF werd onderzocht mbv een ELISA uitgevoerd voor 0,5 cm segmenten van zenuw proximaal en distaal van de plaats van injectie. De resultaten toonden aan dat met behulp van deze injectie techniek hoge concentraties GDNF kunnen worden bereikt in de nervus peroneus, net distaal van de bifurcatie, zonder verhoging van de concentratie in de proximale nervus ischiadicus of in de andere distale tak, de nervus tibialis. Wel wisselden de concentraties GDNF van dier tot dier.

Vervolgens onderzochten wij in een grotere studie het effect van GDFN injectie in de nervus peroneus met behulp van simultane retrograde tracing 4 weken na transectie en chirurgisch herstel van de nervus ischiadicus. Deze studie toonde dat een verhoogd aantal motoneuronen waren uitgegroeid richting de nervus peroneus na LV-GDNF injectie vergeleken met de controle groep waarbij een lentivirale vector coderend voor green fluorescent protein (LV-sGFP) werd geïnjecteerd. Hoewel dit verschil niet statistisch significant was, werd in twee van de acht dieren na LV-GDNF injectie een opvallend uitgesproken effect gevonden. De normale ratio van tibialis en peroneus motoneuronen van 2:1 bleek volledig omgekeerd naar 1:2. Daarnaast toonde immunohistochemie met choline acetyl transferase (ChAT) een verhoogd aantal motor axonen in de nervus peroneus na LV-GDNF injectie,

alhoewel dit laatste ook kan worden verklaard door *sprouting* (het splitsen van axonen in meerdere distale uitlopers).

Conclusie en toekomstige richting van het onderzoek met gentherapie

De resultaten van **hoofdstuk 9** zijn een eerste aanwijzing dat motor axonen kunnen worden geleid met behulp van gentherapie. Meer onderzoek is echter nodig om constante concentraties van groeifactoren na de injectie te verkrijgen. Daarnaast worden op dit moment reguleerbare vectoren ontwikkeld om de *trapping* van axonen bij de plaats van verhoogde concentratie groeifactor (*candy store phenomenon*) te voorkomen. Mogelijke toekomstige toepassing van selectieve injectie zou zijn om motor axonen te geleiden naar de motorische tak, zoals bijvoorbeeld na herstel van de nervus medianus bij de pols (figuur 3) [12]. Andere mogelijke toekomstige toepassingen van gentherapie in zenuwchirurgie zijn upgrading van de autograft door selectieve overexpressie van groeifactoren of verhoging van de snelheid van regeneratie. Dit laatste is met name van belang in het herstel van proximale zenuwletsels, waarbij er een grote afstand is naar het uiteindelijk doelorgaan, zoals bijvoorbeeld het herstel van handfunctie in letsels van de plexus brachialis [13]. Tenslotte, zouden combinaties van de bovenvermelde strategieën (bijvoorbeeld multichannel zenuwbuizen met genetisch gemodificeerd Schwann cellen) kunnen leiden tot verbetering van de resultaten na chirurgisch zenuwherstel.

REFERENTIES:

1. Cajal, S., *Degeneration and regeneration of the nervous system.* London: Oxford University Press, 1928.
2. Varejao, A.S., et al., *Functional evaluation of peripheral nerve regeneration in the rat: walking track analysis.* J Neurosci Methods, 2001. **108**(1): p. 1-9.
3. Puigdellivol-Sanchez, A., A. Prats-Galino, and C. Molander, *Estimations of topographically correct regeneration to nerve branches and skin after peripheral nerve injury and repair.* Brain Res, 2006.
4. Brushart, T.M., *Motor axons preferentially reinnervate motor pathways.* J Neurosci, 1993. **13**(6): p. 2730-8.
5. Navarro, X., V. Meritxell, and A. Valero-Cabre, *Neural plasticity after peripheral nerve injury and regeneration.* Prog in Neurobiology, 2007. **82**: p. 163-201.
6. Maripuu, A., et al., *Reconstruction of sciatic nerve after traumatic injury in humans - factors influencing outcome as related to neurobiological knowledge from animal research.* J Brachial Plexus and Peripheral Nerve Injury, 2012. **7**(7): p. EPub ahead of print.
7. Post, R., K.S. de Boer, and M.J. Malessy, *Outcome following nerve repair of high isolated clean sharp injuries of the ulnar nerve.* PLoS One, 2012. **7**(10): p. e47928.
8. Malessy, M.J., et al., *Evaluation of suprascapular nerve neurotization after nerve graft or transfer in the treatment of brachial plexus traction lesions.* J Neurosurg, 2004. **101**(3): p. 377-89.
9. Yao, L., et al., *Multichanneled collagen conduits for peripheral nerve regeneration: design, fabrication, and characterization.* Tissue Engineering Part C, 2010. **16**(6): p. 1585-1596.
10. de Ruiter, G.C., et al., *Designing ideal conduits for peripheral nerve repair.* Neurosurg Focus, 2009. **26**(2): p. E5.
11. de Boer, R., et al., *Rat sciatic nerve repair with a poly-lactic-co-glycolic acid scaffold and nerve growth factor releasing microspheres.* Microsurgery, 2011. **31**(4): p. 293-302.
12. Hoyng, S.A., et al., *Nerve surgery and gene therapy: a neurobiological and clinical perspective.* J Hand Surg (Eur), 2011. **36E**(9): p. 735-746.
13. Pondaag, W. and M.J. Malessy, *Recovery of hand function following nerve grafting and transfer in obstetric brachial plexus lesions.* J Neurosurgery (Pediatrics), 2006. **105**(1 Suppl): p. 33-40.

Acknowledgements

The completion of this book was made possible thanks to support from many people inside and outside the lab.

Supervisors
Martijn Malessy (promotor), Robert Spinner (co-promotor), Anthony Windebank, Joost Verhaagen

Mayo Clinic
Robert Spinner, Alexandra Wolanskyj, Anthony Windebank, Michael Yaszemski, Bradford Currier, Kenton Kaufman, Eris Sorenson, Peter J. Dyck, JaNean Engelstad, Sandeep Vaishya, Huan Wang, Awad Alaid, Ellen Liang, Irene Onyeneho, Andrew Knight, BingKun Chen, LouAnn Gross, Jewel Podratz, Tony Koch, Jane Meyer, Michael Moore, Lichun Lu, Frederick Schultz, Mark Zobitz, Qingshan (Frank) Chen, Scott Gamb, Wijdicks family, Mikko Larsen, Diederik Kempen.

Netherlands Institute for Neuroscience
Joost Verhaagen, Martijn Malessy, Stefan Hoyng, Martijn Tannemaat, Ruben Eggers.

Text and lay-out
Nick van Silfhout van Textcetera, Department of Scientific Publications Mayo Clinic, Dave Factor, Peggy Chihak, Geraldine Bernard, Jurgen Kuivenhoven, Brenda Vollers, Felix Chorus.

Paranymfen
Quintijn de Ruiter, Co Bosch

Colleagues, friends and family, especially my mom and my girlfriend Max

I THANK YOU ALL!

List of publications

1. Evaluation of suprascapular nerve neurotization after nerve graft or transfer in the treatment of brachial plexus traction lesions. Malessy MJ, de Ruiter GC, de Boer KS, Thomeer RT. J Neurosurg 2004 Sep; 101(3):377-89.
2. Type grouping in skeletal muscles after experimental reinnervation: another explanation. Vleggeert-Lankamp CL, de Ruiter GC, Wolfs JF, Pego AP, Feirabend HK, Lakke EA, Malessy MJ. Eur J Neurosci 2005 Mar;21(5):1249-56.
3. Neurovascular compression following isolated popliteus muscle rupture: a case report. de Ruiter GC, Torchia ME, Amrami KK, Spinner RJ. Journal of Surgical Orthopaedic Advances 2005 Fall;14(3):129-32.
4. Benign metastasizing leiomyomatosis with massive brachial plexus involvement mimicking neurofibromatosis type 1. de Ruiter GCW, Scheithauer BW, Amrami KK, Spinner RJ. Clin Neuropathol. 2006 Nov-Dec 25(6): 282-7.
5. Pores in synthetisch nerve conduits are beneficial to regeneration. Vleggeert-Lankamp CL, de Ruiter GC, Wolfs JF, Pego AP, van den Berg RJ, Feirabend HK, Malessy MJ, Lakke EA. J Biomed Mater Res A. 2007 Mar 15;80(4):965-82.
6. Methods for in vitro characterization of multichannel nerve tubes. de Ruiter GCW, Onyeneho IA, Liang ET, Moore MJ, Knight AM, Malessy MJ, Spinner RJ, Lu L, Currier BL, Yaszemski MJ, Windebank AJ. J Biomed Mater Res A. 2008 Mar 1;84(3):643-51.
7. Two-dimensional digital video ankle motion analysis for assessment of function in the rat sciatic nerve model. de Ruiter GC, Spinner RJ, Alaid AO, Koch AJ, Wang H, Malessy MJ, Currier BL, Yaszemski MJ, Kaufman KR, Windebank AJ. J Peripher Nerv Syst. 2007 Sept; 12 (3):216-22.
8. An anatomic study of the spinal accessory nerve: extended harvest permits direct nerve transfer to distal plexus targets. Vathana T, Larsen M, de Ruiter GC, Bishop AT, Spinner RJ, Shin AY. Clin Anat 2007 Sep 18;20(8): 899-904.
9. A 67-year-old woman who mistook her daughter for a double: differential diagnosis of misidentification delusion. Vinkers DJ, van der Lubbe N, de Reus R, de Ruiter GC, Pondaag W. Ned Tijdschr Geneeskd 2007 Dec 22;151(51):2841-4. Dutch.
10. Misdirection of regenerating motor axons after nerve injury and repair in the rat sciatic nerve model. de Ruiter GC, Malessy MJ, Alaid AO, Spinner RJ, Engelstad JK, Sorenson EJ, Kaufman KR, Dyck PJ, Windebank AJ. Exp Neurol. 2008 Jun;211(2):339-50.
11. Accuracy of motor axon regeneration across autograft, single-lumen, and multichannel poly(lac-co-glycolic acid) nerve tubes. de Ruiter GC, Spinner RJ, Malessy MJ, Moore MJ, Sorenson EJ, Currier BL, Yaszemski MJ, Windebank AJ. Neurosurgery 2008 Jul;63(1):144-53; discussion 153-5.
12. Differential effects of lentiviral vector-mediated overexpression of nerve growth factor and glial cell line-derived neurotrophic factor on regenerating sensory and motor axons in the transected peripheral nerve. Tannemaat MR, Eggers R, Hendriks WT, de Ruiter

GC, van Heerikhuize JJ, Pool CW, Malessy MJ, Boer GJ, Verhaagen J. Eur J Neurosci 2008 Oct;28(8):1467-79.
13. Nerve tube for peripheral nerve repair. de Ruiter GC, Spinner RJ, Yaszemski MJ, Windebank AJ, Malessy MJ. Neurosurg Clin N Am. 2009 Jan;20(1):91-105,vii. Review.
14. Axon regeneration through scaffold into distal spinal cord after transection. Chen BK, Knight AM, de Ruiter GC, Spinner RJ, Yaszemski MJ, Currier BL, Windebank AJ. J Neurotrauma. 2009 Oct;26(10):1759-71.
15. Designing ideal conduits for peripheral nerve repair. de Ruiter GC, Malessy MJ, Yaszemski MJ, Windebank AJ, Spinner RJ. Neurosurg Focus. 2009 Feb;26(2):E5. Review.
16. Controlling dispersion of axonal regeneration using a multichannel collagen nerve conduit. Biomaterials. Yao L, de Ruiter GC, Wang H, Knight AM, Spinner RJ, Yaszemski MJ, Windebank AJ, Pandit A. 2010 Aug;31(22):5789-97.
17. Type grouping in rat sceletal muscle after crush injury. Bovenberg MS, Degeling MH, de Ruiter GC, Feirabend HK, Lakke EA, Vleggeert-Lankamp CL. J Neurosurg 2010 Nov.
18. Cerebral fluid ascites from a ventriculoperitoneal shunt. Houtman-van Duinen Wj, Ende-Verhaar YM, de Ruiter GC, van der Torren-Conze AM. Ned Tijdschr Geneesk. 2011; 155(50):A4035.
19. Decision making in the surgical treatment of meralgia paresthetica: neurolysis versus neurectomy. de Ruiter GC, Wurzer JA, Kloet A. Acta Neurochir (Wien). 2012 Jul 6.
20. Risk factors for survival of 106 surgically treated patients with symptomatic spinal epidural metastases. Bollen L, de Ruiter GC, Pondaag W, Arts MP, Fiocco M, Hazen TJ, Peul WC, Dijkstra PD. Eur Spine J. 2013 Mar 2.

Curriculum Vitae

Godard de Ruiter was born on March 24, 1978 in Nieuwerkerk a/d IJssel in The Netherlands. He graduated from high school (Marnix Gymnasium, Rotterdam) in 1996. Due to the Dutch numerus fixus system he was not able to start studying Medicine until 1999. Meanwhile he studied Biomedical Sciences in Leiden for two years and Pharmacy at the University of Utrecht for one year. In 2001 he completed both his studies Medicine and Biomedical Sciences. As part of the study Biomedical Sciences he performed a 9-month basic research project on peripheral nerve regeneration in the Neuromodulation Group under supervision of Dr. Carmen Vleggeert-Lankamp, which provided the basis for this thesis. For his Medical study, he completed a 3-month clinical research project on brachial plexus repair at the Department of Neurosurgery under supervision of Prof. Martijn Malessy. After his clinical rotations he received his Medical Degree in 2003. In January 2004 he moved to the US to do a two-year research fellowship with Prof. Robert Spinner at the Mayo Clinic, during which he completed most of the articles presented in this thesis. He also passed his US Medical License Exams (USMLE). The work on *multichannel nerve tubes* was awarded the *Best Basic Science Award* at the American Society for Peripheral Nerve (ASPN) in Tuscon Arizona in 2006. After the fellowship he returned to Leiden in 2006 and started his residency in Neurosurgery (head: Prof. Dr. R.T.W.M. Thomeer, later Prof. Dr. Wilco C. Peul). From 2007 he has worked on the final project of this thesis, *guidance of regeneration using gene therapy*, in the Netherlands Institute for Neuroscience in Amsterdam under supervision of Prof. Martijn Malessy and Prof. Joost Verhaagen. In 2012 he completed his residency. He now works as a Neurosurgeon at the Medical Center Haaglanden and Bronovo hospital, both in The Hague. His areas of interest in Neurosurgery are Spine, Nerve and Neurotrauma.